

Cationic Polymerization

August 20, 2012 | <http://pubs.acs.org>
Publication Date: May 1, 1997 | doi: 10.1021/bk-1997-0665.fw001

ACS SYMPOSIUM SERIES

665

Cationic Polymerization

Fundamentals and Applications

Rudolf Faust, EDITOR

University of Massachusetts Lowell

Timothy D. Shaffer, EDITOR

Exxon Chemical Company

Developed from a symposium sponsored
by the Division of Polymer Chemistry, Inc.



American Chemical Society, Washington, DC

American Chemical Society

Library

1155 16th St., N.W.

Washington, D.C. 20036

In Cationic Polymerization; Faust, R., et al.;

ACS Symposium Series; American Chemical Society: Washington, DC, 1997.



Cationic polymerization

Library of Congress Cataloging-in-Publication Data

Cationic polymerization: fundamentals and applications / Rudolf Faust, editor, Timothy D. Shaffer, editor.

p. cm.—(ACS symposium series, ISSN 0097-6156; 665)

“Developed from a symposium sponsored by the Division of Polymer Chemistry, Inc., at the 211th National Meeting of the American Chemical Society, New Orleans, Louisiana, March 24–28, 1996.”

Includes bibliographical references and indexes.

ISBN 0-8412-3507-4

1. Addition polymerization—Congresses.

I. Faust, Rudolf, 1951– . II. Shaffer, Timothy D. (Timothy Daniel), 1960– . III. American Chemical Society. Division of Polymer Chemistry. IV. American Chemical Society. Meeting (211th: 1996: New Orleans, La.) V. Series.

QD281.P6C3863 1997
547'.28—dc21

97-6912
CIP

This book is printed on acid-free, recycled paper.



Copyright © 1997 American Chemical Society

All Rights Reserved. Reprographic copying beyond that permitted by Sections 107 or 108 of the U.S. Copyright Act is allowed for internal use only, provided that a per-chapter fee of \$17.00 plus \$0.25 per page is paid to the Copyright Clearance Center, Inc., 222 Rosewood Drive, Danvers, MA 01923, USA. Reproduction or reproduction for sale of pages in this book is permitted only under license from ACS. Direct these and other permissions requests to ACS Copyright Office, Publications Division, 1155 16th Street, N.W., Washington, DC 20036.

The citation of trade names and/or names of manufacturers in this publication is not to be construed as an endorsement or as approval by ACS of the commercial products or services referenced herein; nor should the mere reference herein to any drawing, specification, chemical process, or other data be regarded as a license or as a conveyance of any right or permission to the holder, reader, or any other person or corporation, to manufacture, reproduce, use, or sell any patented invention or copyrighted work that may in any way be related thereto. Registered names, trademarks, etc., used in this publication, even without specific indication thereof, are not to be considered unprotected by law.

PRINTED IN THE UNITED STATES OF AMERICA

American Chemical Society
Library
1155 16th St., N.W.
Washington, D.C. 20036

In Cationic Polymerization; Faust, R., et al.;

ACS Symposium Series; American Chemical Society: Washington, DC, 1997.

Advisory Board

ACS Symposium Series

Mary E. Castellion
ChemEdit Company

Arthur B. Ellis
University of Wisconsin at Madison

Jeffrey S. Gaffney
Argonne National Laboratory

Gunda I. Georg
University of Kansas

Lawrence P. Klemann
Nabisco Foods Group

Richard N. Loepky
University of Missouri

Cynthia A. Maryanoff
R. W. Johnson Pharmaceutical
Research Institute

Roger A. Minear
University of Illinois
at Urbana-Champaign

Omkaram Nalamasu
AT&T Bell Laboratories

Kinam Park
Prudue University

Katherine R. Porter
Duke University

Douglas A. Smith
The DAS Group, Inc.

Martin R. Tant
Eastman Chemical Co.

Michael D. Taylor
Parke-Davis Pharmaceutical
Research

Leroy B. Townsend
University of Michigan

William C. Walker
DuPont Company

Foreword

THE ACS SYMPOSIUM SERIES was first published in 1974 to provide a mechanism for publishing symposia quickly in book form. The purpose of this series is to publish comprehensive books developed from symposia, which are usually “snapshots in time” of the current research being done on a topic, plus some review material on the topic. For this reason, it is necessary that the papers be published as quickly as possible.

Before a symposium-based book is put under contract, the proposed table of contents is reviewed for appropriateness to the topic and for comprehensiveness of the collection. Some papers are excluded at this point, and others are added to round out the scope of the volume. In addition, a draft of each paper is peer-reviewed prior to final acceptance or rejection. This anonymous review process is supervised by the organizer(s) of the symposium, who become the editor(s) of the book. The authors then revise their papers according to the recommendations of both the reviewers and the editors, prepare camera-ready copy, and submit the final papers to the editors, who check that all necessary revisions have been made.

As a rule, only original research papers and original review papers are included in the volumes. Verbatim reproductions of previously published papers are not accepted.

ACS BOOKS DEPARTMENT

Preface

THE FIELD OF CARBOCATIONIC POLYMERIZATION has undergone rapid growth in recent years. In just over a decade, this field has expanded from the first examples of living polymerization to numerous monomers that undergo living polymerization by a variety of initiator–coinitiator pairs. These newly discovered living systems have permitted the synthesis of advanced materials such as block copolymers and end-functional polymers. Preparation of these materials was either not possible or extremely difficult using conventional techniques.

This volume was developed from an international symposium titled “Carbocationic Polymerization and Related Ionic Processes”, which was held at the 211th National Meeting of the American Chemical Society in New Orleans, Louisiana, March 24–28, 1996. The symposium marked continuing progress in the field of cationic polymerization. This book documents some of the newest results presented at the meeting.

Not surprisingly, more than half of the lectures presented at the symposium, and documented in this book, deal with the use of living cationic polymerization for the synthesis of advanced materials. In the early years after the original discoveries, research focused mainly on the expansion of the scope of living carbocationic polymerization. During the last five years, the emphasis has focused on improving our understanding of the elementary mechanistic steps and using the technique for the synthesis of advanced materials. Its great value as a premier technique for material synthesis validates the role of living carbocationic polymerization as a synthetic tool despite ongoing debate regarding the appropriate name (controlled, living, quasi-living, etc.), the role of additives (nucleophiles), and some other aspects of these polymerizations. The field has matured to a point where some of these processes may advance into commercialization (witness the increased patent activity).

Although scientists engaged in ionic (cationic and anionic) polymerizations frequently exchange ideas at specialized meetings, and are thus aware of these developments, these meetings are not easily accessible to a general audience. Researchers not directly associated with this field may be genuinely surprised by the powerful capabilities now made available by cationic polymerization.

With the organization of this symposium, and the publication of this book, we hope to present the favorable features of cationic polymerizations to a general audience.

RUDOLF FAUST
Polymer Science Program
Department of Chemistry
University of Massachusetts Lowell
One University Avenue
Lowell, MA 01854

TIMOTHY D. SHAFFER
Baytown Polymers Center
Exxon Chemical Company
5200 Bayway Drive
Baytown, TX 77522-5200

January 28, 1997

Chapter 1

Carbocationic Polymerization: A Rejuvenation

Timothy D. Shaffer

Baytown Polymers Center, Exxon Chemical Company, 5200 Bayway Drive,
Baytown, TX 77522-5200

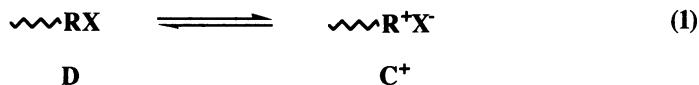
The discovery of living carbocationic polymerization has rejuvenated the field of carbocationic polymerization by creating new opportunities for alkene polymer synthesis. This review discusses the key mechanistic elements of living carbocationic polymerization emphasizing control of the propagation equilibria and the initiation step. This review further shows how living processes have enabled the synthesis of new alkene based polymers that exhibit remarkable properties.

Why has interest in this field increased in the past ten years? The discovery of living vinyl/alkene polymerization is the main reason. This breakthrough has impacted the polymer community in two ways. First, the living technique provides for precise control of initiation, polymer growth and termination. Control of molecular weight, its distribution, end groups, pendant groups, sequence distribution, and steric structure of the polymer is all possible with this technique. The preparation of well defined architectural polymers such as star-shaped polymers becomes accessible with this level of control, creating new opportunities for the total synthetic design of alkene-based macromolecules. Secondly, kinetic and mechanistic studies of carbocationic polymerization systems have led to an improved understanding of many of the previously observed, but poorly explained phenomena. This activity may have the largest future impetus in this field. Previous studies have often generated contradictory findings from seemingly identical experiments. Such confusion has hurt efforts to understand the fundamentals of carbocationic polymerization. The extreme dependence on, and susceptibility of carbocations to, impurities in the solvents and monomers triggers what look like inconsistent results. This fact alone contributed significantly to the time lag between discovery of the living technique in anionic and cationic polymerization.

In the current period of heightened interest, many books have been published on carbocationic polymerization (1-4). Several reviews have also appeared (5-11). As these materials provide a sufficiently up to date and comprehensive review of this subject, one will not be provided here. Instead, the key elements of living vinyl/alkene polymerization will be generally presented here, followed by a discussion of how living carbocationic polymerization is used in new material synthesis.

The Key Elements of Living Polymerization

Living polymerization of alkenes became possible when two important concepts were clearly understood: the dynamics of the propagation equilibria and the control of the number and type of initiating species. The growing chain end may be represented by a Winstein equilibrium. A simplified representation is shown below.



This simplification is justified by the independence of the carbenium ion's reactivity regardless of the degree of dissociation (12,13). Both the dormant (D) and active (C⁺) chain ends are interchangeable through this equilibrium. The exchange rate around the equilibrium is influenced by the mode of initiation, the temperature, the solvents, the presence of nucleophilic additives in the system and the nature of the monomer. Molecular control is only possible when the exchange rate between D and C⁺ is faster than propagation. In essence, the lifetime of the ion is relatively small, producing a low instantaneous concentration of active growing chain ends. This low level of carbocations results in a low overall polymerization rate. Because of the rapid turnover, only a few monomer units are added to the chain before collapse to the dormant state. The length of all the polymer chains becomes more homogeneous as the polymerization proceeds.

To understand this, let us consider a living polymerization system at low conversion. The oligomers formed have an average length of ten, but vary from this average by two or three monomer units. This variation originates from the short lifetime of the active chain ends and the statistical probability of adding a number of monomers before collapse to dormancy. This addition or propagation probability is not broad because of the rapid exchange rate between D and C⁺. At this point, however, polydispersity is fairly large. Assuming that the system continues in this manner, propagation to high molecular weight polymer may still result in chain length differences of two or three monomer units. This difference in chain length for an average of 1000 monomer units is not as significant as it was when the average chain length was ten. Often observed in cationic polymerization, this trend can be followed by plotting the change of molecular weight distribution (M_w/M_n) versus conversion. If $M_w/M_n = 1.1$ for a degree of polymerization of ten to twenty then the D-C⁺ exchange and propagation rates are well balanced.

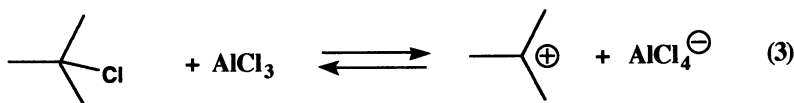
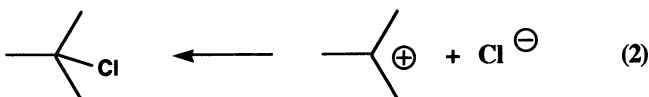
Living cationic polymerization systems are not exempt from transfer or termination (11). They are usually carried out in molecular weight regimes where the influence of chain transfer or termination is not observable. The ratio of propagation to transfer rates ($k_p/k_{tr,M}$) then becomes the limit of molecular control. Since transfer to monomer ($k_{tr,M}$) is the most important chain breaking event for most cationic systems, its rate is used in this determination. Matyjaszewski suggests the expression $DP_n < 0.1 k_p/k_{tr,M}$ be used as a guide in choosing the polymerization conditions (9). DP_n is the number average degree of polymerization for the desired polymer molecular weight. There are a set of k_p , $k_{tr,M}$, etc. values for each type of monomer. By knowing these values and using the DP_n rule of thumb above, we may choose conditions under which polymerization of the chosen monomer can easily reach the desired DP_n and maintain control of the molecular weight, chain end structure, etc. For a given monomer, the temperature dependence of k_p is not the same as $k_{tr,M}$ due to different activation energies for each (14). Since the activation energy for chain transfer is higher than propagation, lower temperatures afford higher molecular weight polymer because $k_p/k_{tr,M}$ is larger. Obviously, a broader range of temperatures may be used to make low molecular weight polymers. In addition, because k_p , $k_{tr,M}$, etc. values are

monomer dependent, a condition which achieves living polymerization for one monomer may not work for another.

Besides its influence on the rates of propagation and transfer, temperature also influences the position of the propagation equilibrium. At lower temperatures, the equilibrium shifts to the right. Solvent polarity increases and is better able to support charged species at lower temperatures.

In general, more polar solvents lead to higher concentrations of ions and therefore higher apparent rates of polymerization. This condition makes exchange slower than propagation leading to nonliving polymerization. Nonpolar solvents, such as hexane, have the opposite effect. At this extreme, exchange may be so slow that initiation becomes impossible. A careful balance of solvent polarity is often required to achieve the correct balance between exchange and propagation. Several systems in isobutylene polymerization, for example, require mixed solvents to achieve the desired polarity (15).

The nature of the counterion is very important in determining the position of the equilibrium and the exchange rates. Nucleophilic counterions move the equilibrium to the left. Reaction of HCl with isobutylene does not yield polymer, but results in 2-chloro-2-methyl propane (2) which does not ionize. The Cl⁻ ion is highly nucleophilic, shifting the equilibrium to the left. The addition of aluminum trichloride to this example converts the system into one which polymerizes isobutylene (3). The more complex, less nucleophilic



AlCl₄⁻ counterion is formed. The nucleophilicity of the Cl⁻ fragment toward the cation is altered by the strong Lewis acid. The Lewis acid in this example activates the t-butylchloride to provide a cation and complex counterion capable of sustaining polymerization.

The nucleophilicity of the labile ligand (Cl⁻ in the example above) in a Lewis acid - complex counterion is affected by the electrophilicity of the metal and the ligands around the metal. This principle is clearly exemplified for living isobutylene polymerization. Under conditions for which titanium tetrachloride causes the living polymerization of isobutylene, substitution of TiCl₄ with AlCl₃ does not afford the same result. The AlCl₃ mediated polymerization is not living. Conditions have not been found in which AlCl₃ achieves living isobutylene polymerization. The weaker Lewis acid, TiCl₄, is preferred. Thus, the strength of the Lewis acid and its concentration should be adjusted for each particular monomer to establish fast propagation exchange.

The method of initiating carbocationic polymerizations directly influences the propagation equilibrium. This equilibrium can itself be considered an initiation step in which the polymer chain end is the initiator. Thus, a fragment from the initiator becomes a part of or is the entire counterion for the polymerization. For example, styrene polymerizations initiated with perchloric acid are mediated by the ClO₄⁻ counterion. Initiation of isobutylene with 2-chloro-2-methylpropane requires a neutral

Lewis acid, such as titanium tetrachloride, which gives rise to the $Ti_2Cl_9^-$ counterion. One of the Cl^- ligands comes from the initiator. In both cases the initiator played a role in creating the gegenion which participates in the propagation equilibrium. If the counterion produced does not lend itself to a balance between active species in propagation, living polymerization will never be achieved. Consequently, the ability to balance the propagation step is usually determined during initiation.

Two other factors greatly influence the ability to produce a living polymerization: the initiation rate and the number of initiating species. Initiation must be equal to or faster than propagation to ensure that all of the polymer chains start at the same time. The goal here is to quickly enter the propagation equilibrium and establish control of monomer addition. Since the propagation equilibrium can be viewed as an initiation step, making the initiator look as much as possible like the polymer chain end is desirable. In isobutylene polymerization, 2-chloro-2,4,4-trimethylpentane (TMPCl) is a better initiator for living polymerization than 2-chloro-2-methylpropane (4). In essence, an initiator's ability to rapidly begin a polymer chain is dependent on the stability of the carbocation it forms. For living polymerization, the stability of the carbocations from the initiator and the polymer chain end should match as closely as possible.

All growing chains should follow the same rapid propagation equilibrium. This implies that the species involved in this equilibria are the same from chain to chain. One way to insure chain end uniformity is to minimize the different types of initiating species. Multiple initiating species lead to multiple propagation equilibria. Theoretically, control of initiating species should be easy, as they are added purposely into the polymerization system. Unfortunately, adventitious water often functions as an efficient initiator in the presence of Lewis acids. The concentration of water in a typical anhydrous solvent preparation (CaH₂, Na/benzophenone, distillation, etc.) is generally close to 10⁻⁴ mol/L in hydrocarbons and can be much higher in polar solvents (16-18). Given that added initiators are used in concentrations between 10⁻⁴ and 10⁻³ mol/L, adventitious water can be a serious threat to initiation control. Precise determination of water concentration at this level is difficult. In addition, water concentration can vary between different batches of solvent. Complex counterions with OH⁻ ligands generate different propagation equilibria than that from the added organic initiators. Water can also impact the polymerization in other ways, but overall the result is the same: loss of molecular control and loss of living polymerization.

Water based initiation can be prevented by the use of a proton trap or an electron donor such as dimethylphthalate (4). Proton traps, including 2,6-di-tert-butylpyridine, preferentially react with the proton generated by water's reaction with the Lewis acid (15b). Electron donors may also trap a formed proton or may simply complex with water. With more active carbocationic monomers, well defined polymers can be prepared in the presence of water, provided that $[H_2O] < 0.1[I]$ and $[M]_0/[H_2O] \sim 1000$ (19).

Additives can also influence propagation equilibria through alteration of the counterion's nature, reversibly transforming the carbocation into a more stable onium ion, or changing the ionic environment. Electron donors such as esters, amides, and sulfoxides bind directly to the Lewis acid. They are typically used in concentrations lower than the Lewis acid concentration. Thus, two Lewis acid components exist in the polymerization: complexed and uncomplexed. Uncomplexed acid ionizes the chain end. The complexed acid may reversibly deactivate the growing chain or speed collapse of the ion pair. Together, these Lewis acid species permit rapid exchange between dormant and active species bringing about living polymerization.

In polymerizations of more active monomers, nucleophilic donors are used at higher concentrations. Here, the donor transforms the carbocation into an onium ion. For example, isobutyl vinyl ether polymerizations in the presence of sulfides generate sulfonium dormant chain ends (20). In this deactivated state, monomer cannot add to

the polymer chain. The Lewis acid retains enough reactivity to re-ionize the sulfonium to the carbocation where monomer addition can take place.

Addition of salts to a polymerization changes the propagation equilibria by modifying the ionic strength of the solution, suppressing the concentration of free ions by the common salt method or by improving ligand/anion exchange (the "special salt" effect). Salt addition can even influence the nature of the counterion in cases where more than one coordination geometry is available to the metal (8). Such is the case with tin (IV) chloride. Addition of one equivalent of quaternary ammonium chloride (Q^+Cl^-) to $SnCl_4$ creates the $SnCl_5^-$ counterion. To this counterion can be added a second equivalent of Q^+Cl^- to become $SnCl_6^{2-}$ (8). The latter counterion is more nucleophilic and more readily collapses the ion pair to the dormant species. It is preferred for living polymerization.

New Polymers

All of the tools that I have described above may be utilized to bring about the preparation of new polymers. Living systems are now known for vinyl ethers, isobutylene, styrene and its derivatives, as well as N-vinylcarbazole. Polymer structures which are well defined and may even carry functional groups can now be prepared from these monomers. Many structural variations are possible and include end functional, block, graft, star, and hyperbranched polymers. Variations on these themes are possible by incorporating comonomers and tailoring their placement in the polymer. Excellent book chapters and review articles cover the range of structural variations that have been created from these building blocks (1-5). I do not choose to retrace these steps. Instead, I will highlight three areas in which living carbocationic polymerization has permitted the preparation of polymers with unique properties which otherwise would be difficult to obtain.

I. PIB Thermoplastic Elastomers. Polyisobutylene (PIB) based rubbers are commercially important materials. The defining characteristics of PIB, low permeability and low modulus, are instrumental in its utility for tire applications (21). Yet all applications which utilize these properties require vulcanization of the raw rubber. Thermoplastic elastomers (TPE's) offer an alternative way to use rubbery materials. TPE's are well known for their ability to be extruded and shaped like a plastic, but perform like a crosslinked rubber thereafter. Reprocessing of the rubber only requires melting of the thermoplastic phase. An ideal molecular combination for a TPE is an ABA triblock copolymer. The A segment is composed of a thermoplastic such as polystyrene. PIB or another rubbery polymer constitutes the B segment. This concept was realized for PIB in 1987, but the system used could not completely suppress the formation of diblocks and homopolymer. As a result, far from optimal properties were observed. The simplest and most convenient method of block copolymer synthesis is a sequential living polymerization. Discovered in 1984 (23), living isobutylene polymerization was successfully used for triblock synthesis in 1990 (24). Since then, many ABA triblocks based on PIB (B block) have been synthesized and mechanically tested. A list of reported PIB based TPE's and the best realized mechanical properties are shown in Table 1. The references indicated refer to the system which gave the best reported mechanical properties. In addition to PIB's inherent advantages, these polymers are expected to have excellent oxidative and thermal properties because of the saturated rubbery segment.

Other ABA triblock copolymers based on PIB have been synthesized in which the A segment is formed by alternate means of polymerization. Examples of these include polymethyl methacrylate (anionic) (36,37) and polyamides (condensation) (38).

Table 1
ABA Triblock Copolymers with Polyisobutylene (B) Midblocks

End Block Monomer(s)	T _g (°C)	Tensile Strength (MPa)	Elongation at Break (%)	Ref.
styrene	~ 100	23-25	700-800	25
p-methylstyrene	~ 105	22	500	26
p-t-butylstyrene	~ 140	8.7	300	27, 28
p-chlorostyrene	~ 123	21	460	29
α-methylstyrene	~ 175	24	300-400	30
indene	~ 200	20	350	31
acenaphthalene	< 250	15	700-800	32
cyclized isoprene	~ 183	10	1200	33, 34
p-methylstyrene / indene	105 - 200	23	460	35
p-t-butylstyrene / indene	140 - 200	20	400	27

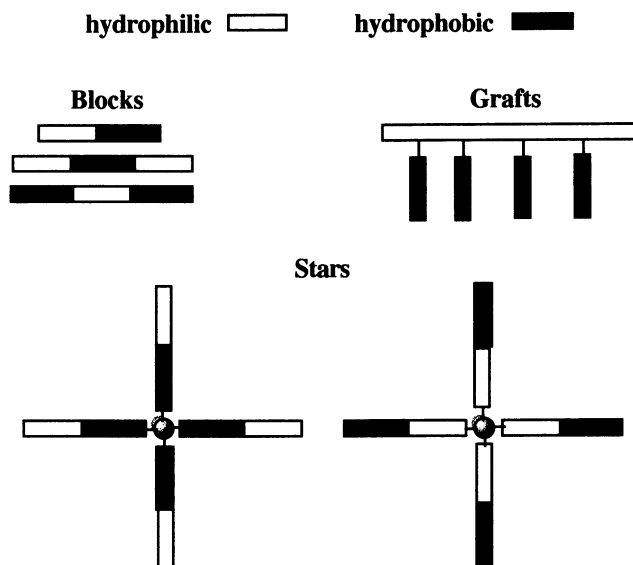
II. Amphiphilic Block Copolymers. These copolymers consist of hydrophobic and hydrophilic segments (1). Because of their dual characteristics, they can be used as surfactants, dispersants, membranes and amphiphilic networks. A considerable amount of attention is given to their biocompatibility. A few have been found to be blood compatible (39).

Again, sequential living polymerization has been vital in the development of these materials. The diagram below depicts the types of architectures that have been used to construct amphiphilic polyvinyl ether block copolymers (40-45). The hydrophobic segments are C₄ or longer polyalkyl vinyl ethers. Hydrophilic segments are functional vinyl ether monomers which are converted after polymerization to water soluble groups like -OH, -NH₂, -NH₃⁺Cl⁻, -COO⁻Na⁺, etc.. The utility of the final amphiphilic copolymer may be tailored by controlling the concentration and type of polar functionality in the polymer. Architectural variations provide an additional means of modifying properties.

Amphiphilic block copolymers have also been prepared from styrenics (46,47) and PIB (39,48-54). One of the PIB systems uses a macromer approach. A three armed methacrylate terminated PIB is radically copolymerized with methacrylate to yield amphiphilic networks. These networks swell in hydrocarbons or water, changing their morphologies relative to the swelling agent. These networks have been found to be blood compatible (39).

III. Hyperbranched Polymers. Three dimensional polymers (i.e., dendrimers) are attractive for applications such as catalysis and drug delivery systems (55, 56). These molecules are regular, well-defined polymers that require multi-step syntheses to

Amphiphilic Block Copolymers of Various Molecular Architecture



guarantee their regularity. The long process of synthesis also limits their availability. Less regular hyperbranched polymers are prepared by polycondensation of AB_2 monomers (57-62). This type of monomer carries two sets of reactive groups that are capable of reacting with each other. An example is an ester (A) diol (2B) that when

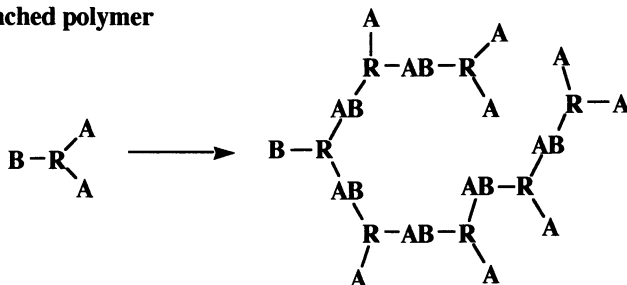
**Illustration of Condensation Polymers Prepared by
AB and AB_2 Type Condensation Monomers**



linear polymer



hyperbranched polymer



Literature Cited

1. *Cationic Polymerizations: Mechanisms, Synthesis and Applications* Matyjaszewski, K. Ed.; Marcel Dekker, Inc.: New York, NY, 1996.
2. Szwarc, M. *Ionic Polymerization Fundamentals*; Hanser: New York, NY 1996.
3. Szwarc, M.; Van Beylen, M. *Ionic Polymerization and Living Polymers*; Chapman & Hall; New York, NY, 1993.
4. Kennedy, J.P.; Ivan, B. *Designed Polymers by Carbocationic Macromolecular Engineering: Theory and Practice*; Hanser: New York, NY 1992.
5. Sawamoto, M.; Kamigaito, M. *New Methods of Polymer Synthesis* Ebdon, J.R.; Eastmond, G., Ed.; Chapman Hall; London, UK, 1995.
6. Sigwalt, P.; Polton, A.; Tardi, M. *J. Macromol. Sci., Pure Appl. Chem.* **1994**, *A31*, 953.
7. Matyjaszewski, K. *J. Macromol. Sci., Pure Appl. Chem.* **1994**, *A31*, 989.
8. Matyjaszewski, K.; Lin, C.-H.; Bon, A.; Xiang, J.S.; *Macromol. Symp.* **1994**, *85*, 65.
9. Matyjaszewski, K. *J. Polym. Sci., Polym. Chem.* **1993**, *31*, 995.
10. Matyjaszewski, K. *Makromol. Chem., Macromol. Symp.* **1992**, *54/55*, 51.
11. Sigwalt, P. *Makromol. Chem., Macromol. Symp.* **1991**, *47*, 179.
12. Mayr, H. in *Cationic Polymerizations: Mechanisms, Synthesis and Applications* Matyjaszewski, K. Ed.; Marcel Dekker, Inc.: New York, NY, 1996, pg.87f.
13. Matyjaszewski, K.; Pugh, C. in *Cationic Polymerizations: Mechanisms, Synthesis and Applications* Matyjaszewski, K. Ed.; Marcel Dekker, Inc.: New York, NY, 1996, pg 207f.
14. Kennedy, J.P.; Marechal, E. *Carbocationic Polymerization*; John Wiley & Sons: New York, NY, 1982.
15. See for example: a). Majoros, I.; Kennedy, J.P.; Kelen, T.; Marsalko, T.M. *Polym. Bull.*, **1993**, *31*, 255. b). Gyor, M.; Wang, H.-C.; Faust, R. *J. Macromol. Sci.*, **1992**, *A29*, 639. c). Shaffer, T.D. US Patent 5,350,819; Sept. 1994.
16. Plesch, P.H. *High Vacuum Techniques for Chemical Synthesis and Measurements*, Cambridge University Press: Cambridge, Great Britain, 1989.
17. Biddulph, R.H.; Plesch, P.H.; Rutherford, P.P. *J. Chem. Soc.* **1965**, 275.
18. Longworth, W.R.; Panton, C.J.; Plesch, P.H. *J. Chem. Soc.* **1965**, 5579.
19. Matyjaszewski, K.; Sawamoto, M. in *Cationic Polymerizations: Mechanisms, Synthesis and Applications* Matyjaszewski, K. Ed.; Marcel Dekker, Inc.: New York, NY, 1996, pg.368f.
20. Cho, C.G.; Feit, B.A.; Webster, O.W. *Macromolecules*, **1990**, *23*, 1918.
21. Kresge, E.N.; Schatz, R.H.; Wang, H.-C. in *Encyclopedia of Polymer Science and Engineering*, John Wiley & Sons: New York, NY, 1987, p. 423 - 448.
22. Fodor, Zs.; Kennedy, J.P.; Kelen, T., Tüdös, F. *J. Macromol. Sci.-Chem.*, **1987**, *A24*, 735.
23. a) Kennedy, J.P.; Faust, R. US Patent Application 746,835; 1985. b). Faust, R.; Kennedy, J.P. *Polym. Bull.*, **1986**, *15*, 317. c) Kennedy, J.P.; Faust, R. Eur. Patent 0206756; 1986.
24. a). Kaszas, G.; Puskas, J.E.; Kennedy, J.P. *J. Appl. Polym. Sci.*, **1990**, *39*, 119. b). Kennedy, J.P.; Puskas, J.E.; Kaszas, G.; Hager, W.G. US Patent 4,946,899; 1990.
25. Gyor, M.; Fodor, Zs.; Wang, H.-C.; Faust, R. *J. Macromol. Sci. Pure Appl. Chem.* **1994**, *A31*, 2055.
26. Fodor, Zs.; Faust, R. *J. Macromol. Sci. Pure Appl. Chem.*, **1995**, *A32*, 575.
27. Puskas, J.E.; Kaszas, G.; Kennedy, J.P.; Hager, W.G. *J. Polym. Sci. Polym. Chem.* **1992**, *30*, 41.
28. Kennedy, J.P.; Meguriya, N.; Keszler, B. *Macromolecules* **1991**, *24*, 6572.
29. Kennedy, J.P.; Kurian, J. *J. Polym. Sci. Polym. Chem.* **1990**, *28*, 3725.
30. Li, D.; Faust, R. *Macromolecules* **1995**, *28*, 4893.

31. Kennedy, J.P.; Midha, S.; Tsunogae, Y. *Macromolecules* **1993**, *26*, 429.
32. Fodor, Zs.; Kennedy, J.P. *Polym. Bull.* **1992**, *29*, 697.
33. Kaszas, G.; Puskas, J.E.; Kennedy, J.P. *J. Appl. Polym. Sci.* **1990**, *39*, 119.
34. Puskas, G.; Kaszas, J.E.; Kennedy, J.P. *J. Macromol. Sci. Chem.* **1991**, *A28*, 65.
35. Tsunogae, Y.; Kennedy, J.P. *J. Macromol. Sci., Pure Appl. Chem.* **1993**, *A30*, 269.
36. Kennedy, J.P.; Price, J.L. *Polym. Mater. Sci. Eng.* **1991**, *64*, 40.
37. Gyor, M.; Kitayama, T.; Fujimoto, N.; Nishiura, T.; Hatada, K. *Polym. Bull.* **1994**, *32*, 155.
38. Zaszke, B.; Kennedy, J.P. *Macromolecules* **1995**, *28*, 4426.
39. Chen, D.; Kennedy, J.P.; Kory, M.M., Ely, D.L. *J. Biomed. Mater. Res.* **1989**, *23*, 1327.
40. Kanaoka, S.; Sawamoto, M.; Higashimura, T. *Makromol. Chem.* **1993**, *194*, 2305.
41. Kanaoka, S.; Omura, T.; Sawamoto, M.; Higashimura, T. *Macromolecules* **1992**, *25*, 6407.
42. Kanaoka, S.; Sawamoto, M.; Higashimura, T. *Macromolecules* **1991**, *24*, 5741.
43. Kanaoka, S.; Sawamoto, M.; Higashimura, T. *Macromolecules* **1991**, *23*, 2309.
44. Minoda, M.; Sawamoto, M.; Higashimura, T. *Macromolecules* **1991**, *24*, 1897.
45. Minoda, M.; Sawamoto, M.; Higashimura, T. *Macromolecules* **1987**, *20*, 2045.
46. Kanaoka, S.; Minoda, M.; Sawamoto, M.; Higashimura, T. *J. Polym. Sci. Polym. Chem. Ed.* **1990**, *28*, 1127.
47. Kojima, K.; Sawamoto, M.; Higashimura, T. *Polym. Bull.* **1990**, *23*, 149.
48. Keszler, B.; *Polymer Bull.* **1992**, *29*, 681.
49. Keszler, B.; Kennedy, J.P.; Mackey, P.W. *J. Controlled Release* **1993**, *25*, 115.
50. Keszler, B.; Kennedy, J.P. *J. Polym. Sci. Polym. Chem.* **1994**, *32*, 3153.
51. Blezer, R.; Lindhout, T.; Keszler, B.; Kennedy, J.P. *Polym. Bull.* **1995**, *34*, 101.
52. Park, D.; Keszler, B.; Galiatsatos, V.; Kennedy, J.P. *Macromolecules* **1995**, *28*, 2595.
53. Pernecker, T.; Kennedy, J.P.; Ivan, B. *Macromolecules* **1992**, *25*, 1642.
54. Hadjikyriacou, S.; Faust, R. *Macromolecules* **1996**, *29*, 5261.
55. Tomalia, D.A.; Durst, H.D. *Top. Curr. Chem.* **1993**, *165*, 193.
56. Newkome, G.R. *Advances in Dendritic Macromolecules*; JAI: Greenwich, CT, 1993; Vol. 1, p 1.
57. Hawker, C.J.; Chu, F.; Pomery, P.J.; Hill, D.J.T. *Macromolecules* **1996**, *29*, 3831.
58. Hawker, C.J.; Frechet, J.M.; Grubbs, R.B.; Dao, J. *J. Am. Chem. Soc.* **1995**, *117*, 10763.
59. Kricheldorf, H.R.; Stober, O.; Lubbers, D. *Macromolecules* **1995**, *28*, 2118.
60. Turner, S.R.; Walter, F.; Voit, B.I.; Mourey, T.H. *Macromolecules* **1994**, *27*, 1611.
61. Kricheldorf, H.R.; Stober, O. *Macromol. Rapid Commun.* **1994**, *15*, 87.
62. Percec, V.; Chu, P.; Kawsumi, M. *Macromolecules* **1994**, *27*, 4441.
63. Frechet, J.M.; Henmi, M.; Gitsov, I.; Aoshima, S.; Leduc, M.R.; Grubbs, R.B. *Science* **1995**, *269*, 1080.
64. see for example:
 - a). Rodriguez-Parada, J.E.; Percec, V. *J. Polym. Sci., Polym. Chem. Ed.* **1986**, *24*, 1363.
 - b). Sagane, T.; Lenz, R.W. *Polymer* **1989**, *30*, 2269.
 - c). Heroguez, V.; Deffieux, A.; Fontanille, M. *Makromol. Chem. Macromol. Symp.* **1990** *A31*, 937.
 - d). Percec, V. Zheng, Q. *Polym. Bull.* **1992**, *29*, 501.

65. see for example:

- a). Shohi, H.; Sawamoto, M.; Higashimura, T. *Macromolecules* **1992**, *25*, 58.
- b). Si, J.; Kennedy, J.P. *J. Macromol. Sci. Pure Appl. Chem.* **1993**, *A30*, 863.
- c). Hashimoto, T.; Suemoto, A.; Okano, K.; Kodaira, T. *J. Polym. Sci. Polym., Chem. Ed.* **1995**, *33*, 1921.
- d). Li, D.; Faust, R. *Macromolecules* **1995**, *28*, 4893.

66. see for example:

- a). Ivan, B. Kennedy, J.P. *J. Polym. Sci. Polym. Chem. Ed.* **1990**, *28*, 89.
- b). Aoshima, S.; Ebara, K.; Higashimura, T. *Polym. Bull.* **1985**, *14*, 425.
- c). Schappacher, M.; Deffieux, A. *Makromol. Chem. Rapid Commun.* **1991**, *12*, 447.
- d). Nemes, S. Pernecker, T.; Kennedy, J.P. *Polym. Bull.* **1991**, *25*, 633.

67. a). Schappacher, M.; Deffieux, A. *Macromolecules* **1992**, *25*, 6744.

- b). Deffieux, A.; Schappacher, M.; Rique-Lurbet, L. *Polymer* **1994**, *35*, 4562.

Chapter 2

Comparison of Controlled Living Carbocationic and Radical Polymerizations

Krzysztof Matyjaszewski

Department of Chemistry, Carnegie Mellon University, 4400 Fifth Avenue,
Pittsburgh, PA 15213-2683

New controlled/"living" carbocationic and radical polymerizations are compared from the point of view of basic mechanisms including spontaneous and catalyzed equilibration between dormant covalent species and growing species, equilibration between onium ions / carbenium ions and persistent radicals / growing radicals, as well as the corresponding degenerative transfer reactions. Similarities and peculiarities of carbocationic and radical systems are reviewed. Fundamental requirements for the synthesis of controlled polymers such as quantitative initiation, fast exchange and low contribution of chain breaking reactions are discussed.

For a long time, carbocationic and radical polymerizations have been considered to be very difficult, if not impossible, to control at the level attainable for anionic polymerization of styrene and dienes. Polymers with unpredictable molecular weights, broad polydispersities and uncontrolled end-functionalities are usually obtained in both systems. Different reasons, related to the very fundamental nature of carbocations and radicals, are responsible for such behavior. Carbocations react extremely rapidly with alkenes ($k_p \approx 10^5 \pm 1 \text{ mol}^{-1} \cdot \text{L} \cdot \text{s}^{-1}$) and readily participate in transfer reactions by loss of β -protons, especially in the presence of basic impurities (1,2). On the other hand, radicals recombine and disproportionate with rates close to the diffusion controlled limits (3). Thus, in typical carbocationic and radical polymerizations, the concentration of growing species (carbocations or radicals) must be very low ($< 10^{-7} \text{ mol/L}$), otherwise cationic polymerization would proceed too rapidly and/or radicals would recom-

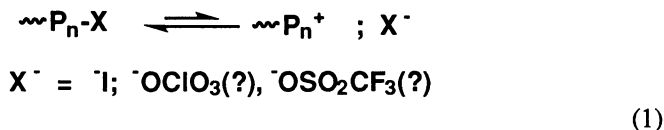
bine too quickly. However, the molecular weight of resulting polymers would be too high and most likely limited by transfer if the concentration of polymer chains is so low ($<10^{-7}$ mol/L). The proportion of chains marked by transfer and/or termination increases with increasing molecular weight, therefore the control of molecular weights, polydispersities and functionalities is satisfactory only for relatively short chains ($M_n \leq 100,000$). To prepare these polymers while maintaining a low concentration of active species, it is necessary to establish a dynamic equilibrium between growing species and dormant species. Some approaches toward the controlled/"living" carbocationic and radical polymerizations based on the concept of reversible activation of dormant species are discussed.

Exchange Reactions

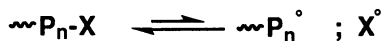
There are three types of reactions in which reactive carbocations and radicals can be formed reversibly from dormant species: spontaneous and catalyzed equilibration between dormant covalent species and growing species, equilibration between onium ions / carbenium ions and persistent radicals / growing radicals, as well as the corresponding degenerative transfer reactions. Similarities and peculiarities of carbocationic and radical systems are reviewed in respect to these three approaches.

1.1 Spontaneous equilibration between covalent species and growing species:

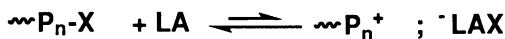
A. Carbocations:



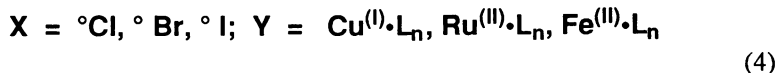
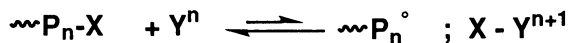
It is not certain how many of these systems actually ionize spontaneously and how many are formed via elimination of the corresponding protonic acid, which subsequently catalyzes the equilibration process (1.2.A), but it seems that polymerization of vinyl ethers with iodide counterions proceeds in a spontaneous way (4), while polymerization of styrenes with perchlorate and triflate anions is probably catalyzed by protonic acid (5). Additional complications are related to the dissociation of ion pairs to free ions. In some systems it is necessary to add salts with common ions to suppress free ion formation in order to control the polymerization.

B. Radicals:

This type of equilibration is probably the simplest and most common, (6-12) where weak covalent bonds are homolytically cleaved using sufficiently high temperatures. A key factor for control here is that the counter-radical, X^\bullet , should not initiate polymerization. This is not the case for dithiocarbamates and some diaryl organic counter-radicals, but the role of the counter-radical may also be played by an organometallic species with an odd number of electrons such as Co^{II} . (13,14) It is not yet clear if the counter-radicals remain in the cage or they diffuse freely to the reaction solution. However, counter-radicals X^\bullet , are present in a very large excess over growing radicals ($[\text{P}^\circ] < 10^{-3}[\text{X}^\circ]$) (15-17). This, so called persistent radical effect (18), is responsible for the reduced proportion of terminated chains.

1. 2. Catalyzed equilibration between covalent species and growing species:**A. Carbocations:**

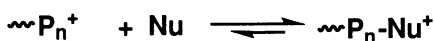
This is certainly the most important class of controlled carbocationic polymerizations (5,19,20). The strength of the Lewis acid must be adjusted for the stability of the corresponding carbocations, and, ideally, ligand X at the chain end and the Lewis acid ligand should be the same. If this is not the case, ligand exchange may occur as in, for example, polymerization of styrene and isobutene initiated by acetates and catalyzed by BCl_3 , leading to chloro-terminated dormant chain ends (21). Protonic acids as well as Lewis acids may be used to catalyze this process.

B. Radicals:

This is the most recent method for controlling radical polymerizations.(15,22-24) The methodology of these atom transfer radical polymerizations (ATRP) is based on catalyzed atom transfer radical reactions (25,26). The main advantage of this system over 1.1.B is that the equilibrium position can easily be adjusted by varying the catalyst concentration, which participates in the redox process by changing from a lower to a higher oxidation state with the simultaneous transfer of ligand X from the dormant chain. Radicals rapidly abstract the ligand back from the X-Y species assuring their low stationary concentration ($\approx 10^{-7} \pm 1$ mol/L).

2. Equilibration between onium ions/carbenium ions and persistent radicals/growing radicals:

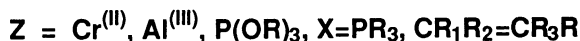
A. Carbocations:



(5)

Carbocations react with non-charged nucleophiles to form onium ions (27-29). The equilibrium position depends on the concentration and strength of the nucleophile and also on the stability of the carbocation. Esters, ethers, and sulfides work efficiently in vinyl ether polymerization, however they seem to be too strongly nucleophilic for the polymerization of styrene and isobutene. In the latter two cases, controlled polymerization can be obtained if a small amount of the nucleophile is added to systems like 1.2.A, in which a complex of the nucleophile and Lewis acid probably forms, having a lower nucleophilicity than the original nucleophile. This may be the case with polymerization in the presence of DMSO, DMF and other two-centered nucleophiles.

B. Radicals:

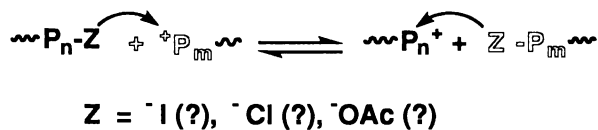


(6)

This is a relatively rare case but possible with metals and organometallic compounds having an even number of electrons such as Cr(II) (30,31) and aluminum and also with non-metallic boron and phosphorous derivatives (32,33) and potentially with non-polymerizable and non-copolymerizable kinetically reactive alkenes.

3. Degenerative transfer:

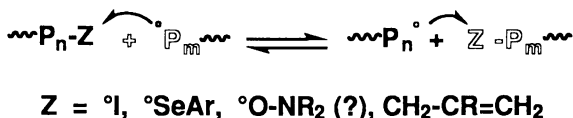
A. Carbocations:



(7)

This system had originally been presented as the first living carbocationic process based on so called inifer process (34,35) in which cumyl chlorides were thought to act as initiators in the polymerization of isobutene catalyzed by BCl_3 , however some later model studies (36) indicate that it is probably the reversible deactivation of carbocations (system 1.2.A) operating in this system rather than 3.A. Nevertheless, a degenerative transfer process may contribute to reducing polydispersities in some carbocationic reactions, for example, vinyl ethers (37).

B. Radicals:



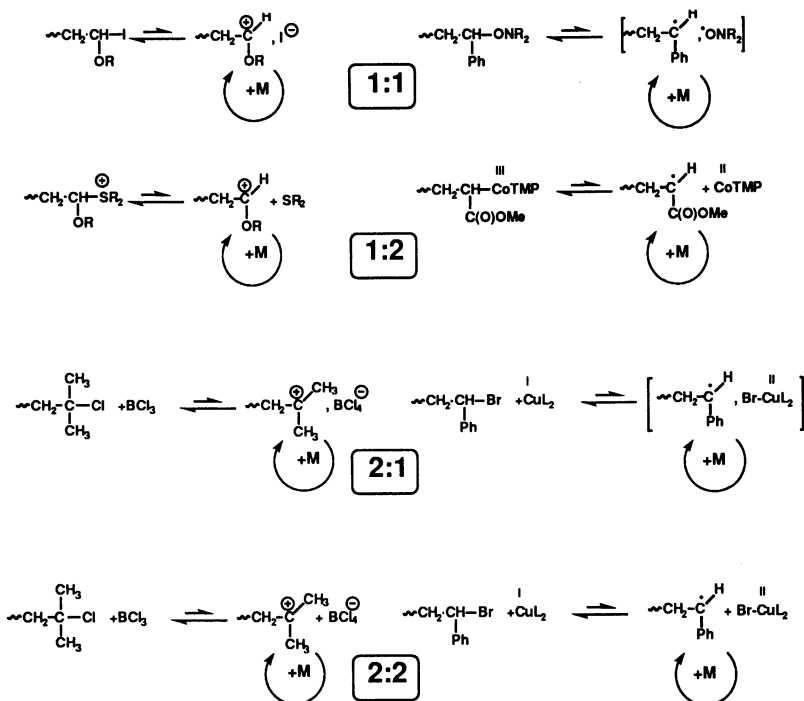
(8)

A degenerative process seems to operate in the polymerization of acrylates and styrenes with iodo- terminated chains (38). Alkyl iodides do not initiate polymerization, but in the presence of conventional radical initiators such as 2,2'-azobisisobutyronitrile (AIBN) or benzoyl peroxide (BPO), they do control molecular weights. Alkyl bromides and chlorides seem to be inactive in this respect, but there is information on the successful use of organoselenium compounds in organic synthesis (39). It is also possible that some nitroxide mediated polymerizations include a degenerative transfer process. Similar reactions may occur in anionic-like reactions, as in, for example, group transfer polymerization, GTP (40). A very special case of degenerative transfer process, is so called addition-fragmentation polymerization mechanism which involves the unsaturated poly(methyl methacrylate) oligomers (41). By definition, the equilibrium constant in such a process is $K=1$.

Formal Stoichiometry of Exchange Reactions

The carbocationic and radical reactions may also be compared from the point of view of the formal stoichiometry of the reactions between dormant and active species. The possibility of 1:1, 1:2, 2:1 and 2:2 systems are shown in eq. (9). Typically, 1:1 systems involve active species in the form of a carbocation

pair or a cage structure for a radical system, although the contribution of the latter may be very small. A 1:2 system is exemplified by the existence of an equilibrium between the onium ion and carbocation where the dissociation state of ionic species is irrelevant; in a radical system some organometallic (cobaltoxime) or alkoxyamine dissociates to form the growing radical and a counter radical.



(9)

A 2:1 system for carbocations operates in non polar solvents when the proportion of free ions is negligible; such a system may also exist in atom transfer polymerization if the growing species is predominantly in the cage structure. The last, a 2:2 system, occurs in polar media for cationic polymerization and usually leads to poor control; on the other hand, 2:2 systems are the best examples of controlled radical polymerization. However, it must be stressed that the discussed system can only be considered in terms of formal stoichiometry and do not reflect real ratios of the species involved in the corresponding equilibria. For example, in cationic systems, traces of nucleophilic impurities (e.g. moisture) will form onium ions and produce an excess of counterion, creating a "spontaneous" common ion effect (2). In radical systems, growing radicals terminate, producing an excess (10^3 to 10^5 fold) of scavenging counter-radical. This persistent radical effect (18) is in fact the most

typical and beneficial phenomenon, provided that proportion of terminated chains does not exceed 1-5%.

Requirements for the controlled polymerization

The position of the equilibrium between dormant and active species defines the overall concentration of propagating species and therefore the overall propagation rate, but preparation of well defined polymers using the controlled system requires fulfillment of some additional criteria.

I. Ratio of rates of deactivation and propagation.

The most important parameter in controlling molecular weights and polydispersities in systems with equilibria between dormant and active species is the relative rate of deactivation versus propagation. With the increasing number of monomer molecules added during each activation period, polydispersities increase and control is lost.

In most systems with slow exchange, polydispersities decrease with increasing molecular weight and conversion (42-44). This is in contrast to transfer/termination dominated systems. At complete conversion in slow exchange systems, when dormant species are present in large excess, initiation is complete and only one type of growing species is active (42).

$$M_w/M_n = 1 + ([I]_0 k_p) / (k_{dact}[D]) \quad (10)$$

Thus, if the initiator concentration ($[I]_0$) is reduced, longer chains are formed, more exchange reactions occur during polymerization, and more chains have the same probability of growth, leading to lower polydispersities. If the concentration of deactivator ($[D]$) increases, the lifetime of the growing species during each activation period is reduced as are polydispersities. Eventually, the ratio of the rate constant of propagation to the rate constant of deactivation (k_p/k_{dact}) becomes the most important factor. For rapidly propagating systems fast deactivation is necessary. Here, catalytic systems are very helpful because spontaneous homolytic and/or heterolytic cleavage may produce too low a concentration of deactivator. It must be remembered that the rate of propagation is reduced with conversion, whereas the rate of deactivation usually stays constant, which is an additional reason for the reduction of polydispersities with conversion. Polydispersity may be also defined as the ratio of the number of monomer units which are incorporated at the single activation period (λ) to the final polymerization degree (DP_n) (42):

$$M_w/M_n = 1 + \lambda/DP_n \quad (11)$$

II. Effect of temperature and contribution of chain breaking reactions

The above considerations were based on ideal systems in which no side reactions are involved. In carbocationic systems transfer is the most important chain breaking reaction. Because elimination of β -protons (transfer) proceeds with a higher activation energy than electrophilic addition of carbocations to alkenes (propagation), synthesis of high molecular weight polymers requires sufficiently low temperatures. Thus, high molecular weight ($M_n \gg 100,000$) polyisobutene is prepared at temperatures below -80°C (19).

On the other hand, the most difficult chain breaking reaction to control in radical systems is termination. Termination is diffusion controlled and has a much lower activation energy than propagation. Thus, in many cases higher temperature may lead to better controlled radical polymerization (45). Nevertheless, there is a temperature limit because above a certain temperature, transfer may become significant and limit molecular weights. Therefore, the temperature range used must be optimal for controlled radical polymerization. This range will depend on particular monomer and initiating system, but also on the particular molecular weight of the targeted polymer. Higher molecular weights will require reduced temperatures, which in turn requires an additional shift toward the dormant species to suppress bimolecular termination.

III. Initiation

Synthesis of polymers with degrees of polymerization predetermined by the ratio of concentrations of reacted monomer to the introduced initiator requires quantitative initiation. In systems with equilibria between active and dormant species it is necessary to assure that the apparent rate constants of initiation is at least comparable to the apparent rate constant of propagation, $k_i^{\text{app}} \geq k_p^{\text{app}}$. ($k_i^{\text{app}} = k_i K_O$, where k_i and K_O refer to the absolute rate constant of addition of the initiating radical to the alkene and the equilibrium constant for the initiating species, respectively; in the same way the apparent propagation rate constant is defined, $k_p^{\text{app}} = k_p K_{\text{eq}}$). If $k_i^{\text{app}} \ll k_p^{\text{app}}$, initiation is incomplete, molecular weights are higher than expected and polydispersities are high.

There is a multitude of initiators for ATRP. Any alkyl halide with activated substituents on an α -carbon such as an aryl, carbonyl, or allyl can be used, in addition to polyhalogenated compounds (CCl_4 , HCCl_3) and those with a weak X bonding such as N-X, S-X, O-X, etc. This includes not only low molar mass compounds but macromolecular species as well, used to form the corresponding block/graft copolymers.

Group X must rapidly and selectively migrate between the growing chain and transition metal. Bromine and chlorine function best in this exchange. Fluorine is bound too strongly to the growing chain, and although iodine is a

good leaving group for acrylate polymerizations, it is involved in side reactions in styrene polymerization (heterolytic cleavage). Some pseudohalogens, thiocyanates for example, have also been used successfully for the polymerization of acrylates and styrenes.

IV. Other effects

There are a few additional requirements for controlled radical and carbocationic polymerizations. The latter, as with any ionic process, must be carried out in the absence of moisture. Water may act not only as the transfer/termination agent but also as a coinitiator, especially when a large excess of Lewis acid is used. Protons generated under such conditions may be scavenged with proton traps such as hindered pyridines, however the resulting pyridinium ions may produce various salt effects which in turn affect polymerization.

In radical processes, moisture is well tolerated and many of them are in fact carried out in aqueous media. On the other hand, compounds with mobile groups/atoms can act as transfer agents and should be avoided. Oxygen, which may not affect carbocationic processes, is a dreadful inhibitor to the radical reaction and must be carefully removed from all reaction mixtures.

If the ion pairs described in systems 1.1.A and 1.2.A dissociate to free ions it may be necessary to trap them using salts with common ions or reduce their concentration by using less polar solvents. It is not yet clear what the proportion of free radicals to caged radicals is in new controlled systems but the addition of an extra scavenger is very beneficial for such systems, indicating the presence of some free radicals.

Conclusions

The above discussion demonstrates similarities between new controlled/"living" carbocationic and radical systems. Below, in Tables 1 and 2, a comparison between conventional and the new controlled cationic and radical systems is presented. Although conventional processes show many similarities to the new systems, there are significant differences between the conventional and controlled systems.

Most conventional carbocationic systems polymerize faster than radical systems due to higher propagation rate constants and higher concentration of active sites. Initiation is relatively much slower than propagation for both systems which are very sensitive to either oxygen (radical) or moisture

(cationic). The main differences are related to reaction temperatures, chain breaking reaction and monomers polymerizable via certain mechanism.

Table 1
Comparison of Carbocationic & Radical Polymerization
I. Conventional Systems

Mechanism	Cationic	Radical
Propagation	$k_p^+ \approx 10^{5 \pm 1} \text{ mol}^{-1} \cdot \text{L} \cdot \text{s}^{-1}$	$k_p \cdot \approx 10^{3 \pm 1} \text{ mol}^{-1} \cdot \text{L} \cdot \text{s}^{-1}$
R_i/R_p	$\approx 10^{-3}$	$\approx 10^{-3}$
$[P^*]$	$\approx 10^{-6 \pm 2} \text{ mol/L}$	$\approx 10^{-7 \pm 1} \text{ mol/L}$
Main Chain Breaking	Transfer	Termination
T	low (e.g. $< -100 \text{ }^\circ\text{C}$)	$80 \pm 20 \text{ }^\circ\text{C}$
$\text{O}_2; \text{H}_2\text{O}$	OK (?); $< 10 \text{ ppm}$	$< 10 \text{ ppm (N}_2)$; OK
Monomers	only IB, VE, ST, NVC	nearly all alkenes

General features of conventional systems include:

- broad molecular weight distribution
- uncontrolled molecular weights
- uncontrolled end-functionalities
- no control of topologies
- random copolymers only by radical process, no block copolymers

There are smaller differences between the corresponding controlled/"living" systems. Overall rates are similar, concentration of active sites are also similar, rates of initiation are close to those of propagation, degrees of polymerization are limited to minimize the effect of side, and the effect of impurities is also smaller.

Table 2
Comparison of Carbocationic & Radical Polymerization
II. Controlled/"Living" Systems

Mechanism	Cationic	Radical
$k_p^{\text{app}} = k_p^+ [P^*]$	$k_p^{\text{app}} \approx 10^{-3 \pm 1} \text{ s}^{-1}$	$k_p^{\text{app}} \approx 10^{-4 \pm 1} \text{ s}^{-1}$
R_i/R_p	≈ 1	≈ 1
$[P^*]/[I]_0$	$\approx 10^{-6 \pm 1}$	$\approx 10^{-6 \pm 1}$
DP_n	$< 0.1 R_p/R_{tr}$	$< 0.1 R_p/R_t$
T	low (e.g. $< -30 \text{ }^\circ\text{C}$)	$80 \pm 20 \text{ }^\circ\text{C}$
$\text{O}_2; \text{H}_2\text{O}$	OK (?); $\approx 100 \text{ ppm}$	$\approx 100 \text{ ppm (N}_2)$; OK
Monomers	only IB, VE, ST, NVC	nearly all alkenes

General features of the new controlled systems include:

- narrow molecular weight distribution ($M_w/M_n \approx 1.1 - 1.5$)
- controlled molecular weights ($M_n \approx 1,000 - 100,000$) predetermined by $\Delta[M]/[I]_0$ ratio
- end-functionalities by termination (side functionalities are usually found only in cationic polymerization of vinyl ethers, radical polymerization is much more tolerant)
- efficient copolymerization (block copolymers by both cationic and radical process; random and gradient copolymers only by radical process)
- new topologies and architectures (stars, combs, hyperbranched)

The three basic methods of establishing equilibria between dormant species and growing carbocations/radicals are nearly identical in the controlled systems. They include spontaneous (or catalytic) homolytic/heterolytic cleavage of covalent bonds in dormant species, formation of stable (persistent) cations (onium ions) and radicals, and the degenerative transfer process. Control of the position of the equilibrium is important but controlling the dynamics of the exchange reactions is of utmost importance in order to prepare well defined polymers in both the carbocationic and radical controlled polymerization systems.

Acknowledgments.

Support from the Petroleum Research Fund administered by the American Chemical Society, the Office of Naval Research, and industrial sponsors of Atom Transfer Radical Polymerization Consortium at Carnegie Mellon University is acknowledged.

Literature Cited:

- (1) Matyjaszewski, K. *Makromol. Chem., Macromol. Symp.* **1992**, 54/55, 51.
- (2) Matyjaszewski, K. *Cationic Polymerizations: Mechanisms, Synthesis and Applications*; Marcel Dekker: New York, 1996.
- (3) Eastmond, G. C. in *Comprehensive Chemical Kinetics*, C. H. Bamford and C. F. H. Tipper, Eds.; Elsevier: New York, 1976; Vol. 14A.
- (4) Cramail, H.; Deffieux, A. *Macromol. Chem. Phys.* **1994**, 195, 217.
- (5) Matyjaszewski, K.; Sigwalt, P. *Polymer Int.* **1994**, 35, 1.
- (6) Borsig, E.; Lazar, M.; Capla, M.; Florian, S. *Angew. Makromol. Chem.* **1969**, 9, 89.
- (7) Otsu, T.; Yoshida, M. *Makromol. Chem., Rapid Commun.* **1982**, 3, 133.

- (8) Solomon, D. H.; Rizzardo, E.; Cacioli, P. U. S. Pat. 4, 581, 429, **1986**
- (9) Bledzki, A.; Braun, D. *Makromol. Chem.* **1983**, *184*, 745.
- (10) Georges, M. K.; Veregin, R. P. N.; Kazmaier, P. M.; Hamer, G. K. *Macromolecules* **1993**, *26*, 2987.
- (11) Mardare, D.; Shigemoto, T.; Matyjaszewski, K. *ACS Polymer Preprints* **1994**, *35(2)*, 557.
- (12) Gaynor, S.; Greszta, D.; Mardare, D.; Teodorescu, M.; Matyjaszewski, K. *J. Macromol. Sci., Pure Appl. Chem.* **1994**, *A31*, 1561.
- (13) Harwood, H. J.; Arvanitopoulos, L. D.; Greuel, M. P. *ACS Polymer Preprints* **1994**, *35(2)*, 549.
- (14) Wayland, B. B.; Pszmik, G.; Mukerjee, S. L.; Fryd, M. *J. Am. Chem. Soc.* **1994**, *116*, 7943.
- (15) Patten, T. E.; Xia, J.; Abernathy, T.; Matyjaszewski, K. *Science* **1996**, *272*, 866.
- (16) Greszta, D.; Matyjaszewski, K. *Macromolecules* **1996**, *29*, 7661.
- (17) Fukuda, T.; Terauchi, T.; Goto, A.; Ohno, K.; Tsujii, Y.; Miyamoto, T.; Kobatake, S.; Yamada, B. *Macromolecules* **1996**, *29*, 6393.
- (18) Fisher, H. *J. Am. Chem. Soc.* **1986**, *108*, 3925.
- (19) Kennedy, J. P.; Ivan, B. *Designed Polymers by Carbocationic Macromolecular Engineering. Theory and Practice*; Hanser: Munich, 1992.
- (20) Sawamoto, M.; Higashimura, T. *Makromol. Chem., Macromol. Symp.* **1990**, *32*, 131.
- (21) Matyjaszewski, K.; Lin, C.-H. *J. Polym. Sci., Part A, Polym. Chem.* **1991**, *29*, 1439.
- (22) Wang, J. S.; Matyjaszewski, K. *J. Am. Chem. Soc.* **1995**, *117*, 5614.
- (23) Kato, M.; Kamigaito, M.; Sawamoto, M.; Higashimura, T. *Macromolecules* **1995**, *28*, 1721.
- (24) Percec, V.; Barboiu, B. *Macromolecules* **1995**, *28*, 7970.
- (25) Bellus, D. *Pure & Appl. Chem.* **1985**, *57*, 1827.
- (26) Curran, D. P. in *Comprehensive Organic Synthesis*; Pergamon: Oxford, 1991; Vol. 4, pp 715.
- (27) Cho, C. G.; Feit, B. A.; Webster, O. W. *Macromolecules* **1990**, *23*, 1918.
- (28) Lin, C.-H.; Matyjaszewski, K. *ACS Polymer Preprints* **1990**, *31(1)*, 599.
- (29) Higashimura, T.; Aoshima, S.; Sawamoto, M. *Makromol. Chem., Macromol. Symp.* **1988**, *13/14*, 457.
- (30) Gaynor, S.; Mardare, D.; Matyjaszewski, K. *ACS Polymer Preprints* **1994**, *36(1)*, 700.
- (31) Espenson, J. H. *Acc. Chem. Res.* **1992**, *25*, 222.
- (32) Greszta, D.; D. Mardare; Matyjaszewski, K. *ACS Polym. Preprints* **1994**, *35(1)*, 466.

- (33) Mardare, D.; Gaynor, S.; Matyjaszewski, K. *ACS Polym. Preprints* **1994**, *35(1)*, 700.
- (34) Kennedy, J. P.; Smith, R. A. *J. Polym. Sci., Polym. Chem. Ed.* **1980**, *18*, 1539.
- (35) Kennedy, J. P.; Marechal, E. *Carbocationic Polymerization*; Wiley Interscience: New York, 1982.
- (36) Mayr, H.; Schade, C. *Makromol. Chem., Rapid Commun.* **1988**, *9*, 483.
- (37) Cramail, H.; Deffieux, A. *Macromolecules* **1994**, *27*, 1401.
- (38) Matyjaszewski, K.; Gaynor, S.; Wang, J. S. *Macromolecules* **1995**, *28*, 2093.
- (39) Curran, D. P.; Eichenberger, E.; Collis, M.; Roepel, M. G.; Thoma, G. J. *Am. Chem. Soc.* **1994**, *116*, 4279.
- (40) Mueller, A. H. E.; Zhuang, R.; Yan, D.; Litvinienko, G. *Macromolecules* **1995**, *28*, 4326.
- (41) Moad, C. L.; Moad, G.; Rizzardo, E.; Tang, S. H. *Macromolecules* **1996**, *29*, 7717.
- (42) Matyjaszewski, K.; Lin, C.-H. *Makromol. Chem. Macromol. Symp.* **1991**, *47*, 221.
- (43) Puskas, J. E.; Kaszas, G.; Litt, M. *Macromolecules* **1991**, *24*, 5278.
- (44) Kunkel, D.; Mueller, A. H. E.; Janata, M.; Lochman, L. *Makromol. Chem., Macromol. Symp.* **1992**, *60*, 315.
- (45) Greszta, D.; Mardare, D.; Matyjaszewski, K. *Macromolecules* **1994**, *27*, 638.

Kinetics of Carbocationic Polymerizations: Initiation, Propagation, and Transfer Steps

Herbert Mayr, Michael Roth, and Gabriele Lang

Institut für Organische Chemie der Ludwig-Maximilians-Universität,
Karlstrasse 23, D-80333 München, Germany

In extension of earlier work on the initiation of carbocationic polymerization and the systematic selection of comonomers which is shortly summarized, we describe model studies on the propagation step of carbocationic polymerization of isobutylene **2a** and the importance of hydride transfer processes. The 2,4,4-trimethyl-2-pentyl cation **1**⁺ reacts five times faster with trimethyl(2-methylallyl)silane **2b** than with isobutylene **2a** as derived from competition experiments. This reactivity ratio is combined with the diffusion controlled rate constant for the reaction of **1**⁺ with **2b** ($3 \times 10^9 \text{ L mol}^{-1} \text{ s}^{-1}$) to yield a rate constant of $k = 6 \times 10^8 \text{ L mol}^{-1} \text{ s}^{-1}$ for the reaction of the tertiary alkyl cation **1**⁺ with isobutylene **2a**. Rate constants for the abstractions of hydride from hydrocarbons by benzhydryl cations **8**⁺ have been determined and compared with the rate constants for the addition of benzhydryl cations **8**⁺ to CC-double bonds. It is found that in the case of 1,1-dialkyl and higher alkylated ethylenes the attack of carbocations at the CC-double bond is generally preferred. In the case of mono- and 1,2-dialkyl-substituted ethylenes, however, electrophilic attack at the double bond and hydride abstraction have comparable activation energies.

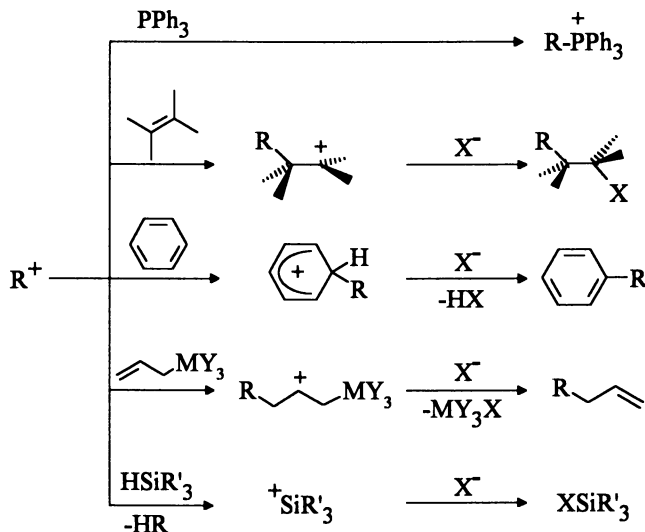
During the past decade we have systematically investigated the kinetics of the reactions of carbocations with uncharged nucleophiles, e.g., alkenes (1), arenes (2), allylsilanes and -stannanes (3), and hydride donors (4,5). When properly selecting the reaction conditions (6), all these reactions – even those with alkenes – terminate after the reaction of the carbocation with one molecule of the nucleophile, and the 1:1-products depicted in Scheme 1 can be isolated in high yield. In all cases discussed in this report the reaction of the carbocation with the nucleophile, i.e., the first steps of the sequences depicted in Scheme 1 have been proven or by analogy assumed to be rate-determining.

NOTE: Dedicated to Professor George A. Olah, the father of modern carbocation chemistry, on the occasion of his 70th birthday.

© 1997 American Chemical Society

25

Since charge is neither "destroyed" nor "created" during the reaction of a carbocation with a neutral nucleophile, it is understandable that the rates of all these reactions show only very little dependence on solvent polarity (7).



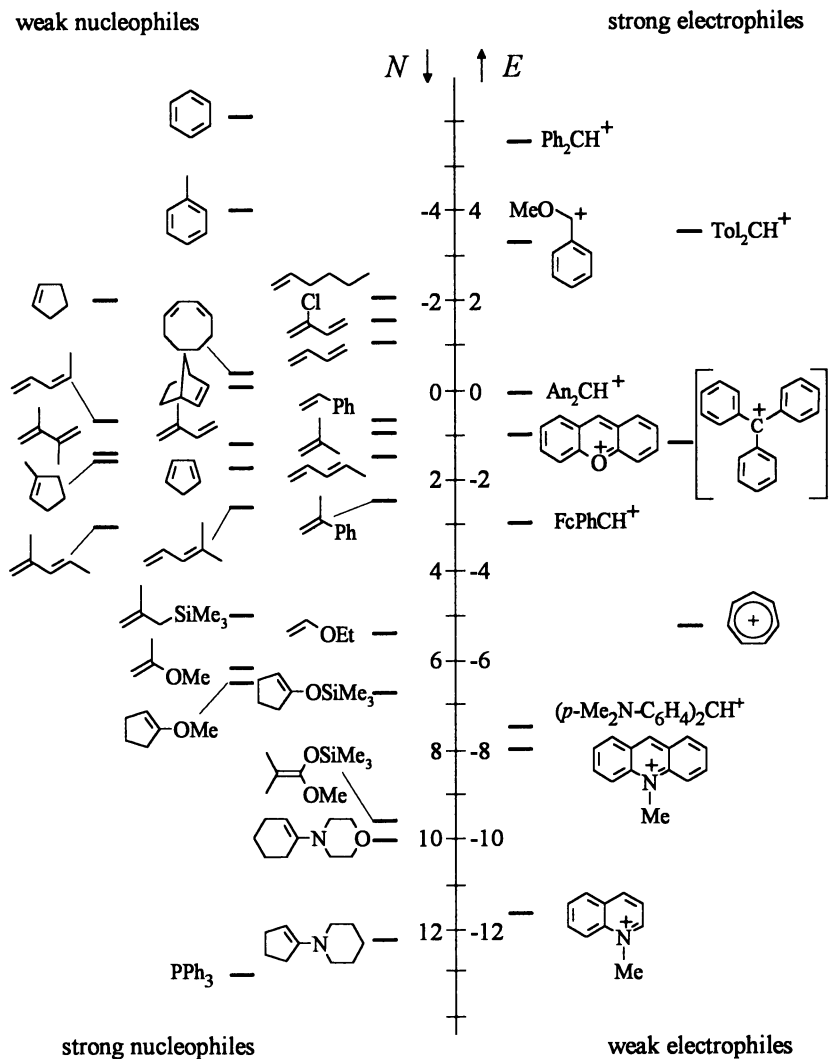
Scheme 1. Single-step and multi-step reactions of electrophiles (R^+) with nucleophiles ($M = \text{Si, Ge, Sn}$).

The reactions of benzhydryl cations with 2-methyl-1-pentene, for example, are only three times faster in nitromethane than in dichloromethane (8), and identical rates have been observed for the hydride transfer from dimethylphenylsilane to the bis(*p*-anisyl)carbenium ion (4). Identical rate constants have been observed when carbocations with complex counter-ions of different structure have been employed or when the reactions have been performed in presence of 0.1 M tetraalkylammonium salts with complex counter-ions, indicating that paired and non-paired carbocations show equal reactivities (8,9). An explanation for this behavior comes from the observation that the dissociation constant K_D for pairs of a wide variety of carbocations and complex counter-ions is almost constant and varies only between 1.9×10^{-4} and 2.9×10^{-4} mol L^{-1} (CH_2Cl_2 , -70°C) (10), i.e., under these conditions free ions are generally less stable by $(13.8 - 14.5) \times 10^{-4}$ kJ mol^{-1} than the corresponding ion-pairs. If this energy difference also holds for the free and paired activated complexes, ΔG^\ddagger is not affected by ion-pairing and equal reactivities of free and paired ions must result (11).

Three independent methods for determining rate constants of the cation-nucleophile combination reactions have been employed by us:

- Photometric and/or conductometric measurements of the consumption of persistent carbocations in presence of various nucleophiles (8). It is obvious that the conductometric method is only applicable when the fast reactions succeeding the rate-determining step give rise to non-ionic products.

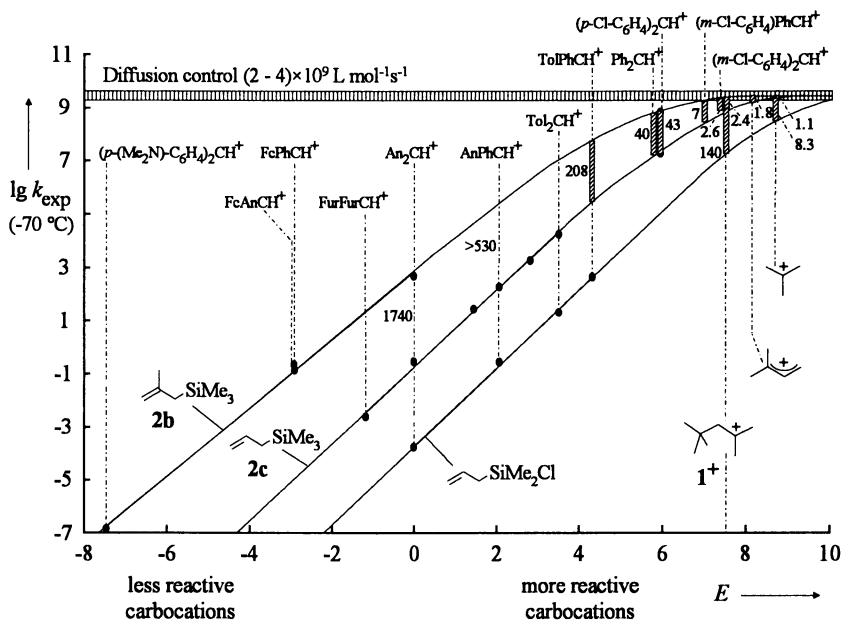
- b) Photometric detection of the decay of Laser-flash photolytically generated carbocations in presence of various nucleophiles (12-14,17).
 c) Competition experiments, where the relative reactivities of the two nucleophiles are derived from the product ratio obtained by *in situ* generation of carbocations in presence of these two nucleophiles (15,16).



Scheme 2. Reactivity scales for nucleophiles and electrophiles.

These three sets of experiments yield results which are consistent with each other (17) and correlation analysis has shown that the reactions with $k < 10^7 \dots 10^8 \text{ L mol}^{-1} \text{ s}^{-1}$

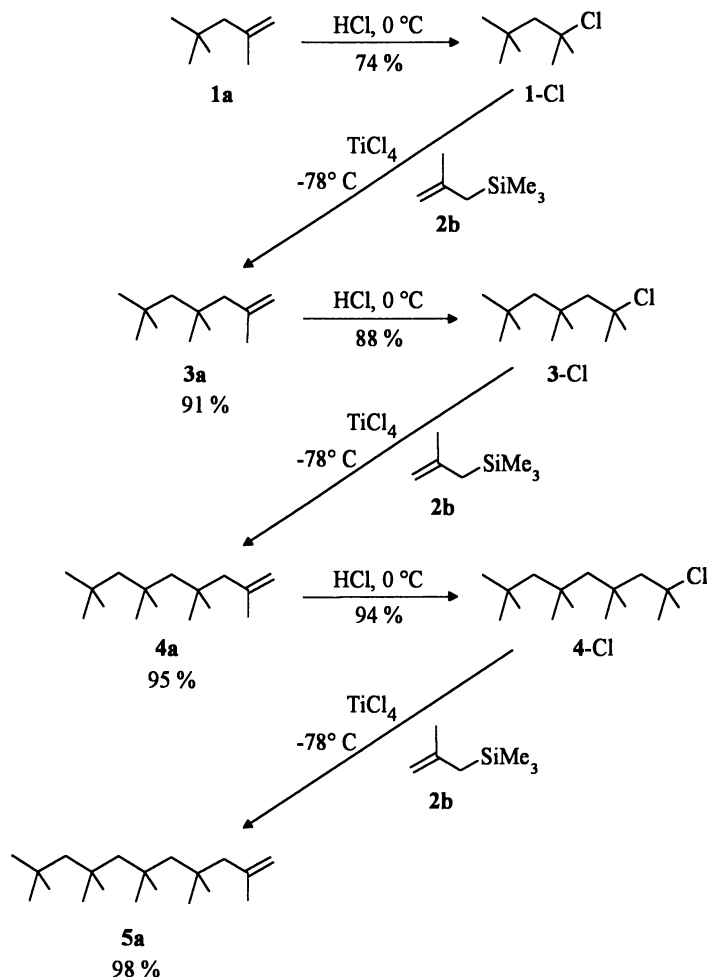
the reactions of carbenium ions with allylsilanes are plotted against the electrophilicity parameters E of the carbenium ions. Since weakly electrophilic carbocations react more than three orders of magnitude faster with **2b** than with **2c** (Scheme 3), the reactivity ratio $k(\mathbf{2b})/(\mathbf{2c}) = 2.4$ indicates that the reaction of $\mathbf{1}^+$ with the more nucleophilic of these two competitors (**2b**) is diffusion controlled.



Scheme 3. Changeover from the constant selectivity relationship to the reactivity selectivity principle. – Fc = ferrocenyl, Fur = 2,3-dihydrobenzofuran-5-yl. Directly measured rate constants are marked by dots, results from competition experiments by shaded bars (from ref. (19)).

Investigations of the reactions of Laser flash photolytically generated carbocations with highly nucleophilic π -systems in acetonitrile gave maximum rate constants between 2×10^9 and $4 \times 10^9 \text{ L mol}^{-1} \text{ s}^{-1}$ (diffusion control). This value was assumed also to correspond to the diffusion rate constant in dichloromethane since the viscosity coefficients at 20°C are almost identical for both solvents. For these reasons, a rate constant of $(2-4) \times 10^9 \text{ L mol}^{-1} \text{ s}^{-1}$ can be assumed for the reaction of $\mathbf{1}^+$ with trimethyl(2-methylallyl)silane **2b**.

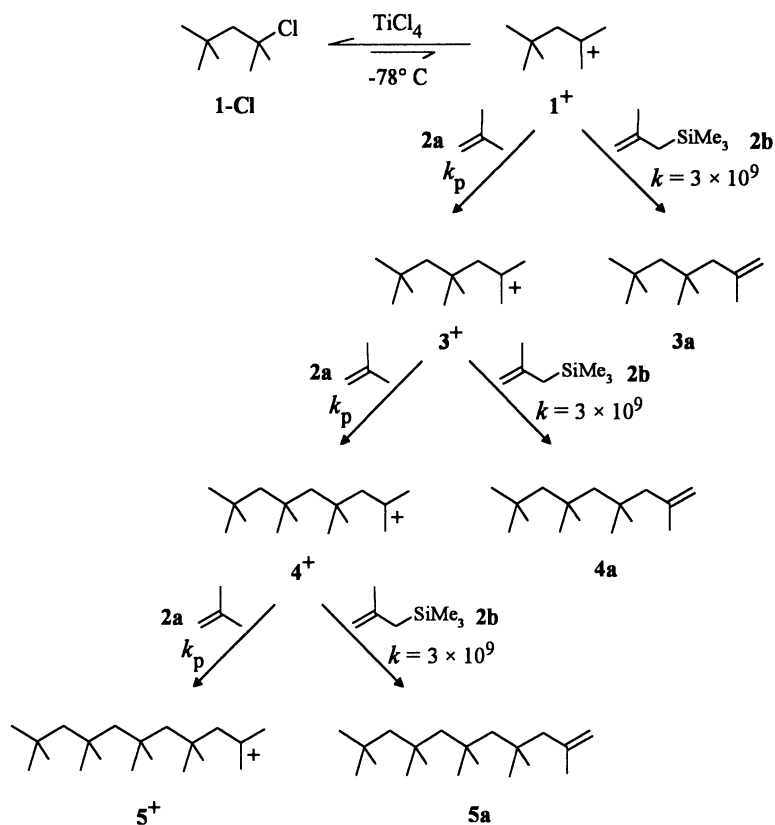
With this information another type of competition experiment has been designed (23). Scheme 4 shows that the TiCl_4 catalyzed reaction of 1-Cl with trimethyl(2-methylallyl)silane **2b** yields the alkene **3a** quantitatively. The sequence, addition of HCl and treatment with **2b**/ TiCl_4 has been repeated to selectively produce the isobutylene tetramer **4a** and pentamer **5a**.



Scheme 4. Trimethyl(2-methylallyl)silane **2b** is a terminator for the carbocationic polymerization of isobutylene **2a**.

When diisobutylene hydrochloride **1-Cl** is treated with TiCl_4 in presence of isobutylene **2a** and allylsilane **2b** (Scheme 5), the initially generated carbocation 1^+ can select between two different reaction channels. It may either undergo a diffusion-controlled reaction with **2b** to yield the isobutylene trimer **3a** or react with isobutylene **2a** to produce the homologous cation 3^+ which can again select between **2a** and **2b**. Since the isobutylene oligomers, **4a** and **5a** as well as the higher ones, are consecutive products of cation 3^+ , the relative reactivities of **2b** and **2a** can be derived from the ratio $[\mathbf{3a}]/([\mathbf{4a}] + [\mathbf{5a}] + [\text{higher oligomers}])$. Combination of the relative rate constants thus obtained with the known absolute rate constant for **2b** (diffusion control, 3×10^9)

yields the rate constant for the reaction of 1^+ with **2a**. In an analogous competition experiment, the relative reactivities of isobutylene **2a** and allyltrimethylsilane **2c** have been determined, which, in combination with the relative reactivities of **2b** and **2c** (19), also provide the rate constant for the reaction of 1^+ with **2a**.

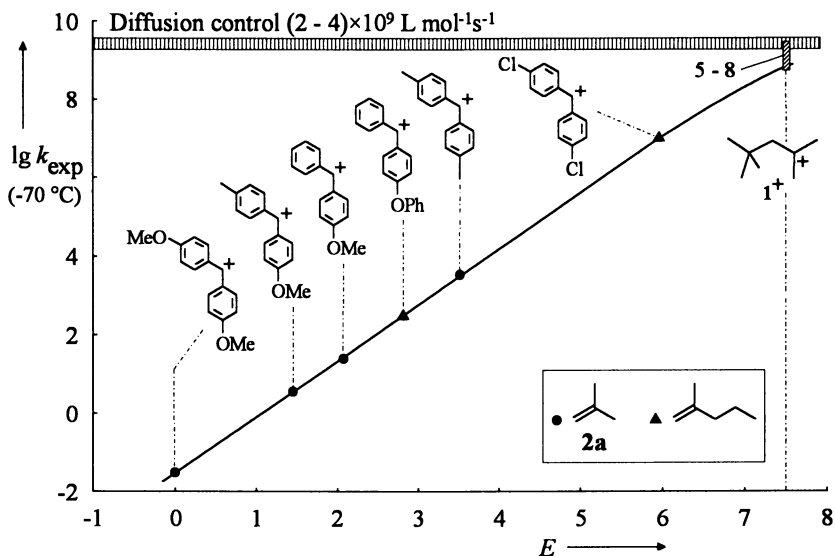


Scheme 5. Competition experiments for the determination of the propagation rate constant of isobutylene **2a**.

Unexpectedly for the reasons discussed above, exactly the same rate constant ($6 \times 10^8 \text{ L mol}^{-1} \text{ s}^{-1}$) (23) has been determined in this way as derived from the linear free energy relationship 1 (see above).

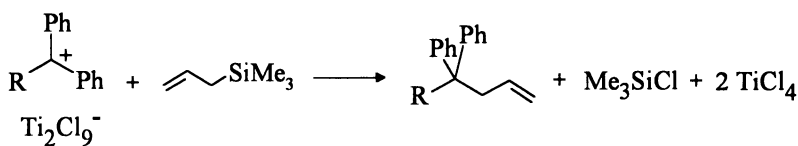
Reaction 2 can be considered as a model for the propagation step of carbocationic polymerization of isobutylene **2a**. Since for this polymerization propagation rate constants between 10^3 and $10^8 \text{ L mol}^{-1} \text{ s}^{-1}$ have been reported (24-32), and the most reliable values were considered to be around $10^4 \text{ L mol}^{-1} \text{ s}^{-1}$ (24-28,30-32), the high rate constant determined for reaction 2 appears surprising, and the question arises whether there is a principal difference between the electrophilicity of low molecular weight carbocations and their high-molecular weight homologues.

We would like to stress that the rate constant $k \geq 10^8 \text{ L mol}^{-1} \text{ s}^{-1}$ for the reaction of the tertiary carbenium ion 1^+ with isobutylene **2a** matches well with the directly measured rate constants for the reactions of other carbenium ions with isobutylene **2a**. Scheme 6 shows, for example, that a rate constant close to $10^4 \text{ L mol}^{-1} \text{ s}^{-1}$ has already been observed for the reaction of isobutylene **2a** with the highly stabilized bis(*p*-tolyl)carbenium ion $[(p\text{-H}_3\text{CC}_6\text{H}_4)_2\text{CH}^+]$ (21), and for the corresponding reaction with the chloro substituted benzhydryl cation $[(p\text{-ClC}_6\text{H}_4)_2\text{CH}^+]$ a rate constant of $10^7 \text{ L mol}^{-1} \text{ s}^{-1}$ has been measured (17). Since both benzhydryl cations have been found to be less Lewis-acidic than 1^+ (9), the observed ranking of the electrophilic reactivities of these carbocations is in accord with expectation.



Scheme 6. Comparison of the rate constant for $(1^+ + 2a)$ with the directly measured rate constants for the reactions of benzhydryl cations with isobutylene **2a** or 2-methyl-1-pentene (CH_2Cl_2 , -70°C). – An = *p*-MeO- C_6H_4 , Tol = *p*-Me- C_6H_4 (rate constants from ref. (1,8,17,20,21); *E*-values from ref. (7,19)).

In order to examine whether the length of the polyisobutylene chain may account for the different reactivities of the carbocations, we have synthesized alkyldiphenylcarbenium ions with different lengths of the alkyl chain by ionization of the corresponding ethers (33). Scheme 7 shows that the neopentyldiphenylcarbenium ion **6b** is 20 to 50 times less reactive than the methyldiphenylcarbenium ion **6a** but that a further increase of the alkyl chain length has little influence on reactivity. Comparable results were obtained for the reactions of these carbocations with dimethylphenylsilane (33). Since Scheme 7 refers to a relatively slow reaction, i. e., a reaction which can easily be followed by conventional kinetic methods, there remains the possibility that chain length affects the rate constants of very fast reactions and we have to restrict the validity of k_p determined for reaction 2 to oligomerization reactions of isobutylene.



	$k(-70\text{ }^\circ\text{C}) / \text{L mol}^{-1}\text{s}^{-1}$	k_{rel}
	$(2 - 6) \times 10^1$	20 - 50
	1.10×10^{-1}	1.0
	3.38×10^{-2}	0.31
	3.41×10^{-2}	0.31

Scheme 7. Reactivities of alkyldiphenylcarbenium ions with different lengths of the alkyl chains.

There are arguments, however, which support a propagation rate constant for the carbocationic polymerization of isobutylene **2a** as determined for reaction 2. Kaszás, Puskás and Kennedy (34), for example, studied the cationic copolymerization of isobutylene **2a** and 2,4-dimethyl-1,3-pentadiene **2d** and found that the diene **2d** is consumed approximately three times faster than isobutylene **2a**. As a consequence of the highly different nucleophilicity parameters, $N(\mathbf{2a}) = 1.07$ (7), $N(\mathbf{2d}) \approx 3.7$ (Mayr, H., Hartnagel, M., *Liebigs Ann.*, in press) one would expect the diene **2d** to be approximately 400 times more reactive than isobutylene **2a**, if both reactions fall in the linear range of Scheme 3. Only with the assumption that the propagation rate constants are close to the diffusion limit, the reported copolymerization data can be rationalized.

Plesch's chain transfer ratio from growing polyisobutylene to anisole also roughly agrees with our estimates ($k_{\text{tr}}/k_{\text{p}} = 5.3 \times 10^{-3}$) (35). For the reaction of 1^+ ($E = 7.50$) (19) with anisole ($N = -1.56$, $s = 1.17$) (7) a second-order rate constant (20 °C) of $9 \times 10^6 \text{ L mol}^{-1} \text{ s}^{-1}$ is calculated by equation 1 which is combined with the rate constant for reaction 2 ($6 \times 10^8 \text{ L mol}^{-1} \text{ s}^{-1}$) to yield a transfer ratio of $k_{\text{tr}}/k_{\text{p}} = 1.5 \times 10^{-2}$, 3

times larger than directly observed (35). Only by assuming an even larger propagation rate constant for the polymerization of isobutylene (**2a**) a better match of data could be obtained.

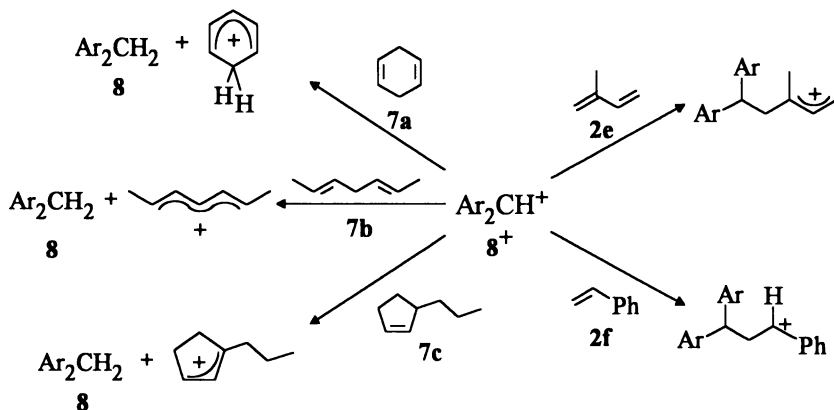
Because of these consistencies it is suggested to examine whether the previously published, considerably lower values of the propagation rate constants k_p of isobutylene **2a** may be reinterpreted in terms of $K_1 k_p$.

Hydride Transfer Reactions

Transfer processes are the most important chain-breaking reactions in cationic polymerizations. While we do not yet have a possibility to predict the rates of proton transfer reactions and of intramolecular Friedel-Crafts alkylations, the relative rates of intermolecular Friedel-Crafts alkylations can be derived from the nucleophile ranking in the left column of Scheme 2.

Hydride transfer reactions represent a third class of transfer processes, which have been reported to be of great importance, especially during the polymerization of non-branched olefins as 1-butene, 2-butene, pentenes, octenes and decenes (36). The question arises whether one might be able to generally predict the relative rates of hydride transfer and propagation reactions in carbocationic polymerizations.

When 1,4-cyclohexadiene **7a**, (2*E*,5*E*)-heptadiene **7b**, or 3-propylcyclopentene **7c** were combined with the benzhydryl salts 8^+Z^- ($Z^- = BCl_4^-, Ti_2Cl_9^-, CF_3SO_3^-$) in CH_2Cl_2 , the diarylmethanes **8** were produced and isolated in 87 to 99 % yield (Scheme 8). Thus, unlike the alkenes and dienes investigated previously (1), the compounds **7** act as hydride donors and do not behave as π -nucleophiles.

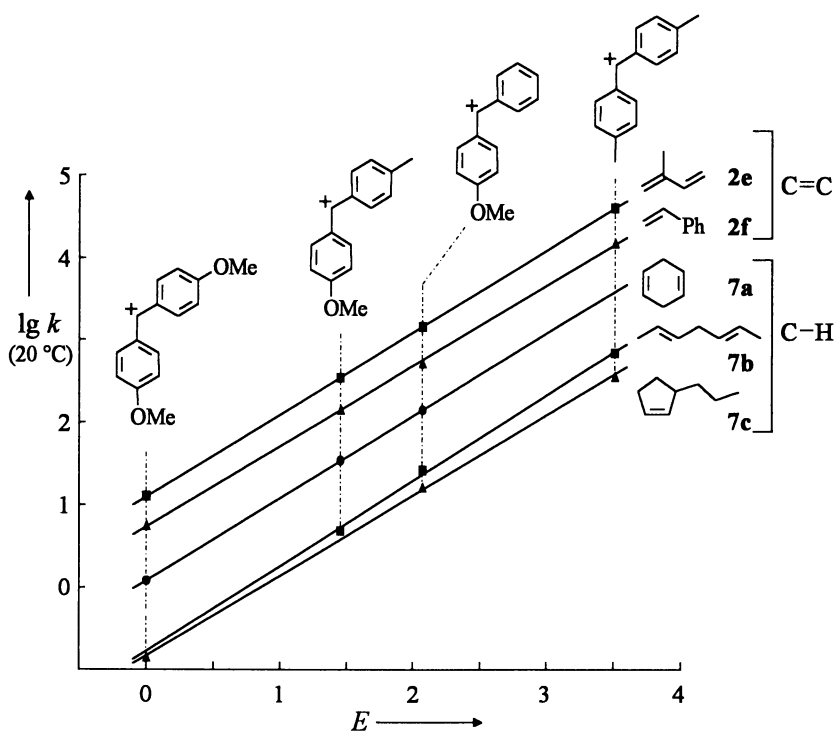


Scheme 8. Reactions of benzhydryl cations 8^+ with unsaturated hydrocarbons which act as hydride donors (**7a**, **7b**, **7c**) or π -nucleophiles (**2e**, **2f**).

By determining the rate of consumption of the benzhydryl cations 8^+ , the hydride transfer reactions were found to follow second-order kinetics. In some cases the coun-

ter-ion was varied (BCl_4^- , Ti_2Cl_9^- , CF_3SO_3^-) and found not to affect the rate constant indicating the rate determining nature of the hydride transfer step.

When these rate constants ($\lg k$) are plotted versus the electrophilicity parameters E of the benzhydryl cations (Scheme 9) linear correlations are found which are not only parallel with each other but also with the corresponding graphs for styrene **2f** and isoprene **2e**, i.e., compounds which act as π -nucleophiles. This means that any benzhydryl cation $\mathbf{8}^+$ reacts 30 times faster with styrene **2f** (C-C bond formation), for example, than with 3-propylcyclopentene **7c** (hydride transfer), i.e., the reactivity ratio is independent of the electrophilicity of the benzhydryl cation. In other words, Scheme 9 indicates that the hydride transfers from hydrocarbons to carbenium ions also follow the linear free enthalpy relationship 1 with a slope similar to that previously found for π -nucleophiles with terminal double bonds ($s \approx 1.0$).

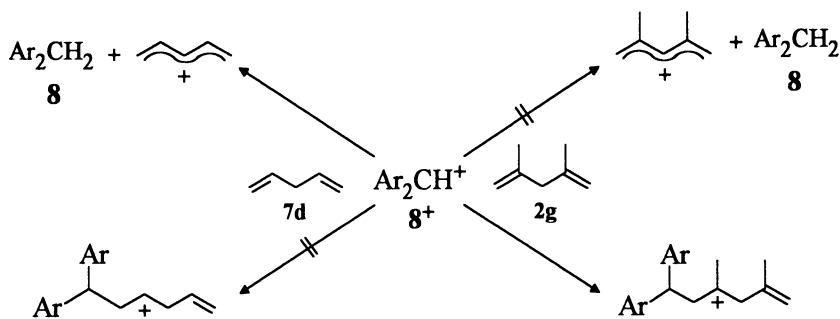


Scheme 9. Constant selectivity relationships for the reactions of benzhydryl cations $\mathbf{8}^+$ with hydride donors and π -nucleophiles (CH_2Cl_2 , 20 °C).

The hydride transfer abilities of the other hydride donors listed in Scheme 10 have only been measured with respect to one benzhydryl cation $\mathbf{8}^+$. Assuming that the linear free enthalpy relationship 1 with slope $s = 1$ also holds for these compounds, the corresponding nucleophilicity parameter N was determined by substituting $\lg k$, E , and $s = 1$ into equation 1.

However, the reactivities of **7e** and **7f** very closely resemble those of **7b** and **7d**, respectively, and we found that the reduction of ΔH^\ddagger caused by the extra methyl group is counterbalanced by an increase of the negative value of ΔS^\ddagger . It, therefore, depends on the temperature whether the methyl groups in bisallylic position cause a slight increase or decrease of reactivity.

In contrast to the 1,4-dienes **7b**, **7d**, **7e**, and **7f**, 2,4-dimethyl-1,4-pentadiene **2g** was found to react as a π -nucleophile. Since the two methyl groups in **2g** are located at nodal positions of the pentadienyl cation LUMO, the hydride abstraction can be expected to be of comparable rate as in 1,4-pentadiene **7d**. This reaction is not observed, however, since it is surmounted by the electrophilic attack at the methylene termini yielding a tertiary carbenium ion (Scheme 11). This is a more favorable process than the formation of secondary carbenium ions that might be produced by addition of electrophiles to the double bond of 1,4-pentadiene **7d** or the other 1,4-dienes on the left side of Scheme 10.



Scheme 11. 1,4-Dienes reacting as σ - (left) or π -nucleophiles (right).

Scheme 10 furthermore shows that 1,1-dialkylated or more highly alkylated ethylenes as well as 1,3-dienes generally behave as π -nucleophiles (formation of allyl or *tert.*-alkyl cations) towards carbenium ions, while monoalkylated or 1,2-dialkylated ethylenes can either react as π -nucleophiles (propene **2h**, 2-butene **2i**) or hydride donors (3-propylcyclopentene **7c**) towards benzhydryl cations. Since in the latter cases electrophilic attack at the double bond is less favorable due to the formation of secondary carbenium ions, the π - and σ -route have comparable activation energies, and one can expect that the ratio of the two competing processes strongly depends on the steric requirement of the attacking carbenium ion.

On this background it is understandable that the carbocationic polymerization of non-branched alkenes does not give high-molecular weight compounds (**34,36**). Even if the π -nucleophilicity (relevant for propagation) is higher than the σ -nucleophilicity (relevant for hydride transfer) the reactivity difference is too small to provide a sufficient number of propagation steps before transfer occurs.

According to Scheme 10, the π -nucleophilicity of isobutylene **2a** is approximately two orders of magnitude greater than the σ -nucleophilicity of **7c**. Though allylic cations in five-membered rings are somewhat more favorable than their acyclic analogues, one

Literature Cited

- (1) Mayr, H. *Angew. Chem.* **1990**, *102*, 1415-1428; *Angew. Chem., Int. Ed. Engl.* **1990**, *29*, 1371-1384.
- (2) Mayr, H.; Bartl, J.; Hagen, G. *Angew. Chem.* **1992**, *104*, 1689-1691; *Angew. Chem., Int. Ed. Engl.* **1992**, *31*, 1613-1615.
- (3) Hagen, G.; Mayr, H. *J. Am. Chem. Soc.* **1991**, *113*, 4954-4961.
- (4) Mayr, H.; Basso, N.; Hagen, G. *J. Am. Chem. Soc.* **1992**, *114*, 3060-3066.
- (5) Mayr, H.; Basso, N. *Angew. Chem.* **1992**, *104*, 1103-1105; *Angew. Chem., Int. Ed. Engl.* **1992**, *31*, 1046-1048.
- (6) Mayr, H. in *Selectivities in Lewis Acid-Promoted Reactions* (Schinzer, D.; Ed.), NATO ASI Series C, Vol. 289, **1989**, p. 21.
- (7) Mayr, H.; Patz, M. *Angew. Chem.* **1994**, *106*, 990-1010; *Angew. Chem., Int. Ed. Engl.* **1994**, *33*, 938-957.
- (8) Mayr, H.; Schneider, R.; Schade, C.; Bartl, J.; Bederke, R. *J. Am. Chem. Soc.* **1990**, *112*, 4446-4454.
- (9) Mayr, H. in *Cationic Polymerization: Mechanisms, Synthesis, and Applications* (Matyjaszewski, K.; Ed.), Marcel Dekker: New York, **1996**, 51-136.
- (10) Schneider, R.; Mayr, H.; Plesch, P. H. *Ber. Bunsenges. Phys. Chem.* **1987**, *91*, 1369-1374.
- (11) Mayr, H.; Schneider, R.; Schade, C. *Makromol. Chem., Macromol. Symp.* **1988**, *13/14*, 43-59.
- (12) McClelland, R. A.; Banait, N.; Steenken, S. *J. Am. Chem. Soc.* **1986**, *108*, 7023-7027.
- (13) McClelland, R. A.; Kanagasabapathy, V. M.; Steenken, S. *J. Am. Chem. Soc.* **1988**, *110*, 6913-6914.
- (14) McClelland, R. A.; Kanagasabapathy, V. M.; Banait, N. S.; Steenken, S. *J. Am. Chem. Soc.* **1989**, *111*, 3966-3972.
- (15) Mayr, H.; Pock, R. *Chem. Ber.* **1986**, *119*, 2473-2496.
- (16) Pock, R.; Mayr, H. *Chem. Ber.* **1986**, *119*, 2497-2509.
- (17) Bartl, J.; Steenken, S.; Mayr, H. *J. Am. Chem. Soc.* **1991**, *113*, 7710-7716.
- (18) Patz, M.; Mayr, H. *Makromol. Chem., Macromol. Symp.* **1996**, *107*, 99-110.
- (19) Roth, M.; Mayr, H. *Angew. Chem.* **1995**, *107*, 2428-2430; *Angew. Chem., Int. Ed. Engl.* **1995**, *34*, 2250-2252.
- (20) Mayr, H.; Schneider, R.; Irrgang, B.; Schade, C. *J. Am. Chem. Soc.* **1990**, *112*, 4454-4459.
- (21) Mayr, H.; Schneider, R.; Grabis, U. *J. Am. Chem. Soc.* **1990**, *112*, 4460-4467.
- (22) Patz, M.; Mayr, H.; Bartl, J.; Steenken, S. *Angew. Chem.* **1995**, *107*, 519-521; *Angew. Chem., Int. Ed. Engl.* **1995**, *34*, 490-492.
- (23) Roth, M.; Mayr, H. *Macromolecules* **1996**, *29*, 6104-6109.
- (24) Plesch, P. H. *Prog. React. Kinet.* **1993**, *18*, 1-62.
- (25) Marek, M.; Chmelir, M. *J. Polym. Sci.* **1968**, *C22*, 177-183.
- (26) Toman, L.; Marek, M. *Makromol. Chem.* **1976**, *177*, 3325-3343.
- (27) Magagnini, P. L.; Cesca, S.; Giusti, P.; Priola, A.; Di Maina, M. *Makromol. Chem.* **1977**, *178*, 2235-2248.
- (28) Ueno, K.; Yamaoka, H.; Hayashi, K.; Okamura, S. *Int. J. Appl. Radiat. Isotopes* **1966**, *17*, 595-602.

- (29) Taylor, R. B.; Williams, F. *J. Am. Chem. Soc.* **1969**, *91*, 3728-3732.
- (30) Sigwalt, P.; Matyjaszewski, K. *Polym. Int.* **1994**, *35*, 1-26.
- (31) Matyjaszewski, K. *Makromol. Chem., Macromol. Symp.* **1992**, *54/55*, 51-71.
- (32) Freyer, C. V.; Mühlbauer, H. P.; Nuyken, O. *Angew. Makromol. Chem.* **1986**, *145/146*, 69-87.
- (33) Mayr, H.; Roth, M.; Faust, R. *Macromolecules* **1996**, *29*, 6110-6113.
- (34) Kaszás, G.; Puskás, J.; Kennedy, J. P. *Macromolecules* **1992**, *25*, 1775-1779.
- (35) Penfold, J.; Plesch, P. H. *Proc. Chem. Soc. London* **1961**, 311.
- (36) Kennedy, J. P.; Maréchal, E., *Carbocationic Polymerization*, John Wiley & Sons: New York, **1982**, p. 211.

Chapter 4

Cationic Copolymerization of Methyl Glyoxylate with Cyclic Acetals

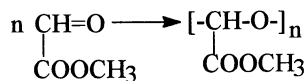
Structure of Active Species by Phosphine Ion Trapping

M. Basko, P. Kubisa, and Stanislaw Penczek

Center of Molecular and Macromolecular Studies, Polish Academy of Sciences,
Sienkiewicza 112, 90-363 Łódź, Poland

Cationic copolymerization of methyl glyoxylate with 1,3-dioxolane leads to functionalized polyacetals. In this system, active species participate not only in homo- and cross-propagation but also in depropagation and transacetalization reactions. All of these processes lead to interconversion of active species. The knowledge of relative concentrations of active species in the course of copolymerization is thus important for understanding the factors governing the composition and the microstructure of the copolymers formed at different conditions. To determine the relative concentrations of active species in the cationic copolymerization of aldehydes with 1,3-dioxolane, the ion-trapping with tertiary phosphines was applied. The results were correlated with relative reactivities of active species.

Methyl glyoxylate (GM) is a monomer containing an ester function in addition to polymerizable aldehyde function. The presence of the ester function in the monomer molecule does not prohibit its ionic polymerization, thus poly(methyl glyoxylate) was prepared recently by both anionic and cationic polymerization of GM (1,2,3). The resulting polymer is a polyacetal containing ester side groups:



Vairon a.o. published extensive studies on the thermodynamics and kinetics of GM polymerization (1,2).

Ionic polymerization of GM offers an interesting possibility of preparing functionalized polyacetals. Polyacetals derived from aldehydes are, however, thermally unstable. Depropagation is typically initiated by decomposition of the thermally unstable hemiacetal end-groups (4). Polyformaldehyde, for example, has to be stabilized by end-capping i.e. be converting unstable hemiacetal groups into the stable ester groups. Alternative method is based on cationic copolymerization of formaldehyde cyclic trimer

(1,3,5-trioxane) with a suitable comonomer, providing chain units interrupting the sequence of carbon and oxygen atoms in the chain. Typical comonomers are 1,3-dioxolane (DXL) or ethylene oxide (EO), providing $-\text{CH}_2-\text{CH}_2-$ units, on which depropagations stops (5).

Homopolymers of GM, like other polyacetals, are thermally unstable. The thermal stability may be greatly improved by copolymerization with suitable comonomer. This would be one-step method of preparing stable functionalized polyacetals.

In the present paper we report on the preliminary results concerning the cationic copolymerization of GM with 1,3-dioxolane (DXL). In order to understand the copolymerization process, this first part is devoted to the determination of the structure of active species.

Results and Discussion

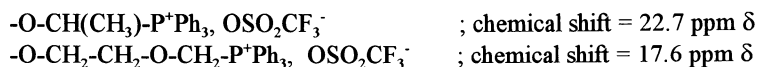
Our preliminary results on the GM-DXL copolymerization revealed, that although the relatively high molecular weight copolymers can be prepared, transacetalization proceeds fast, reshuffling the monomer units and changing the structure of active species. Therefore first we elaborated the method allowing these structures to be determined.

Structure of Active Species by Ion-trapping Method. Ion-trapping with tertiary phosphines has been successfully used for the determination of structures and concentrations of active species in the cationic polymerization of heterocyclic and vinyl monomers (6,7,8,9). The principle of the method is outlined in the scheme below (counterions omitted):



Applied to the cationic copolymerization of DXL with aldehydes, this method should allow to determine the relative concentrations of active species containing terminal DXL or GM units i. e. $\dots\text{-DXL}^+$ vs $\dots\text{-GM}^+$ species, although it would not provide any information concerning the form in which these active species exist (e.g. oxonium vs carboxonium ions) because the structure of resulting phosphonium ions is in both cases the same.

Application of the Ion-trapping Method for the Model System : Cationic Copolymerization of 1,3-Dioxolane (DXL) with Acetaldehyde (AA). Homopolymerizations of two monomers: AA and DXL (initiated with trifluoromethanesulfonic acid and conducted at $[\text{M}]_0 = 3.5 \text{ mol/L}$ and $[\text{I}]_0 = 5 \cdot 10^{-2} \text{ mol/L}$ in CH_2Cl_2 solution at -78°) were terminated with an excess of triphenylphosphine (PPh_3) and the chemical shifts of the corresponding phosphonium ions were determined as equal to:



Copolymerization of both comonomers was carried out at the same conditions. In the $^{31}\text{P-NMR}$ spectrum of the reaction mixture terminated with triphenylphosphine,

initially mostly the signal at 22.7 ppm δ was observed, corresponding to the species containing terminal aldehyde unit (Fig. 1a). Concentration of these species, determined by the integration of the corresponding signal with respect to the signal of the known excess of unreacted phosphine, was close to the initial concentration of initiator. When, however, the terminated reaction mixture was kept for the prolonged period of time, the changes in the spectrum occurred. The over-all concentration of phosphonium ions did not change but the signal corresponding to phosphonium ions formed from the active species terminated with AA unit at 22.7 ppm δ was gradually converted into a signal corresponding to the active species terminated with DXL unit at 18.0 ppm δ (Fig. 1b,c).

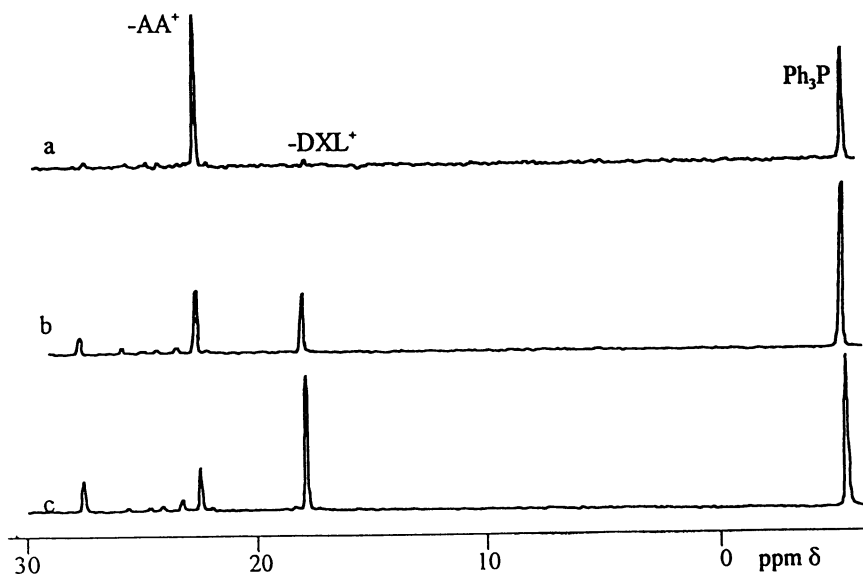
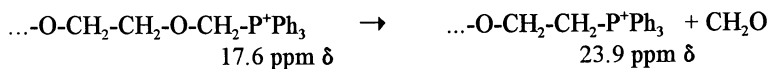


Fig. 1. ^{31}P NMR spectra of reaction mixture after termination of copolymerization of acetaldehyde (AA) and 1,3-dioxolane (DXL) with triphenylphosphine. Conditions: $[\text{CF}_3\text{SO}_3\text{H}]_0 = 9 \cdot 10^{-2}$ mol/L, $[\text{AA}]_0 = [\text{DXL}]_0 = 3.5$ mol/L, CH_2Cl_2 , -78°C , time = 20 h. $[\text{Ph}_3\text{P}] = 1.95 \cdot 10^{-1}$ mol/L. Spectra recorded at room temperature: a - 0.5 h, b - 30 h, c - 144 h. after termination.

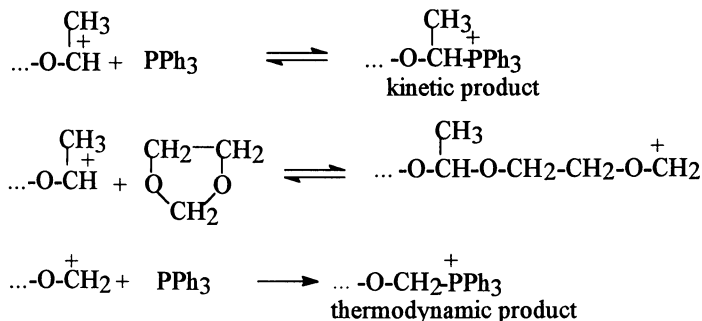
In the spectra 1b and 1c additional signals of low intensity appear at 23-30 ppm δ region. The signal at 23.5 ppm δ may be attributed to observed earlier (10) very slow interconversion of terminated $-\text{DXL}^+$ species according to the scheme below (giving only the formal notation, without indicating the mechanism of conversion):



The signal at ~ 28 ppm δ is probably due to $\text{Ph}_2\text{RP}=\text{O}$ formed by hydrolysis of R-PPh_3^+ phosphonium ion (R stands for polymeric ligand), occurring when the solution is kept for a prolonged period of time (144 h) in capped (not sealed) NMR tubes (11). The signals of very low intensity at 26-27 ppm δ , corresponding to $< 3\%$ -mol of total phosphorus, are due to unidentified impurities.

The observation of the slow interconversion of phosphonium ions in the terminated reaction mixture implies, that in contrast to the cationic polymerization of cyclic ethers or vinyl ethers, termination of active species of cationic aldehyde polymerization is not completely irreversible. Apparently, certain fraction of active species of $-\text{AA}^+$ type, stabilized by the inductive effect of methyl group, exist in equilibrium with the corresponding phosphonium ion. These species may participate in propagation-depropagation equilibria or in transacetalization. By any of these processes, $-\text{AA}^+$ active species are converted into the less stabilized $-\text{DXL}^+$ active species.

In such a situation, when termination of $-\text{AA}^+$ active species is to some extent a reversible process, while the termination of $-\text{DXL}^+$ active species is irreversible (or at least the equilibrium is shifted more strongly towards phosphonium ion), the interconversion of $-\text{AA}-\text{P}^+\text{Ph}_3$ species (the kinetic product) into the $-\text{DXL}-\text{P}^+\text{Ph}_3$ species (the thermodynamic product) should proceed, as shown in scheme below (only carboxonium form of active species shown, counterions omitted):



The reversibility of the termination may affect the results, thus in order to terminate the copolymerization irreversibly, more nucleophilic aliphatic phosphine, namely tributylphosphine (PBu_3) was used as a terminating agent.

The chemical shifts of the corresponding phosphonium ions, determined by terminating the homopolymerization of both monomers with tributylphosphine, are equal to:



In the ^{31}P -NMR spectrum of the copolymerizing mixture, terminated with tributylphosphine, signals of phosphonium ions corresponding to both types of active species appear; signal corresponding to $-\text{AA}^+$ species has much higher intensity. At the

copolymerization conditions: $[DXL]_0 = [AA]_0 = 3.5 \text{ mol/L}$, CH_2Cl_2 , 25° , the following results were obtained:

Overall concentration of active species = $5.05 \cdot 10^{-2} \text{ mol/L}$ (= 1.01 $[I]_0$).
 Concentration of $-AA^+$ active species = $4.60 \cdot 10^{-2} \text{ mol/L}$ (91 mol-%).
 Concentration of $-DXL^+$ active species = $0.45 \cdot 10^{-2} \text{ mol/L}$ (9 mol-%).

There were no changes in the ^{31}P -NMR spectrum within 24 h, indicating, that in this system termination was indeed irreversible and determined concentrations of both types of phosphonium ions were equal to the concentrations of both types of active species in the reaction mixture at the moment of termination.

Ion-trapping Method in the Cationic Copolymerization of 1,3-Dioxolane with Methyl Glyoxylate. It was established on the basis of termination of homopolymerizations of DXL and GM with triphenylphosphine, that the chemical shifts of corresponding phosphonium ions are equal to:

$\dots\text{-OCH}_2\text{CH}_2\text{OCH}_2\text{-PPh}_3^+$; chemical shift = 17.6 ppm δ
 $\dots\text{-OCH}(\text{COOCH}_3)\text{-PPh}_3^+$; chemical shift = 25.5 ppm δ
 (homopolymerizations initiated with trifluoromethanesulfonic acid and conducted at $[M]_0 = 3.5 \text{ mol/L}$ and $[I]_0 = 5 \cdot 10^{-2} \text{ mol/L}$ in CH_2Cl_2 solution at -78°)

In contrast, however, to the earlier studied copolymerization of DXL with AA, GM reacts with both electrophilic reagents (e.g. initiators of cationic polymerization) and nucleophilic reagents (e.g. tertiary phosphines used as a trapping agents). Thus, unreacted GM reacts with an excess of a trapping agent (needed to provide internal standard) complicating the analysis. According to the literature, reaction of aldehydes with tertiary phosphines gives the corresponding zwitterion, which, depending on reaction conditions, may undergo further transformations (12).

When the homopolymerization of GM was terminated with PPh_3 two signals were observed in ^{31}P -NMR spectra. There was no signal corresponding to free phosphine, although phosphine was used in > 2 -fold excess. The signal at 25.5 ppm δ was attributed to the terminal $-\text{GM-PPh}_3^+$ unit resulting from reaction of $\dots\text{-GM}^+$ active species with phosphine. The other signal at 31 ppm δ was tentatively assigned to $\text{Ph}_3\text{P}^+\text{-GM}^-$ zwitterion (3). The chemical shift of phosphorus in zwitterion is higher (signal is shifted downfield) than the signal of phosphorus in terminal phosphonium ion in spite of the fact, that in the former the strong donor group ($-\text{CH}(\text{COOCH}_3)\text{O}^-$) is present. The chemical shift of phosphorus in terminal phosphonium ion is, however, affected by the presence of counteranion (triflate anion) and other donor group ($-\text{OCH}(\text{R})-$). The combined effect of two donor group (but also one acceptor ester group (R)) in close proximity to the phosphorus atom leads to the upfield shift of the signal, compared to the signal of zwitterion. If this assignment is correct, then it would be possible to distinguish phosphonium ion formed by termination of cationic active species from phosphonium ion formed by reaction of phosphine with GM monomer. However, it can not be ruled out, that the originally formed zwitterionic species may induce an anionic polymerization of GM leading to longer chain phosphonium ion, indistinguishable from the phosphonium ion resulting from termination of the cationic species.

In the spectrum, signal of free phosphine (at about -5 ppm δ) as well as signal at about 30 ppm δ (corresponding to zwitterion) were present, indicating, that concentration of remaining unreacted GM monomer in the system was much lower than the concentration of phosphine.

This unreacted GM converted part of an excess of phosphine into the corresponding zwitterion. Since concentration of GM was too low to consume the excess of phosphine completely, the possibility of formation of a longer chains by anionic process may be excluded. Consequently, signal observed at 23 ppm δ is due exclusively to the active species ...-GM⁺ terminated with phosphine. Because the signal of active species ...DXL⁺ at 17.8 ppm δ is observed independently, the relative concentrations of both types of active species may be determined. At the conditions given in caption to Fig. 2, the following results were obtained:

Overall concentration of active species = $5.25 \cdot 10^{-2}$ mol/L (= 0.99 [I]₀).
 Concentration of -GM⁺ active species = $0.89 \cdot 10^{-2}$ mol/L (17 mol-%).
 Concentration of -DXL⁺ active species = $4.36 \cdot 10^{-2}$ mol/L (83 mol-%).

Table 1 gives the summary of the values of ³¹P-NMR chemical shifts of phosphonium ions formed by termination of studied copolymerization systems by tertiary phosphines.

Table 1. ³¹P-NMR Chemical Shifts of Phosphonium Ions Formed by Termination of Cationic Copolymerization of 1,3-Dioxolane (DXL) with Acetaldehyde (AA) and Methyl Glyoxylate (GM) by Tertiary Phosphines (spectra recorded in CHCl₃ solvent at 25 °C)

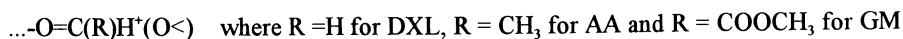
System	Structure of phosphonium ion	Chemical shift ppm δ
DXL-AA	-OCH ₂ CH ₂ OCH ₂ P ⁺ Ph ₃	18.0
	-OCH(CH ₃)P ⁺ Ph ₃	22.7
	-OCH ₂ CH ₂ OCH ₂ P ⁺ Bu ₃	35.5
	-OCH(CH ₃)P ⁺ Bu ₃	34.4
DXL-GM	-OCH ₂ CH ₂ OCH ₂ P ⁺ Ph ₃	17.2
	-OCH(COOCH ₃)P ⁺ Ph ₃	21.6

Comparison of DXL-AA System and DXL-GM System. It should be pointed out, that in both studied systems, i.e. DXL-AA and DXL-GM, the relative concentrations of active species were determined after the ultimate conversions of comonomers had been reached i.e. at equilibrium (or close to equilibrium) conditions.

In the cationic copolymerization of cyclic acetals with aldehydes, after reaching the ultimate conversions of comonomers, the system is still in dynamic equilibrium. By

propagation-depropagation equilibria or by transacetalization, active species containing terminal units derived from an aldehyde may be converted into active species containing terminal units derived from a cyclic acetal and vice versa. Thus the determined proportions of active species correspond to the fractions of active species of both types, being in equilibrium with chains containing equimolar fractions of both types of units (at $[\text{aldehyde}]_0 = [\text{DXL}]_0$ and almost complete conversions of comonomers). This proportion should be related to the relative reactivities of active species.

Although both types of active species may exist in various forms, (carboxonium ions, cyclic or linear oxonium ions) (13), the nature of substituent at the carbon atom on which positive charge is partly located, should affect the reactivity in a similar way. The structure of active species derived from AA, GM and DXL units is shown below (only carboxonium structure shown):



In the pair DXL-AA, the electron donating inductive effect of the (R = CH₃) group leads to stabilization of positive charge, decreasing the reactivity of -AA⁺ active species as compared to -DXL⁺ active species (R = H). The observed concentration of -AA⁺ active species is therefore considerably higher than -DXL⁺ active species (although with time, the reversibility of the reaction between -AA⁺ active species and phosphine leads to the decrease of the [-AA⁺]/[-DXL⁺] ratio, as described in the previous section). In the pair DXL-GM, the electron withdrawing inductive effect of the ester group leads to the increase of the effective positive charge on carbon atom and to the enhanced reactivity of the -GM⁺ active species as compared to -DXL⁺ active species. In accordance with this reasoning, the observed equilibrium concentration of -GM⁺ active species is considerably lower than this of the -DXL⁺ active species.

The number of elementary reactions involved in establishing the equilibria is too large to permit the quantitative interpretation, thus the ion-trapping method allows only to confirm the expected order of relative reactivities of active species in cationic copolymerization of aldehydes with 1,3-dioxolane.

Acknowledgment: This work was supported in part by a grant PAN/NSF-90-31 from II M. Sklodowska-Curie Fund.

Literature Cited

1. Vairon, J.-P.; Muller, E.; Brunel, C. *Makromol. Chem., Macromol. Symp.* **1994**, *85*, 307.
2. Vairon, J.-P.; Muller, E.; Brunel, C. *J. Macromol. Sci., Macromol. Reports* **1994**, *A31*, 821.
3. Muller, E.; *Ph. D. Thesis, University Paris VI, Paris, France, 1992*
4. Vogl, O. In *Encyclopedia of Polymer Science and Engineering*; Mark, H. F.; Bikales, N. M.; Overberger, C. H.; Menges, G.; Kroschwitz, J. I., Eds.; John Wiley & Sons, New York, 1985, Vol. 1; p. 623.
5. Dolce, T. J.; Grates, J. A. In *Encyclopedia of Polymer Science and Engineering*; Mark, H. F.; Bikales, N. M.; Overberger, C. H.; Menges, G.; Kroschwitz, J. I., Eds.; John Wiley & Sons, New York, 1985, Vol. 1; p. 61.

6. Brzezinska, K.; Chwialkowska, W.; Kubisa, P.; Matyjaszewski, K.; Penczek, S. *Makromol. Chem.* **1977**, *178*, 2491.
7. Penczek, S.; Kubisa, P.; Brzezinska, K.; Basko, M. *ACS Polym. Prepr.* **1993**, *34(1)*, 812
8. Penczek, S.; Brzezinska, K. *Makromol. Chem., Macromol. Symp.* **1994**, *85*, 45
9. Matyjaszewski, K.; Penczek, S. *Makromol. Chem.* **1981**, *182*, 1735.
10. Chwialkowska, W.; Kubisa, P.; Penczek, S. *Makromol. Chem.* **1982**, *183*, 753
11. Cristau, H.J.; Plenat, F. In *The chemistry of organophosphorus compounds*; Hartley, F. R. Ed. John Wiley & Sons, Chichester, 1984, Vol. 3, p. 113
12. Hudson, H. R. In *The chemistry of organophosphorus compounds*; Patai, S. Ed.; The chemistry of functional groups; John Wiley & Sons, Chichester, 1990, Vol. 1, p. 415
13. Penczek, S.; Szymanski, R. *Polymer J.* **1980**, *12*, 617

Chapter 5

Thermodynamic Study of the Ionic Polymerization of *n*-Butyraldehyde

F. Mohamed, M. Moreau, and J. P. Vairon¹

Laboratoire de Chimie Macromoléculaire, Unité de Recherche Associée 24,
Université Pierre et Marie Curie, 4 Place Jussieu, 75252 Paris Cedex 05, France

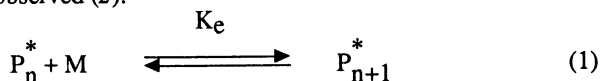
The polymerization of *n*-butyraldehyde, initiated in various solvents and in bulk with as well cationic (CF₃SO₃H, BF₃:OEt₂) as anionic (alkoxides) initiators, has been reinvestigated from -78° to +60 °C by ¹H, ¹³C NMR and UV spectrophotometry. The virtual equilibrium between the monomer and the cyclic trimer, previously reported for cationic initiation at high temperature has been confirmed over the whole temperature range. Anionic initiation in THF led to side reactions with formation of aldol derivatives. A monomer - polymer equilibrium was only observed in *n*-pentane. The thermodynamic parameters and ceiling temperatures have been determined for both anionic and cationic initiations. When using initiation by CF₃SO₃H and alkoxides, a crotonization took place for reaction temperatures above 5°C, with formation of 2-ethyl-hexenal. Using alkoxides, the polymer is rapidly formed in *n*-pentane at -78°C and slowly in THF only after initiation at -95°C. Using triflic acid, no polymer is observed even at -95°C in dichloromethane, but polymer is obtained in *n*-pentane at such a low temperature. Another way to get crystalline high polymer consists in condensing monomer vapor onto the anionic or cationic initiator solution cooled at T ≤ -50°C.

Aliphatic aldehydes are known to polymerize ionically leading to the formation of the corresponding polyacetals. The polymerization occurs via the formation of a carboxonium ion (a) in cationic polymerization and an alkoxide ion (b) in anionic polymerization (1).



¹Corresponding author

In aldehyde polymerization, the ΔH_{polym} is low and an equilibrium between polymer and monomer is observed (2):



but the aldehyde polymerization is generally favoured by formation of insoluble crystalline polymers in the medium (3).

For higher aldehydes such as n-butyraldehyde a ceiling temperature of -18°C was estimated (4) but the determination of the thermodynamic parameters is difficult due to the low reliability of the equilibrium monomer concentration measurements after deactivation (5). Moreover, in the case of n-butyraldehyde (6) and higher aliphatic aldehydes (7), cationic initiation with protic or Lewis acids led to cyclotrimerization.

In the present paper, the thermodynamic parameters of the polymerization of n-butyraldehyde initiated either cationically with $\text{CF}_3\text{SO}_3\text{H}$ (triflic acid), $\text{BF}_3\cdot\text{OEt}_2$ and SnCl_4 , or anionically with potassium and cesium alkoxides and $(\text{CH}_3)_3\text{SiOCs}$ have been reinvestigated from -78°C to $+60^\circ\text{C}$. The monomer concentration at equilibrium was determined in situ by ^1H NMR and by UV spectrophotometry (monomer absorption at 290 nm). Influence of the solvent nature on the equilibrium and on polymer formation is discussed.

Experimental

Materials. n-Butyraldehyde was purified as described in literature (5). The main distillation fraction was collected under nitrogen in a tube equipped with a Rotaflo stopcock. The monomer (GC purity higher than 99.8%) is dried under vacuum over molecular sieves for 5 days, then transferred and stored in calibrated tubes. Alcohols (tBuOH, n- $\text{C}_6\text{H}_{13}\text{OH}$) and silanol ($(\text{CH}_3)_3\text{SiOH}$) were distilled over sodium under reduced pressure and collected in a calibrated tube equipped with a stopcock.

Dichloromethane (SDS pestipur) was purified as previously described (8). After drying, under vacuum (10^{-5} mmHg), over phosphorous pentoxide and successive sodium mirrors, dichloromethane was stored in calibrated tubes equipped with a breakseal. Benzene was distilled over sodium-potassium alloy, tetrahydrofuran over sodium wires and n-pentane over CaH_2 , and stored under vacuum in calibrated tubes.

Initiators, $\text{CF}_3\text{SO}_3\text{H}$ (triflic acid, TfOH) and $\text{BF}_3\cdot\text{OEt}_2$ were purified by successive high vacuum distillations (10^{-5} mmHg) of the commercial products (Fluka) into sealed tubes. SnCl_4 (Aldrich) was distilled under nitrogen in the presence of copper cuttings. The main fraction collected in a tube equipped with a Young stopcock was transferred by distillation, under vacuum, over a sodium mirror for 2 hours at -30°C , and then into calibrated tubes equipped with breakseals.

Cesium alkoxides (tBuOCs, n- $\text{C}_6\text{H}_{13}\text{OCs}$) and silanolate $(\text{CH}_3)_3\text{SiOCs}$ were obtained in a sealed reactor by reacting an excess of the corresponding alcohol with metallic cesium. After elimination by condensation of the unreacted alcohol in a side tube, cesium salts were washed with dry benzene. After drying, known amounts of solid initiator were distributed in breakable phials. Potassium t-butoxide in THF solution (1M) was transferred under vacuum before use.

The cyclic trimer was synthesized under nitrogen at 2°C from neat n-butyraldehyde (70 ml) and $\text{BF}_3\cdot\text{OEt}_2$ (0.8 ml). After 2 hours, 5.2 ml of pyridine, and then 200 ml of dichloromethane were added. After washing with water, drying of the organic phase, dichloromethane and n-butyraldehyde were removed by distillation under reduced pressure. The crude trimer was obtained with a yield of 60%. The product was distilled and the main fraction (b.p. $107^\circ\text{C}/15$ Torr) was collected in a

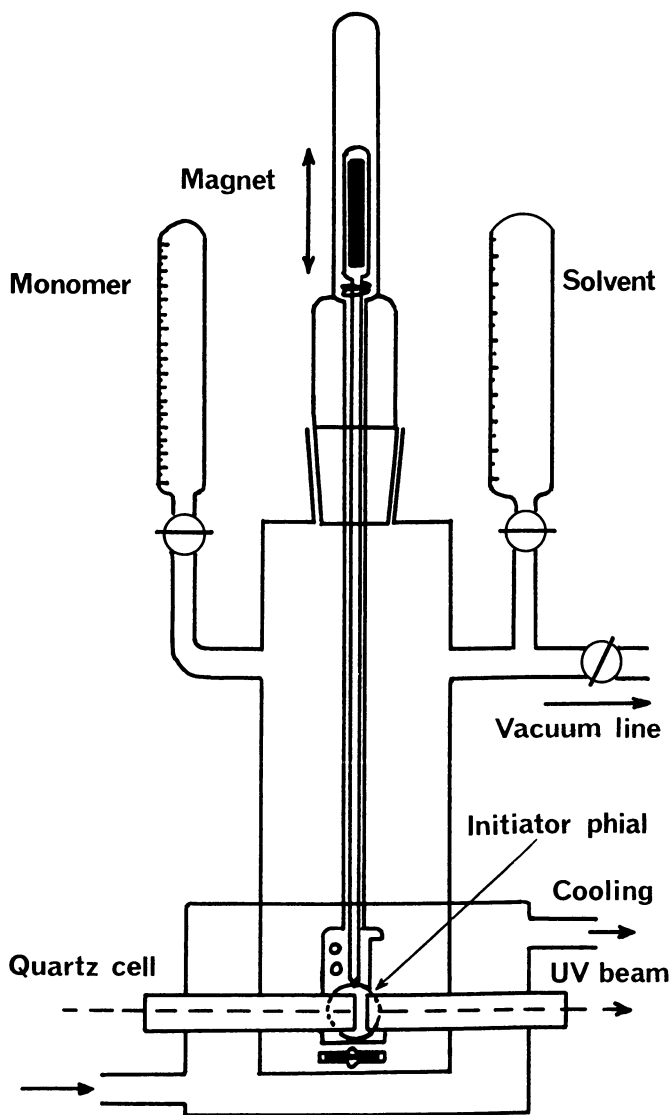
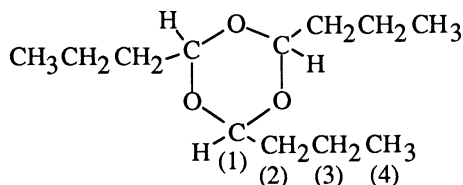


Figure 1. UV-Cell apparatus.

calibrated tube equipped with a Rotaflo stopcock. For analysis, cyclic trimer was kept with 0.5% of pyridine but for the UV-study in presence of triflic acid, pyridine was previously removed.

(2)



$\delta_{\text{ppm}} \text{ } ^1\text{H} / \text{}^{13}\text{C}$: (1) 4.85 / 102.5 (2) 1.55 / 38.1 (3) 1.45 / 18.2 (4) 0.98 / 15.0
(Ref TMS ; See Fig. 2) (m.p. -19°C ; $d_{20}^{20} = 0.919$)

Poly(*n*-butyraldehyde) synthesized for NMR analysis (see Fig. 6a) was obtained under vacuum in a sealed reactor. After introduction of the monomer and *n*-pentane by bulb-to-bulb vacuum distillation and cooling at -78°C , a phial of anionic initiator was broken in the stirred solution. Initiator (Cesium alkoxide) was insoluble in *n*-pentane but a rapid solubilization was observed in the course of the polymerization. After polymerization, the reaction was stopped by addition of cold solutions of different endcapping reagents. After elimination of the solvent, washing with acetone and drying, samples were stored under vacuum until NMR analysis. The most efficient endcapping reagent was trichloroacetylisocyanate but the most stable polymer was obtained after treatment with a pyridine - acetic anhydride solution (1 : 8) as previously observed (9).

Procedures

NMR Spectrometry. The initiators were introduced in the NMR tube either under nitrogen for the solid cesium alkoxides or silanolate, or by bulb-to-bulb vacuum distillation for TfOH and $\text{BF}_3 \cdot \text{OEt}_2$. After freezing of the initiator, the solvent and *n*-butyraldehyde were respectively introduced at low temperature by bulb-to-bulb distillation. NMR tube was sealed off at -78°C and the two layers of reagents were quickly mixed at -60°C just before analysis. A capillary of toluene- d_8 previously introduced into the NMR tube was used as external lock.

NMR spectra were recorded on Bruker spectrometers (AC 200, ARX 250).

UV Spectrophotometry. Experiments were carried out under vacuum by using a thermoregulated quartz cell (Fig.1). The reactor was equipped with UHV Young joints allowing easy connections of the calibrated tubes containing the *n*-butyraldehyde and the solvent (dichloromethane, THF or *n*-pentane). The reaction was started by breaking the initiator phial in the monomer solution, using an outside magnet. Monomer concentration was followed through its absorption at 290 nm ($\epsilon_{\text{max}} = 21.5 \text{ l} \cdot \text{mol}^{-1} \cdot \text{cm}^{-1}$ in dichloromethane, 19.8 in THF and 19.4 in *n*-pentane) using a Cary 118 spectrophotometer.

Results and Discussion

All cationic and anionic polymerizations were followed by NMR spectrometry and UV spectrophotometry.

Cationic Polymerization

The cationic polymerizations were carried out in dichloromethane and *n*-pentane solutions with monomer concentrations in the range of 1-2 M and initiator concentrations in the range of 4-16 mM for triflic acid, 16-40 mM for $\text{BF}_3 \cdot \text{OEt}_2$ and 40 mM for SnCl_4 .

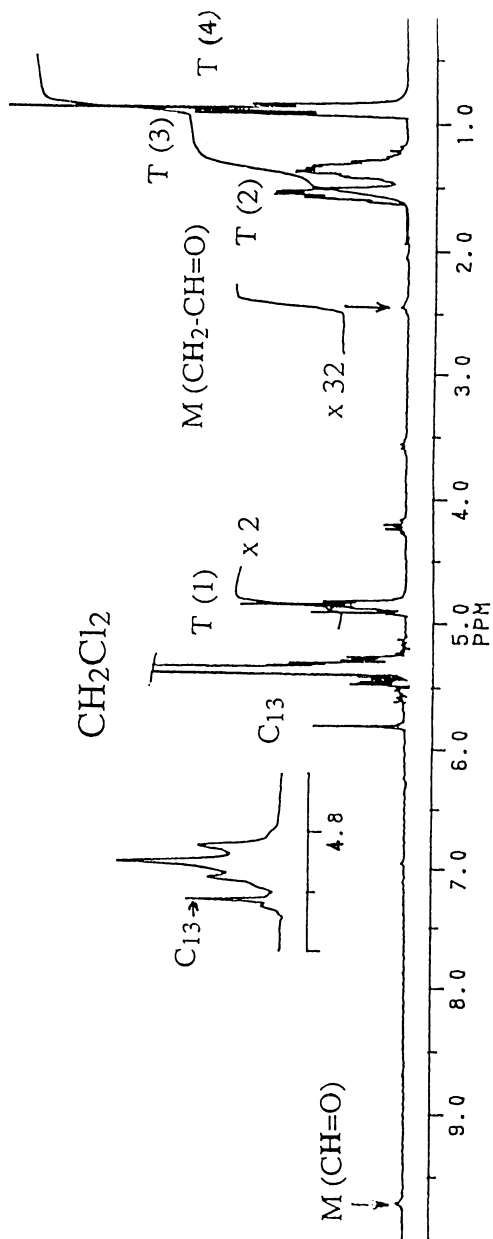
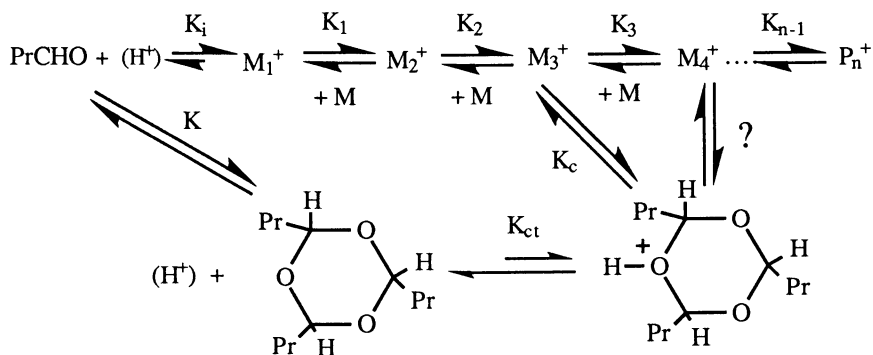


Figure 2. 200 MHz ^1H NMR spectrum after reaction of n-butylaldehyde with $\text{BF}_3 \cdot \text{OEt}_2$ in CH_2Cl_2 . $[\text{M}]_0 = 1.25 \text{ M}$; $[\text{BF}_3 \cdot \text{OEt}_2] = 40 \text{ mM}$ $T = -60^\circ\text{C}$ $t = 2 \text{ min}$.

In dichloromethane, with $\text{BF}_3 \cdot \text{OEt}_2$ as the initiator, the ^1H NMR spectrum recorded at -60°C two minutes after mixing (Fig. 2) shows the presence of only two products : a small amount of *n*-butyraldehyde (aldehydic proton at 9.74 ppm) and a major product which can be assigned to the cyclic trimer ($-\text{OCH}(\text{Pr})\text{O}-$ at 4.85 ppm identical to resonances observed for higher aliphatic aldehydes (7)). The ^{13}C NMR spectrum confirms that no band characteristic of the polymer is present (i.e. at 99.4 ppm/TMS for the acetal methine group) and that the only product formed at this temperature is the cyclic trimer (methine at 102.5 ppm). This result is in good agreement with those obtained with acetaldehyde (10).

By increasing the temperature no new products are observed. This variation of the reaction temperature modified the cyclic trimer and residual monomer concentrations indicating that the two species are in equilibrium as previously suggested (6) (see scheme 1).

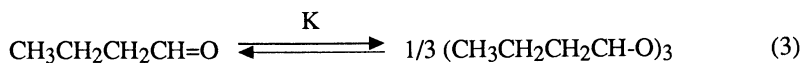
In *n*-pentane, in the same conditions of concentrations and for temperatures higher than -40°C , the monomer / cyclic trimer equilibrium was also observed by NMR, without formation of high polymer.



Scheme 1

Changing the initiators, the same species are found with SnCl_4 and $\text{CF}_3\text{SO}_3\text{H}$. With triflic acid, an absorption band near 260 nm is observed, even at low temperature, most probably due to aldol derivatives. For highest concentrations of initiator, this absorption disturbed the measurement of the monomer concentration at 290 nm whereas no products except monomer, cyclic trimer and initiator are observable on the NMR spectrum under -5°C . As observed for acetaldehyde and paraldehyde in presence of H_2SO_4 (11), at temperatures higher than 5°C , a slow crotonization took place with irreversible formation of 2-ethyl-hexenal ($\lambda_{\text{max}} = 318$ nm). Thus, with TfOH, thermodynamic parameters deduced from NMR study appeared more reliable.

If we consider the virtual cyclotrimerization equilibrium (6),



its constant is equal to :

$$K = \frac{[\text{Trimer}]_e^{1/3}}{[\text{M}]_e} \quad (4)$$

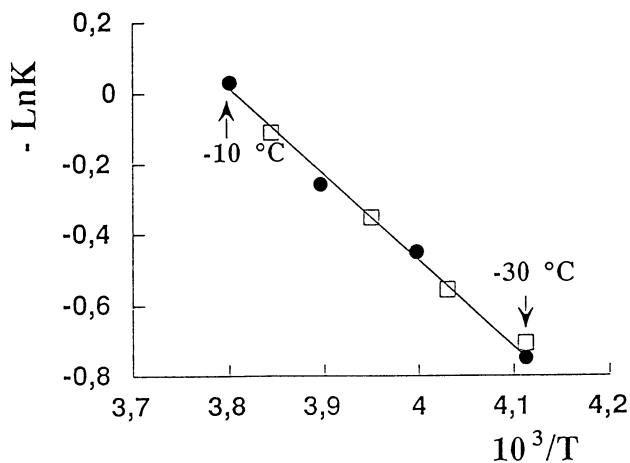


Figure 3. Variation of K with the temperature in the cationic cyclotrimerization of *n*-butyraldehyde in CH_2Cl_2 . Influence of the concentration of the initiator. $[\text{M}]_0 = 0.9 \text{ M}$ (□) $[\text{TfOH}]_0 = 6.7 \text{ mM}$ (●) $[\text{TfOH}]_0 = 3.9 \text{ mM}$

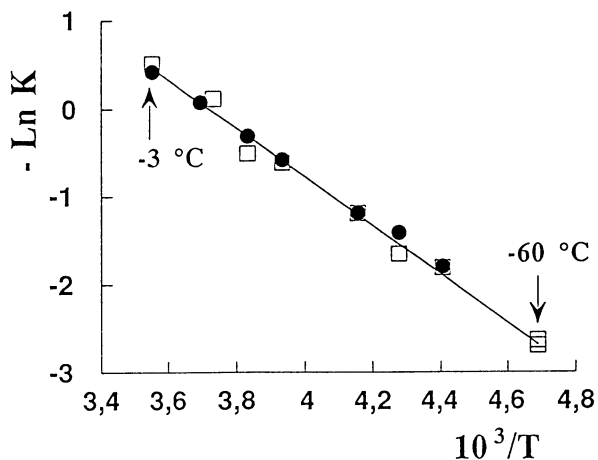


Figure 4. Variation of K with the temperature in the cationic cyclotrimerization of *n*-butyraldehyde in CH_2Cl_2 . Influence of the nature of the initiator. (□) $[\text{M}]_0 = 1.7 \text{ M}$; $[\text{TfOH}]_0 = 54 \text{ mM}$ (●) $[\text{M}]_0 = 1.25 \text{ M}$; $[\text{BF}_3 \cdot \text{OEt}_2]_0 = 40 \text{ mM}$

and different from the equilibrium constant calculated for a monomer / active polymer equilibrium (eq. 1) where $K_e = 1/[M]_e$ (considering a high \overline{DP}_n).

Linear plots of $-\ln K$ versus reciprocal temperature are obtained (see Fig. 3, 4, 5). The cyclotrimerization equilibrium is found independent of the concentration and the nature of the initiator (Fig. 3 and 4). The linear plots allow to determine the thermodynamic parameters of the cyclotrimerization in solution from

$$\Delta G/RT = -\ln K = \Delta H_{SS}/RT - \Delta S_{SS}/R \quad (5)$$

The enthalpies, entropies and critical temperatures values obtained from NMR and UV spectrophotometry are reported in table I. The critical temperature of the cyclotrimerization (T_e) corresponds to the temperature at which $K = 1$.

By comparison, in dichloromethane with $BF_3 \cdot OEt_2$, the UV and NMR techniques led to very similar values of ΔH_{SS} , ΔS_{SS} and T_e . The lower values of enthalpy and entropy determined by UV in n-pentane with triflic acid might be explained by the presence of the aldol absorption band.

The thermodynamic parameters obtained in dichloromethane ($\Delta H_{SS} = -22$ $KJ \cdot mol^{-1}$; $\Delta S_{SS} = -80$ $J \cdot mol^{-1} \cdot K^{-1}$) are lower than those previously reported ($\Delta H_{SS} = -25$ $KJ \cdot mol^{-1}$; $\Delta S_{SS} = -96$ $J \cdot mol^{-1} \cdot K^{-1}$), with a critical temperature observed at $5^\circ C$ instead of $-9^\circ C$ (6).

Starting from the cyclic trimer in dichloromethane solution and after initiation with TfOH ($[Trim]_0 = 0.3$ M; $[I]_0 = 40$ mM), an UV study showed also that a cyclic trimer - monomer equilibrium is raised which led to ΔH_{SS} and ΔS_{SS} close to the ones observed starting from monomer (see Table I). With $SnCl_4$, the same thermodynamic parameters are obtained.

Table I. Thermodynamic parameters for the cationic cyclotrimerization of n-butyraldehyde in various solvents ($K = 1$)

<i>Solvent</i>	<i>[M]₀</i> Mol.l ⁻¹	<i>Initiator</i>	<i>-ΔH_{SS}</i> KJ.mol ⁻¹	<i>-ΔS_{SS}</i> J.mol ⁻¹ K ⁻¹	<i>T_e</i> °C
n-Pentane	0.8 (c)	TfOH (a)	24 ± 1	78 ± 1	35 ± 2
	1.2	BF ₃ ·OEt ₂ (b)	32.5	103	43
	1.2 (d)	BF ₃ ·OEt ₂ (a)	30	93	49
n-Pentane/ CH ₂ Cl ₂ 80/20	1.2	BF ₃ ·OEt ₂ (a)	28	92	32
CH ₂ Cl ₂	0.8	SnCl ₄ (a)	22	80	2
	1.2	BF ₃ ·OEt ₂ (a)	24 ± 2	85 ± 5	9 ± 1
	1.25	BF ₃ ·OEt ₂ (b)	22 ± 1	80 ± 4	2 ± 1
	1.7	TfOH (b)	21.5	80	-4
Trimer	0.3	TfOH (a)	21 ± 2	70 ± 5	27 ± 5
			<i>-ΔH_{Is}</i> KJ.mol ⁻¹	<i>-ΔS_{Is}</i> J.mol ⁻¹ K ⁻¹	<i>T_e</i> °C
Bulk	11.3	BF ₃ ·OEt ₂ (b)	45 ± 1	152 ± 3	23 ± 1

(a) UV (b) NMR (c) initiation at +10°C (d) initiator in CH₂Cl₂ (2.5% in volume)

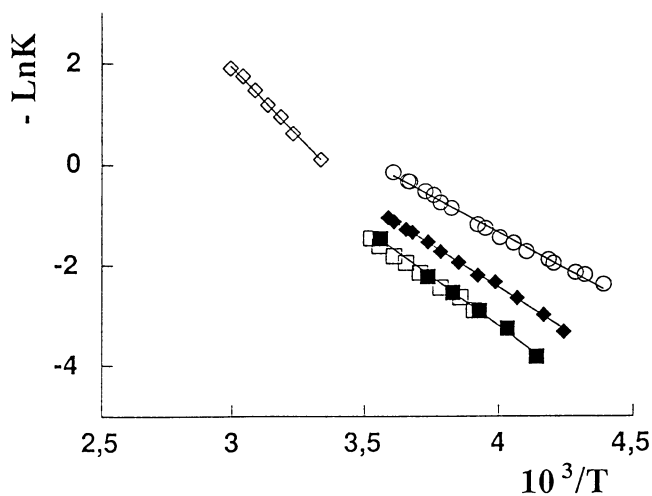


Figure 5. Variation of K with the temperature in the cationic equilibrium cyclotrimerization of *n*-butyraldehyde. Influence of the nature of the solvent .

- in solution $[M]_0 = 1.25 \text{ M}$; $[\text{BF}_3:\text{OEt}_2] = 40 \text{ mM}$
 - (O) CH_2Cl_2 (◆) *n*-pentane / CH_2Cl_2 (80 : 20) (◻) (■) *n*-pentane
- in bulk (◊) $[M]_0 = 11.3 \text{ M}$; $[\text{BF}_3:\text{OEt}_2] = 40 \text{ mM}$

By contrast, a variation of the solvent nature pointed out that cyclotrimerization in a non polar solvent such as n-pentane is more favoured than in a polar solvent such as dichloromethane. Highest values of ΔH_{SS} , ΔS_{SS} and T_e are observed in n-pentane. This is particularly true for T_e which increased from 2°C in dichloromethane to 46°C in pure n-pentane. Two experiments with a mixture of both solvents (2.5 and 20% of CH_2Cl_2) showed that the thermodynamic equilibrium is depending on the polarity of the medium (see Fig 5 and table I) as previously observed with toluene (6) and benzene (12).

Bulk reactions of the neat n-butyraldehyde (11.3 M) with $\text{BF}_3\cdot\text{OEt}_2$ (40 mM) at high temperature (25 to 60°C) showed by NMR the presence of the monomer and cyclic trimer alones, as observed by Hashimoto et al (6), but the enthalpy and entropy computed from the linear plot of $-\ln K$ vs $1/T$ (see Fig. 5) differ noticeably from the values reported by these authors.

It should be noticed that taking the values given by Hashimoto et al, and considering the cyclic trimer - monomer equilibrium, a correct linear plot of $-\ln K$ versus reciprocal temperature is also obtained, with no significant upward deviation as considered by these authors. But the thermodynamic parameters deduced from the corresponding plot ($\Delta H_{1S} = -23 \text{ KJ.mol}^{-1}$; $\Delta S_{1S} = -78 \text{ J.mol}^{-1} \text{ K}^{-1}$) are similar to those we observed in dichloromethane and definitively different that the ones we obtained in bulk, even if the values of T_e are very close (23 °C) (see Table I).

Considering the low polarity of the cyclic trimer (6), the high enthalpy and entropy determined in bulk should be closer to those obtained in n-pentane.

Although it seemed that only the cyclic trimer could be obtained at very low temperature, a rapid polymerization, with formation of an insoluble high polymer, took place at -95°C in n-pentane with TfOH initiation ($[\text{M}]_0 = 3.25 \text{ M}$; $[\text{TfOH}]_0 = 11.2 \text{ mM}$ in a phial of dichloromethane). At this temperature, with the same concentrations, no polymer is obtained in dichloromethane. This might be explained by a competition at -95°C between polymerization and backbiting of the active polymer, more especially endbiting of M_3^+ , with formation of the stable cyclic trimer (see scheme 1), and/or by the poor solubility and favoured crystallization of the growing polymer in n-pentane compared to dichloromethane.

Anionic Polymerization

In THF, the NMR study of the reaction at -60°C of n-butyraldehyde ($[\text{M}]_0 = 1.7 \text{ M}$) with tBuOCs or tBuOK (60 mM) showed an almost complete consumption of the monomer with no apparent formation of polymer. Obviously the cyclic trimer cannot be anionically formed. In the spectrum (Fig. 6b) a weak but broad band is observed near 8 ppm due to the presence of hydroxy groups in the solution. By comparison with anionic poly(n-butyraldehyde) (Fig. 6a), other resonances are observed between 4 and 5 ppm which might be assigned to acetal and hydroxy derivatives (oligomers?). Increasing the temperature of the reacting medium slightly modified the concentration of the different species present in the solution but strongly changed the chemical shift of the hydroxy groups. Above 5°C, crotonization took place and 2-ethyl-hexenal was slowly formed implying the presence of aldol, even at low temperatures.

The UV study in THF confirmed the NMR observations. After initiation with tBuOK (or tBuOCs) in the range of -50°C - -78°C, only a few percents of monomer remained. Increasing the temperature up to -10°C modified slightly this low monomer concentration but no equilibrium was found. The observation at -78°C of a broad absorption band at 250 - 260 nm agreed also with possible aldol formation at low temperature.

In THF, polymer is only obtained when the initiation by tBuOK is performed at -95°C. After introduction of the initiator, the solution was kept 4 hours at -95°C. In

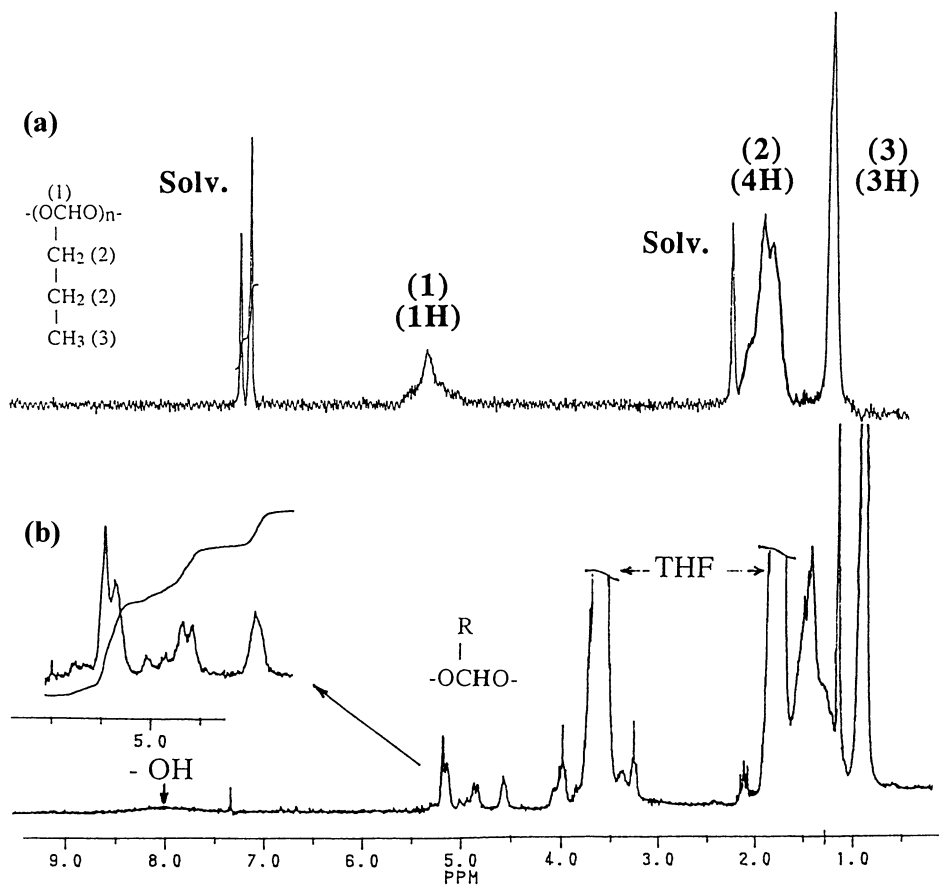


Figure 6. 200 MHz ^1H NMR spectra of anionic poly(*n*-butylaldehyde) in toluene- d_8 at 80°C (a) and after the reaction of *n*-butylaldehyde with *t*BuOK in THF (b). $[\text{M}]_0 = 1.7 \text{ M}$; $[\text{tBuOK}]_0 = 60 \text{ mM}$; $T = -60^\circ\text{C}$

Conclusion

NMR and UV spectrophotometry studies of the ionic polymerization of n-butyraldehyde showed that using the conventional way of polymerization (introduction of the initiator into the monomer solution) the monomer-polymer equilibrium strongly depends on solvent nature, on the type of initiation and on temperature.

In case of cationic initiation an equilibrium between the cyclic trimer and the monomer, without formation of high polymer, is always observed in dichloromethane but only in the range of -40 - +60°C in n-pentane. The increase of enthalpy and entropy of the cationic cyclotrimerization observed with BF₃:OEt₂ in dichloromethane, n-pentane and in bulk is in agreement with the former proposal of Vogl (16, 17) who explained this increase by aggregation of the aldehyde molecules through dipolar interactions. This aggregation is modified by changing dielectric constant of the medium, and increases from dichloromethane to n-pentane. The low polarity of the cyclic trimer (6) and the high monomer concentration could explain the higher values observed in bulk for thermodynamic parameters.

For anionic initiation, in polar solvents, side reactions like aldolization can be observed but in non polar solvents like n-pentane, aldolization appears very limited at low temperature and this can explain the high polymer formation in n-pentane at T ≤ -50°C as it has been already observed for aliphatic aldehydes (5).

The large endothermicity of the dissolution of the monomer, the poor solubility and the crystallization of the growing polymer at low temperature in non polar solvents such as n-pentane compared to polar solvents such as THF and dichloromethane might favour the formation of high polymer (16).

References

- (1) Vogl, O. *Plastiques* **1965**, 2 (3), 224
- (2) Kubisa, P. ; Vogl, O. *Polymer* **1980**, 21, 525
- (3) Kubisa, P. ; Neeld K. ; Starr J. ; Vogl, O. *Polymer* **1980**, 21, 1433
- (4) Vogl, O. *J. Macromol. Sci.* **1967**, A1 (2), 243
- (5) Vogl, O. *J. Polym. Sci.* **1964**, part A , 2, 4607
- (6) Hashimoto, K.; Sumimoto, H.; Ohsawa, S. *J. Polym. Sci.* **1977**, 15, 1609
- (7) Starr, J. ; Vogl, O. *J. Macromol. Sci.* **1978**, A12 (7), 1017
- (8) Sauvet, G.; Vairon, J. P.; Sigwalt, P. *Bull. Soc. Chim. Fr.* **1970**, 403
- (9) Vogl, O. *Belg. Pat.* n° 580,553 **1959**
- (10) Vogl, O. *J. Polym. Sci.* **1964**, part A , 2, 4591
- (11) Delépine, M. *Compt. Rend. Ac. Fr.* **1908**, 147, 1316
- (12) Ogorodnikov, A.L. ; Katsnel'son, M.G. ; Pinson, V.V. ; Levin, Yu.V. *Zh. Prikl. Khim.* **1990**, 63, 1340
- (13) Takida, H. ; Noro, K. *Kobunshi Hagaku* **1964** , 21, 467
- (14) Mita, I. ; Imai, I. ; Kambe, H. *Makromol. Chem.* **1970**, 137, 169
- (15) Hashimoto, K.; Sumimoto, H.; Ohsawa, S. *J. Polym. Sci.* **1976**, 14, 1221
- (16) Vogl, O. ; Bryant, W.M.D. *J. Polym. Sci.* **1964**, part A , 2, 4633
- (17) Schneider, W. G. ; Bernstein, H. J. *Trans. Faraday Soc.* **1956**, 52, 13

Chapter 6

Stability of Propagating Species in Living Cationic Polymerization of Isobutylene

Daniela Held¹, Béla Iván^{1,3,4}, Axel H. E. Müller¹, Feike de Jong²,
and Teun Graafland²

¹Institute of Physical Chemistry, University of Mainz, Welderweg 15,
D-55099 Mainz, Germany

²Shell Research and Development Centre, Postbus 3033, NL-1003 AA,
Amsterdam, Netherlands

The stability of living polyisobutylene chains (PIB) obtained by di- and monofunctional initiators in conjunction with TiCl_4 coinitiator was investigated under monomer starved conditions (i. e. after 100 % monomer conversion) in the absence and presence of different additives, such as *N,N*-dimethylacetamide (DMA), 2,6-di-*tert*-butylpyridine (*DtBP*), pyridine (Py) and 2,4-dimethylpyridine (DMPy), in CH_2Cl_2 /hexane (40:60 v/v) mixture at -78°C . Only negligible amounts of chain ends with expected double bonds were formed as verified by ^1H NMR, and all the additives, with the exception of *DtBP*, resulted in constant molecular weights for a period of four hours. However, chain coupling occurred in the presence of *DtBP*. On the basis of our experimental findings this effect is interpreted by proton abstraction in a reaction between *DtBP* and propagating chains leading to external double bonds which further react with active chain ends. Molecular weight distribution data indicate that there are differences among the examined nucleophilic compounds in their mode of action during living polymerization of isobutylene.

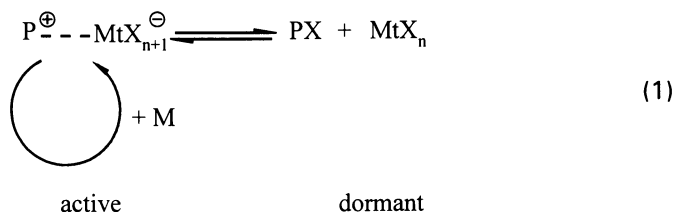
There have been significant developments in the field of living carbocationic polymerization (LCCP) during the past few years (see Refs. 1-5 for recent reviews). LCCP offers process control for the synthesis of a wide variety of novel materials with potential commercial interest. These include new macromonomers, telechelics, polymers with pendant functional groups (liquid crystalline homo- and copolymers, non-linear optical materials etc.), star-shaped macromolecules, block and graft copolymers (thermoplastic elastomers, amphiphilic blocks), cyclic

³Permanent address: Central Research Institute for Chemistry of the Hungarian Academy of Sciences, Puzstaszeri u. 59-67, P.O. Box 17, H-1525 Budapest, Hungary

⁴Corresponding author

macromolecules and specialty networks (polyurethanes, polyepoxides, ionomers and amphiphilic networks as potential new biomaterials) (1-5).

LCCP is a process in which active (propagating) chains are in equilibrium with dormant (inactive) species (1,6-8). For instance, halogen-terminated chains (P-X) are in equilibrium with the active species (P^{\oplus}) propagating by monomer addition in living polymerization of olefins, such as isobutylene and styrene and its derivatives, in the presence of Lewis acids (MtX_n), e. g. BCl_3 , $TiCl_4$, SnX_4 ($X = Cl, Br$) etc.

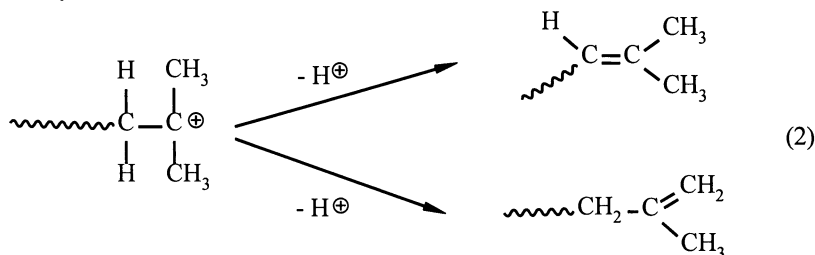


On the basis of this mechanistic scheme, a kinetic model has been recently developed by us to evaluate LCCP systems of alkyl vinyl ethers and decomposition of propagating species in such polymerizations (9).

Most of the LCCP systems contain either a nucleophilic additive (also referred to as Lewis base or electron donor), such as esters, ethers, amines, amides etc. (see Refs. 1-5 for review), chelating compounds (10), or a tetraalkylammonium salt (11-15). In the current practice, six major classes of additives are used to mediate LCCP of isobutylene (IB): (1) inert nucleophiles (DMA, dimethylsulfoxide, N-methyl-pyrrolidone, esters etc.) (see Refs. 1-5 for review), (2) strong bases, such as Py and DMPy (16,17), (3) DtBP proton trap (18,19), (4) chelating agents, such as 2,5-pentandione and N,N,N',N'-tetramethylethylenediamine (10), (5) inhibitors (*inhibitor* + *retarder* agent) (1), (6) tetra-*n*-butylammoniumchloride (13,14). The exact role of these compounds has not been completely revealed yet, and there are several interpretations on their beneficial effects for LCCP to occur: (i) by pushing the ionic equilibria through interaction of the nucleophilic additives or their complexes with carbocations towards less reactive cationic species which are in equilibrium with dormant terminated chains as shown in equation 1 (1), (ii) by serving as a proton trap exclusively, as in the case of DtBP proton trap (19), and (iii) by forming dormant onium-type chain ends, as in the case of ethers and thioethers (20), which are in equilibrium with reactive ion-pairs and free ions that propagate by "classical" carbocationic polymerization.

On the basis of "classical" carbocationic polymerizations, decomposition of the propagating carbocationic species is expected to lead to proton expulsion and formation of a double bond at chain ends as in chain transfer processes. This process is viewed to result from hyperconjugation between the inherently instable carbocationic center and neighboring protons (1) leading to proton expulsion and formation of a π -bond. In polymerization of IB, this means the appearance of *exo* and *endo* olefinic endgroups by chain transfer (see equation 2). Polyisobutylene (PIB) chains with external double bond terminus are able to react with the polymeric

carbocations leading to coupling of PIB molecules, i. e. to increase of molecular weight (MW). It is expected that internal double bond containing PIBs do not react further because of steric hindrance. Therefore, proton expulsion in LCCP of IB under monomer starved conditions (i. e. after complete monomer consumption) can be detected by chain end structure and MW determinations.



The stability of propagating species, that is their ability to participate only in the desired propagation and to avoid side reactions leading to permanently terminated polymer chains, is a critical factor not only for the fundamental understanding of particular living polymerization processes but it is important from synthetic and technological point of view as well. This chapter deals with the results of our recent systematic investigations carried out to obtain information on the effect of different nucleophilic additives on the stability of active (propagating) species in isobutylene (IB) polymerization under monomer starved conditions.

Results and Discussion

The Effect of Different Additives on the Chain End Structure and on Molecular Weight Distributions of PIBs Obtained by Difunctional Initiator. On the basis of the above thoughts, IB polymerizations initiated by a difunctional initiator, 1,3-di(2-chloro-2-propyl)-5-*tert*-butylbenzene (*t*BuDiCumCl), in conjunction with TiCl_4 in the presence of different additives, such as DMA, *Dt*BP, Py and DMPy, were allowed to run to complete monomer conversions (reached in less than five min); then samples were withdrawn at predetermined time intervals up to four hours as described in the Experimental Section. For all the additives, a yellow to red precipitate was observed on the addition of TiCl_4 to the solution of initiator, monomer and additive. Since precipitates were not observed in IB polymerization in the absence of additives, the formation of a Lewis base - Lewis acid complex is assumed in line with earlier results (1,18). On addition of methanol, the complex dissolved and discolored immediately for DMA, *Dt*BP and DMPy. In case of Py, the discoloration was very slow. At the reaction time of four hours, a second portion of monomer was charged to the polymerization system in order to check the activity of the chains toward further polymerization.

Surprisingly, significant amounts of double bond containing chain ends were not detected even after four hours of standing under monomer starved conditions, i. e. in polymerization systems with 100 % monomer conversion, neither in the absence

nor in the presence of the different additives. Data obtained by molecular weight determination with GPC indicate lower than theoretical initiating efficiencies at complete monomer conversion in all cases. However, as shown in Table 1, the molecular weights and polydispersities (M_w/M_n) of PIBs did not change in the presence of DMA, Py and DMPy after complete monomer conversion was reached. Negligible changes in molecular weight distribution (MWD) were obtained in the absence of additives and in the presence of DMA, and no changes occurred in the MWD in the presence of Py and DMPy for four hours. However, as indicated in Table 1 and Figure 1, MWs of PIB initiated by *t*BuDiCumCl, a bifunctional initiator, significantly increased in the presence of *Dt*BP. As shown in Figure 1, the GPC traces of PIBs obtained in the presence of *Dt*BP after quenching at 5, 60 and 240 mins clearly exhibit that PIB chains with higher MW are formed even after 100 % monomer conversion. This means that chain coupling of PIB molecules formed by LCCP of IB occurs in the presence of *Dt*BP. The extent of coupling depends on the concentration of *Dt*BP. Higher *Dt*BP concentration leads to higher rates and extents of PIB chain coupling as data indicate in Table I.

Table I. M_n and M_w/M_n as a function of time in isobutylene polymerization by the *t*BuDiCumCl/TiCl₄ initiating system in the absence and presence of different additives (see Experimental Section for polymerization conditions)

Time (min)	$M_n \cdot 10^3 (M_w/M_n)$					
	-	DMA	Py	DMPy	<i>Dt</i> BP	<i>Dt</i> BP ^a
5	7.04	7.49	8.96	6.96	9.76	7.01
	(2.53)	(1.29)	(1.16)	(1.43)	(1.54)	(1.31)
10	7.55	7.44	9.08	6.86	10.4	7.12
	(2.40)	(1.34)	(1.15)	(1.49)	(1.52)	(1.26)
30	7.84	7.43	8.71	6.88	10.5	7.43
	(2.37)	(1.32)	(1.17)	(1.44)	(1.74)	(1.31)
60	7.17	7.48	8.67	7.09	11.0	7.90
	(2.74)	(1.33)	(1.18)	(1.46)	(1.75)	(1.30)
120	8.08	7.48	8.53	7.09	12.0	8.12
	(2.35)	(1.31)	(1.21)	(1.46)	(1.71)	(1.35)
180	8.04	7.39	8.40	6.97	12.6	7.93
	(2.40)	(1.34)	(1.21)	(1.46)	(1.73)	(1.38)
240	8.55	7.37	8.44	7.14	12.3	7.86
	(2.30)	(1.32)	(1.22)	(1.45)	(1.77)	(1.36)
250 ^b	-	-	11.4	10.8	21.3	-
			(1.39) ^c	(1.49)	(1.70)	

^a $[t\text{BuDiCumCl}]_0/[Dt\text{BP}] = 1$

^b IB added to the remaining solution after 240 min: $\Delta[\text{IB}] = 0.89 \text{ M (Py)}, 0.99 \text{ M (DMPy)},$ and 0.89 M (DtBP)

^c Bimodal

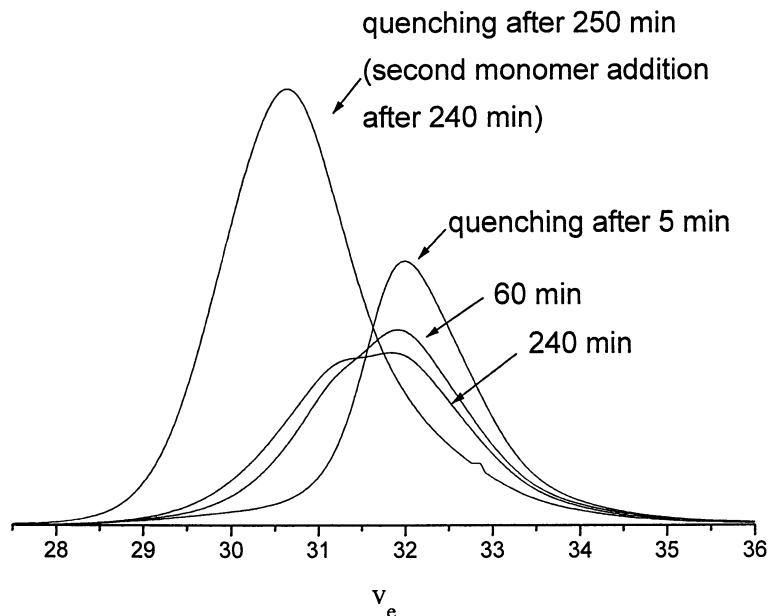


Figure 1. GPC traces of PIB obtained by *t*BuDiCumCl in the presence of *Dt*BP at different times.

The GPC trace of PIB obtained by adding IB to the polymerization system after four hours reaction time is also displayed in Figure 1. According to this Figure, higher MW polymer was formed, i. e. polymer chain ends were still active after four hours in this LCCP system of isobutylene. Similar observations were obtained in the presence of other additives as shown by data in the last row in Table I.

It is noteworthy that the MWDs are different in the presence of the different additives under identical conditions as indicated by the M_w/M_n data in Table I. This reflects that there are differences in their mode of action which affect the kinetics of LCCP of isobutylene. In other words, the mode of action of nucleophilic additives in LCCP of olefins is most likely a complex process, and the differences indicate that a simple interpretation, such as exclusive proton scavenging (19) by all the known additives, is not sufficient as explanation for the occurrence of LCCP.

Chain End Stability of Monofunctional PIBs under Monomer Starved Conditions. The surprising chain coupling which occurred in the presence of *Dt*BP was further studied by using monofunctional TMPCl as initiator for LCCP of IB. Theoretically, a bifunctional initiator can act not only as an initiating entity but also as chain coupling agent. This effect can be completely avoided by using monofunctional initiator, i. e. if chain coupling would also occur in this case it would exclusively involve reactive chain ends. Figure 2 shows the GPC traces of PIBs prepared by 2-chloro-2,4,4-trimethylpentane (TMPCl) as initiator for LCCP of IB in

the presence of *DtBP* at 5, 60 and 240 mins reaction times, i. e. after 100 % monomer conversion. As this Figure indicates, similar coupling phenomenon is observed as with the bifunctional initiator. These experiments prove that coupling under monomer starved conditions occurs by a reaction between two PIB chains. It is also exhibited in Figure 2 that increase of MW can be obtained when a second charge of monomer was added after four hours of reaction time.

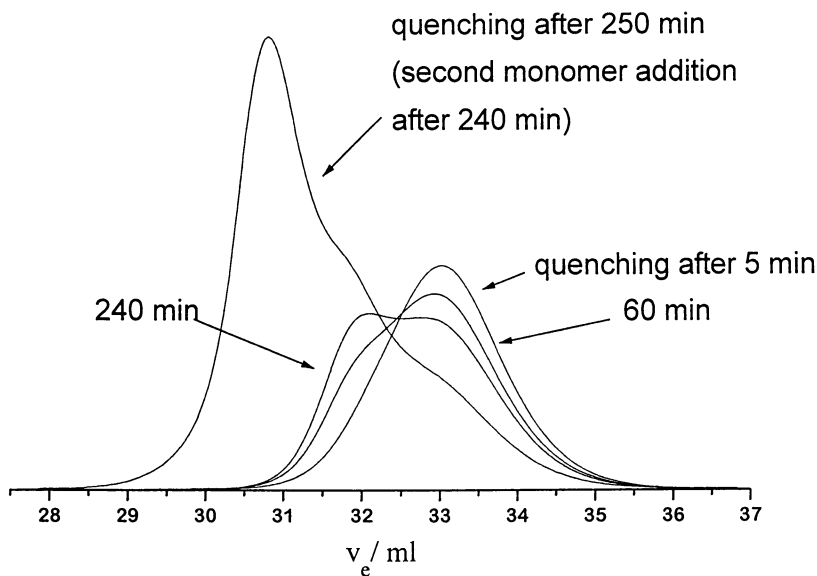
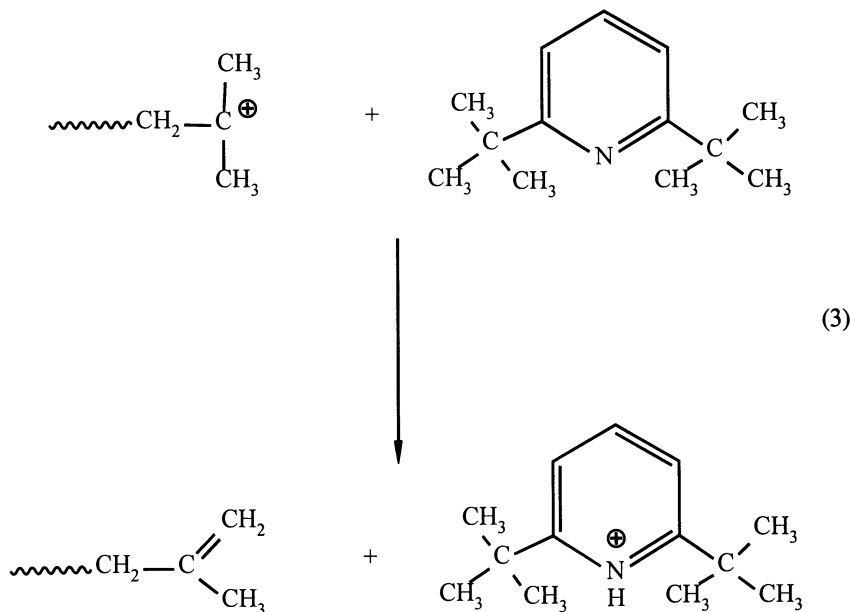


Figure 2. GPC traces of PIB obtained by TMPCl in the presence of *DtBP* at different times.

Under monomer starved conditions, molecular weight increase was not observed with PIBs prepared by TMPCl in the presence of DMA, Py and DMPy in accordance with experimental findings described in the previous section for polymers obtained by the difunctional initiator. These results also indicate that the equilibrating propagating species and terminated polymer chains as shown in equation 1 possess long stability in the presence of nucleophilic additives.

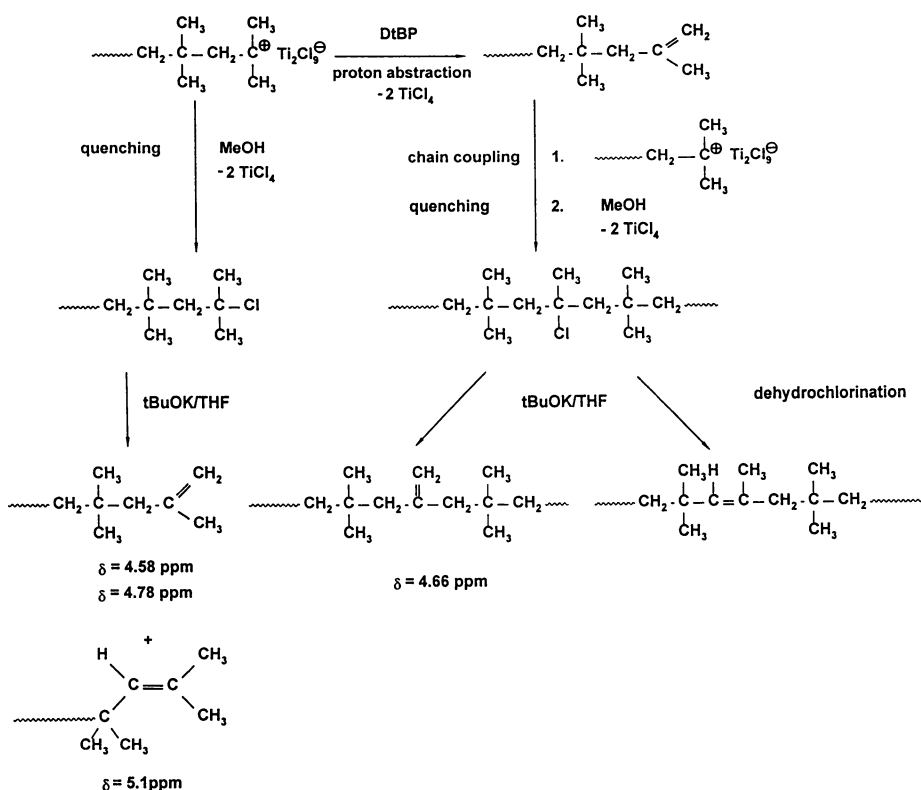
The Mechanism of Chain Coupling in the Presence of *DtBP*. Experiments with TMPCl (see previous Section) proved that chain coupling occurs by a direct interaction between two PIB chains in the presence of *DtBP*. Regular proton expulsion by "classical" carbocations would theoretically lead to 25 % *endo* and 75 %

exo olefinic chain ends. The *exo* olefins can react with polymeric carbocationic species leading to chain coupling. Due to steric hindrance the *endo* olefins would not take part in such reactions, and these double bonds could be detected in PIBs after quenching the polymerization systems. However, neither external nor internal olefins were detected by ^1H NMR in PIBs obtained in the presence of *DtBP* after four hours of reaction time. This means that *exo* olefins leading to chain coupling were not formed by a classical chain transfer process. The concentration dependence of chain coupling in the presence of *DtBP* as shown by the experimental results in Table I indicates that *DtBP* is directly involved in the formation of external olefins. *DtBP* is a widely known proton trap, and it has been claimed that it interacts only with protons and does not react with other species, such as Lewis acids and carbocations (19,21-23). This means that in contrast to other basic additives, which form strong complexes with Lewis acids, free *DtBP* exists in TiCl_4 cointiated LCCP of IB. It is postulated by us that this free *DtBP* abstracts a proton from a methyl group of the propagating chain ends leading exclusively to external double bonds as shown in equation 3. The resulting polymer is an isobutenyl ended PIB macromonomer which quickly reacts with the active cationic species yielding chain coupling. Due to steric hindrance proton abstraction cannot take place from the $-\text{CH}_2-$ methylene group next to the carbocation by *DtBP*. Therefore *endo* olefins cannot be detected even after long reaction times.



The coupling process and the structure of the resulting polymer were verified by dehydrochlorination experiments. As shown in Scheme 1, when only low extent of coupling occurs, *tert*-chlorine chain ends are formed and dehydrochlorination by

*t*BuOK yields $\sim\text{CH}_2\text{-C}(\text{CH}_3)=\text{CH}_2$ chain ends (24) together with low concentrations of $\sim\text{CH}=\text{C}(\text{CH}_3)_2$ *endo* olefins ($\sim 3\text{-}8\%$ of total double bonds) (25-27). Indeed, as shown in Figure 3, after dehydrochlorination, the characteristic signals at 4.58 and 4.78 ppm appear in the ^1H NMR spectrum of PIB that was produced with a 5 min reaction time. A small peak can be also observed at 4.64, 4.74 and 5.1 ppm. The latter is attributed to the *endo* olefinic proton (26,27) while the signals at 4.64 and 4.74 ppm indicates the presence of pendant $\sim\text{CH}_2\text{-C}(\text{CH}_3)=\text{CH}_2$ and most likely internal $\sim\text{CH}=\text{C}(\text{CH}_3)\text{-CH}_2\sim$ olefinic groups, respectively. Figure 4 exhibits the ^1H NMR spectrum, after dehydrochlorination with *t*BuOK, of PIB that was produced with a 240 min reaction time. Comparison of Figures 3 and 4 clearly indicates that the relative ratios between the NMR signals of *exo* and pendant olefin groups significantly decreased. The majority of double bonds in the dehydrochlorinated PIB with 240 mins reaction time is in the form of pendant olefinic groups. As shown in Scheme 1, proton abstraction by *Dt*BP yields *exo* olefins which react with cationic chain ends leading to chain coupling. Termination of the coupled PIB gives a pendant *tert*-chlorine group the dehydrochlorination of which by *t*BuOK results in the pendant double bond.



Scheme 1

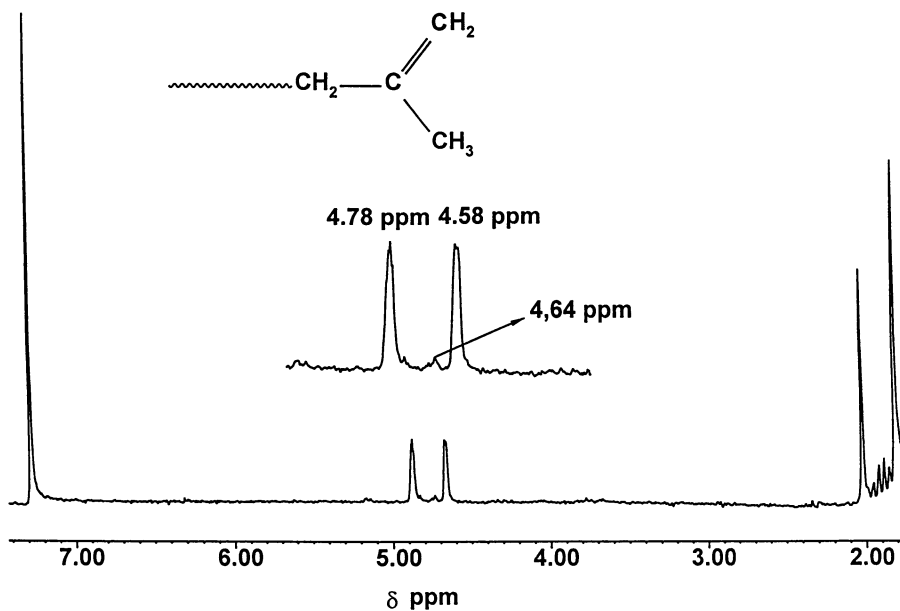


Figure 3. ¹H NMR spectrum of monofunctional PIB with 5 mins reaction time after dehydrochlorination with *t*BuOK.

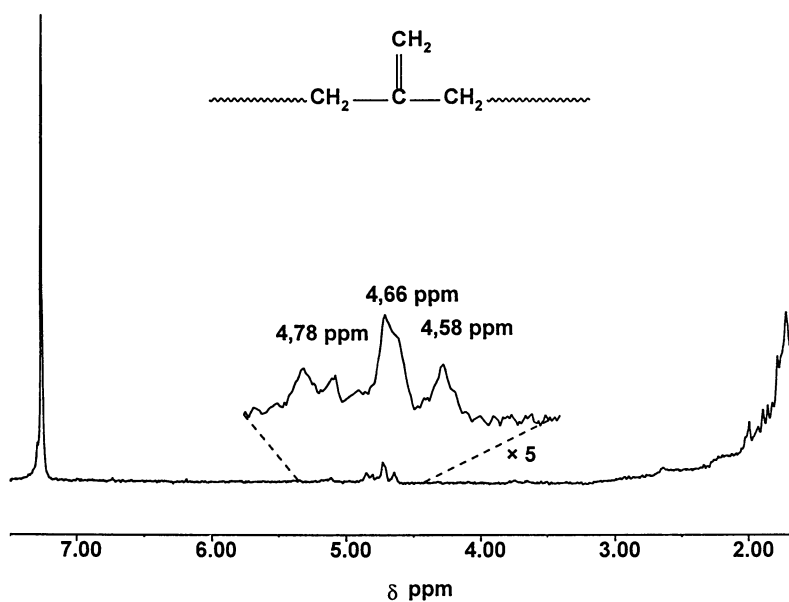


Figure 4. ¹H NMR spectrum of monofunctional PIB with 240 mins reaction time after dehydrochlorination with *t*BuOK.

Conclusions

In line with earlier findings (30-32), the plausible explanation of the results obtained in the presence of *DtBP* is abstraction of a proton by free *DtBP* from the methyl groups adjacent to the cationic center as shown in equation 3. Due to steric reasons this process leads exclusively to external double bonds and forms isobutenyl ended macromonomers which quickly react with the active cationic species. Although the other additives, such as Py and DMPy, are strong bases as well, free additives are most likely absent in the polymerization systems containing these compounds since they form strong complexes with Lewis acids.

It could also be argued that proton expulsion might occur in all LCCP systems through the gegenion, and terminal double bonds and HCl are formed. In the presence of additives forming complexes with the Lewis acids, complete hydrochlorination of double bonds takes place immediately, and olefinic chain ends cannot be detected. If spontaneous proton expulsion would occur, free *DtBP* as proton trap captures the protons, and the *exo* olefins from the ensuing double bonds react with the carbocationic species leading to chain coupling. One can argue that because sterically hindered non-reactive internal (*endo*) olefins were not detected, this explanation has no sufficient ground, and the existing data indicate direct proton abstraction by free *DtBP*. Therefore protonation of the double bond can be imagined only by assuming reversible proton trapping by *DtBP*, i. e. efficient protonation-deprotonation equilibrium for protonation of the internal double bonds by the proton released from the proton trap. It has also to be noted that in case of the existence of spontaneous proton expulsion followed by re-hydrochlorination, proton scavenging by the nucleophilic additives, or more precisely by the Lewis acid-Lewis base complexes, in LCCP (19) cannot be accepted as explanation for the effect of these compounds in such polymerization systems. However, these complexes prevent initiation by protic impurities, such as H₂O, indicating efficient proton scavenging. Therefore there is no reason to doubt that scavenging the much stronger protic acid, HCl, if it was formed, also occurs in the presence of all the nucleophilic additives, on the one hand. If proton trapping was rapidly reversible, it would also prevent coupling with the involvement of the *exo* olefins, on the other hand. Thus, on the basis of the currently available results one must conclude that spontaneous β -proton expulsion does not take place in the presence of additives mediating LCCP of IB, i. e. chain coupling is the result of direct, bimolecular abstraction of the β -protons from the carbocationic species in the investigated living polymerization systems.

In all the investigated polymerizations in the presence of additive, MW increased by adding a new charge of isobutylene after four hours of standing under monomer starved conditions indicating the living nature of these polymerizations even after such extremely long reaction times. These results indicate that the propagating species are unexpectedly stable in LCCP of isobutylene in the investigated polymerization systems. Comparison of our new experimental results also indicates that the different additives influence the polymerization process differently. This is clearly shown by M_w/M_n data in Table I.

Data obtained in this study also provide some basis for a critical evaluation of the different mechanistic schemes proposed for LCCP so far, i. e. (1) LCCP occurs by "classical" propagating species (free cations and contact ion pairs) (20), and (2) non-dissociated species (stretched covalent bonds) are the active (propagating) species (1). One would expect detectable proton expulsion in the absence of monomer if the active chain ends were "classical" ion pairs and/or free cations. However, as results of our studies under monomer starved conditions indicate, the active sites show significant stability in LCCP of isobutylene.

There are also different opinions on the mode of action of additives in LCCP of olefins: (1) the Lewis acid (MtX_n) forms a strong complex with the nucleophilic additive and this complex with reduced nucleophilicity mediates LCCP (see *Ref. 1* and references therein), (2) the only role of all the nucleophilic additives (DMA, Py, DMPy etc.) is proton scavenging similar to that of *DtBP* (19). If the sole role of nucleophilic additives was only proton scavenging, then exactly the same results should have been obtained under identical conditions with all the additives. *DtBP* suppresses chain transfer during polymerization (19), i. e. in the presence of monomer. However, it leads to MW increase in the absence of monomer due to proton abstraction from the chain ends.

Experimental

Initiator (1,3-di(2-chloro-2-propyl)-5-*tert*-butylbenzene, *t*BuDiCumCl) was synthesized as described (16). $TiCl_4$, N,N-dimethylacetamide (DMA), 2,6-di-*tert*-butylpyridine (*DtBP*), pyridine (Py) and 2,4-dimethylpyridine (DMPy) (all from Aldrich) were used as received. Solvents and IB were purified as described (28). LCCP was carried out by a simple conventional laboratory technique (28,29) in 40:60 v/v CH_2Cl_2 -hexane mixture at $-78\text{ }^\circ C$; $[tBuDiCumCl]_0 = [additive]/2 = [TiCl_4]/32 = 0.01\text{ M}$, $[IB]_0 = 0.88\text{ M}$. Samples were withdrawn at predetermined times and quenched with prechilled methanol. A second charge of IB was added to the polymerization mixture after 4 hours, and it was allowed to polymerize for additional 10 mins. After evaporation of the solvent mixture the polymer was dried in vacuo at room temperature. Molecular weight averages and MWD were determined with GPC calibrated with PIB standards. 1H NMR spectra were recorded in $CDCl_3$ on a Bruker AC-200 equipment.

Acknowledgments: This study was supported by Shell Research BV, Amsterdam.

Literature Cited

1. Kennedy, J. P.; Iván, B. *Designed Polymers by Carbocationic Macromolecular Engineering: Theory and Practice*, Hanser Publishers: Munich, New York, 1992
2. Iván, B.; Kennedy, J. P. In *Macromolecular Design of Polymeric Materials*; Hatada, K; Kitayama, T.; Vogl, O., Eds.; Marcel Dekker: New York, 1996; pp. 51-84

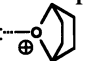
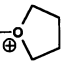
3. Iván, B; Kennedy, J. P. *Ind. J. Technol.* **1993**, *31*, 183
4. Iván, B. *Makromol. Chem., Macromol. Symp.* **1993**, *75*, 181
5. Sawamoto, M. *Prog. Polym. Sci.* **1991**, *16*, 111
6. Iván, B; Kennedy, J. P. *Macromolecules* **1990**, *23*, 2880
7. Iván, B. *Makromol. Chem., Macromol. Symp.* **1993**, *67*, 311
8. Iván, B. *Macromol. Symp.* **1994**, *88*, 201
9. Iván, B.; Müller, A. H. E. In *Preprints of 11th IUPAC Symp. on Cationic Polymerization and Related Processes*; Borovets, July 5-8, 1993; p. 44
10. Ref. 1, pp. 37, 64
11. Ishihama, Y.; Sawamoto, M.; Higashimura, T. *Polym. Bull.* **1990**, *23*, 361
12. Ishihama, Y.; Sawamoto, M.; Higashimura, T. *Polym. Bull.* **1990**, *24*, 201
13. Pernecker, T.; Kennedy, J. P. *Polym. Bull.* **1991**, *26*, 305
14. Pernecker, T.; Kennedy, J. P.; Iván, B. *Macromolecules* **1992**, *25*, 1642
15. Lin, C. H.; Xiang, J. S.; Matyjaszewski, K. *Macromolecules* **1993**, *26*, 2785
16. Storey, R. F.; Lee, Y. *J. Macromol. Sci.-Pure Appl. Chem.* **1992**, *A29*, 1017
17. Storey, R. F.; Choate, K. R., Jr. *Macromol. Symp.* **1995**, *95*, 71
18. Faust, R.; Iván, B.; Kennedy, J. P. *J. Macromol. Sci.-Chem.* **1991**, *A28*, 1
19. Gyor, M.; Wang, H.-C.; Faust, R. *J. Macromol. Sci.-Pure Appl. Chem.* **1992**, *A29*, 639
20. Matyjaszewski, K.; Sigwalt, P. *Polym. Int.* **1994**, *35*, 1
21. Brown, H. C.; Kanner, B. V. *J. Am. Chem. Soc.* **1953**, *75*, 3865
22. Brown, H. C. *J. Chem. Soc.* **1956**, 1248
23. Brown, H. C.; Kanner, B. V. *J. Am. Chem. Soc.* **1966**, *88*, 986
24. Kennedy, J. P.; Chang, V. S. C.; Smith, R. A.; Iván, B. *Polym. Bull.* **1979**, *1*, 575
25. Kitayama, T.; Nishiura, T.; Hatada, K. *Polym. Bull.* **1991**, *26*, 513
26. Lubnin, A. V.; Kennedy, J. P.; Goodall B. L. *Polym. Bull.* **1993**, *30*, 19
27. Feldthusen, J.; Iván, B.; Müller, A. H. E. *unpublished results*
28. Everland, H.; Kops, J.; Nielsen, A.; Iván, B. *Polym. Bull.*, **1993**, *31*, 159
29. Feldthusen, J.; Iván, B.; Müller, A. H. E.; Kops, J. *to be published*
30. Guhaniyogi, S.C.; Kennedy, J. P.; Ferry, W. M. *J. Macromol. Sci.-Chem.* **1982**, *A18*, 25
31. Nuyken, O.; Park, S. D.; Walter, M. *Polym. Bull.*, **1982**, *8*, 451
32. Ref. 1, pp. 128-136

Chapter 7

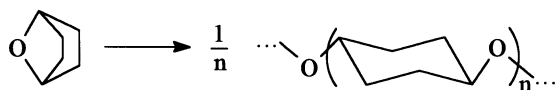
Copolymerization of 7-Oxabicyclo[2.2.1]heptane with Tetrahydrofuran

Stanislaw Penczek, Ryszard Szymanski, Julia Pretula, Krzysztof Kaluzynski, and Jan Libiszowski

Center of Molecular and Macromolecular Studies, Polish Academy of Sciences, Sienkiewicza 112, 90–363 Łódź, Poland

Statistical, pseudoperiodic and block copolymers of 7-oxabicyclo[2.2.1]heptane (**B**) and tetrahydrofuran (**T**) were prepared. Sequences of **B** provide stiff, mesogenic units, whereas units of **T** provide elastic units. The corresponding rate constants of homo- and crosspropagation were determined. Active species provided by **B** (B^* : , anion omitted) are much more reactive than species formed from **T** (T^* : , due to the higher strain of the "bicyclic ion". Due to the high reactivity of B^* these species attack the -TT- units, resulting in transesterification, observed for the first time in the polymerization of cyclic ethers. Therefore, formation of pure block copolymers in sequential copolymerization, starting from living poly-**T** was not possible. Nevertheless, multiblock copolymers were prepared, having long enough poly-**B** units to exhibit LC properties. Above the ceiling temperature (T_c) of **T** (longer poly-**T** units could not be formed) the pseudoperiodic copolymers of the structure close to $[(\text{T})_1(\text{B})_x]_n$ were also prepared.

7-Oxabicyclo[2.2.1]heptane (**B**) is an oxygen-bridged bicyclic ether giving in cationic polymerization a high-melting, crystalline product with 1,4-trans configuration of the cyclohexane rings in the chains (*I*):



Introduction of some flexible repeating units into the rigid chains of poly-**B**, e.g. the tetramethyleneoxy units (from THF) should decrease the melting point of the product and allow the mesogenic (LC) properties (2) of such copolymers. The copolymerization of **B** and **T** has not been studied yet in any detail. Some information on the copolymer

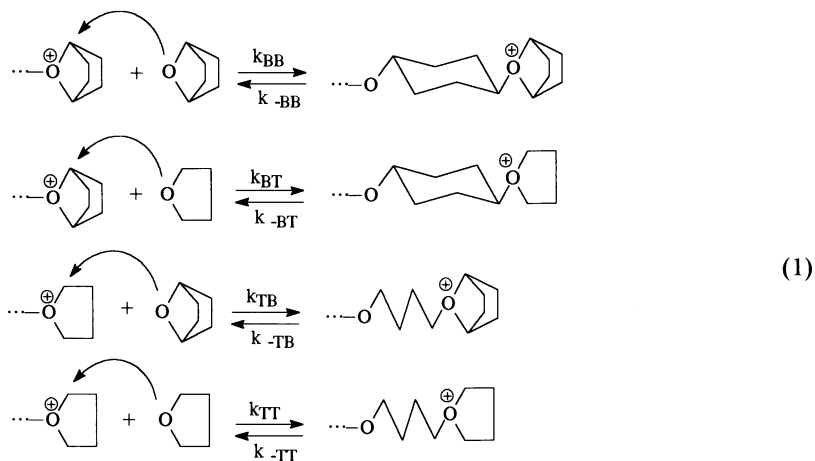
properties were however published (1). The fiber forming properties of these copolymers were also described (3).

In this paper we give a short account of our already published results (4) and some other data being either in press (5) or not intended to be published elsewhere. Therefore, in some parts this paper has a form of an extended abstract.

Results and Discussions

Reactivities of Active Species

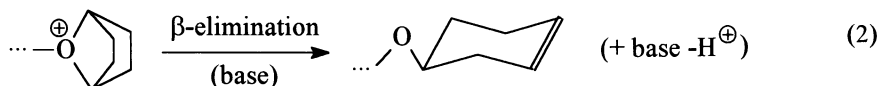
In the copolymerization of **B** and **T** homo- and crosspropagations can be accompanied by the corresponding depropagation reactions. This is shown in the scheme (1) below.



Polymerization was mostly initiated with $C_6H_5CO^+SbF_6^-$ and conducted in CH_2Cl_2 solvent, however in the scheme the anions are omitted.

Determination for such a scheme of all of the rate constants is not possible if the corresponding rate constants of homopropagation and homodepropagation are not known for both comonomers from independent studies. Nevertheless, since we were able to determine concentrations of both B^* and T^* growing species, several rate constants from scheme (1) were numerically estimated on the basis of kinetic measurements.

Below, in Fig. 1 the $^{31}P\{^1H\}$ NMR spectrum is given of one of the copolymerization mixtures, in which active species were killed with $P(n-C_4H_9)_3$. Besides the B^* and T^* active species, converted into the corresponding phosphonium salts (formulae shown in the spectrum) the $H-P^+(n-C_4H_9)_3$ (the protonated phosphine) signal is present. This indicates, that termination on the B^* active species (by β -elimination) takes place:



Thus, we were able to follow in addition to the concentrations of the active species B^* and T^* also the concentration of " H^{\oplus} ", formed as the result of chain termination.

Then, measuring the comonomers consumption as a function of time (in CH_2Cl_2 solvent, 30°C) we were able to estimate the following rate constants of reactions and the following ratios of the rate constants (numerical curve fitting was applied): $k_{\text{TT}} = 2.2 \cdot 10^{-2}$ (the most reliable k_{TT} known from literature is equal to $3.9 \cdot 10^{-2}$) (6), $k_{\text{BB}} = 2.0 \cdot 10^{-1}$, $k_{\text{TB}} = 3.7 \cdot 10^{-2}$ and $k_{\text{BT}} = 1.9 \cdot 10^{-1}$ (all in $\text{mol}^{-1} \cdot \text{L} \cdot \text{s}^{-1}$). Thus, since $k_{\text{TT}}/k_{\text{TB}} \approx 0.6$ and $k_{\text{BB}}/k_{\text{BT}} \approx 1.0$ but $k_{\text{BB}}/k_{\text{TB}} = 5.4$ and $k_{\text{BT}}/k_{\text{TT}} = 8.6$, we conclude, that the corresponding rate constants of elementary reactions are mostly governed by the reactivity of the active species, as it was observed several times in the cationic ROP (7), proceeding by the borderline $\text{S}_{\text{N}}2$ reaction. The observed difference of reactivities stems from a higher ring strain of the "bicyclic active species" B^* than that of "monocyclic" ones T^* . These ring strains are probably close to the enthalpies of polymerization of the corresponding monomers (T : $\Delta H_{\text{ic}} = -15 \text{ kJ mol}^{-1}$ (8); B : $\Delta H_{\text{ic}} = -44.3 \text{ kJ mol}^{-1}$ (9)).

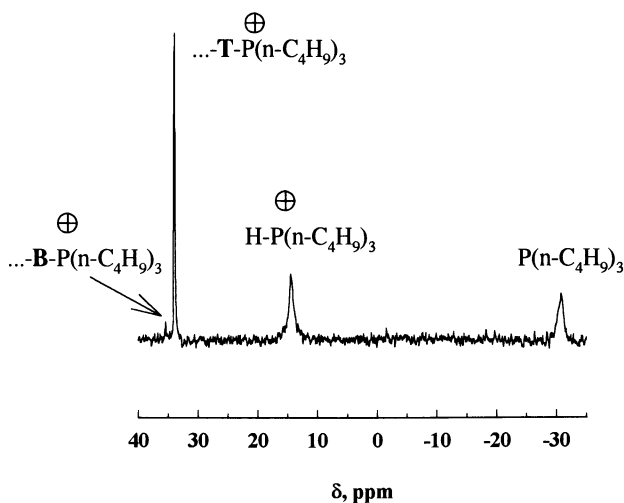
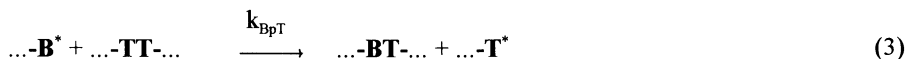


Figure 1. $^{31}\text{P}\{\text{H}\}$ NMR spectrum of the copolymerization mixture, killed with $\text{P}(\text{n-C}_4\text{H}_9)_3$. $[\text{B}]_0 = 1.46$, $[\text{T}]_0 = 2.08$, $[\text{C}_6\text{H}_5\text{CO}^{\oplus}\text{SbF}_6^{\ominus}]_0 = 0.067$, all in mol L^{-1} ; copolymerization reaction time 11 min., temp. 25°C .

Besides these rate constants we were also able to estimate the rate constant k_{BpT} ($\approx 6 \cdot 10^{-2} \text{ mol}^{-1} \cdot \text{L} \cdot \text{s}^{-1}$ at 25°C), i.e. the rate constant of attack of the B^* active species on the $-\text{TT}-$ repeating unit:



This rate constant was estimated on the basis of the polymer microstructure analysis carried out for homopolymerization of B in the presence of poly- T (5).

Thus, the rate constant of breaking of the $-\text{TT}-$ unit in copolymer by the B^* active species is only a few times (~ 3 times at r.t.) lower than rate constant of crosspropagation of B^* active species with T . Therefore, at least for this reason (other reasons will be discussed in the next section), although r_{B} and r_{T} are known ($k_{\text{BB}}/k_{\text{BT}}$ and $k_{\text{TT}}/k_{\text{TB}}$ respectively) one cannot relate the copolymer microstructure to the feed composition by

using the known equations. Chain transfer to polymer (\mathbf{B}^* to $-\mathbf{TT}-$) does influence the microstructure although does not influence directly the copolymer composition. This, however, depends as well on the depropagation reactions.

Statistical copolymerization

In the studies of random (or statistical) copolymerization, usually the dependence of the copolymer composition on the feed is to be determined. In the simplest case the reactivity ratios r_1 and r_2 in the Mayo equation determine this dependence for a given temperature.

In our work, described in the previous paragraph, these ratios were measured. However, the simple Mayo equation together with the reactivity ratios are not sufficient to describe the system, since additional reactions (depropagations and the chain transfer) take place.

There are two general ways to find a proper solution: either by determining the rate constants of the involved reactions (either all or most of them), or by finding formal parameters and using them for the Mayo equation, relating the copolymer composition with the feed. These parameters may depart more or less from the genuine reactivity ratios r_1 and r_2 , defined as in the Mayo equation, since they may include (e.g.) rate constants of depropagation.

Thus, although we have in our disposal several rate constants (as determined in the our previous work (5) and described in the preceding paragraph), we used the second of the discussed above approaches, namely using formal parameters, that encompass several rate constants.

First we used the "composition reactivity ratios", $\bar{r}_B^{(c)}$ and $\bar{r}_T^{(c)}$. In our previous paper we have shown, that these parameters can be determined from the least square fit of the observed copolymer composition (e.g. $\text{fr}(\mathbf{B})$, being the fraction of units \mathbf{B} in copolymer) and the fraction of monomer \mathbf{B} in the feed F_B ($F_B = [\mathbf{B}]_0 / ([\mathbf{B}]_0 + [\mathbf{T}]_0)$) to the equation derived directly from the Mayo relationship:

$$\text{fr}(\mathbf{B}) = \frac{F_B^2 \cdot (\bar{r}_B^{(c)} - 1) + F_B}{F_B^2 \cdot (\bar{r}_B^{(c)} + \bar{r}_T^{(c)} - 2) + 2 \cdot F_B \cdot (1 - \bar{r}_T^{(c)}) + \bar{r}_T^{(c)}} \quad (4)$$

(this form of the Mayo relationship is more convenient in fitting the experimental data than the classical equation)

On the other hand, having determined the polymer microstructure by ^1H and ^{13}C -NMR (the corresponding spectra are given in Refs 4,5), we could determine the so called "microstructure reactivity ratios".

$$\bar{r}_B^{(m)} = \frac{[\mathbf{T}]_0}{[\mathbf{B}]_0} \cdot \frac{\text{fr}(\mathbf{BB})}{\text{fr}(\mathbf{BT})}; \quad \bar{r}_T^{(m)} = \frac{[\mathbf{B}]_0}{[\mathbf{T}]_0} \cdot \frac{\text{fr}(\mathbf{TT})}{\text{fr}(\mathbf{BT})}, \quad (5)$$

(where $\text{fr}(\mathbf{XY})$ denotes the fraction of dyads \mathbf{XY} ; i.e. $\text{fr}(\mathbf{BT}) = 0.5 \text{fr}(\mathbf{BT} + \mathbf{TB})$).

The above equations give the real reactivity ratios (k_{BB}/k_{BT} and k_{TT}/k_{TB} , respectively) for copolymerization without depropagations and other side reactions (at low comonomer conversion).

Below, in Figure 2, the dependence of $\text{fr}(\mathbf{B})$ on $F_{\mathbf{B}}$ is given on the basis of the previously determined parameters. Points are experimental (4), lines are calculated, using the parameters $\bar{r}_{\mathbf{B}}^{(c)}$, $\bar{r}_{\mathbf{T}}^{(c)}$ and $\bar{r}_{\mathbf{B}}^{(m)}$, $\bar{r}_{\mathbf{T}}^{(m)}$. Both equations, generating the compositional and microstructure reactivity parameters, stem from the Mayo approach, and ignore all reactions but the homo- and crosspropagations. Therefore, although equations (4) and (5) have entirely different forms, these parameters should have the same values, if indeed the other reactions (depropagations and reshuffling in our system) can be ignored.

In Figure 2 we give dependence of $\text{fr}(\mathbf{B})$ on $F_{\mathbf{B}}$, computed for both sets of parameters determined for 25°C. The agreement is relatively fair, indicating, that for the chosen conditions the influence of side reactions is self-compensating. Actually, the corresponding parameters used have the following values: $\bar{r}_{\mathbf{B}}^{(c)} = 0.62$, $\bar{r}_{\mathbf{T}}^{(c)} = 0.10$, and $\bar{r}_{\mathbf{B}}^{(m)} = 0.70$, 0.70 , 0.44 , 0.84 ; $\bar{r}_{\mathbf{T}}^{(m)} = 0.09$, 0.13 , 0.19 , and 0.13 , respectively (in order of increasing $F_{\mathbf{B}}$). The calculated lines are computed, in the case of the (m) series, applying eq. (4) and the corresponding pairs of $\bar{r}_{\mathbf{X}}^{(m)}$ values (where \mathbf{X} is either \mathbf{B} or \mathbf{T}), instead of the analogous parameters (c).

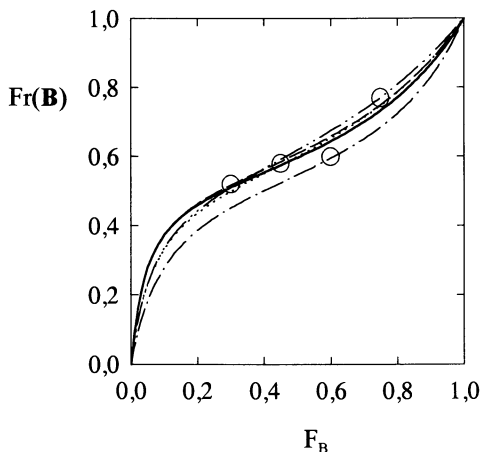


Figure 2. Experimental points and the computed curves relating the copolymer composition with the monomer feed. Solid line: based on $\bar{r}_{\mathbf{B}}^{(c)} = 1.0$, $\bar{r}_{\mathbf{T}}^{(c)} = 0.6$ (the best fit curve); lines --; ...; -.-; -.-: based on $\bar{r}_{\mathbf{B}}^{(m)}$ and $\bar{r}_{\mathbf{T}}^{(m)}$ parameters, determined for copolymers obtained at 25°C at different feed (order of increasing $F_{\mathbf{B}}$, respectively): 0.70, 0.09; 0.70, 0.13; 0.44, 0.19; 0.84, 0.13. $[\mathbf{B}]_0 + [\mathbf{T}]_0 = 1 \text{ mol} \cdot \text{L}^{-1}$.

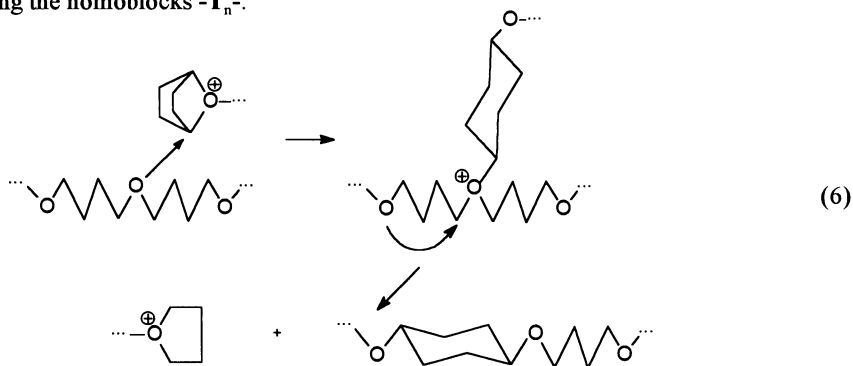
We suspect, that the compensation effect takes place, because, although the agreement at 25°C is relatively good between the (c) and (m) parameters for at least three sets of data, the reactivity ratios computed on the basis of the estimated rate constants (cf. previous paragraph) differ from both (c) and (m) parameters ($r_{\mathbf{B}} = 1.0$, $r_{\mathbf{T}} = 0.6$). Besides, at -23°C the same comparison gave a large difference between parameters (c) and (m), and between parameters (m) of the same series ($\bar{r}_{\mathbf{B}}^{(c)} = 0.06$, $\bar{r}_{\mathbf{T}}^{(c)} = 1.32$, and $\bar{r}_{\mathbf{B}}^{(m)} = 0.50$, 0.37 , 0.31 , 0.32 ; $\bar{r}_{\mathbf{T}}^{(m)} = 1.72$, 1.86 , 2.48 , and 2.72 , respectively (in order of increasing $F_{\mathbf{B}}$: 0.33, 0.50, 0.58, 0.67; $[\mathbf{B}]_0 + [\mathbf{T}]_0 = 8 \text{ mol} \cdot \text{L}^{-1}$)(4). It should be noted that at 25°C larger difference is observed for $\bar{r}_{\mathbf{T}}$ than for $\bar{r}_{\mathbf{B}}$. This is because \mathbf{T} is more prone to depropagation.

We expected that a better agreement between (c) and (m) parameters should be observed at lower temperature, when not only the depropagation of the $-\text{BX}^*$ units ($\text{X} = \text{B}$ or T), but also of $-\text{TX}^*$ units would be hampered. We also expected, that the third reaction, not encompassed by the simple Mayo scheme that we used, namely the chain transfer to $-\text{T}_n-$ units from the B^* active species should be relatively slowed down (having higher activation energy than that of propagation). The different results, however, indicate the importance either of the reshuffling reaction or of some other reactions not taken into account (e.g. the exchange of active species: $-\text{XB}^* + \text{T} \rightleftharpoons -\text{XT}^* + \text{B}$).

Copolymers that were prepared in the experiments described in this section are not random, as they were expected to be, provided that both homo- and crosspropagation proceed randomly without additional influences. Actually, according to the analysis of the polymer microstructure (5) the average length of homoblocks is shorter than calculated for random copolymers of the same composition.

Indeed, some tendency to alternation ($r_{\text{B}} r_{\text{T}} < 1$) was noted. This results from the transesterification reaction (with k_{BPT} rate constant) and the determined values of r_{T} and r_{B} , both lower or equal to 1. Considering the value of r_{T} ($=k_{\text{TT}}/k_{\text{TB}}$) = 0.6 we note, that the higher nucleophilicity of B overshadows the possible steric strain, when B adds to T^* , in comparison with when T adds to T^* . On the other hand, if we take r_{B} ($=k_{\text{BB}}/k_{\text{BT}}$) ≈ 1 , then we have a similar phenomenon. B adds to B^* at the same rate as T adds to B^* . Thus, although B is more nucleophilic, it brings more strain in its reaction with B^* than T does in its reaction with B^* .

Statistical copolymers of B and T have the average lengths of homoblocks shorter than random copolymers of the same composition, and exhibit some tendency to alternation. This mostly results from the high efficiency of the transesterification reaction, cutting the homoblocks $-\text{T}_n-$:



On top of this effect $r_{\text{B}} r_{\text{T}} < 1$, as required for alternation.

Pseudoperiodic copolymers

High homopolymerization equilibrium concentration of T at room temperature ($[\text{T}]_{\text{e}} = 3.1 \text{ mol L}^{-1}$ in bulk at 25°C)⁽¹⁰⁾ allows carrying out copolymerization with concentration of T lower than its equilibrium concentration. This enables the thermodynamic control of the process, because at these conditions homodepropagation of T^* is (due to the thermodynamic reasons) much faster than the corresponding homopropagation. Consequently, the number of homosequences of T in resulting copolymer is very low and

the final product can be regarded as a pseudoperiodic copolymer: $(\mathbf{T})_1(\mathbf{B})_n$. We introduced the term "pseudoperiodic", because the corresponding product differs from the periodic one in a distribution of the lengths of blocks **B**. In the periodic copolymer blocks have uniform size. Formation of such a copolymer is additionally enhanced by the described above transesterification reaction, involving homosequences of $-\mathbf{T}-$ and \mathbf{B}^* . For instance, copolymerization of **B** and **T** carried out in CH_2Cl_2 solvent at 0°C with initial concentrations of comonomers equal to 3.78 and $0.87 \text{ mol}\cdot\text{L}^{-1}$, respectively, yielded copolymer with an average lengths of homosequences ($-\mathbf{B}-$ and $-\mathbf{T}-$) equal to 4.8 and 1.06, respectively.

The homopolymerization equilibrium concentration of **T** can be estimated to be at these conditions equal to about $2.8 \text{ mol}\cdot\text{L}^{-1}$, (11) much higher than the initial concentration of **T** taken for copolymerization. Usually, even if the copolymerization is conducted above the T_c of one of the comonomers, some dyads are present. Practical absence of dyads of **T** in the described above product can be explained by the effective transesterification reaction as discussed above.

Thus, copolymers prepared this way are good candidates for tractable LC polymers. To the best of our knowledge, our original paper on this subject was the first attempt of preparing LC pseudoperiodic copolymers by a direct one step copolymerization.

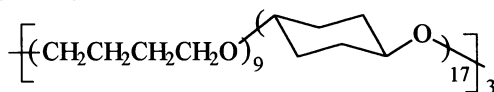
Block copolymers (5)

An efficient transesterification involving poly-**T** sequences, described in the previous paragraphs, prevented the preparation of pure block copolymers of **B** and **T** by sequential polymerization of **T** and **B** monomers (adding **B** to the living poly-**T**). Moreover, the reverse order of polymerization (addition of **T** to the still reactive poly-**B**) was not effective, because of the practical insolubility of poly-**B** and relatively fast termination involving \mathbf{B}^* (cf. the paragraph on kinetic). Thus, copolymers obtained by the procedures comprising reaction of the living poly-**T** with **B** resemble statistical copolymers. Moreover, even the product of homopolymerization of **B** in the presence of a dead poly-**T** gives apparently statistical copolymer with only slightly longer homoblocks than in random copolymer of the same composition.

Copolymers obtained by adding **B** to living poly-**T** without removing free monomer **T** have homoblocks shorter than calculated for random copolymers of the comparable compositions, similarly as it was observed for statistical copolymers. For instance, one of copolymers obtained at 0°C had the average lengths of homosequences of **B** and **T** equal to 1.58 and 1.90, respectively, whereas the computed lengths for random copolymer of the same composition were equal to 1.62 and 2.22. At 25°C the differences of lengths of homoblocks were even more pronounced (1.41 and 2.21 versus 1.61 and 2.63, respectively). When however, most of **T** was removed (by distillation off at low temperature) before adding **B**, the lengths of homoblocks were found to be a little longer than in random copolymer of the same compositions. This difference was not however really significant: the observed lengths of homoblocks of **B** and **T** in one of copolymers (obtained at 25°C) were equal to 1.72 and 3.83, respectively, while a random copolymer of the same composition would have 1.45 and 3.22, respectively.

Copolymers with a multiblock structure were nevertheless finally obtained when active species were generated at both ends of poly-**T**, terminated with iodide groups and activated (ionized) with AgSbF_6 , directly in the reaction mixture, with high concentration of **B**. When reaction was carried out in CH_2Cl_2 solvent (copolymer was soluble in this solvent, provided that fraction of **B** units was not too high) the average lengths of

homoblocks were about 3 times larger than in a comparable random copolymer (lengths of **B** and **T** sequences equal to 4.59 and 7.50, respectively, compared with 1.61 and 2.63 computed for this composition in a random copolymer. A much more pronounced multiblock structure was obtained when nitromethane was used as the reaction medium. The copolymer precipitates at these conditions and a multiblock product results of the following average structure:



Thus, the transesterification was slowed down much more than propagation, due to the difference of the segmental mobility when compared with the mobility of the monomer molecules.

Conclusions

Copolymerization of **B** with **T** is governed by a relatively high difference of reactivities of active species **B*** and **T*** ($k_{BB}/k_{TB} = 5.4$ and $k_{BT}/k_{TT} = 8.6$) and by a fast chain transfer of the **B*** active species to the poly-**T** segments (e.g. $k_{BB}/k_{BT} \sim 3$). Transesterification, bearing resemblance to the transacetalization (12) in the polymerization of cyclic acetals, results from the high reactivity of **B*** active species. Nevertheless, it was possible to prepare both pseudoperiodic copolymers ($\{T_x B_y\}_n$) as well as the multiblock copolymers ($\{T_y B_x\}_n$), with sufficiently long **B_x** segments; e.g. $x = 17$ and $y = 9$, i.e. more than required for the promesogenic units.

Literature cited

1. Wittbecker, E. L., Hall, H. K., Jr., Campbell, T. W., *J. Am. Chem. Soc.* **1960**, *82*, 1218
2. Kops, J., Spanggaard, H., *Polym. Bull.* **1986**, *16*, 507
3. Sikkema, D. J., Hoogland, P., *Polymer* **1986**, *27*, 1443
4. Libiszowski, J., Szymanski, R., Penczek, S., *Macromol. Rapid Commun.* **1995**, *16*, 687
5. Pretula, J., Kaluzynski, K., Szymanski, R., Penczek, S., *Macromolecules* **1996**, in press
6. Matyjaszewski, K., Slomkowski, S., Penczek, S., *J. Polym. Sci., Polym. Chem. Ed.* **1979**, *17*, 2413
7. Goethals, E.J., Penczek, S., In *Comprehensive Polymer Science*; Allen, G., Bevington, J.C., Eds.; Chain Polymerization, Part I; Pergamon Press: Oxford, **1989**; Vol. 3, p. 173
8. Leonard, J., Maheux, D., *J. Macromol. Sci.-Chem.* **1973**, *A7*, 1421
9. Andruzzi, F., Pilcher, G., Virmani, Y., Plesh, P.H., *Makromol. Chem.* **1977**, *178*, 2367
10. Penczek, S., Matyjaszewski, K., *J. Polym. Sci., Symp.* **1976**, *56*, 255
11. Penczek, S., Kubisa, P., Matyjaszewski, K., *Adv. Polym. Sci.* **1985**, *68/69*, 1
12. Chwialkowska, W., Kubisa, P., Penczek, S., *Makromol. Chem.* **1982**, *183*, 753

Chapter 8

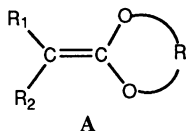
The Synthesis and Photoinitiated Cationic Polymerization of Cyclic Ketene Acetals

J. V. Crivello, Y.-L. Lai¹, and R. Malik

Department of Chemistry, Cogswell Laboratory, Rensselaer Polytechnic Institute,
Troy, NY 12180-3590

A new, high yield synthesis of novel cyclic and acyclic ketene acetals has been developed which makes these compounds readily available. The ketene acetal monomers were fully characterized by IR, NMR and by elemental analysis. A study of the photoinduced cationic polymerization of a series of cyclic and acyclic ketene acetal monomers was carried out using various onium salt photoinitiators. It was observed that the cyclic monomers underwent facile cationic polymerization to give high molecular weight polymers while the acyclic ketene acetals did not. The position and type of substituents in the cyclic ketene acetals were the major factors in determining the proportion of vinyl to ring-opening polymerization which took place.

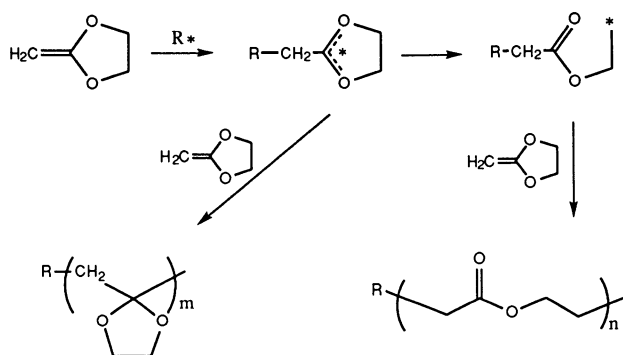
Cyclic ketene acetals (A) are a well known class of compounds having the general structure shown below.



¹Current address: East Bamboo Company Limited, 11F Number 35, Section 1, Cheng-Tech Road, Taipei, Taiwan, Republic of China

Due to the strong electron releasing effects of the two alkoxy groups, cyclic ketene acetals display a pronounced dipolar character which confers great reactivity towards attack by electrophiles, nucleophiles and free radicals (1). Schildknecht (2) reported that ketene acetals are more reactive than the related vinyl ethers in cationic polymerization. McElvain, et al. (3) observed that ketene acetals undergo facile cationic polymerization even in the presence of such acids as sulfuric acid as initiator. More recently, the polymerization of ketene acetals under both free radical (4,5) and cationic (6-11) conditions was reported. It was further shown that the polymerizations of cyclic ketene acetals can lead to both vinyl and ring-opening polymerization as depicted in Scheme 1 where * indicates either a free radical or a cation.

Scheme 1



While it appears that there is a very rich polymer chemistry associated with ketene acetals, this chemistry has not been thoroughly investigated, primarily due to the difficulty of synthesizing the monomers and to the low yields which are usually obtained. This article reports the results of recent work conducted in this laboratory directed the development of a general method for preparation of ketene acetals bearing methyl or ethyl groups on the carbon-carbon double bond. We also report the behavior of these monomers in photoinitiated cationic polymerization.

EXPERIMENTAL

Preparation of Monomers

The following are typical synthetic procedures used for preparation of cyclic ketene acetals.

Synthesis of 2-Propylidene-1,3-dioxolane (1) Crotonaldehyde (2.01 g, 28.7 mmol), ethylene glycol (2.14 g, 34.4 mmol), benzene (50 mL) and p-toluenesulfonic acid (PTSA) (2 mg) were placed in a 100 mL flask equipped with a magnetic stirrer, Dean-Stark trap and condenser. The mixture was heated at 95 °C in an oil bath for 3 h until about 0.5 mL of water had collected in the trap. After cooling, the solution was washed with 30 mL of 1% sodium bicarbonate and then with 30 mL of saturated aqueous sodium chloride solution. The organic solution was dried over anhydrous potassium carbonate and fractionally distilled to give 2-(1-propenyl)-1,3-dioxolane, bp 73-75 °C/185 mm Hg (2.48 g, 21.7 mmol, 76% yield).

$^1\text{H-NMR}$ (CDCl_3) δ (ppm) = 1.70-1.75 (2d, 3H, CH_3); 3.82-4.02 (m, 4H, $\text{OCH}_2\text{CH}_2\text{O}$); 5.14-5.18 (d, 1H, OCHO); 5.42-5.55 (m, 1H, $\text{CH}_3\text{-CH=CH}$); 5.84-6.02 (m, 1H, $\text{CH}_3\text{-CH=CH}$).

2(1-Propenyl)-1,3-dioxolane (2.48 g, 21.7 mmol) and tris(triphenylphosphine)ruthenium(II) dichloride (10 mg) were placed in a 50 mL flask. The flask was fitted with a magnetic stirrer, nitrogen inlet and reflux condenser and then heated at 125 °C in an oil bath. The course of the reaction was monitored by ^1H NMR and the isomerization was completed in 3 h. The mixture was distilled to give 2-propylidene-1,3-dioxolane (**1**), bp 75-78 °C/185 mm Hg (2.25 g, 19.74 mmol, 91% yield).

^1H NMR (CDCl_3) δ (ppm) = 0.90-0.98 (t, 3H, CH_3); 1.90-2.05 (m, 2H, CH_2); 3.60-3.68 (t, 1H, CH); 4.12-4.18 (m, 4H, $-\text{OCH}_2$).

IR (neat) 2953, 2896, 1812, 1712, 1477, 1463, 1382, 1287, 1231, 1162, 1002, 958, 852, 753, 667 cm^{-1} .

Synthesis of 2,2'-Diethylidene-4,4'-bis(1,3-dioxolane) (15) Acrolein (6.55 g, 0.12 mol), erythritol (7.14 g, 58.5 mmol), benzene (150 mL) and PTSA (30 mg) were placed in a 250 mL flask equipped as described above. The mixture was heated at 95 °C in an oil bath for 12 h until 2.1 mL of water collected in the trap. After cooling, the solution was washed with 100 mL of a 1% aqueous sodium bicarbonate solution and then with 70 mL of a saturated aqueous sodium chloride solution. The organic solution was dried over anhydrous potassium carbonate, and fractionally distilled to give 2,2'-divinyl-4,4'-bis(1,3-dioxolane) bp 67-71 °C/0.5 mm Hg (6.02 g, 30.4 mmol, 52% yield).

^1H NMR (CDCl_3) δ (ppm) = 3.62-4.30 (m, 6H, $\text{OCH}_2\text{-CH-O}$); 5.02-5.20 (m, 2H, OCHO); 5.27-5.53 (m, 4H, $\text{CH}=\text{CH}_2$); 5.69-5.89 (m, 2H, $\text{CH}=\text{CH}_2$).

2,2'-Divinyl-4,4'-di-(1,3-dioxolane) (2.11 g, 10.7 mmol) and tris(triphenylphosphine)ruthenium(II) dichloride (15 mg) were placed in a 50 mL flask. The flask was equipped as described previously and heated at 125 °C in an oil bath. The reaction was followed by ^1H NMR for 7 h until the isomerization had reached completion. The mixture was cooled and fractionally distilled to give 2,2-diethylidene-4,4'-bis(1,3-dioxolane) (**15**), bp 75-79 °C/0.5 mm Hg (1.50 g, 7.62 mmol, 71% yield).

^1H NMR (CDCl_3) δ (ppm) = 1.47-1.54 (m, 6H, CH_3); 3.55-3.70 (m, 2H, $\text{CH}_2\text{-CH=C}$); 4.13-4.38 (m, 6H, $\text{OCH}_2\text{-CH-O}$).

IR (neat) 2920, 2860, 1710, 1470, 1440, 1360, 1280, 1060, 950, 840, 745 cm^{-1} .

Cationic Polymerizations

Bulk Polymerizations Samples were prepared as follows: 1-2 g of the ketene acetal monomer and 0.1-1.0 wt% of the appropriate photoinitiator were placed in a 10 mL vial. After the photoinitiator had dissolved in the monomer by shaking, the mixture was placed in an aluminum pan. The samples were then irradiated at room temperature for 1-120 seconds using a 200 W GE H3T-7 medium-pressure mercury arc lamp mounted at a distance of 10 cm from the samples. The samples were transferred back to the vial, and allowed to stand in the dark at room temperature for 1-60 hours. Table 1 shows the photoinitiators their concentrations, the irradiation times and polymerization times for each monomer. The polymers were purified by dissolving in chloroform and precipitating into methanol (monomers **1-3**, **5-11**, **14** and **17**) or n-hexane containing ~1% of ammonium hydroxide. The polymers were isolated by either filtration of the precipitated polymers or by decantation of the solvent from the liquid polymers. The polymers were washed with fresh solvent and dried in vacuo.

Fourier Transform Real-Time Infrared Spectroscopic (FT-RTIR) Studies (12)

Kinetic and conversion data for the cationic photopolymerizations of the monomers were obtained using Fourier transform real-time infrared analysis (FT-RTIR). This

method involves the monitoring of an appropriate IR band due to the polymerizing group while simultaneously irradiating the thin film sample with UV light. Measurements were performed on a Midac Series M-1300 Fourier Transform Infrared Spectrometer equipped with a liquid nitrogen cooled MCT detector. The instrument was fitted with a UVEXS Co SCU 110 UV lamp equipped with a flexible liquid optic cable directed at a 45° angle onto the sample window. All studies were conducted using broad band, unfiltered UV light at an intensity of 15.8 mW/cm². Samples were prepared by placing thin films (0.1 - 0.3 mm) of the liquid monomers containing 0.02 mol% of onium salt (4-n-octyloxyphenyl)phenyliodonium hexafluoroantimonate (IOC10) or S,S-diphenylsulfonium-S-4-thiophenoxyphenyl- hexafluoroantimonate (SS) onto a NaCl plate. The samples were irradiated with UV light for 150 sec. and simultaneously monitored for decrease of the band at 845-860 cm⁻¹. Data were collected on a Bit-Wise Co. 486 PC computer, reduced and plotted as conversion versus time curves with the aid of Galactic Industries Corp. Grams 386, Version 3.0 software. Light intensity measurements were made with the aid of an International Light Co. Control-Cure Radiometer.

The kinetic parameter, $R_p/[M_0]$, was determined from the slopes of the conversion versus irradiation time curves according to equation 1.

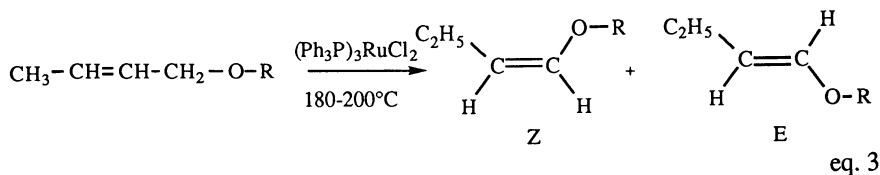
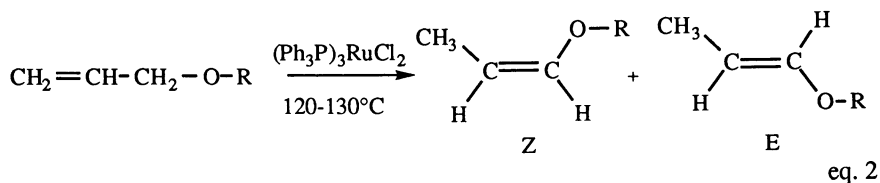
$$R_p/[M_0] = ([\text{conversion}]_{t_2} - [\text{conversion}]_{t_1}) / (t_2 - t_1) \quad \text{eq. 1}$$

Where R_p and $[M_0]$, are respectively, the rate of polymerization and the initial monomer concentration. The conversions were determined directly from the curves at irradiation times t_1 and t_2 .

RESULTS AND DISCUSSION

Synthesis of Monomers

Recently, we reported that 1-propenyl ethers (13) and 1-butenyl ethers (12) can be prepared in quantitative yields by the ruthenium catalyzed rearrangement of allyl and crotyl ethers, respectively (equations 2 and 3).



The isomerization of alkyl allyl ethers proceeds smoothly at temperatures from 120-130 C while alkyl crotyl ethers are isomerized at higher temperatures. A mixture of cis and trans isomers are obtained in both cases.

This isomerization method was also be applied to the preparation of cyclic ketene acetals (Scheme 2). Table 1 shows structures of the ketene acetal monomers prepared using this approach.

Scheme 2

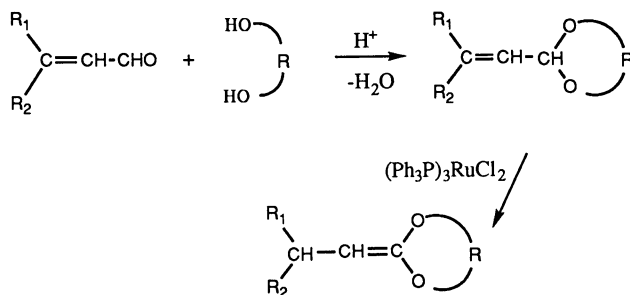


Table 1
Synthesis of Ketene Acetal Monomers

Notation	Monomer	Yield (%)	Notation	Monomer	Yield (%)
1		91	10		94
2		80	11		88
3		75	12		86
4		67	13		80
5		77	14		75
6		80	15		71
7		91	16		68
8		84	17		81
9		67	18		73

A wide variety of monomers were prepared having various ring sizes and either a methyl or an ethyl substituent on the ketene acetal double bond. By selection of the proper diol, both aliphatic and aromatic groups could be placed at various positions on the rings. All the monomers shown in Table 1 were liquids which could be purified by distillation. Yields of the resulting ketene acetals from the corresponding vinyl precursors were not optimized but were uniformly good-to-excellent. All monomers were characterized by IR, ^{13}C and ^1H MNR spectroscopy, and elemental analysis.

It should be noted that in all cases, the ketene acetals exist as a mixture of *cis*,

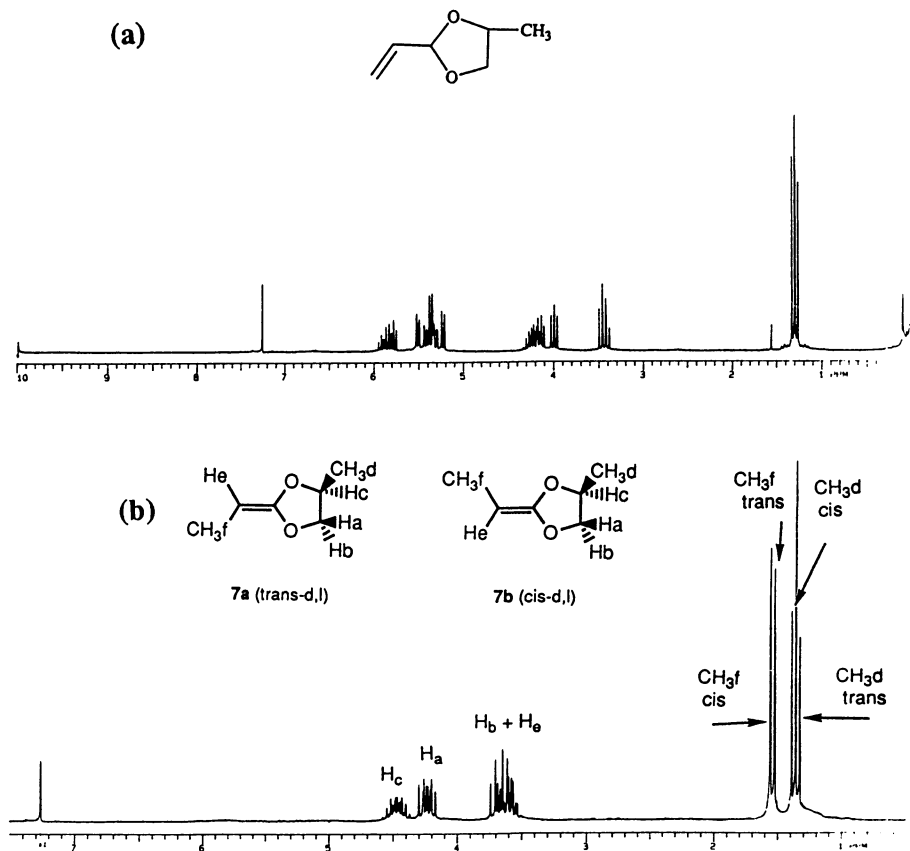


Figure 1. 200 MHz ^1H -NMR spectra of (a) 2-vinyl-4-methyl-1,3-dioxolane and (b) 2-propylidene-4-methyl-1,3-dioxolane (7).

trans and stereoisomers resulting from the presence of the double bond and an asymmetric center at the carbon bearing the substituent on the ring. Due to the close boiling points of these compounds and their tendency to polymerize during attempted purification by column chromatography, no separation of the isomers was possible. Instead, the mixtures of isomers were carried directly into the polymerization studies. The presence of isomers was clearly observable using high field (500 MHz) $^1\text{H-NMR}$. For example, in Figure 1, the presence of *cis*-*d,l* and *trans*-*d,l* isomers of monomer **7** can be clearly seen by the splitting of the protons of the methyl groups on the double bond which appear as separate doublets at $\delta = 1.35\text{--}1.55$ ppm. Integration of the doublets provides an estimate of the isomer ratio for this monomer (*cis*-*d,l* / *trans*-*d,l* = 50:50).

The cyclic ketene acetal monomers were found to be highly reactive and these compounds had a marked tendency to polymerize on standing. This problem was overcome by either adding small amounts of a strong inorganic base as a stabilizer, or by washing the glassware storage containers with base prior to use.

Cationic Photopolymerization

Acyclic ketene acetals **17** and **18** underwent cationic polymerization to give low molecular weight polymers probably due to competing chain transfer reactions. In contrast, the cyclic ketene acetal monomers are cationically photopolymerized using onium salt photoinitiators to give higher molecular weight polymers. The results of bulk photopolymerizations are given in Table 2. Typical photoinitiator concentrations were 0.1 to 0.5 mol%.

In Table 2, SS is S,S-diphenyl-S-4-thiophenoxyphenylsulfonium SbF_6^- , IOC is (4-decyloxyphenyl)phenyliodonium SbF_6^- and UV9380C is di(4-docecylphenyl)iodonium SbF_6^- . As may be noted in Table 2, high molecular weight polymers were obtained for many of these monomers. Monomers **15** and **16** gave crosslinked polymers insoluble in common solvents.

Table 2
Cationic Photopolymerization of Ketene Acetals

Monomer	Photo-initiator	Yields (%)	M_n	Monomer	Photo-initiator	Yields (%)	M_n
1	SS	100		10	SS	84	57700
2	IOC	30	6600	11	SS	71	23500
3	IOC	18	5200	12	IOC	17	550
4	IOC	7	450	13	IOC	10	450
5	IOC	67	40600	14	IOC	21	2800
6	IOC	52	24800	15	IOC	100	
7	SS	81	26600	16	IOC	100	
8	SS	80	35900	17	UV9380C	5	2200
9	SS	70	15000				

The reactivity of the monomers was monitored using real-time infrared spectroscopy. Employing this rapid monitoring technique, it was possible to follow the progress of the rapid photoinitiated cationic polymerizations of the monomers in thin films. An example of this technique is shown in Figure 2. Determination of the slopes of the linear portion of the curves (R_p/M_0) gives a direct measure of the reactivity of the monomers while the conversions after 100 seconds irradiation could also be directly determined. The data obtained in the real-time infrared studies is presented in Table 3.

Table 3
The Rates and Conversions of Ketene Acetals in
Photoinitiated Cationic Polymerization

Monomer	Photoinitiator (conc.)	$R_p/[M_0]$ (s^{-1})	Conversion* (%)
1	SS, 0.02 mol%	1.75	92
2	SS, 0.02 mol%	2.29	95
3	SS, 0.02 mol%	2.21	92
4	SS, 0.02 mol%	2.23	93
5	SS, 0.02 mol%	1.50	89
6	SS, 0.02 mol%	2.96	85
7	SS, 0.02 mol%	20.8	99
8	SS, 0.02 mol%	7.76	98
9	SS, 0.02 mol%	19.5	97
10	SS, 0.02 mol%	3.95	95
11	SS, 0.02 mol%	3.01	84
12	IOC-10, 0.02 mol%	3.56	81
14	IOC-10, 0.02 mol%	5.62	99

*Measured after 100 seconds irradiation.

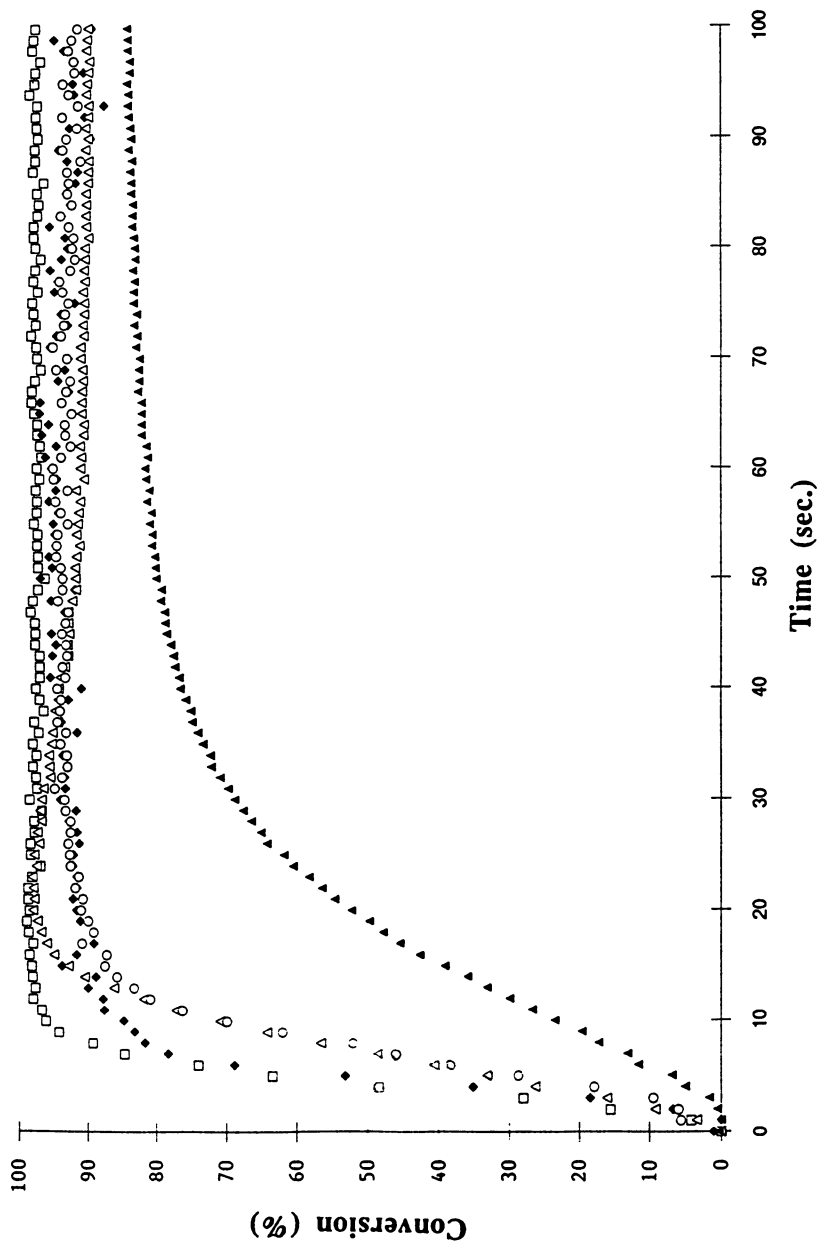
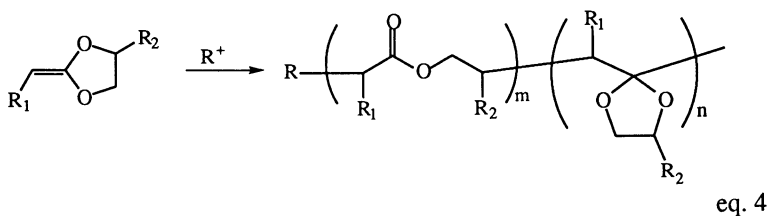


Figure 2. FT-RTIR Study of the photopolymerization of monomers 7 (□), 8 (△), 9 (◆), 10 (○) and 11 (▼) in the presence of 0.02 mol% SS.

Determination of the Microstructure of the Polymers

Studies of the microstructure of the polymers formed from the cationic photopolymerization of cyclic ketene acetals by ^1H NMR and IR spectroscopy

showed that both vinyl and ring-opening polymerization occurred. There is a good correlation between these two methods. Thus, the resulting polymers consist of both types of repeating units as depicted in equation 4.

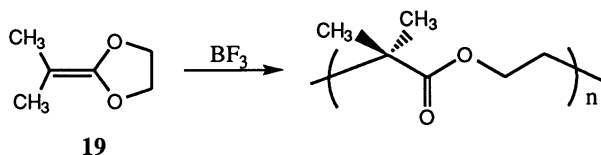


The ratio of the two modes of polymerization depended on three factors: 1) the substitution on the ketene acetal double bond, 2) the character of the substitution on the ring and 3) the ring size of the cyclic acetal. By manipulation of these factors, the ratio could be varied. Given in Table 4 is the data obtained from these studies.

Table 4
Calculated % Ring-Opening For Various Cyclic Ketene Acetals

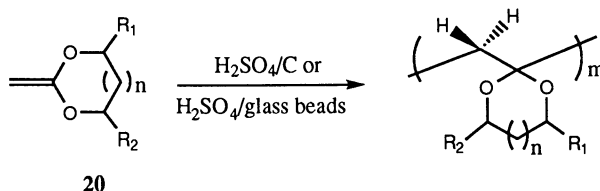
Monomer	Photo-initiator.	% Ring-Opening		Monomer	Photo-initiator.	% Ring-Opening	
		NMR	IR			NMR	IR
1	SS			8	SS		3
2	IOC		31	9	SS		2
3	IOC		48	10	SS		3
4	IOC		38	11	SS	54	54
5	IOC		13	12	IOC		45
6	IOC	82	89	13	IOC		81
7	SS		3	14	IOC	52	58

Among the three factors listed above which determines the ratio of ring-opening to vinyl polymerization, the kind and number of substituents on the double bond appears to be dominant. Mukiyama et al. (14) have reported that the dimethylketene acetal **19** undergoes mainly ring-opening polymerization in the presence of BF_3 to give mainly the polyester shown in equation 5.



eq. 5

In contrast, Zhu and Pitman (15) have reported that unsubstituted cyclic ketene acetals **20** of various ring sizes and with a variety of ring substituents undergo exclusive cationic vinyl polymerization on treatment with either sulfuric acid treated carbon or glass beads (equation 6).



eq. 6

The results of the above two observations indicate that the increasing steric hindrance provided by the two methyl substituents of **19** essentially inhibits vinyl polymerization and promotes ring-opening polymerization. Conversely, no matter what substituent was placed on the ring of **20**, polymerization occurs exclusively by a vinyl polymerization pathway. Based on these observations, it would be predicted that placing a single alkyl substituent onto the ketene acetal double bond should result in mixed vinyl and ring-opening modes of polymerization. Indeed, this is exactly what is observed in the monomers prepared in this investigation. Moreover, increasing the bulkiness of the alkyl substituent increased the proportion of ring-opening to vinyl polymerization. Thus, ethyl substituted monomers **1-6** give higher levels of ring-opening polymerization than corresponding methyl substituted monomers **8-10**.

The character of the substituent on the ring influences the degree of ring-opening. Those substituents which can stabilize a cation on the adjacent carbon atom bearing them will favor ring-opening. The degree of ring-opening of the series of cyclic ketene acetal monomers decreased in the following order: phenyl > ethyl > methyl > chloromethyl which correlates with the ability of those ring substituents to stabilize the cationic intermediate.

The ring size of the cyclic ketene acetal also plays a role in the amount of ring-opening. The larger the ring, the greater the proportion of ring-opening compared to vinyl polymerization. Seven-membered ring monomers have greater ring strain than the corresponding six or five-membered ring analogues so that they give a higher ratio of ring-opening to vinyl polymerization.

Depolymerization

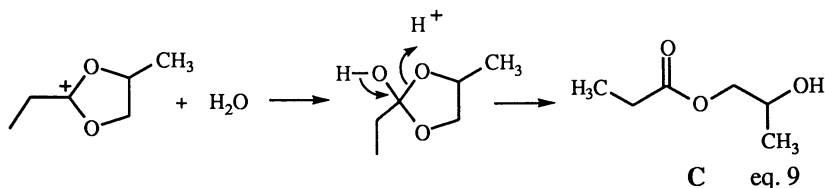
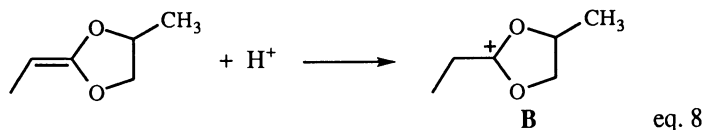
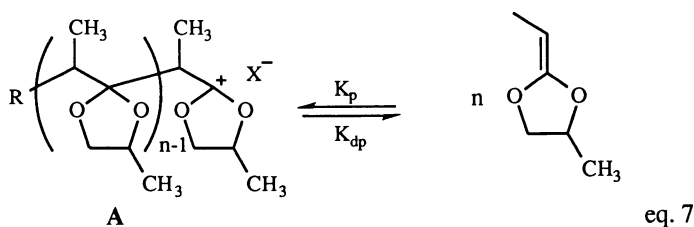
In certain cases, high molecular weight polymeric cyclic ketene acetals which were not subjected to deliberate termination with base were observed to undergo reversion to low molecular weight species. For example, the polymer derived from monomer **7** containing 3% polyester units and 97% cyclic acetal units underwent extensive spontaneous depolymerization on standing in air at room temperature after approximately 3 weeks. Analysis of the reaction mixture by gas chromatography

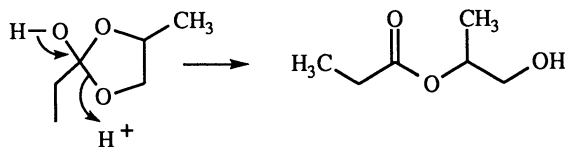
showed that the two major components formed which accounted for 82% of the mixture. Infrared spectroscopy showed bands at 1737 and 3444 cm^{-1} which were assigned respectively to ester carbonyl and hydroxyl groups. Chemical ionization mass spectroscopy gave a major $M + 1$ peak at 133 mass units. Assignment of the ^1H NMR bands was consistent with the structure for 2-hydroxypropyl propionate as the major product together with a small amount of 2-hydroxy-1-methylethyl propionate. In agreement with this conclusion, the ^{13}C NMR spectrum displayed eleven major resonances with closely related chemical shifts and a prominent carbonyl resonance at 174.55 ppm.

Scheme 3 shows the proposed mechanism for the depolymerization of polymer from **7**. The above results can be explained by assuming that the ceiling temperature for the vinyl polymer **A** derived from the cationic photopolymerization of monomer **7** is rather low. In the presence of photogenerated acid, the polymer is first depolymerized to **7** that thereafter is reprotonated to yield a carbocation intermediate **B** which is subsequently attacked and hydrolyzed by water. Attack can occur as noted in Scheme 3 at either of the two acetal ring carbons to form the observed two hydroxyester products **C** and **D**.

Only polymers containing a high ratio of vinyl to ring-opened units in the backbone displayed a marked tendency to undergo depolymerization on standing. Thus, while the polymer derived from **7** is highly sensitive towards depolymerization and hydrolytic degradation, the corresponding polymers from monomers **6** and **11** contained respectively 89% and 54% polyester units were stable in the presence of a high ambient humidity and high concentrations of photoinitiators. The polyester units, therefore, form sites along the polymer backbone beyond which unzipping of the polymer chain cannot occur. Based on this rationale it appears possible to regulate the depolymerizability of a ketene acetal polymer by controlling the ratio of ring-opened (i.e. ester) to vinyl units in the backbone.

Scheme 3





D

eq. 10

CONCLUSIONS

A series of cyclic and acyclic ketene acetal monomers have been prepared by a straightforward, high yield method and their photoinitiated cationic polymerization studied. On irradiation with UV light in the presence of onium salt photoacid generators, these ketene acetal monomers underwent facile cationic polymerization which involved both ring-opening and vinyl polymerization. The relationship between monomer structure and the ratio of these two modes of polymerization was investigated. Polymers derived from monomers which give a high degree of vinyl polymerization showed a marked tendency to undergo depolymerization due to their inherent low ceiling temperatures. Conversely, polymers with higher degrees of ring-opening showed little tendency towards depolymerization.

ACKNOWLEDGMENT

Financial support of this work by the Petroleum Research Fund administered by the American Chemical Society is gratefully acknowledged.

LITERATURE CITED

1. Brassard, P. In: *The Chemistry of Ketenes, Allenes and Related Compounds*, S. Patai, editor, John Wiley & Sons, New York, 1980, p. 488.
2. Schildknecht, C.E. *Vinyl and Related Polymers*, John Wiley & Sons, New York, 1952, p. 700.
3. Johnson, P.R., Barnes, H.M. and McElvain, S.M. *J. Am. Chem. Soc.*, **1940**, 62, 964; *ibid.*, **1936**, 58, 529.
4. Sadhir, R.K. and Luck, R.M. *Expanding Monomers*, CRC Press, Boca Raton, 1992, p. 197.
5. Bailey, W.J., Ni, Z. and Wu, S.-R. *Macromolecules*, **1982**, 15, 711.
6. Cho, I. and Gong, M.S. *J. Polym. Sci., Polym. Lett. Ed.*, **1982**, 20, 361.
7. Yokozawa, T., Hayashi, R. and Endo, T. *Macromolecules*, **1992**, 25, 3313.
8. Park, J. Yokozawa, T. and Endo, T. *Makromol. Chem.*, **1993**, 194, 2017.
9. Park, J., Yokozawa, T. and Endo, T. *J. Polym. Sci., Polym. Chem. Ed.*, **1993**, 31, 1141.
10. Park, J., Kihara, N., Ikeda, T. and Endo, T. *J. Polym. Sci., Polym. Chem. Ed.*, **1993**, 31, 1083.
11. Zhu, P.C. and Pittmann, Jr., C.U. In: *Chemical and Engineering News*, **1995**, July 17, 16.
12. Crivello, J.V. and Yang, B. *J. Polym. Sci., Polym. Chem. Ed.*, **1995**, 33, 1381.
13. Crivello, J.V. and Jo, K.D. *J. Polym. Sci., Polym. Chem. Ed.*, **1993**, 31(6), 2193.
14. Mukaiyama, T., Fujisawa, T., Nohira, H. and Hyugaji, T. *J. Org. Chem.*, **1962**, 27, 33337.
15. Zhu, P.C. and Pittman, Jr., C.U. *J. Polym. Sci., Part A: Polym. Chem.*, **1996**, 34, 73.

Chapter 9

Noncoordinating Anions in Carbocationic Polymerization

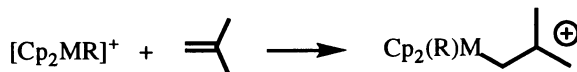
Tris(pentafluorophenyl)boron as a Lewis Acid Catalyst

Timothy D. Shaffer

Baytown Polymers Center, Exxon Chemical Company, 5200 Bayway Drive,
Baytown, TX 77522-5200

This chapter reports on several aspects of isobutylene homo- and copolymerization catalyzed by trispentafluorophenylboron, $B(pfp)_3$. The nature of initiation, termination and chain transfer are addressed by kinetic analysis. The first order chain transfer constant ($k_{tr,M}/k_p$) at -40°C is also reported. Comonomers addressed by this account include isoprene (2.1 mol%) and p-methylstyrene (2.0 mol%). The characteristics (i.e. M_n , M_w/M_n , comonomer incorporation, branching, BSB triad) of copolymers prepared by $B(pfp)_3$ catalysis are compared with that known from other catalysts.

The initiation of carbocationic polymerizations with metallocene initiators that contain the noncoordinating anions (NCA's), $B(C_6F_4)_4^-$ and $R(B(C_6F_5)_3)^-$, has been recently demonstrated (1-7). Initiation is believed to occur by σ addition of the olefin to the metallocation.



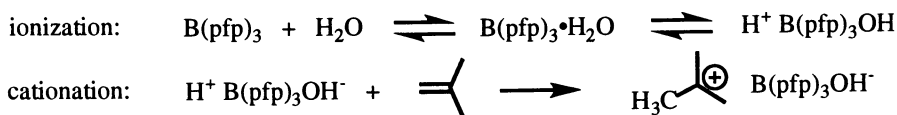
However, protic initiation may also result as a consequence of the metallocation's reaction with adventitious moisture in the solvents (7). The source of initiation is dependent upon the relative concentrations of the metallocation and water. Protic initiation can be avoided with the addition of a proton trap, but the metallocation's concentration must exceed the concentration of adventitious moisture to ensure polymerization. Initiation from the metallocation is very inefficient. Since the metallocation largely participates only in initiation, the attributes of these polymerizations are generally due to the NCA (7).

This realization opens opportunities for NCA catalysts that do not contain expensive metallocenes. Indeed, Ph_3C^+ , Li^+ , and R_3Si^+ salts of NCA's can initiate and catalyze carbocationic homo- and copolymerizations (1,7). These initiators provide many of the attributes observed in the metallocene based systems. In addition, some offer the advantages of stability to water and handling ease. These advantages are offset

NOTE: This article is part two in a series.

by the multistep syntheses required for their preparation. The less synthetically challenging trispentafluorophenylboron ($B(\text{pfp})_3$) may provide similar polymerization attributes when used as a Lewis acid catalyst. If so, this represents a less complicated way to access the advantages offered by NCAs.

The use of $B(\text{pfp})_3$ to catalyze isobutylene polymerization is known (5,7). In both cases, water borne protons are assumed to be the initiator. Evidence of protic initiation came from proton trapping experiments in which the presence of a proton trap successfully prevented polymerization.



The $B(\text{pfp})_3/\text{H}_2\text{O}$ system requires more polar solvents to support ionization as polymerizations do not occur in hydrocarbon solvents. As such, $B(\text{pfp})_3$ behaves more like BCl_3 than BF_3 in this regard. Complexation studies with $B(\text{pfp})_3$ rank it between, BF_3 than BCl_3 in Lewis acid strength (8).

Although the mode of initiation in the $B(\text{pfp})_3/\text{H}_2\text{O}$ system has been addressed, many other aspects of polymerizations catalyzed by $B(\text{pfp})_3$ are not documented. This article preliminarily reports on several aspects of isobutylene homo- and copolymerizations catalyzed by $B(\text{pfp})_3$. The temperature and solvent polarity dependence as well as the determination of a first order chain transfer constant ($k_{tr,M}/k_p$) at -40°C are presented.

Results and Discussion

Homopolymerization of Isobutylene. A number of isobutylene homopolymerizations were run with $B(\text{pfp})_3$ using mostly water and 2-phenylpropan-2-ol (PPOH) as initiators, two different temperatures, and solvents with different polarity. The results of these experiments appear in Table 1. All runs were stopped after 30 minutes of polymerization. Several observations can be made from these data. Polymerizations are generally inefficient in nonpolar solvents like hexane and toluene. Similar results have been reported for polymerization in methylcyclohexane (7). More polar solvents, like methylene chloride, permit higher conversion to polymer. In either case, molecular weight values are significantly higher than expected using $[M]/[I]$ as a guide. As an example, experiment 10 should provide a polymer with a M_n of 101 kD, but the M_n of the prepared material is 908 kD. Although these polymerizations are not living, significantly higher M_n values suggest that slow initiation is responsible for the discrepancy. The use of a more efficient initiator, as in experiment 7, illustrates this point. Use of the *t*-alkyl chloride initiator TBDCC (see Table 1 for definition) provides for a polymer with a M_n of 13.2 kD which is significantly below that expected for this conversion ($M_n = 117$ kD). Even though slow initiation contributes less to this polymerization, the lower M_n suggests the participation of chain transfer.

Improving conversion by moving to more polar solvents suggests a lowering of the activation energy for cation formation. Both initiation and propagation may be more efficient in the polar solvents. Regardless of the solvent used, these polymerizations are slow and are colorless throughout, implying a low concentration of active chain ends. This observation is consistent with slow initiation and perhaps a reversible termination step that is competitive with propagation. Changes in solvent polarity are known to alter propagation equilibria as anticipated from the Winstein model (9,10).

Kinetics of Homopolymerization. The kinetic character of water initiated polymerizations was further defined by analyzing the first order rate plot (Figure 1) and

Table 1: B(pfp)₃ IB Homopolymerizations

Rxn.	[M] (mol/L)	[Cat] x10 ³ (mol/L)	[I] x 10 ³ (mol/L)	initiator, [I] x 10 ³ (mol/L)	Solvent	Temp. (°C)	Yield (%)	M _n	M _w /M _n
1	3.6	3.0		PPOH, 1.8	MeCl ₂	-30	24	159,300	2.2
2	3.4	"		H ₂ O	"	"	75	144,100	2.2
3	4.2	"		"	"	"	32	175,000	2.2
4	5.1	"		"	"	"	2.7	376,500	1.9
5	"	"		PPOH, 1.8	Hexane	"	<1	---	---
6	"	"		"	Chlorobenzene	"	18	80,000	2.1
7	"	"		TBDCC, 2.0	MeCl ₂	"	82	13,200	4.0
8	"	"		BrMP, 1.6	"	"	34	199,600	2.9
9	"	"		H ₂ O, 3.3	"	-50	4	513,300	3.4
10	1.8	4.2		H ₂ O, 1.0	"	"	96	908,000	4.3
11	1.8	3.0		"	"	"	94	225,100	4.9
12	3.6	"		"	"	"	87	410,600	4.2
13	"	"		H ₂ O, <0.1	MeCl	"	17	1,330,880	4.2
14	"	"		"	MeCl ₂ /Hex ^a	"	9.9	711,924	5.6
15	"	"		"	MeCl ₂ /Hex ^b	"	<1	---	---
16	"	"		PPOH, 1.8	Toluene	"	<1	---	---
17	"	"		"	Hexane	"	<1	---	---

run time = 30 minutes; PPOH : 2-phenylpropan-2-ol; TBDCC: 5-tert-butyl-1,3-bis(1-chloro-1-methylethyl)benzene; BrMP: 2-methyl-2-bromopropane; MeCl₂: methylene chloride; MeCl: methylchloride; a: 90/10 v/v; b: 80/20 V/V.

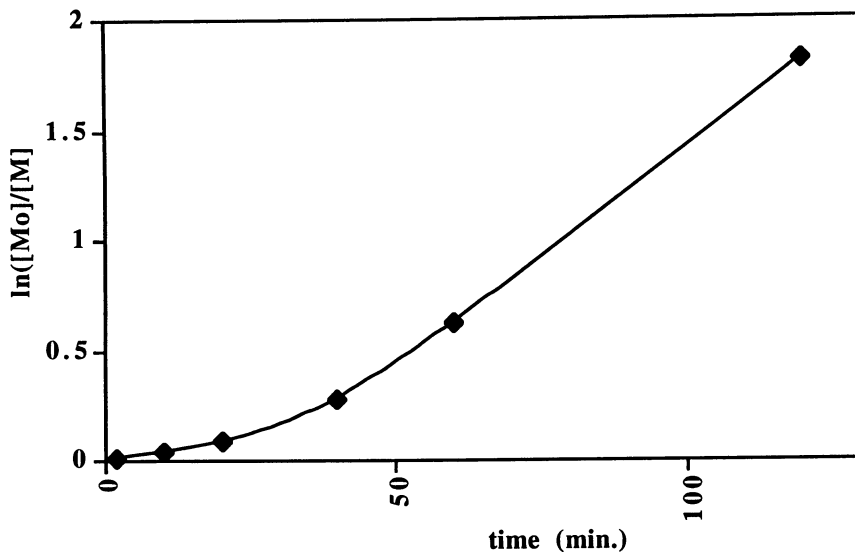


Figure 1: First Order Rate Plot for Isobutylene Homopolymerization in Methylene Chloride at -30°C . $[\text{IB}] = 6.7 \text{ mol/L}$; $[\text{B}(\text{pfp})_3] = 3.1 \times 10^{-3} \text{ mol/L}$; $[\text{H}_2\text{O}] = 1.0 \times 10^{-3} \text{ mol/L}$.

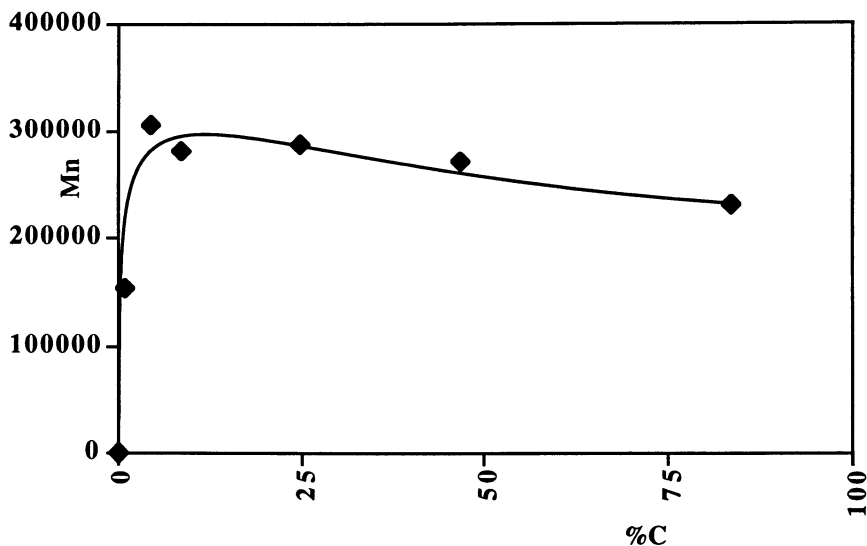


Figure 2: Plot of M_n vs. %C for Isobutylene Homopolymerization in Methylene Chloride at -30°C . Conditions the same as in Figure 1.

following M_n with conversion (Figure 2) for a polymerization in methylene chloride at -30°C . The first order plot is characterized by an upward curve typical of polymerizations with slow initiation (9). Once the plot reaches linearity, it remains so implying the absence of irreversible termination. The slope of the latter linear portion of this curve provides an apparent rate of polymerization, $k_p[P^+] = 0.019 \text{ min}^{-1}$. Because of the high monomer concentration used in this experiment, the acceleration of the polymerization may also result from a change in the solvent polarity as monomer is consumed. This point is exemplified by experiments 2 through 4 of Table 1. As $[M]$ is increased, the conversion to polymer in thirty minutes goes down and M_n values rise. In effect, at higher monomer concentrations the solvent, of which monomer may be considered a component, is less polar and therefore contributes to an overall lowering of polymerization rate. This apparent rate paradox stems from the sensitivity of this catalyst system to solvent polarity.

Polymerizations initiated with water or PPOH are slow and may require several hours to reach complete conversion. In the kinetic example just discussed, 84% conversion required 140 minutes, even at a relatively high monomer concentration.

The molar ratio of $B(\text{pfp})_3$ to initiator is important to increasing the efficiency of initiation. Table 2 lists the results of several polymerizations in which the ratio $[B(\text{pfp})_3]/[\text{PPOH}]$ has been changed. These runs were made in methylene chloride which contained relatively low levels of adventitious water ($\leq 10^{-4} \text{ mol/L}$), so that the added initiator, PPOH, could be used as a controlled, measurable initiation source. For each of these reactions, the theoretical M_n is 40.6 kD and the initiation efficiency (I_{eff}) is calculated accordingly (11). I_{eff} increases with increasing $[B(\text{pfp})_3]/[\text{PPOH}]$ and only reaches 74% at a ratio of 8.6. When the concentration of the initiator is significantly higher than the Lewis acid concentration, no polymer is formed. These observations characterize $B(\text{pfp})_3$ as a weak Lewis acid.

The chain transfer aspects of this catalyst were determined at -40°C , a temperature midway between the majority of the experiments reported here. Polymerizations were run with varying monomer concentrations in a methylene chloride/hexane solvent system. The experiment with the highest monomer concentration defined the volume of the nonpolar component for the rest of the experiments. This experiment contained no hexane. After all, monomer functions as a solvent until it is consumed. At lower monomer concentrations, hexane was added to keep the volume of the nonpolar solvent component constant. This method eliminates or minimizes the effect of solvent polarity changes upon chain transfer that would otherwise occur by simply reducing the amount of the monomer added to the polymerization. Reactions were stopped after 30 seconds in order to stop conversions at less than 5%. The raw data are shown in Table 3. A Mayo plot was constructed and is shown in Figure 3. $1/DP_n$ is plotted as a function of $1/[M]_0$ to give an ordinate equal to $k_{tr}M/k_p$ or $C_{tr}M$ and a slope equal to k_{tr}/k_p or C_{tr} , since $k_{tr} \ll k_p$ (possibly a

Table 2: Dependence of M_n and M_w/M_n of Polyisobutylene on $B(\text{pfp})_3$ Concentration in Methylene Chloride at -50°C

Rxn.	$[B(\text{pfp})_3]$ $\times 10^3 \text{ (mol/L)}$	$[B]/[I]$	Yield (%)	M_n	M_w/M_n	I_{eff} (%)
1	0.78	0.27	0	----	----	----
2	3.13	1.1	93	111,100	2.8	34
3	6.25	2.2	89	93,400	3.0	39
4	12.5	4.3	91	54,100	3.9	68
5	25.0	8.6	93	51,000	4.2	74

$[\text{IB}] = 2.1 \text{ mol/L}$; run time = 30 minutes; $[\text{I}] = [2\text{-phenylpropan-2-ol}] = 2.9 \times 10^{-3} \text{ mol/L}$; $[\text{B}] = [B(\text{pfp})_3]$

Table 3: Data for Determination of $k_{tr,M}/k_p$ at -40°C

$[M]_0$	$[M]_t$	M_n
0.840	0.833	19,000
2.11	1.98	41,000
3.37	3.29	59,000
4.22	4.19	77,000
6.33	6.31	90,000

$V_t = 30$ ml: methylene chloride (15 ml) + hexane (15ml - volume of monomer); $[PPOH] = 2.4 \times 10^{-3}$ mol/L; $[B(pfp)_3] = 5.4 \times 10^{-3}$ mol/L.

reasonable assumption). From this plot, $k_{tr,M}/k_p$ is 2.4×10^{-4} and k_{tr}/k_p is 2.28×10^{-3} .

The C_{trM} value found here closely agrees with that determined for a $TiCl_4$ catalyzed isobutylene polymerization at -48°C in methylene chloride ($C_{trM} = 3.0 \times 10^{-5}$) (12). However, the C_{tr} value is unexpectedly high. A large C_{tr} value suggests that the counterion is very basic and strongly assists in chain transfer. There are other explanations. My assumption of $k_t \ll k_{tr}$ could be invalidated by chain transfer to initiator, reinitiation of the terminated polymer chains akin to reversible termination or dependency of the transfer constants on monomer concentration (especially high monomer concentration). Regardless, the values of chain transfer seem to conflict with the observed molecular weights of the prepared polyisobutylenes (Table 1). Additional experiments are required to understand this conflict.

Copolymerization of Isobutylene with Isoprene. Copolymerizations with 2.1 mol% isoprene (IP) were run at -30 and -50°C . The results of these experiments are

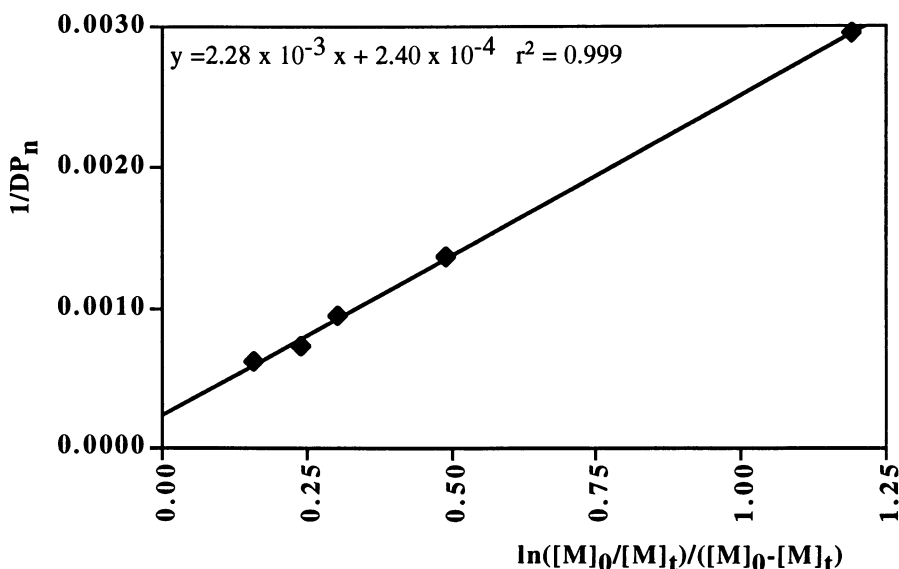
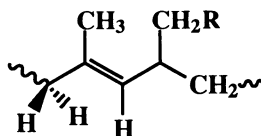


Figure 3: Integrated Mayo Plot for $B(pfp)_3$ Catalyzed Isobutylene Polymerization at -40°C in Methylene Chloride.

shown in Table 4. Yields and molecular weights of the copolymers are lower than comparable isobutylene homopolymerizations. This reduction is expected as a consequence of the combination of the chain transfer constants for each monomer (13). Even so, the M_n values are quite high for isobutylene-isoprene copolymerizations at -30°C . The low incorporation of isoprene compared to its composition in the feed contributes to the high M_n 's; however, slow initiation remains the major player in the preparation of high M_n polymers. For example, with PPOH as the initiator in experiment 1, a copolymer which is prepared with roughly twice the M_n expected based on a $[M]/[I]$ comparison at this conversion (49.5 kD). Using the more efficient initiator (TBDCC), on the other hand, provides for a copolymer with a M_n very close to the theoretical M_n (53.9 kD vs. 55.4 kD).

A minor, but important, structure in isobutylene-isoprene copolymers has been recently identified with NMR spectrometry (14). An olefinic resonance at 4.93 ppm (doublet) characterizes branching in the copolymers. The branch is centered on an IP unit and takes the form:



"R" is a branch of unspecified length. ^1H NMR does not permit any distinction between short and long chain branching. This unit may arise from hydride abstraction by a growing chain end followed by subsequent reinitiation. No 1,2 or 2,3 addition products for isoprene were observed and none are observed here either.

The percent branch column in Table 4 refers to the mole percent of branched isoprene units in the copolymer. Polymer 2, for example, contains 0.07 mol% branch point isoprene units per polymer chain or one branch once every 1429 repeating units. This works out, with a M_n of 94.4 kD, as one branch per chain. The influence of branching on molecular weight determinations and physical property characteristics in these copolymers is not known. Branching at this level is somewhat equivalent to that found in commercial butyl rubber prepared at -100°C (14).

The percentage of isoprene involved in branching was shown to increase with increasing polymerization temperature for ethylaluminum dichloride (EADC) catalyzed polymerizations. At -30°C , copolymers prepared using EADC can have as many as 75% of the isoprene units involved in branching at 2 mol% isoprene incorporation.

Table 4: $\text{B}(\text{pfp})_3$ Isobutylene/Isoprene Copolymerizations in Methylene Chloride

Rxn.	initiator, [I] $\times 10^3$ (mol/L)	Temp. ($^\circ\text{C}$)	Yield (%)	M_n	M_w/M_n	% IP incorp.	% branch
1	PPOH, 1.8	-30	44	94,400	2.1	1.0	0.07
2	TBDCC, 2.0	"	55	53,900	2.5	1.4	0.05
3	BrMP, 1.8	"	7	173,100	2.0	1.0	0.07
4	H_2O , 2.4	"	14	103,800	3.1	1.3	0
5	H_2O , 1.0	-50	21	218,300	2.8	0.7	0

$[\text{IB}] = 3.6$; $[\text{IP}] = 7.8 \times 10^{-2}$ mol/L; $[\text{B}(\text{pfp})_3] = 3.9 \times 10^{-3}$ mol/L; run time = 30 minutes; PPOH : 2-phenylpropan-2-ol; TBDCC: 5-tert-butyl-1,3-bis(1-chloro-1-methylethyl)benzene; BrMP: 2-methyl-2-bromopropane.

Example 2 referred to above exhibits the largest amount of isoprene units involved in branching for any of the copolymers and represents a significant improvement over the EADC system.

Copolymerization of Isobutylene with p-Methylstyrene. A few copolymerizations were also run at -30 and -50 °C with 2.1 mol% p-methylstyrene (pMS) in the feed. The copolymers were analyzed for M_n , M_w/M_n , mol% incorporation of pMS, and %BSB triads. The latter two values were determined from ^1H NMR spectra of the copolymers. Determination of BSB triad information in pMS-IB copolymers has been recently reported (15,16). We have developed a ^1H NMR method (procedure to be disclosed later) to determine BSB values. This procedure is less time consuming than the ^{13}C method and agrees fairly well with its BSB values ($\pm 5\%$). Table 5 contains the data obtained for the copolymers. With organic initiators such as PPOH and TBDCC, high conversions can be reached within a thirty minute reaction time. M_n values at moderate and high conversion fall short of the theoretical M_n values at corresponding conversions (except for rxn. 9). This trend may be explained by improved initiation, perhaps an initiation preference for pMS, or an increased participation of chain transfer due to pMS. These processes may also combine to give this outcome.

Table 5: B(pfp)₃ Isobutylene/p-Methylstyrene Copolymerizations

Rxn.	initiator, [I] x 10 ³ (mol/L)	Temp. (°C)	Yield (%)	M_n	M_w/M_n	% pMS incorp.	% BSB
1	PPOH, 1.8	-30	85	43,500	2.3	1.4	64
2	TBDCC, 2.0	"	94	16,900	2.8	1.7	51
3	BrMP, 1.8	"	53	22,400	3.6	2.0	58
4	H ₂ O, 2.4	"	47			2.0	58
5a	"	"	2.8	59,800	2.1	5.0	46
6b	"	"	33	70,700	2.1	3.8	58
7c	"	"	63	39,000	2.8	2.9	67
8	H ₂ O, 1.0	-50	39	127,700	2.3	1.5	56
9	PPOH, 1.8	"	41	92,900	2.3	1.5	59

except where noted - [IB] = 3.6 mol/L; [pMS] = 7.8×10^{-2} mol/L; [B(pfp)₃] = 3.9×10^{-3} mol/L; run time = 30 minutes; PPOH: 2-phenylpropan-2-ol; TBDCC: 5-tert-butyl-1,3-bis(1-chloro-1-methylethyl) benzene; BrMP: 2-methyl-2-bromopropane; a: [IB] = 6.7 mol/L, [pMS] = 0.13 mol/L, [B(pfp)₃] = 0.003 mol/L; b: same as "a", but 3 hour reaction time; c: same as "a", but 6 hours. ND: not determined

A few experiments suggest a slight preference for pMS, with incorporation levels exceeding feed levels. This preference is supported by pMS incorporation and BSB values at low conversion. Experiments 5,6 and 7 differ only by time and hence conversion. At low conversion, experiment 5, pMS incorporation is more than twice the feed level with the highest BSB value for this experimental set. Thus, pMS is entering the copolymer at a faster rate than IB. The expected trends, lower pMS incorporation and higher BSB values, are observed in experiments 6 and 7. BSB values generally average around 58, with a low of 48 in experiment 5 and a high of 67 in experiment 7. pMS-IB copolymers prepared by a "living" polymerization system in ethyl chloride with a 3:97 molar ratio exhibit similar values (16, 17). In the "living"

system, these BSB values were correlated to calculated reactivity ratios of $r_{\text{pMS}} = 7.99$ and $r_{\text{IB}} = 0.74$. Although the experiments presented here are under different conditions, the similarity of the BSB values strongly suggests that similar reactivity ratios are in effect here.

Conclusions

$\text{B}(\text{pfp})_3$ is an effective catalyst for preparing high M_n isobutylene homo- and copolymers at -30 and -50 °C. The molecular weights observed here are relatively high in light of the polymerization temperatures. The highest M_n polymers and copolymers are prepared with water or PPOH as the initiator as a result of slow, inefficient initiation. The polymerizations are generally slow, but are retarded by increasing the nonpolar character of the solvent. IP copolymerizations result in minor amounts of branching, representing an improvement (in addition to higher M_n) over the use of EADC at these polymerization temperatures. Although M_n values in pMS/IB copolymerizations are lower than either homopolymerizations or copolymerizations of IB with IP, the microstructure of the copolymers compares favorably with similar pMS/IB copolymers prepared at lower temperatures with other catalysts.

Experimental

Materials. Purification of monomers, solvents, synthesis of initiators, etc. have been presented previously (7). 2-phenylpropan-2-ol was purchased from Aldrich Chemical Co. and used as received. Tris(pentafluorophenyl) boron was purchased from Quantum Chemical Co.

Polymerizations. Polymerizations and copolymerizations were run in resin kettles in a dry box. Temperature was maintained with a pentane bath cooled by liquid nitrogen in the dry box. Cooling was controlled with a solenoid operated by a microprocessor set to a specified temperature (± 1 °C). Solvents, monomers and initiators were mixed with mechanical agitation and cooled to the desired temperature in the kettle. Catalyst, dissolved into 1 to 2 ml of solvent, was then added to the charge with a glass pipette or syringe. Quenching of the polymerization was not necessary before precipitation, but, when desired, methanol was added. Polymers were purified by methanol precipitation and dried in vacuo at 50 °C.

Characterization. GPC analyses were run in THF at 45 °C with 5 PSL GPC columns (10^5 , 10^4 , 10^3 , 500 and 100 Å) and a flow rate of 1 ml/min. Calibration was performed using polystyrene standards and Mark-Houwink constants to develop a PIB calibration curve. This curve was tested every 12 samples with two narrow molecular distribution PIB standards (prepared in house). ^1H NMR spectra were recorded on a Bruker AC-250 250 MHz spectrometer in CDCl_3 solutions using residual chloroform as the internal reference.

Isoprene Copolymer Composition and % Branching Determination. Compositions were determined by recording spectra and integration on dried polymer samples. %IP incorporation was determined by measuring the integral values of the 5.1 (A) and 4.93 (B) resonances of the olefinic protons of isoprene and the aliphatic resonances (C). Isoprene incorporation was then calculated from equation 1

$$\% \text{IP} = 100 \times [8(\text{A}+\text{B})]/(\text{A}+\text{B}+\text{C}) \quad (1)$$

and branching was calculated from equation 2

$$\% \text{ branch} = 100 \times (B/[A + B]) \quad (2)$$

p-Methylstyrene Copolymer Composition. From the recorded spectra and integration on cried polymer samples, integral values were compared for the 7.1 to 6.8 ppm region (D) with those of the aliphatic region of 3.0 to 0.5 ppm (E). Using these values and equation 3, we calculated %pMS incorporation.

$$\% \text{pMS} = 100 \times (8D)/(4E + 2D) \quad (3)$$

Literature Cited

1. Shaffer, T.D. *US Patent Appl.* 08/234,782 April 1994.
2. Quyoum, R.; Wang, Q; Turdet, M.-J.; Baird, M.C.; Gillis, D.J. *J. Amer. Chem. Soc.* **1994**, *116*, 6435.
3. Barsan, F.; Baird, M.C. *J. Chem. Soc. Chem. Commun.* **1995**, 2065.
4. Baird, M.C. *US Patent* 5,439,996 August 8, 1995.
5. Baird, M.C. *US Patent* 5,448,001 September 5, 1995.
6. Wang, Q.; Quyoum, R.; Gillis, D.J.; Tudoret, M.J.; Jeremic, D.; Hunter, B.K.; Baird, M.C. *Organometallics* **1996**, *15*, 693.
7. Shaffer, T.D.; Ashbaugh, J.R. *J. Polym. Sci. Polym. Chem. Ed.* **1996**, *34*, 0000.
8. Massey, A.G.; Park, A.J. *J. Organomet. Chem.* **1966**, *5*, 218.
9. *Cationic Polymerizations: Mechanisms, Synthesis and Applications* Matyjaszewski, K. Ed.; Marcel Dekker, Inc.: New York, NY, 1996.
10. Matyjaszewski, K. *J. Macromol. Sci., Pure Appl. Chem.* **1994**, *A31*, 989.
11. Faust, R.; Kennedy, J.P. *J. Polym. Sci. Polym. Chem.* **1987**, *25*, 1847.
12. Biddulph, R.H.; Plesch, P.H.; Rutherford, P.P. *J. Chem. Soc.* **1965**, 275.
13. Kennedy, J.P.; Marechal, E. *Carbocationic Polymerization*; John Wiley & Sons: New York, NY, 1982.
14. White, J.L.; Shaffer, T.D.; Ruff, C.J.; Cross, J.P. *Macromolecules* **1995**, *28*, 3290.
15. Lubnin, A.; Orszagh, I.; Kennedy, J.P. *J. Macromol. Sci., Pure Appl. Chem.* **1995**, *A32*, 1809.
16. Nagy, A.; Orszagh, I.; Kennedy, J.P. *J. Phys. Org. Chem.* **1995**, *8*, 273.
17. Orszagh, I.; Nagy, A.; Kennedy, J.P. *J. Phys. Org. Chem.* **1995**, *8*, 258.

Chapter 10

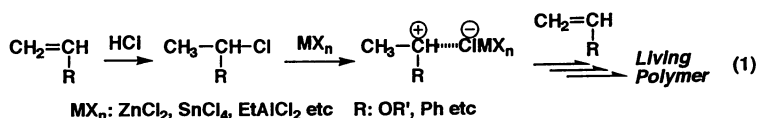
Living Cationic Polymerization with $\text{Yb}(\text{OSO}_2\text{CF}_3)_3$ as a Water-Resistant, Recoverable Lewis Acid

Kotaro Satoh, Hiroshi Katayama, Masami Kamigaito, and Mitsuo Sawamoto¹

Department of Polymer Chemistry, Graduate School of Engineering,
Kyoto University, Kyoto 606-01, Japan

Living cationic polymerization of isobutyl vinyl ether (IBVE) has been achieved with $\text{Yb}(\text{OTf})_3$ -based initiating systems ($\text{OTf} = \text{OSO}_2\text{CF}_3$) where the ytterbium salt is a Lewis acid-type activator coupled with the hydrogen chloride-adduct of IBVE as an initiator and a nitrogen-based nucleophilic additive such as triethylamine. The polymerization proceeds even in the presence of strong nucleophiles like the aliphatic amine and pyridines to give narrowly distributed polymers with controlled molecular weights. $\text{Yb}(\text{OTf})_3$ can be recovered from the reaction mixtures by extraction with water, followed by drying, and the recovered salt can induce similar living polymerization, indicating that $\text{Yb}(\text{OTf})_3$ is a water-resistant, recoverable unique Lewis acid for cationic polymerization, where water and amines are usually strong inhibitors and/or chain transfer agents.

Lewis acids play important roles in cationic polymerizations of vinyl monomers. For example, cationic polymerizations are often initiated with combinations (initiating systems) of a protonic acid and a Lewis acid (MX_n); see eq 1. Generally, the protonic acid forms an adduct with a monomer, e.g., the alkyl chloride in eq 1, and in this particular example, the Lewis acid interacts with the chlorine to ionize the adduct; propagation thus commences. The interaction thereby generates a complex anion (e.g., $-\text{ClMX}_n$ in eq 1) that serves as the counteranion of the propagating carbocation. As seen from such a brief description, the Lewis acid components affect not only the initiation but also the propagation processes by associating with the growing carbocation and thereby controlling its nature.

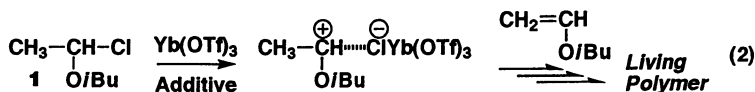


¹Corresponding author

The selection of Lewis acids is equally important in designing living cationic polymerization (1,2). We have already shown that one of the crucial factors in this aspect is the Lewis acidity, as affected by the central metal and its substituents (halogen, alkoxy group, etc.) (3,4). In contrast to the large variety of initiators (protonic acids and their derivatives), however, the scope of the Lewis acids for living cationic polymerization is rather limited, confined to the halides and alkoxides of boron, aluminum, zinc, tin, and titanium.

In this study we focus our attention to rare earth metal or lanthanide salts as new Lewis acids (activators) for living cationic polymerization. Among them, ytterbium trifluoromethanesulfonate [$\text{Yb}(\text{OTf})_3$; $\text{OTf} = \text{OSO}_2\text{CF}_3$] is of interest, which is known as a unique Lewis acid characterized by the strong Lewis acidity, the large ionic radius of the central metal, and, in particular, its tolerance towards water (5–7). For example, the triflate can mediate aldol and other organic reactions in aqueous media where conventional metal halide-type Lewis acids are of course inactivated.

Thus, we herein employed $\text{Yb}(\text{OTf})_3$ for the living cationic polymerization of isobutyl vinyl ether (IBVE) in conjunction with its adduct (1) with hydrogen chloride as an initiator (eq 2). Proper choice of reaction conditions and nucleophilic additives in fact led to living cationic IBVE polymerization. The controlled polymerization is possible even in the presence of strong amines, and $\text{Yb}(\text{OTf})_3$ can be repeatedly used after recovery from the reaction mixtures by extraction with water, despite the fact that amines and water are well-known inhibitors and/or chain transfer agents in cationic polymerization with conventional metal halides.



Living Cationic Polymerization with $\text{Yb}(\text{OTf})_3$

Cationic polymerization of IBVE was carried out in dichloromethane (CH_2Cl_2) at -15°C with the $1/\text{Yb}(\text{OTf})_3$ initiating system [$\mathbf{1}$, 5.0 mM; $\text{Yb}(\text{OTf})_3$, 2.0 mM] (see Experimental Section). Throughout this study, the ytterbium salt was of the anhydrous form, obtained by vacuum drying a commercial hydrate under heating at 200°C , and it was employed as a solution in tetrahydrofuran (THF); unless otherwise specified, the reaction medium therefore consisted of a $\text{CH}_2\text{Cl}_2/\text{THF}$ mixture with 10 vol% THF. Under these conditions the polymerization was almost instantaneous and resulted in polymers with uncontrolled molecular weights and broad molecular weight distributions (MWDs).

Subsequent search of nucleophilic additives showed that the $\text{Yb}(\text{OTf})_3$ -mediated polymerization was clearly retarded in the presence of a sterically hindered pyridine, 2,6-di-*tert*-butyl-4-methylpyridine (DTBMP; 2.0 mM) and was completed in 12 hr (Figure 1). A similar and slightly slower polymerization occurred with tin tetrachloride (SnCl_4) in place of $\text{Yb}(\text{OTf})_3$. On the other hand, the use of ytterbium chloride (YbCl_3), instead of the triflate counterpart, led to a much slower polymerization, showing the marked effect of the strongly electron-withdrawing triflate groups on the ytterbium center.

In the presence of the pyridine, the polymerizations with $\text{Yb}(\text{OTf})_3$ and SnCl_4 gave polymers with narrow MWDs ($M_w/M_n = 1.1\text{--}1.2$), whereas the polymers with YbCl_3 had broader distributions. Separate analysis of number-average molecular weights (M_n) as a function of conversion showed that the former two systems yielded living polymers whose molecular weights are directly proportional to conversion. Thus, living cationic polymerization of IBVE has been achieved with $\text{Yb}(\text{OTf})_3$ in the

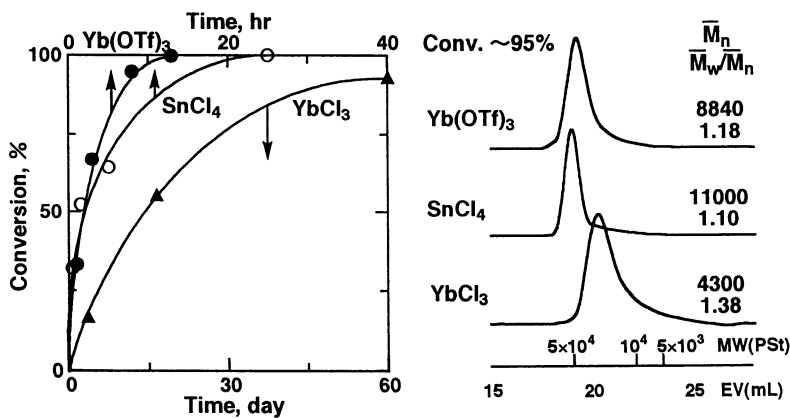


Figure 1. Polymerization of IBVE with **1**/Lewis acid initiating systems in CH₂Cl₂ at -15 °C: [IBVE]₀ = 0.38 M; [**1**]₀ = 5.0 mM; [Lewis acid]₀ = 2.0 mM; [DTBMP]₀ = 2.0 mM; THF, 10 vol%. Lewis acids: (●) Yb(OTf)₃; (○) YbCl₃; (▲) SnCl₄. The MWDs are for the polymers obtained at ca. 95 % conversion

presence of DTBMP. As will be discussed later in this paper, the added pyridine may serve as a proton scavenger to prevent an uncontrolled polymerization with adventitious water and, additionally, may interact with the ytterbium salt to modify its Lewis acidity (8).

Effects of Nitrogen Nucleophiles

The possibility of Yb(OTf)₃-mediated living polymerization of IBVE was further examined with the use of a series of pyridines and amines, as summarized in Figures 2 and 3.

Sterically Hindered Pyridines. Living cationic polymerization with Yb(OTf)₃ proved also possible in the presence of 2,6-disubstituted, sterically hindered pyridines, such as 2,6-diphenylpyridine and 2,4,6-trimethylpyridine, along with DTBMP (Figure 2). All these systems gave polymers with narrow MWDs, and their molecular weights M_n are in direct proportion to monomer conversion and in good agreement with the calculated values based on the initial monomer/initiator (IBVE/**1**) feed mole ratio.

Triethylamine and Pyridine. More important, similar living polymerizations proceeded even in the presence of triethylamine and pyridine (unsubstituted), i.e., strong nucleophiles without steric hindrance. As shown in Figure 3, the reactions are slower than those with the hindered derivatives (Figure 1), nevertheless the product polymers had narrow MWDs and controlled molecular weights. Under otherwise the same conditions, SnCl₄ can hardly induce polymerization, as has been known in conventional cationic systems.

Thus, Yb(OTf)₃, coupled with initiator **1**, mediates living cationic polymerization of IBVE in the presence of suitable nitrogen-based nucleophiles as additives. It is particularly interesting that the Yb(OTf)₃-mediated reaction is not inhibited by the sterically unhindered, strongly basic amines (triethylamine and pyridine), in sharp contrast to the extremely slow polymerization with SnCl₄ under similar conditions (Figure 3).

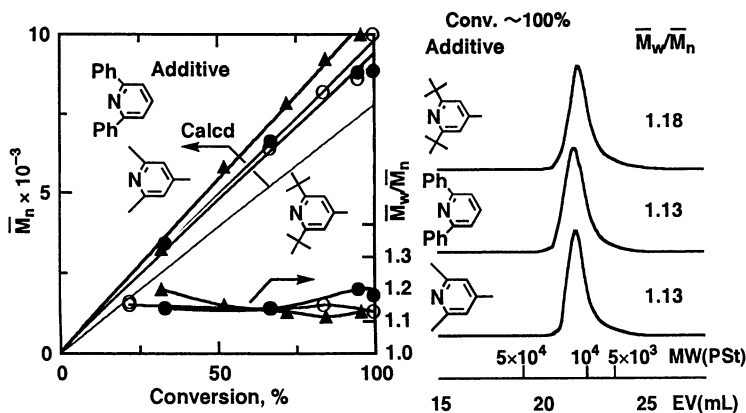


Figure 2. M_n , M_w/M_n , and MWD of poly(IBVE) obtained with **1**/ $Yb(OTf)_3$ in CH_2Cl_2 at $-15^\circ C$ in the presence of hindered pyridines: $[IBVE]_0 = 0.38 M$; $[I]_0 = 5.0 mM$; $[Yb(OTf)_3]_0 = 2.0 mM$; $[pyridine]_0 = 2.0 mM$; THF, 10 vol%. Pyridines: (●) 2,6-di-*tert*-butyl-4-methylpyridine; (○) 2,4,6-trimethylpyridine; (▲) 2,6-diphenylpyridine.

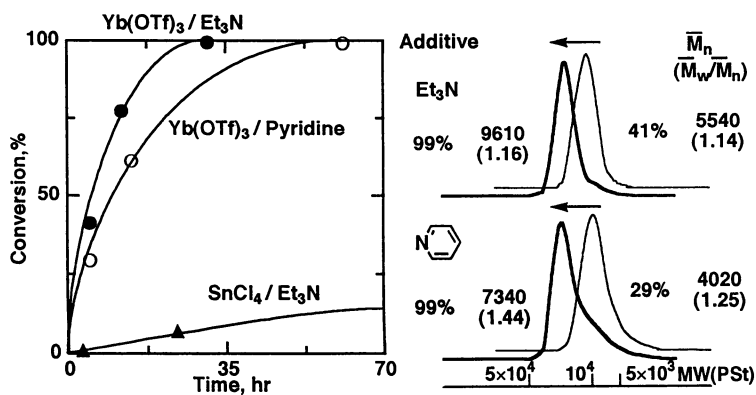


Figure 3. Polymerization of IBVE with **1**/Lewis acid initiating systems in CH_2Cl_2 at $-15^\circ C$ in the presence of triethylamine (Et_3N) or pyridine: $[IBVE]_0 = 0.38 M$; $[I]_0 = 5.0 mM$; $[Lewis\ acid]_0 = 2.0 mM$; $[additive]_0 = 2.0 mM$; THF, 10 vol%. Lewis acid/additive: (●) $Yb(OTf)_3/Et_3N$; (○) $Yb(OTf)_3/pyridine$; (▲) $SnCl_4/Et_3N$

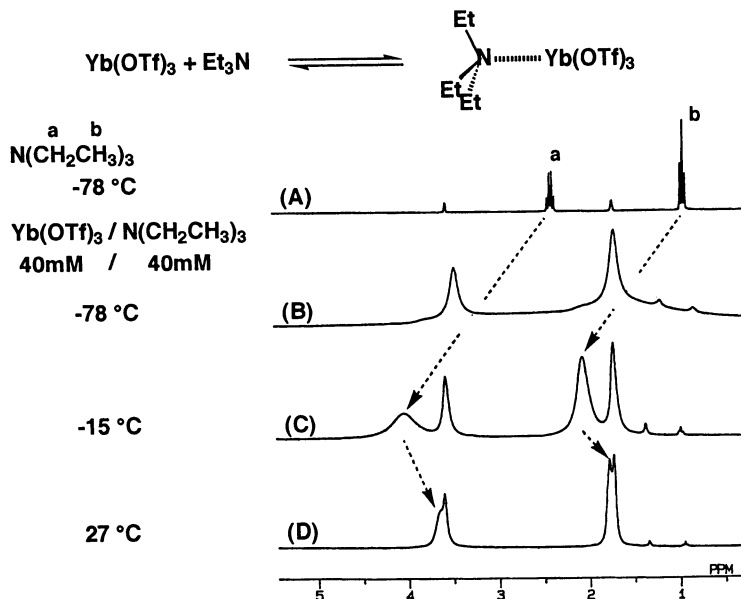


Figure 4. ^1H NMR spectra (270 MHz) of triethylamine (A) and its mixtures with $\text{Yb}(\text{OTf})_3$ (B–D) in $\text{THF-}d_8$ at varying temperatures ($^\circ\text{C}$): (A,B) -78 ; (C) -15 ; (D) 27 . $[\text{Yb}(\text{OTf})_3]_0 = [\text{Et}_3\text{N}]_0 = 40$ mM.

Interaction of $\text{Yb}(\text{OTf})_3$ with Triethylamine: ^1H NMR Study. Figure 4 illustrates a series of ^1H NMR spectra for an equimolar mixture of $\text{Yb}(\text{OTf})_3$ and triethylamine in $\text{THF-}d_8$. At -78 $^\circ\text{C}$ the amine alone exhibits characteristic signals of the ethyl groups in the region of 1–2.4 ppm (Figure 4A). On addition of $\text{Yb}(\text{OTf})_3$, these peaks became very broad and shifted to lower field to overlap with the sharp resonances of the undeuterated THF solvent (Figure 4B). The shifted ethyl signals sharpened at higher temperatures (Figures 4C and 4D), and they were well separated from the THF peaks at -15 $^\circ\text{C}$, the temperature at which the living polymerization proceeded.

These spectral changes show that the ytterbium salt interacts with triethylamine, as schematically shown in Figure 4, and this interaction most probably induces electron-donation from the amine to $\text{Yb}(\text{OTf})_3$ and thereby renders the latter a weaker Lewis acid that would be suitable for living cationic polymerization. The specific interaction of the amine also prevents its termination on the growing carbocation.

Living Polymerization with Recovered $\text{Yb}(\text{OTf})_3$

An expected feature of the use of $\text{Yb}(\text{OTf})_3$ is its tolerance towards water (see above), and to demonstrate that, we carried out the following experiments. Thus, the IBVE polymerization with the $1/\text{Yb}(\text{OTf})_3$ system was run at -15 $^\circ\text{C}$ in CH_2Cl_2 in the presence of DTBMP additive (2 vol% THF in the solvent). When IBVE conversion reached near 100%, the reaction was quenched with methanol, and the reaction mixture was diluted with hexane. The $\text{Yb}(\text{OTf})_3$ in the diluted reaction mixture was extracted with water (the salt is highly soluble therein), isolated by evaporating off the water, and vacuum dried at 200 $^\circ\text{C}$ for 6 hr. The produced polymers are recovered from the remaining hexane phase via evaporation under reduced pressure.

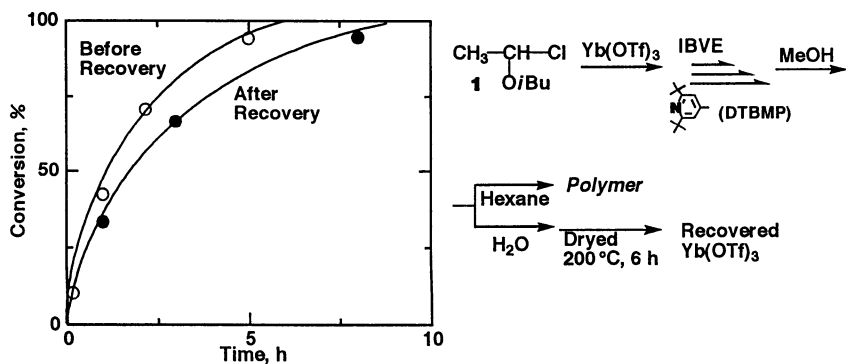


Figure 5. Polymerization of IBVE with **1** and recovered $Yb(OTf)_3$ in CH_2Cl_2 at $-15\text{ }^\circ\text{C}$ in the presence of DTBMP: $[IBVE]_0 = 0.38\text{ M}$; $[1]_0 = 5.0\text{ mM}$; $[Yb(OTf)_3]_0 = 2.0\text{ mM}$; $[DTBMP]_0 = 2.0\text{ mM}$; THF, 2.0 vol%. $Yb(OTf)_3$: (O) pristine; (●) recovered.

The $Yb(OTf)_3$ thus recovered was employed again for the IBVE polymerization under the same conditions as in the first run (Figure 5). The polymerizations with the pristine and the recovered $Yb(OTf)_3$ proceeded at nearly the same rates and reached quantitative conversion in 5–8 hr.

In addition, the polymers obtained in both systems (Figure 6) showed similarly narrow MWDs, and their molecular weights are directly proportional to conversion and close to the calculated values for living polymers. These results demonstrate that the recovered $Yb(OTf)_3$ is able not only to effectively induce IBVE polymerization but to give living polymers as well, despite that the recovery process involves treatment with a large amount of water that might deactivate the strong Lewis acid.

Namely, the ytterbium salt proved to be water-resistant and recoverable Lewis acid that is also effective in the presence of strong nucleophiles such as triethylamine and pyridine. This unique feature suggests that $Yb(OTf)_3$ might mediate cationic polymerization in *aqueous media*, where conventional cationic polymerization is believed to be impossible. Experiments in this line are in progress in our laboratories.

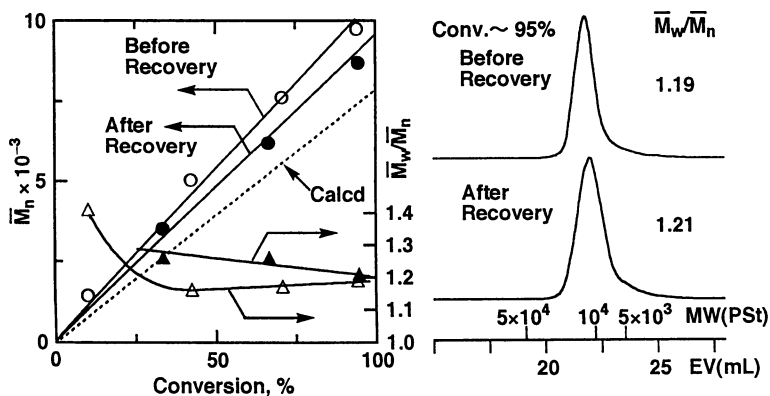


Figure 6. M_n , M_w/M_n , and MWD of poly(IBVE) obtained with **1** and recovered $Yb(OTf)_3$ in CH_2Cl_2 at $-15\text{ }^\circ\text{C}$ in the presence of DTBMP (cf. Figure 5): $[IBVE]_0 = 0.38\text{ M}$; $[1]_0 = 5.0\text{ mM}$; $[Yb(OTf)_3]_0 = 2.0\text{ mM}$; $[DTBMP]_0 = 2.0\text{ mM}$; THF, 2.0 vol%. $Yb(OTf)_3$: (O, Δ) pristine; (●, \blacktriangle) recovered.

Experimental Section

Materials. Yb(OTf)₃ (Aldrich) was obtained commercially as a hydrate. The hygroscopic salt was vacuum dried into the anhydrous form at 200 °C for 6 hr and was immediately dissolved under dry nitrogen in dry THF containing DTBMP or other nucleophiles [Yb(OTf)₃ and the nucleophile, 20 mM each]; without the nucleophile, the anhydrous salt induces cationic ring-opening polymerization of THF. YbCl₃ (Aldrich; hexahydrate, purity >99.9 %) was also dried and treated in the same way. SnCl₄ (Aldrich; 1.0 M solution in CH₂Cl₂) was used as commercially received and diluted with the same solvent before use. IBVE (Tokyo Kasei; purity > 99 %) was washed successively with 10% aqueous sodium hydroxide and deionized water, dried overnight with potassium hydroxide pellets, and doubly distilled over calcium hydride prior to use. Stock solutions of the IBVE-HCl adduct (**1**) was prepared as reported (3,4).

The following hindered pyridines were invariably of commercial source (Aldrich) and used as received: 2,6-di-*tert*-butyl-4-methylpyridine (purity 98 %); 2,4,6-trimethylpyridine (99 %); 2,6-diphenylpyridine (99 %). Pyridine (Aldrich; >99.9 %) and triethylamine (Wako Chemicals; >99 %) were purified by double distillation over calcium hydride and LiAlH₄, respectively. CH₂Cl₂ and THF as solvents and toluene as an internal standard for gas chromatography were distilled twice over calcium hydride (for CH₂Cl₂ and toluene) or LiAlH₄ (for THF).

Procedures. Polymerization was carried out at -15 °C under dry nitrogen in baked glass tubes equipped with a three-way stopcock. Into a monomer solution in CH₂Cl₂ (4.0 mL, with IBVE and toluene 0.50 mL each) was added sequentially a prechilled solution of the initiator **1** (in CH₂Cl₂, 50 mM, 0.50 mL) and the solution of Yb(OTf)₃ and a nucleophilic additive (DTBMP etc., in THF, 0.50 mL; see above), and was terminated by adding prechilled ammoniacal methanol (2.0 mL). IBVE conversion was determined from its residual concentration by gas chromatography with toluene as an internal standard. The product polymers were isolated by evaporating the solvent and other volatiles under reduced pressure, as reported (3,4). Their MWD and Mn were determined by size-exclusion chromatography on the basis of a polystyrene calibration, which is in accordance with absolute M_n by NMR (3,4).

The recovery of Yb(OTf)₃ from the reaction mixture and its re-use for polymerization was described in the text.

Literature Cited

1. Sawamoto, M. *Prog. Polym. Sci.* **1991**, *16*, 111.
2. Matyjaszewski, M.; Sawamoto, M. *Cationic Polymerizations: Mechanisms, Synthesis, and Applications*; Matyjaszewski, M., ed.; Marcel Dekker: New York, NY, 1996; Chapter 4.
3. Kamigaito, M.; Maeda, Y.; Sawamoto, M.; Higashimura, T. *Macromolecules* **1993**, *26*, 2670.
4. Kamigaito, M.; Sawamoto, M.; Higashimura, T. *Macromolecules* **1995**, *28*, 5671.
5. Forsberg, J. H.; Spaziano, V. T.; Balasubramanian, G. K.; Liu, G. K.; Kinsley, S. A.; Duckworth, C. A.; Poteruca, J. J.; Brown, P. S.; Miller, J. L. *J. Org. Chem.* **1987**, *52*, 1017.
6. Kobayashi, S.; Hachiya, I. *Tetrahedron Lett.* **1992**, *33*, 1625.
7. Hachiya, I.; Kobayashi, S. *J. Org. Chem.* **1993**, *58*, 6958.
8. Yb(OTf)₃ may also be solvated preferentially by THF, the solvent for its stock solution (6,7).

Chapter 11

The Heterogeneous Cationic Polymerization of Aromatic Alkenes by Aluminum Triflate

Alessandro Gandini and Yao-Hong Yang

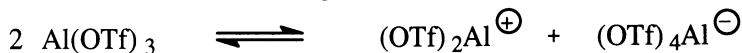
Matériaux Polymères, Ecole Française de Papeterie et des Industries Graphiques, Boite Postal 65, 38402 Saint Martin d'Hères, France

Aluminium triflate is a very convenient initiator for the polymerization of styrenic monomers. The systems investigated in this work call upon the use of that strong Lewis acid suspended in non polar solvents. The behaviour of 4-methylstyrene and indene as representative monomers for the C9 petroleum cut was explored both in heterogeneous homopolymerization and copolymerization conditions. Initiation was found to take place only through cocatalysis and monomer transfer was an important chain-braking event at room temperature. The low DPs thus obtained were deemed interesting in the context of the preparation of resinous materials. After the study of these batch reactions, a continuous mode was tested and the results showed that the catalyst operates adequately, but needs frequent regenerations.

The use of heterogenous means to initiate cationic polymerization has attracted sporadic attention since the late 1940s, with various laboratories becoming involved from time to time with the study of a specific solid catalyst. However, as underlined in a previous survey (1), up to the end of the 1970s, these contributions often lacked the necessary scientific approach to justify reliable mechanistic conclusions. It was at that time that a thorough investigation of the activity of numerous metal perchlorates and triflates in relation to both typical electrophilic reactions and cationic polymerizations was carried out in our laboratory in order to assess both the relative reactivity of the salts used, the initiating mechanisms involved and the kinetic features of the most promising systems (1-3).

In this study, the metal salts were employed in different media, of which some were entirely heterogeneous (1), others involved the presence of both dissolved and solid species (3) and finally, some allowed the complete dissolution of the catalyst (2,3). Aluminium triflate (AT) was found to be one of the most interesting initiators, capable of operating under the different conditions mentioned, albeit through different mechanisms. Among the conventional electrophilic reactions, alkylations, acylations,

carbinol dehydrations, alkene hydrations and esterifications gave very satisfactory results in terms of yields and selectivity (3). Cationic polymerization systems were of course also thoroughly scrutinized using this initiator (1-3). In solvents of low polarity ($\epsilon \sim 2$), **AT** was entirely insoluble and acted therefore at the liquid/solid interphase essentially through cocatalysis. In solvents of medium polarity ($\epsilon \sim 10$), direct initiation was shown to take place even for the predominantly insoluble portion of the salt. In highly polar media, viz. solvents like nitromethane or some bulk *n*-donor monomers, **AT** was soluble up to fairly high concentrations and its mode of initiation was found to occur following its selfionization:



and the subsequent addition of the aluminium cation to the alkenyl unsaturation or the heteroatom of the monomer.

AT can be readily prepared by different synthetic routes, of which two were selected in that work (1-3), namely: (i) the reaction of aqueous triflic acid with an excess of aluminium powder, or (ii) the reaction of triethyl aluminium with a dry solution of triflic acid in methylene chloride. It was found that, provided the salt prepared by the former method was correctly dried, both preparations led to the same species in terms of qualitative and quantitative activity.

A large variety of monomers were found to respond to activation by **AT**. These included aliphatic and aromatic alkenes, vinyl ethers and other *n*, π -donor structures, as well as numerous heterocycles (1-3) and their relative reactivity led to the conclusion that this novel initiator ought to be considered as a particularly strong Lewis acid.

The present study deals with a more specific approach in which we called upon **AT** as a potentially useful *heterogeneous* catalyst for the polymerization of aromatic alkenes in a more practical context. It was in fact thought that we could use this initiator to convert what is usually known as the "*C9 cut*" into a resinous product. This fraction, arising from petroleum cracking, contains a mixture of aromatic structures which include polymerizable species like substituted styrenes and indene together with non-polymerizable components like xylenes. It is used industrially as a source of resins for paint, printing inks, etc. after the various alkenes have been oligomerized cationically by conventional initiators. The replacement of the latter acidic catalysist by **AT** seemed an interesting proposition because of the possibility of using fixed-bed heterogeneous catalysis, i.e. a continuous polymerization system for the *C9 cut*.

In order to acquire a sound understanding of this new system, it was decided to conduct a systematic study of the polymerization of two monomers representative of the *C9 cut*, namely 4-methylstyrene (**MS**) and indene (**IN**), as well as of their copolymerization in toluene, which again would simulate adequately the mixture of aromatic solvents in that cut.

Experimental

Aluminium triflate was synthesized by the simpler route, namely the reaction of aqueous triflic acid with a 20% excess of pure aluminium fine powder at 50°C for twenty hours. After filtration to separate the remaining unreacted metal, the salt was

isolated by vacuum drying at 150°C to constant weight. Various samples of **AT** were prepared following this straightforward technique and gave reproducible results, provided the same average crystal size was employed. **AT** was kept at room temperature in a dry atmosphere since it is quite hygroscopic. Whenever needed, it was submitted to cascade sieving under dry nitrogen in order to separate different granulometric fractions. **AT** is a remarkably stable salt in terms of its resistance or its indifference to photolysis and thermal degradation.

For the sake of comparison, two standard cationic initiators were also employed, namely boron fluoride etherate and titanium tetrachloride. Both were purchased as one molar solutions in methylene chloride and used as received.

The two monomers used in this work, **MS** and **IN**, were commercially available and were purified by fractional distillation. Each middle portion was collected over calcium hydride and left for at least 48 hours before use, in order to ensure adequate drying. The purity of these samples was checked by GLC (>99.5%) and their residual moisture content by Karl-Fischer titration ($<10^{-3}$ M).

The solvents were submitted to a similar procedure. Apart from toluene, which was the standard medium used in this study, xylenes and methylene chloride, were also employed for specific purposes as indicated below. The commercial solvents, used for precipitation and/or fractionation of the polymers, were pure products and did not undergo any treatment. All other reagents employed for specific mechanistic tests, like acetic acid, acetic anhydride and the sterically-hindered pyridine, were used as purchased. Both the silica beads used as support for the **AT**, as well as the molecular sieves used as drying agent in the flow experiments, were commercial products, each chosen for its specific role.

Batch polymerizations were conducted in a nitrogen atmosphere at room temperature, following the typical procedure described hereafter. A known amount of **AT** was introduced into the reaction flask and vacuum dried at 180°C for different periods of time. The salt was then allowed to cool to room temperature in a dry nitrogen atmosphere before the solvent and the monomer were added under vigorous magnetic stirring. Thereafter, samples were withdrawn at regular intervals and analysed by gas liquid chromatography in order to follow the kinetics of monomer consumption. These reactions were quenched by adding an excess of triethylamine. Copolymerizations, as well as reactions involving the addition of specific mechanism-diagnostic reagents, were carried out in the same way, except that in these systems the rate of consumption of each monomer was monitored. In all instances, xylene was used as reference for the GLC analyses.

Continuous polymerizations involved, first of all, the deposit of a thin layer of **AT** onto the silica support made up of beads with a granulometry of 0.04 to 0.063 mm. This was achieved by vacuum evaporation in a rotary system of an aqueous solution of **AT** in the presence of the silica beads. The resulting solid was introduced in a glass column and submitted to the same drying procedure described above for batch systems. The monomer/solvent mixture was then pumped through the column and samples collected continuously at its exit with a merry-go-round system. These samples were analyzed by GLC. In some experiments, as described below, a column containing 3 Å molecular sieves (adapted to the removal of moisture) preceded the catalyst column in order to improve the drying of the monomer solution.

Polymers were isolated by shaking the neutralized final solutions three times with distilled water and extracting the organic layer with methylene chloride. After

separating and drying the latter solution, the solvents and unpolymerized monomer(s) were vacuum evaporated thus leaving only the non-volatile products as residue. This mixture of oligomers and polymers was dissolved in a small amount of methylene chloride and the resulting solution poured into a large excess of methanol under vigorous stirring. This operation allowed the separation of two fractions, namely: an insoluble portion made up of a higher DP constituent and an oligomeric residue which was recovered by vacuum evaporation of the methanol/methylene chloride mixture.

The structures of both polymers and oligomers were characterised by FTIR and NMR spectroscopy, their M_n by vapour pressure osmometry and their molecular weight distribution by GPC using THF as eluent.

Results and Discussion

Batch Homopolymerization of 4-methylstyrene. The first set of experiments involved the batch polymerization of **MS** by **AT** in toluene at room temperature. Under these conditions, the initiator was totally insoluble in the reaction medium as shown by the fact that if **AT** was stirred for several minutes in toluene and the suspension filtered under nitrogen, the filtrate did not display any initiating activity, not only toward **MS**, but neither toward much more nucleophilic monomers like vinyl ethers. This was taken as evidence of complete insolubility of **AT** in toluene. Indeed, in our previous study, conducted in methylene chloride (3), **AT** had been shown in a similar experiment, to operate both as a solid and as a homogeneous initiator, although its solubility in that medium polarity solvent was very modest.

After a wide search concerning the various experimental parameters related to this system, we chose the following conditions as a *standard reference* to which later experiments were always compared:

- A temperature of 20-22°C (room temperature).
- A mixture of solvents made up of toluene containing about 10% of xylene (GLC standard).
- A *nominal* concentration of 5 g/l of **AT**, with an average grain size of 50 mm, which had been dried for five hours at 180°C under a vacuum of 5 Pa immediately before the polymerization.
- A monomer concentration of 1 M.

Under these conditions, polymerizations were quite reproducible even when different batches of **AT** were used. They reached completion within a few hours and the M_n values of the global product, were around 3000, independent of reaction yields. Figure 1 and Table 1 show a typical plot of conversion versus time for two such reactions conducted under the same conditions, as well as the molecular weights of the ensuing products. The corresponding polymerizations of **MS** initiated by $TiCl_4$ or $BF_3 \cdot Et_2O$ in the same solvent at room temperature required catalyst concentrations around $5 \cdot 10^{-3}$ M to give the same kinetic pattern and produced polymers with similar molecular weights. The relative sluggishness of both the heterogeneous and homogeneous reactions is obviously to be attributed to the very low polarity of the medium used in all these experiments.

In the search for the most appropriate polymerization conditions, we discovered that with nominal **AT** concentrations lower than 1 g/l, the reactions were extremely slow. Also, using **AT** without the implementation of the drying procedure

described above, gave low or very low polymerization rates with irreproducible kinetic patterns. The first mechanistic aspect explored was therefore the role of residual moisture on the behaviour of this polymerization. It was in fact very important to establish, on the one hand, the qualitative mechanistic criterion related to the possible action of AT in the absence of water, i.e. the possibility of direct initiation, and, on the other hand, the quantitative role of moisture in terms of cocatalysis versus poisoning.

Table 1. Experimental conditions and number-average molecular weights of two nominally identical polymerizations of MS

Run	[AT] (g/l)	[MS] (M)	Time (h)	Mn
1	4.8	1	4	3100
			8	2700
			24	2800
			96	2900
2	4.8	1	24	3000

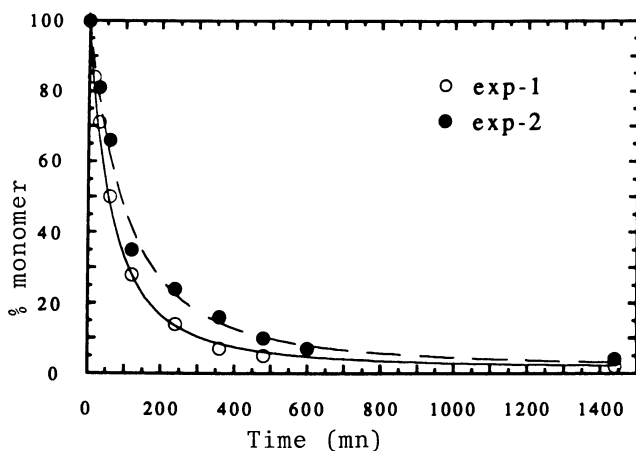


Figure 1. Conversion vs. time plots for the two polymerizations described in Table 1.

Figure 2 shows a series of experiments carried out in the same initial conditions, except for the amount of water present or added. As can be clearly observed, the use of AT without any drying procedure prior to the actual polymerization gave a very modest activity compared with that of the same system in which the standard heating under vacuum preceded the addition of the monomer solution. Specific additions of moisture to the dried initiator resulted in a progressive decrease in its activity, as shown in Figure 2, to the point where, with a water concentration of about 4×10^{-2} M in the reaction medium, the polymerization practically ceased. There is therefore little doubt that water can poison these systems through termination reactions and/or by decreasing the initiating efficiency of AT.

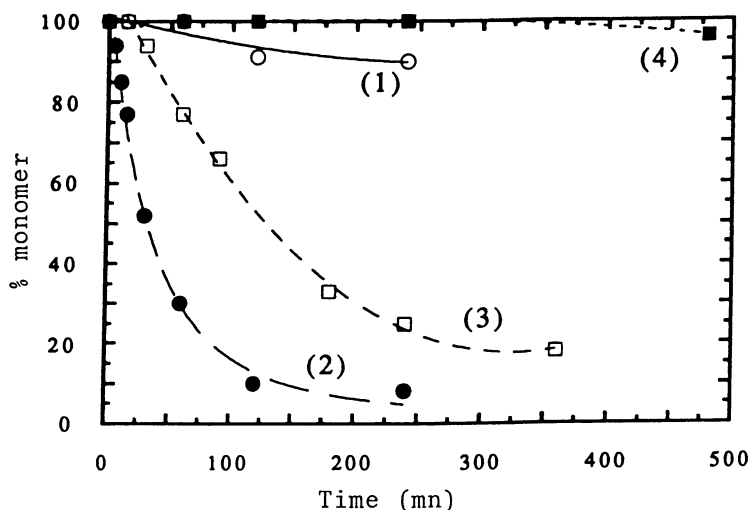


Figure 2. Conversion vs. time plots for a series of standard polymerizations of MS at room temperature. (1): MS not dried; (2): MS dried for 5 hours; (3): MS dried for 5 hours, then water added to give 10^{-2} M concentration; (4): same as (3) but water concentration $3.5 \cdot 10^{-2}$ M.

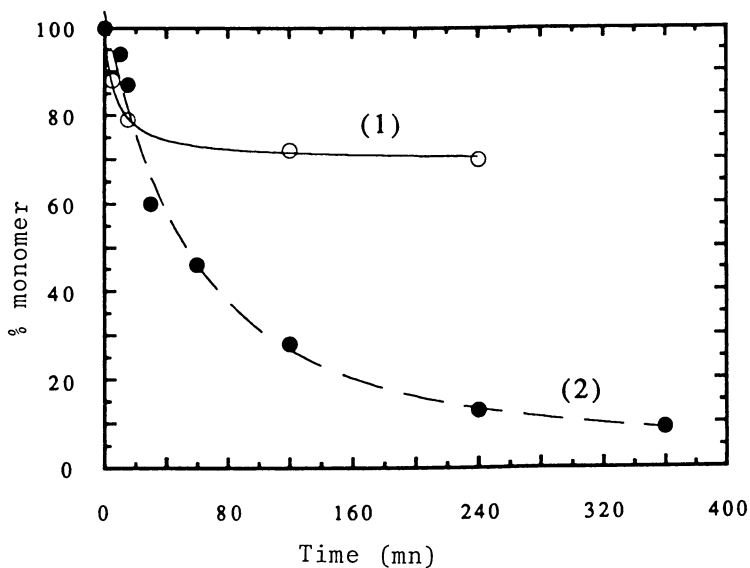


Figure 3. Conversion vs. time plots showing the effect of AT drying time under otherwise standard conditions. (1): 20 h; (2): 5 h standard drying time.

We then moved towards the opposite extreme, namely the reduction of residual moisture. Figure 3 shows the effect of prolonged drying compared with the standard procedure, which indicates a loss of activity, and, more precisely, the rapid cessation of the reaction which attained a limiting yield. This behaviour suggests that water is necessary for the initiation step and that it is probably consumed in the overall process of the formation of a dead polymer molecule, as is often encountered in cocatalytic processes related to cationic polymerization. Figure 4 shows another way of obtaining the same features which consisted in adding a chemical drying agent, viz. triethylaluminium to the standard dried system. This experiment corroborated the conclusion drawn from the results given in Fig. 3 since the activity was progressively reduced as the residual moisture was chemically removed.

Finally, 2,6-di-*t*-butyl-4-methylpyridine (**DBMP**) was used as a diagnostic reagent (4) to ascertain whether or not direct initiation occurred in the present conditions. Figure 5 shows that with progressively higher concentrations of this proton scavenger, polymerizations were slowed down and gave correspondingly lower limiting yields until, with about $2 \cdot 10^{-3}$ M of **DBMP**, they virtually ceased. This behaviour clearly indicates that initiation requires a protonation step which is quenched by the sterically hindered pyridine and that the fact that inhibition can be reached with a critical concentration of **DBMP**, no other cationation reaction takes place.

Thus, contrary to its behaviour in more polar media (1-3), aluminium triflate in toluene at room temperature does not induce the polymerization of 4-methylstyrene in the absence of traces of water. In other words, nodirect initiation was detected in the

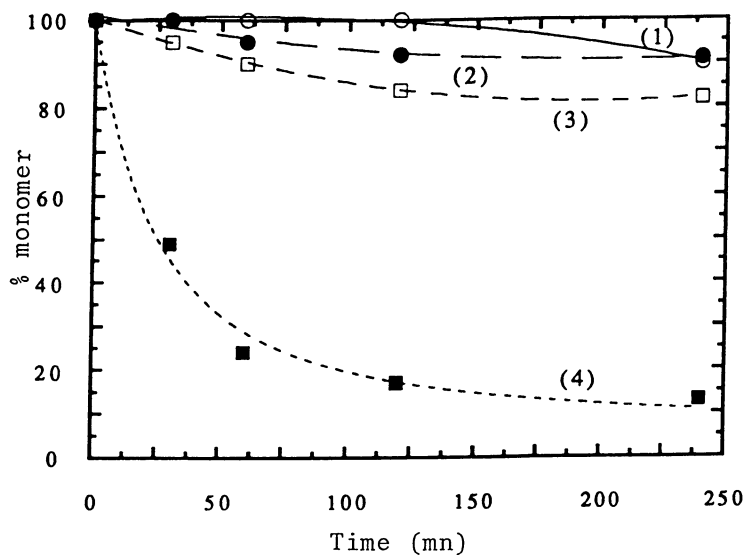
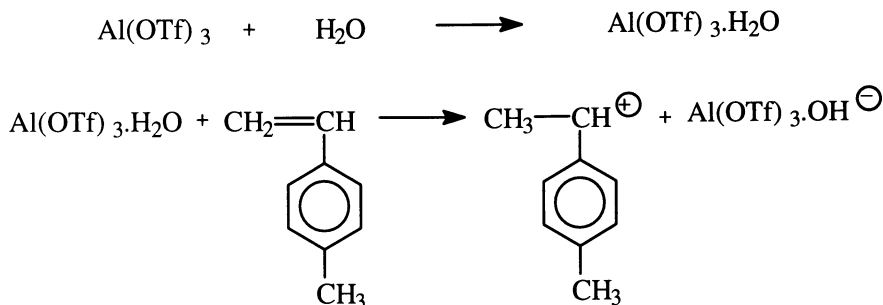


Figure 4. Conversion vs. time plots for a series of MS polymerizations carried out in the presence of $4.5 \cdot 10^{-3}$ M triethyl aluminium. (1): $[AT] = 0.47$ g/l; (2): $[AT] = 2.4$ g/l; (3): $[AT] = 4.8$ g/l; (4): $[AT] = 4.8$ g/l, without $AlEt_3$. In all experiments, AT was dried by the standard technique.

present system. The only initiation mechanism operating in this system is therefore a classical cocatalysis, viz.:



Moreover, the plateau attained with vigorously dried media indicates that water is consumed in the polymerization, probably by incorporation of the hydroxy anion when the propagating ion pair collapses:

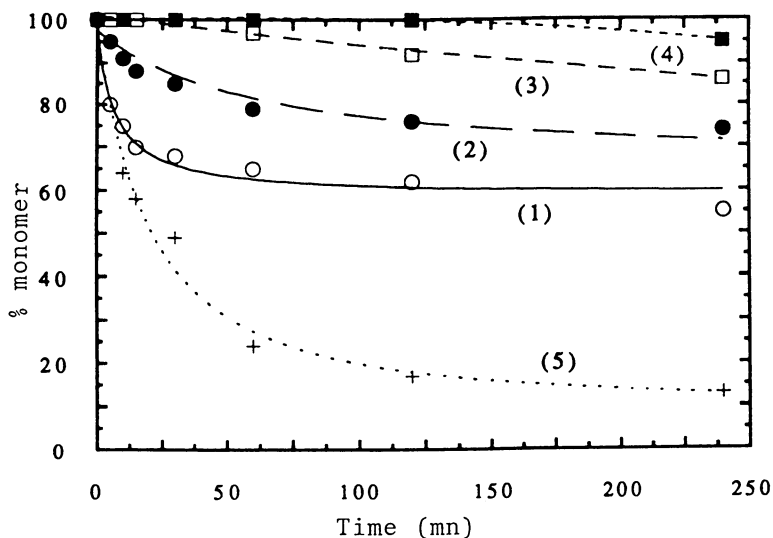
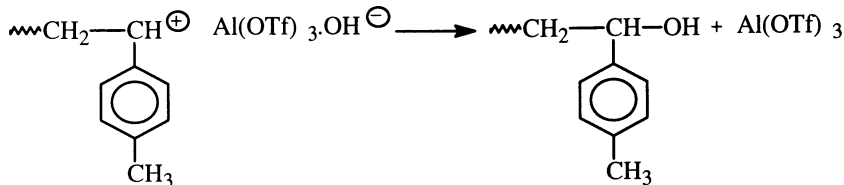


Figure 5. Conversion vs. time plots for a series of standard MS polymerizations in the presence of variable amounts of DBMP. (1): $[DBMP] = 2.5 \cdot 10^{-4} M$; (2): $5 \cdot 10^{-4} M$; (3): $10^{-3} M$; (4): $210^{-3} M$; (5): no DBMP added.

From the experiments with **DBMP** it was possible to estimate the concentration of residual moisture in the "standard" conditions employed to polymerize **MS**, since one molecule of water initiates one chain by protonation through its complex with **AT**. Thus, the concentration of **DBMP** found to give near-inhibition of the polymerization must be close to the concentration of water present in the system, viz. here $2 \cdot 10^{-3}$ M (see Figure 5). This concentration represents the sum of all residual moisture arising from the solid initiator grains, but also from the monomer, the solvent and the walls of the reaction vessel.

The oligomeric and polymeric fractions obtained by precipitation in MeOH of the products of these runs were examined by FTIR and $^1\text{H-NMR}$ spectroscopy. Figures 6 and 7 give typical NMR spectra of the two fractions. The sample of oligomer shown in Fig. 6 had a DP_n close to 4 and therefore both end-groups can be clearly detected, namely the methyl protons at 1.3 ppm and the alkenyl ones around 6 ppm. Such a pattern suggests that monomer transfer dominated in these polymerizations, according to the classical reaction which involves the transfer of a proton from an active species to the monomer which thus leaves a terminal unsaturation and starts a new chain bearing an initial methyl group, viz.:

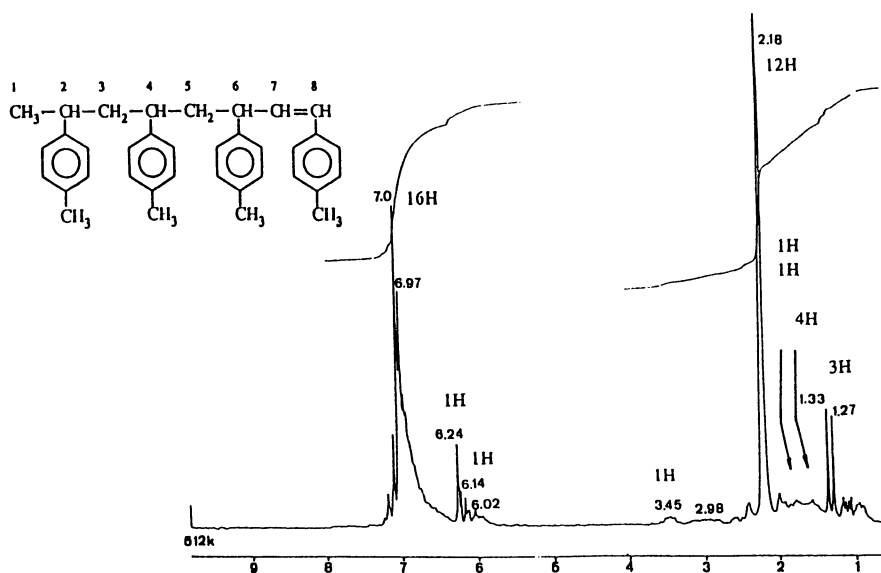
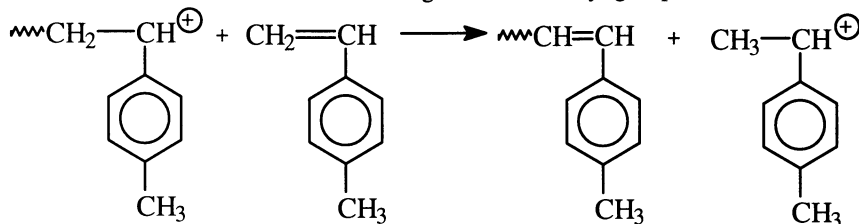


Figure 6. 100 MHz $^1\text{H-NMR}$ spectrum of a typical oligo(**MS**), $M_n=400$, in CD_2Cl_2

Figure 7 shows the resonances of the protons in the unit of a MS polymer with a DP_n close to 30, i.e. the fraction that precipitated in methanol. The correct integration pattern suggests the expected regular structure. The FTIR spectrum of the latter material is given in Figure 8: its analysis confirmed the expected pattern. The same pattern appeared in the FTIR spectrum of the oligomers with an additional strong peak at 960 cm⁻¹ revealing the presence of -CH=CHR moieties (end groups) in the trans conformation. All these spectroscopic features were also found in poly(MS)s prepared with conventional homogeneous cationic initiation.

It can therefore be concluded that AT operating in toluene at its solid surface at room temperature, gives rise to the same basic process of chain growth of 4-methylstyrene as, e.g., TiCl₄ in solution.

The ability of AT to sustain successive polymerizations *in situ* was the next aspect tested in this investigation. Several experiments were conducted in which at the end of a given polymerization another portion of monomer solution was added. Figure 9 shows a typical phenomenology arising from this multiple MS addition. Clearly, the rate of polymerization decreased at each addition. Thus, in the experiment depicted in Fig. 9, at the sixth addition, the rate of monomer consumption had reached an extremely modest value compared with that of the initial situation. This behaviour was common to all reactions of this type and even led to inert systems when the number of monomer additions was large, viz. 8 to 10, depending on the actual conditions.

Various possible causes of this loss of activity were explored and ruled out, namely: (i) the aging of the AT in suspension, since no difference was observed

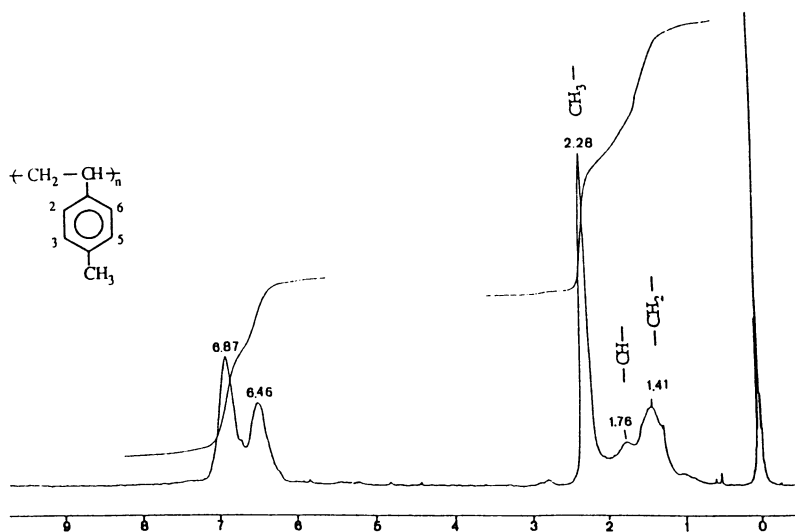


Figure 7. 100 MHz ¹H-NMR spectrum (solvent CD₂Cl₂) of a typical poly(MS) insoluble in MeOH.

between an experiment in which the monomer solution was added shortly after the AT was vacuum dried and one in which several days elapsed between placing the dried initiator in toluene and the addition of the monomer; (ii) the amount of residual moisture, since both the addition of a drying agent and the addition of small amounts of water did not change the general pattern typified in Fig. 9; (iii) a nucleophilic impurity in the monomer, since a double fractional distillation of MS did not alter the slowing trend. It must be emphasized that if a fresh portion of dried AT was added to

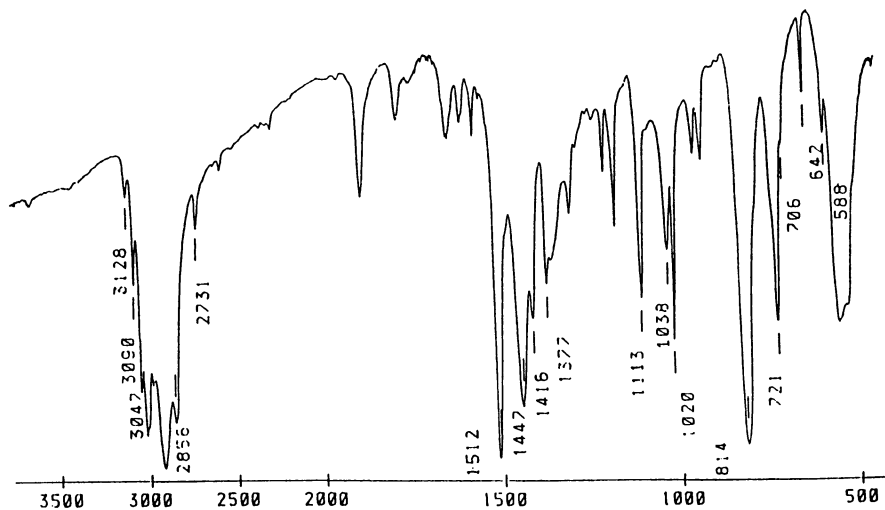


Figure 8. FTIR spectrum (KBr pellet) of the poly(MS) shown in Figure 7.

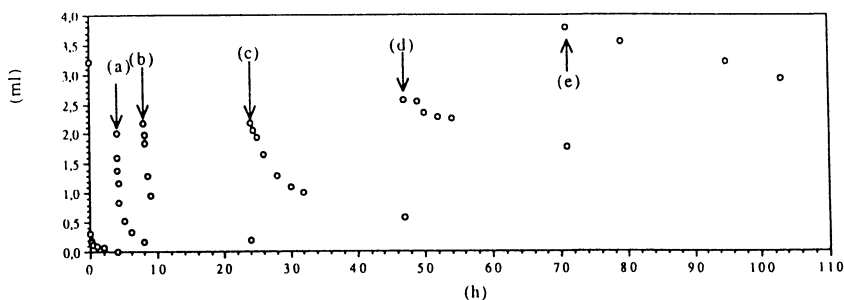


Figure 9. Conversion-vs-time plots of polymerizations resulting from successive additions of MS to a standard medium. Each addition marked by an arrow involved 5 ml of a 1:1 v/v solution of MS in toluene. The total volume of the reaction medium went therefore from 24 to 49 ml, i.e. the nominal concentration of AT was reduced progressively by a factor of two.

a suspension containing unreacted monomer and "spent initiator", i.e. after several successive monomer additions, the polymerization resumed immediately at a high rate, indeed as high as that measured after the first monomer addition. This experiment confirms that the standard solution did not contain any relevant amount of poisoning impurity.

The only plausible explanation for this deterioration of the initiating capability of AT seemed to be the accumulation of polymer in the reaction medium. This point was verified by comparing the course of a standard polymerization with that of one carried out in the same conditions, but in the presence of a high concentration of a poly(MS) prepared previously under standard conditions and long reaction times. The polymer was dissolved in dry toluene and added to the AT suspension in the same solvent before adding the monomer. Figure 10 shows clearly that a drastic reduction in the activity of the initiator occurred under these conditions. The concentration of polymer used in this experiment corresponded to the amount accumulated in a multiple experiment like that shown in Figure 9.

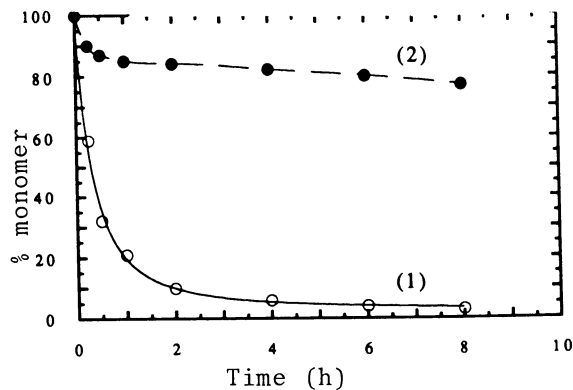
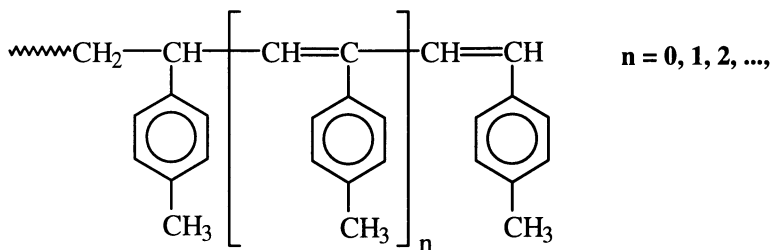


Figure 10. Comparison of a standard polymerization of MS (1) with one in which 124 g/l of standard poly(MS) were introduced in the system (2).

The reason for the poisoning effect of the polymer is to be found in the terminal unsaturations borne by these macromolecules. In fact, this is the only structural difference with respect to toluene or xylenes which obviously did not interact negatively with the surface of AT. It can be argued that the conjugated alkenyl-aromatic moieties at the end of most polymer molecules played the role of Lewis bases and can, as a consequence, formed a donor-acceptor complex with the strong Lewis acid surface of AT. This interaction obviously reduced the electrophilic character of that surface and its corresponding strength as initiator. It is important to underline the fact that the monounsaturated polymer chains, formed by monomer-transfer reactions, can acquire further unsaturation by reacting with active species, following a well-established mechanism already observed in the cationic polymerization styrene (5), indene (6) and 2-alkenylfurans (7). Thus, when the reaction medium containing polymer and active species is left for long periods of time before quenching, as is the case in our systems, a mixture of polymers and oligomers bearing the general structure



accompanied by macromolecules with saturated end-groups, gives a better representation of the situation. This state of affairs will of course enhance the poisoning of AT, because the higher the degree of conjugation through multiple unsaturations, the higher will be the Lewis basicity of the moiety. The visual observation of a progressive coloration (going from light yellow to dark brown) of the initiator's grains, as experiments like that shown in Fig. 10 progressed, confirmed the formation of complexes between polymer molecules and the acidic surface of AT.

The next step in the mechanistic study called upon the use of purposely added cocatalysts, in order to avoid the reliance on residual moisture, and the associated difficulties related to reproduce its content, as a means of initiation. Acetic acid and acetic anhydride were tested for this purpose. A series of experiments with different concentrations of both cocatalysts showed that the rates of polymerization were strongly enhanced and that allowed the actual amount of AT used to be reduced by a factor of two or more. Tables 2 and 3 give an idea of the quantitative role of both cocatalysts as a function of their concentration. Note that under the same operating conditions, water cocatalysis, at its optimum concentration, gave a much slower polymerization.

Table 2. The activity of acetic acid as a cocatalyst in the standard polymerization of MS as shown by the progressive increase in polymerization rate as the concentration of AcOH was increased

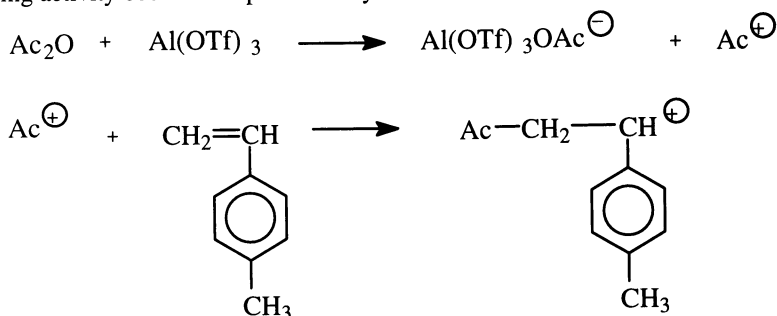
Run	[Ac ₂ O] (M)	Reaction time (min)	Residual monomer (%)
1	10 ⁻⁴	240	30
2	5.10 ⁻⁴	240	15
3	10 ⁻³	150	15
4	10 ⁻²	60	0

Table 3. The cocatalytic role of Ac₂O in the standard polymerization of MS

Run	[Ac ₂ O] (M)	Reaction time (min)	Residual monomer (%)
1	10 ⁻⁴	240	20
2	5.10 ⁻⁴	240	17
3	2.10 ⁻⁴	60	10
4	5.10 ⁻⁴	45	10
5	10 ⁻³	15	10
6	2.10 ⁻³	15	3
7	10 ⁻²	10	0

The role of acetic acid as cocatalyst seems straightforward in that its complexation with **AT** provides a strong Brønsted acid for the protonation of the monomer, stronger than $\text{Al}(\text{OTf})_3 \cdot \text{H}_2\text{O}$. With acetic anhydride, two situations must be considered: (i) the amount of Ac_2O is lower than that of the residual water; in this case AcOH is the relevant cocatalyst, apart from the water remaining after the complete hydrolysis of the anhydride; (ii) the amount of Ac_2O exceeds that of the moisture present in the system; apart from the cocatalysis by the AcOH formed, there seems to be an additional cocatalytic contribution by the excess of anhydride. In fact, the cocatalytic action of this additive was shown to continue well beyond the stoichiometric amount corresponding to the residual moisture, viz. up and above 10^{-2} M, as indicated by the data in Table 3 and many similar experiments.

It seems therefore likely that acetic anhydride could react with the surface of **AT** in toluene to produce acylium ions which would be responsible for the additional initiating activity observed experimentally. Thus:



This mechanism remains to be proved and work is in progress to test its validity.

The effect of the addition of small amounts of AcOH or Ac_2O at different stages of a water-cocatalyzed multiple polymerization of **MS** by **AT** was also examined. Modest accelerations were observed if the additions took place at fairly early stages of the reaction, whereas if the system had reached a quiescent mode, very little effect was registered. These experiments confirmed that the loss of initiating ability of **AT** was not caused by the lack of a cocatalyst, but instead by surface poisoning induced by the donor/acceptor interaction with the unsaturations of the polymer molecules accumulated in the solution.

The last parameter studied in this context was the role of the dielectric constant of the medium on the behaviour of the system. Figure 11 shows the results of three runs carried out in the same conditions except for the fact that the solvent polarity was progressively increased. As expected, the rate of polymerization increased in a corresponding manner. It must be reminded here that our previous investigation (1-3) had shown that CH_2Cl_2 did in fact dissolve small amounts of **AT**, so that apart from the acceleration attributed to the increase in polarity, some homogeneous polymerization of **MS** must have taken place, albeit in modest proportions.

Batch Homopolymerization of Indene. The behaviour of this monomer simulated in every qualitative respect that described above for 4-methylstyrene. The major quantitative difference was found to be a considerably lower rate of polymerization when the same standard operating conditions were applied. Figure 12 illustrates this

point by showing the sluggishness of the reaction with 5 g/l of AT, as compared with the corresponding results referred to MS in Fig. 1. Again acetic acid and acetic anhydride played a very useful cocatalytic role as shown in Figure 13.

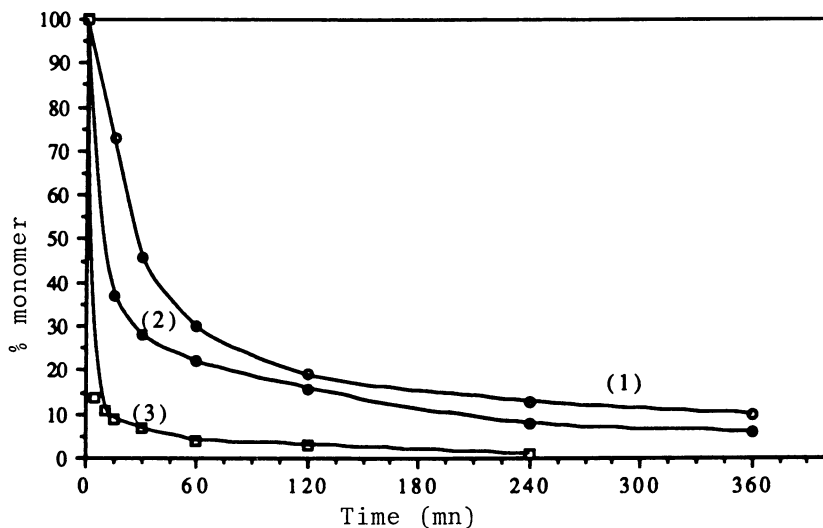


Figure 11. Comparison of the rate of polymerization of MS under standard conditions except for the nature of the medium. (1): toluene; (2): toluene/methylene chloride in a 1/1 v/v proportions; (3) methylene chloride.

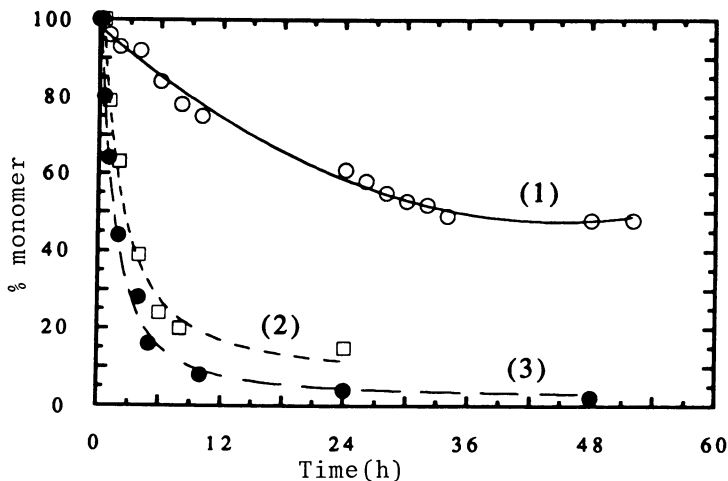


Figure 12. Conversion vs. time plots for three polymerizations of indene (IM) in toluene at room temperature in the presence of variable amounts of AT, dried according to the standard procedure. (1): [AT] = 5 g/l; (2): [AT] = 15 g/l; (3): [AT] = 30 g/l.

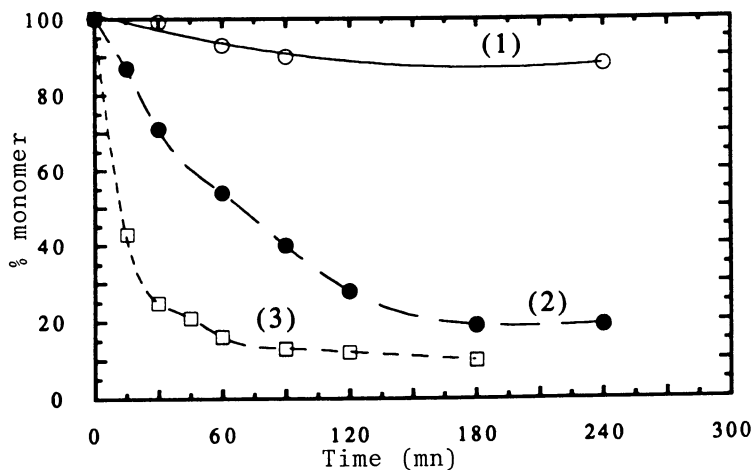


Figure 13. The cocatalytic role of acetic acid and acetic anhydride in the polymerization of indene. (1): standard conditions; (2): $[AcOH] = 3 \cdot 10^{-3} M$; (3): $[Ac_2O] = 3 \cdot 10^{-3} M$.

The oligomers and polymers isolated by fractionation in methanol had, typically, DPs of about 3 and about 15, respectively, i.e. lower values than those of the corresponding poly(MS)s. The 1H -NMR spectra of these products are shown in Figures 14 and 15 and the FTIR spectrum of a typical oligomer is given in Figure 16. All this spectroscopic evidence, coupled with the low values of the molecular weights, corroborated the conclusions drawn above for the polymerization of MS concerning the regularity of the polymeric structures and the predominant role of monomer transfer. Again, these features were compared with those of poly(indene)s prepared with conventional homogeneous cationic initiators and complete similarities were observed.

The additional parameter investigated with indene was the role of the granulometry of AT on its initiating activity. Figure 17 shows a set of polymerizations conducted in the same conditions, except for the average grain size of the catalyst. As expected, the higher the specific surface of AT, the higher was the polymerization rate, although it was difficult to establish more quantitative criteria because of a rather modest reproducibility, as shown in Fig. 17.

Since both monomers tested bear an aromatic moiety, it was important to assess the occurrence of alkylation reactions arising from the interaction between an active species and a solvent molecule, but also from those involving either a benzene ring belonging to a monomer unit in a polymer chain already formed or one pertaining to a monomer molecule. Indene was chosen for these tests because the possible incorporation of solvent moieties would be readily revealed by the presence of methyl groups in a polymer which does not contain any. The comparison between the 1H -NMR and FTIR spectra of polyindenes prepared with AT in toluene, m-xylene and p-xylene clearly showed the absence of peaks around 2.3 ppm (NMR), which could be attributed to the resonance of the methyl group and of bands in the $800-900\text{ cm}^{-1}$ (IR), which could reveal the presence of trisubstituted aromatic structures, even when the polymerizations were left standing for a couple of weeks before quenching.

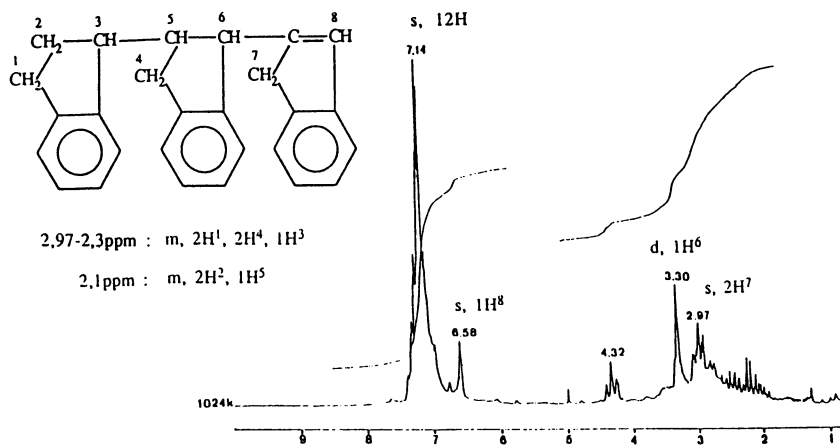


Figure 14. 100 MHz $^1\text{H-NMR}$ spectrum of a typical oligo(IN), $M_n=330$, in CD_2Cl_2

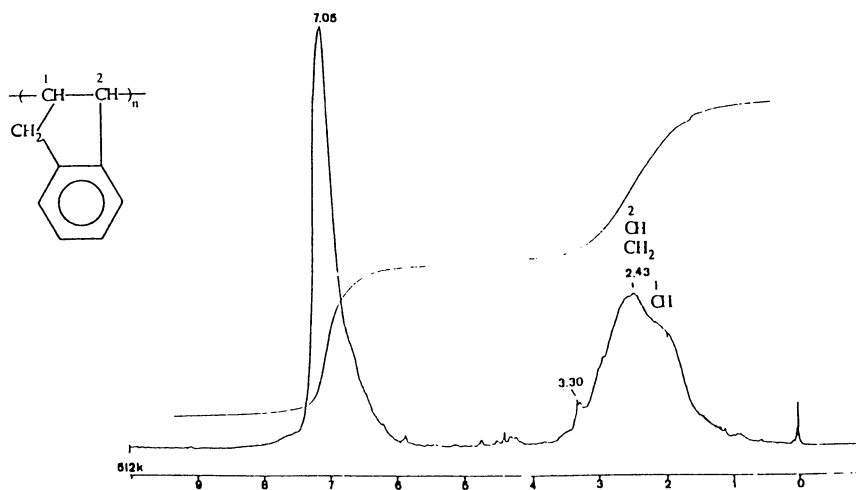


Figure 15. 100 MHz $^1\text{H-NMR}$ spectrum (solvent CD_2Cl_2) of a typical poly(IN) insoluble in MeOH, $M_n=1850$.

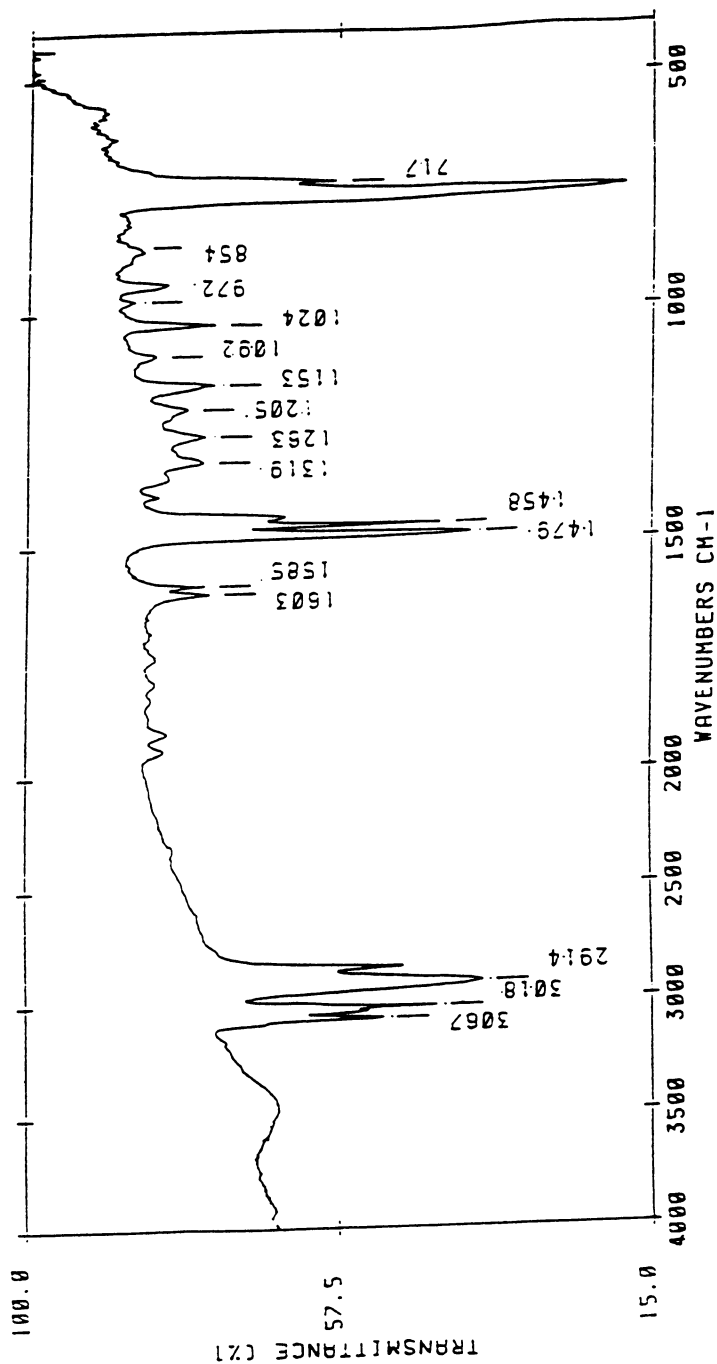


Figure 16. FTIR spectrum of the poly(IN) shown in Figure 15. KBr pellet.

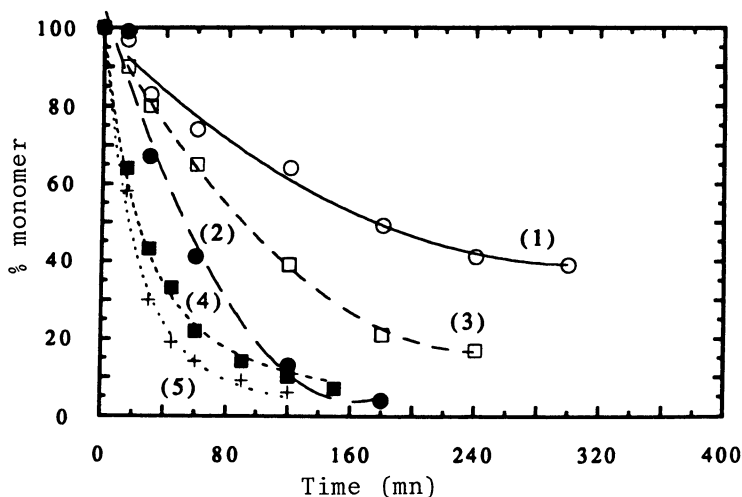


Figure 17. The role of average AT grain size on the rate of polymerization of indene with $[AcOH] = 3 \cdot 10^{-3} M$ and otherwise standard conditions. (1): $<0.025 mm$; (2): $0.025-0.040 mm$; (3): $0.040-0.063 mm$; (4) $0.063-0.080 mm$; (5): $0.080-0.100 mm$.

In other words, the spectra of all these polymers did not differ from those of the corresponding products prepared in methylene chloride. It can therefore be concluded that electrophilic substitution reactions were negligible events in all these systems, if present at all. Curiously, AT had been previously found to act as a good catalyst for alkylation reactions (3, 8). It seems most likely that the lack of intervention of this type of side reaction in the present study comes from the low polarity of the medium employed.

Copolymerization experiments. Having established that both MS and IN can be readily polymerized by AT in toluene, albeit at different rates, it seemed judicious to investigate their copolymerization behaviour in the same experimental conditions. This phase of the study permitted a closer approach to the actual *C9 cut*, since we were now dealing with two typical monomers in a typical solvent.

The first copolymerization experiments were conducted using conventional initiators working homogeneously, namely titanium tetrachloride and boron fluoride etherate. In both instances, and within a fairly wide range of catalyst concentrations, the two monomers were found to be consumed at the same rate. When we switched to our heterogeneous system, calling upon AT as initiator, the same features were encountered and again this concomitant consumption did not depend on the actual polymerization rate, i.e. on the amount of AT used and on the absence or presence of added cocatalysts like acetic anhydride. Figure 18 shows this peculiar behaviour with 3 different polymerizations where the data points reflecting the consumption of each monomer coincide in each run within experimental error.

Having previously established that IN was a less reactive monomer than MS, we had expected a similar trend in the copolymerizations involving these two monomers. However, the results showed unambiguously that this was not the case and that the tendency pointed instead to a rate of polymerization very much the same

for each of them. The obvious consequence of this state of affairs was that the copolymers had 50/50 compositions as indicated by the relative integrations of the typical $^1\text{H-NMR}$ given in Figure 19.

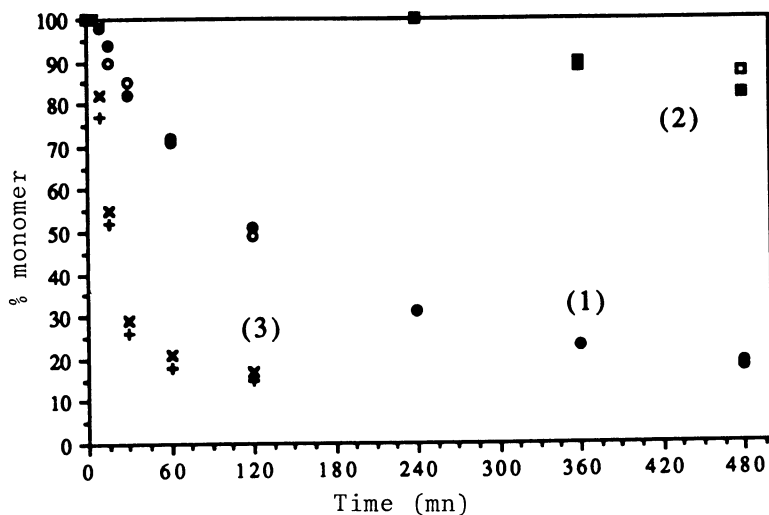
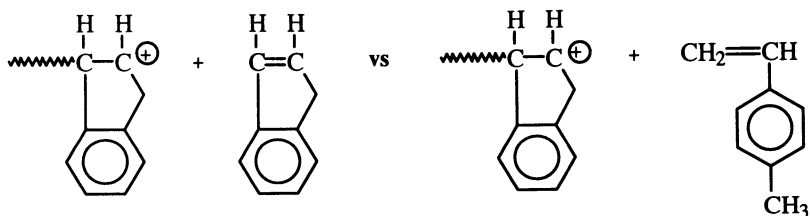


Figure 18. Conversion vs. time plots for copolymerizations of MS and IN under different conditions. (1): $[\text{MS}] = 0.5$, $[\text{IN}] = 0.5$, otherwise standard conditions; (2): $[\text{MS}] = 0.25$, $[\text{IN}] = 0.75$, otherwise standard conditions. (3): $[\text{MS}] = 0.5$, $[\text{IN}] = 0.5$, $[\text{Ac}_2\text{O}] = 5 \cdot 10^{-4} \text{ M}$.

If, on the one hand, it seems reasonable to postulate that the active species arising from each comonomer bear the same degree of stabilisation connected with presence of the aromatic moiety next to the carbon atom holding the positive charge, on the other hand, the kinetic likelihood relative to each of the four propagation steps, is not the same given the important differences in steric hindrance. In particular, the homopolymerization step relative to indene would be the slowest, as indeed already confirmed by the lower reactivity of this monomer with respect to that of MS in our homopolymerization experiments

The following alternative propagation reactions illustrate, through the visualization of the steric problems associated with the addition of a molecule of IN to its own active end, what seems to us as the most plausible interpretation of the copolymerization results:



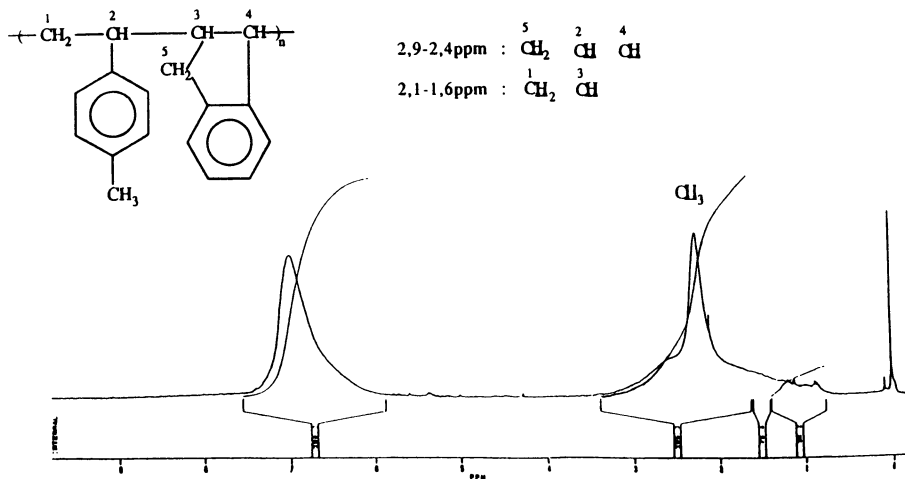


Figure 19. 100 MHz $^1\text{H-NMR}$ spectrum of a typical poly(MS-co-IN) in CD_2Cl_2

This explanation also accounts for the observation of a much lower overall rate of copolymerization measured in the experiment in which the initial concentration of IN was much larger than that of MS (see Figure 18). In conclusion, the elimination of major steric factors seem to narrow down the difference in reactivity between the two monomers and this makes the copolymers' composition close to 1:1, although of course it does not imply necessarily that the structure of the products is mostly alternating.

Flow Experiments. Feeding a toluene solution containing either monomer, or a mixture of both, through a column packed with silica beads covered with a film of AT resulted in continuous systems of polymerization. The amount of initiator deposited on the SiO_2 support was varied over a wide range of proportions with respect to the amount of silica. A w/w ratio close to 1/30 gave the best and most reproducible results. Both acetic acid and its anhydride were tested as cocatalysts. As the samples were recovered and analyzed at the exit, it became clear that the activity of AT decreased in all experiments, although the presence of added cocatalysts improved its performance. Thus, 100 ppm of AcOH in the feed solution gave about 300 g of poly(MS) per gram of AT, before the polymerization started to slacken.

This decrease was attributed to the accumulation of moisture on the surface of AT, i.e. to its excessive hydration caused by the progressive fixation of the residual water contained in the flowing monomer solution. In order to minimize this detrimental feature, a column of activated 3 Å molecular sieves was placed before the SiO_2/AT column. The situation was indeed improved by this measure, but another

source of aging now appeared at longer flow times, namely the same catalyst poisoning encountered in the batch experiments. As already discussed above, this was attributed to the interaction of the unsaturated end-groups of the polymer molecules with the **AT** surface. Here too, the loss of activity was accompanied by the development of a brown colour on the surface of the initiator's grains.

Various means to reactivate the SiO_2/AT beads were explored. Baking them at 180°C in a current of oxygen gave only a partial recovery of their initiating ability, whereas passing a solution of TiCl_4 in CH_2Cl_2 produced excellent results, particularly if its concentration was high, viz. above 0.1 M. It seems likely that the polymer fixed onto the **AT** was removed by the flowing Lewis acid through competitive complexing. The procedure adopted was therefore to let the acidic solution flow through the SiO_2/AT column, wash with dry CH_2Cl_2 , wash with dry toluene and finally carry out the standard thermal activation of the **AT**. This provided the possibility of recycling the catalyst which had recuperated its original activity. This part of the study is being pursued to establish whether the treatment with the solution of titanium tetrachloride leads simply to the reactivation of **AT** or whether some of the Lewis acid remains complexed at its surface thus giving a novel initiating entity.

Conclusion

Aluminium triflate is an efficient heterogeneous initiator for the polymerization of aromatic alkenes in aromatic solvents and could therefore be used to convert the *C9 cut* into a resinous material. The lack of solubility of this catalyst in media of such low dielectric constant allows moreover the use of flow systems which can be optimized in terms of both activity and recyclability.

Acknowledgment

We wish to thank DSM Research for generous financial support.

Literature Cited

1. Collomb, J.; Morin, B.; Gandini, A.; Cheradame, H. *Europ. Polym. J.* **1980**, *16*, 1135.
2. Collomb, J.; Gandini, A.; Cheradame, H. *Makromol. Chem., Rapid Commun.* **1980**, *1*, 489.
3. Arlaud, P.; Collomb, J.; Gandini, A.; Cheradame, H. In *Cationic Polymerization and Processes*; E.J. Goethals Ed., Academic Press, London 1984, p. 49.
4. Gandini, A.; Martinez, A. *Makromol. Chem., Macromol. Symp.* **1988**, *13/14*, 211.
5. Gandini, A.; Plesch, P.H. *Europ. Polym. J.* **1968**, *4*, 55.
6. Prosser, H. J.; Young, R.N. *Europ. Polym. J.* **1972**, *8*, 879.
7. Alvarez, R.; Gandini, A.; Martinez, R. *Makromol. Chem.* **1982**, *183*, 2399.
8. Olah, G.A.; Farooq, O.; Farnia, S.M.F.; Olah, J.A. *J. Am. Chem. Soc.* **1988**, *100*, 2560.

Chapter 12

Heterogeneous Cationic Polymerization Initiators

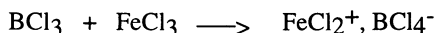
Polymerization of 2-Methylpropene in the Presence of FeCl₃ in Nonpolar Medium

G. Rissoan, S. Randriamahefa, and H. Cheradame¹

University of Evry, Centre National de la Recherche Scientifique, E.P. 109,
2 rue H. Dunant, 94320 Thiais, France

The cationic polymerization of 2-methylpropene in hexane with ferric chloride as initiator proceeds essentially via heterogeneous initiation. Hydrated ferric chloride is more efficient than the anhydrous one. It is suggested that both cocatalysis and direct initiation mechanism occur. Kinetic results show that the polymerization rate orders are respectively zero, one and one, in monomer, catalyst and cocatalyst. The rate determining step is the isomerization of the monomer molecule in the active species. The termination rate is negligible.

The present research is the continuation of our systematic study of the use of metal salts as solid state catalysts for the initiation of the cationic polymerization of alkenes, particularly 2-methylpropene. This polymerization in heterogeneous conditions is scarcely studied. Colomb et al reported that metal salts of strong acid such as perchlorates and trifluoromethanesulfonates (triflates) could be powerful coinitiators for the polymerization of n-donor monomers such as propene sulfide, n- π donor monomers such as isobutylvinylether or π -donors such as butadiene, styrene, α -methylstyrene, 2-methylfuran and 2-methylpropene (1)(2). Marek et al carried out similar polymerization on this last monomer in the presence of a mixture of BCl₃ and FeCl₃ in non polar solvent, but with a small amount of dichloromethane to dissolve the ferric salt (3). This author demonstrated the outstanding efficiency of this initiating system and concluded that initiation was due to direct initiation by the positive moiety FeCl₂⁺ produced by a reaction of heteroionization between the two Lewis acids in homogeneous conditions:



An initiation mechanism by monoelectronic transfer between FeCl₂⁺ formed and the monomer was proposed. The possible initiating efficiency of ferric chloride alone was totally neglected. Ferric perchlorate alone was also used by Collomb (1), but in polar solvent (nitromethane) which dissolved the salt and gave 100% yield in a few minutes.

NOTE: This article is part two in a series.

¹Corresponding author

Direct initiation in non polar medium was also postulated in the polymerization of butadiene, both with mixed catalysts as $\text{CoCl}_2/\text{AlCl}_3$ (4), and with single salts as CoCl_2 or NiCl_2 (5) and in the polymerization of 2-methylpropene with aluminium triflate (6). On the other hand, a cocatalytic initiation mechanism was proposed by Addecott et al. (7) in the polymerization of 2-methylpropene in non polar medium initiated by magnesium chloride.

We describe in this paper the heterogeneous cationic polymerization of 2-methyl propene in non polar medium (hexane) with solid ferric salts as initiator, more particularly focussing on FeCl_3 . In this work we attempt to assess the relative importance of these two possible initiation mechanisms: direct and cocatalytic initiation. Finally, a kinetic study enables us to have better understanding of the chemistry of this heterogeneous polymerization.

Experimental Section

Materials. 2-methylpropene (Aldrich, 99% purity) was dried over calcium hydride and stored under vacuum. Anhydrous or hydrated FeCl_3 (Aldrich, 98% purity) was stored under nitrogen. According to the elemental analysis the water content of hydrated FeCl_3 is 0.5 mole H_2O per mole of salt and ten times lower (0,05 M) for the anhydrous grade. Hexane (Aldrich 99% purity) was dried over calcium hydride, freshly distilled under nitrogen and degassed twice under vacuum. Other ferric salts were used: the synthesis of anhydrous and dihydrate ferric perchlorate was carried out using a procedure described elsewhere (8). FeBr_3 was an ABCR product (99.5% purity). When a cointiator concentration is reported, it is clear that the concentration is calculated as if the salt is soluble in the reaction medium, which is not the case. In order to get rid of the specific surface problem, the cointiator of a given quality (e.g. anhydrous ferric chloride) was always sampled from the same container throughout the whole study.

Procedures. A typical polymerization procedure was as follows: The polymerization reactor was charged with the salt in a glove box under nitrogen and then connected to a vacuum line by teflon taps. The salt was used just as such or dried by heating for two hours at 150 °C. After cooling, hexane and then monomer were cryodistilled into the reactor, and the mixture was magnetically stirred at -10 °C during the reaction time. The polymerization was stopped by quenching with methanol.

After filtration of the reaction mixture, the solvent was evaporated and the weight of polymer formed was determined after drying to constant weight under vacuum.

Molar mass distribution (MMD) was determined by a KNAUER SEC instrument with a series of 4 m Styragel columns (10 , 10 , 500 and 100 Å), a differential refractometer and an UV absorbance detector. Calibration was done using narrow MMD polyisobutenes.

Results and Discussion

Initiation Mechanism.

Initiation by Ferric Salts in Non Polar Medium. The catalysts must have enough acidity to polymerize the monomer in aliphatic solvents such as hexane. FeCl_3 was used but ferric bromide and perchlorate were also tested. Some results are summarized in table I. In this preliminary study, the polymerization yield in a given

time was used as a parameter allowing to appraise the initiating efficiency, while it is clear that this procedure must be used with caution.

Anhydrous ferric perchlorate was efficient enough to give 28% yield of polymer in one hour with a concentration three times lower than that used for anhydrous FeCl_3 (17% yield). It gave also good results under a dihydrated state (23% yield in 30 minutes), unlike the case observed in polar medium (1). However, the perchlorate salt needs drastic conditions of handling to avoid any risk of hydration

Hydrated ferric bromide gave 100% yield in 60 minutes

Hydrated ferric chloride was the more efficient of the tested catalysts based on ferric halides (100% in 30 minutes). It is to be noticed that the polydispersity index is unusually high. This point will be commented later.

For the sake of comparison, the initiating system $\text{FeCl}_3/\text{BCl}_3$ in hexane was also briefly studied.

Table I. 2-methylpropene polymerization (4.5 M) induced by various ferric salt

Run n°	Reaction time (mn)	Catalyst (10^2M)	Yield (%)	Mn	Polydisp. index
1	60	FeCl_3 anhydrous (5.7)	17	4700	8
2	30	$\text{FeCl}_3 \cdot 0.5\text{H}_2\text{O}$ (6.2)	100	800	11
3	60	$\text{Fe}(\text{ClO}_4)_3$ anhydr. (1.7)	28	4400	25
4	30	$\text{Fe}(\text{ClO}_4)_3 \cdot 2\text{H}_2\text{O}$ (4.4)	23	4200	11
5	60	FeBr_3 hydrated (6.2)	100	3350	12
6	30	FeBr_3 hydrated (6.2)	82	800	4

We checked first that BCl_3 alone did not initiate the polymerization of 2-methylpropene in the experimental conditions summarized in table II. In the presence of the two salts in anhydrous conditions, the polymerization is fast enough. The yield of polymer is much higher than that with anhydrous FeCl_3 alone. This difference is important with anhydrous FeCl_3 but not with $\text{FeCl}_3 \cdot 0.5\text{H}_2\text{O}$ which gives similar polymerization yield in similar conditions (compare run 2 table I and run 5 table II). Slight hydration of anhydrous ferric chloride which was not dried under vacuum in the case of run 4 table II did not change the result. Particularly large MMD of the polymers obtained with all these catalysts (see tables I and II) are noticed. This seems to be the case for most of the cationic polymerizations with heterogeneous initiators, as we shall see later.

Table II. 2-methylpropene polymerization initiated by the {anhydrous $\text{FeCl}_3/\text{BCl}_3$ } system in hexane

Run n° ^a	Monomer Mol.l^{-1}	FeCl_3 ^b Mol.l^{-1}	BCl_3 ^c Mol.l^{-1}	T °C	Yield %	Mn	I ^d
1	4.5	0	0.055	-10	0		
2	4.5	0.062	0.055	-13	100	3,900	6
3 ^e	4.5	0.058	0.055	-10	100	6,400	9
4 ^e	4.5	0.062	0.055	-10	100	1,300	8
5	4.5	0.062	0.055 ^f	-10	100	4,700	11
6 (bulk)	11.2	0.062	0.055	-10	61	2,300	23

a: Polymerization time = 30 mn. b: Nominal concentration, as if FeCl_3 is soluble in the medium. c: BCl_3 introduced as a solution in hexane, except for run.5. d: Mw/Mn. e: Anhydrous FeCl_3 not dried under vacuum. f: BCl_3 gas.

This preliminary study allowed us to conclude that direct initiation probably due to coionization between two Lewis acids is observed in our totally non polar medium, but also that cocatalytic initiation could be able to give similar results, at least in term of yield, even if the molecular weights are slightly lower.

Effect of Various Additives on 2-Methylpropene Polymerization Initiated by Ferric Chloride.

Effect of Water. Since it was concluded that hydrated ferric chloride was more efficient than the anhydrous one, and that the initiating efficiency could be due to cocatalytic initiation, it was decided to check this point introducing water in the reaction medium already containing the anhydrous salt, before the introduction of monomer. Some results are presented in table III. The first two experiments were carried out in order to provide a base for comparison. It can be seen that the yield is roughly increasing with time. This point will be extensively checked in the kinetic study below. In the run 3 table III, the concentration of added water was approximately equal to that of the ferric salt not dried ($\text{FeCl}_3 \cdot 0.5\text{H}_2\text{O}$). The same results (100% yield after 30 minutes and average molecular weight about 800) were obtained (table III). The crystallisation water was as active as the added water on the anhydrous salt. It was concluded that this last water was hydrating the surface of FeCl_3 giving 100% yield of polymer by a cocatalytic mechanism.

Table III. Effect of various additives on the heterogeneous polymerization of 2-methylpropene (4.5M) initiated by FeCl_3 in hexane at -10°C

Run n°	FeCl_3 , $10^2 \cdot \text{mol} \cdot \text{l}^{-1}$	Additives $10^2 \cdot \text{mol} \cdot \text{l}^{-1}$	Time min.	yield %
1	anhydrous: 6.2	-	30	7
2	anhydrous: 5.7	-	60	17
3	anhydrous: 6.2	H_2O : 3	30	100
4	anhydrous: 5.9	DTBMP*: 3	30	4
5	anhydrous: 5.9	DTBMP: 19	30	3
6	undried: 5.9	DTBMP: 19	30	3
7	anhydrous: 6.2	BCl_3 : 3	30	88
8	anhydrous: 6.2	BCl_3 : 5.5	30	100

Effect of 2,6-Di-tert-Butyl-4-Methylpyridine (DTBMP). It was reported earlier that the DTBMP selectively reacts with proton donating species, at the exclusion of others electrophiles and can inhibit the proton initiated polymerization (9)(10)(11). The use of this sterically hindered base allows to distinguish the cocatalytic initiation from the direct one. We have introduced DTBMP in the polymerization reactor before all other reagents, by sublimation under vacuum. It's concentration is either in excess (run 5, table III) or half the catalyst concentration (run 4, table III). Anhydrous and hydrated FeCl_3 were tested in the presence of this base. In all cases, total inhibition of the polymerization reaction was not observed with this hindered pyridine, but the yields dropped significantly. Two hypothesis can be proposed to explain this phenomenon of residual polymerization in the presence of DTBMP:

-either, besides the cocatalytic initiation reaction, there are others initiating reactions producing acidic sites which lead to a direct initiation, without protons, as claimed by Marek and coll. (3) who have referred to oxydo-reduction reaction;

-or, the DTBM, too sterically hindered by its tert-butyl side groups, is not able to trap completely the protons on the surface of the catalyst. The latter can initiate the

polymerization before their capture by the bulky base at time of a later transfer reaction.

Effect of Various Cocatalysts. The effect of different cocatalysts on the polymerization of 2-methylpropene in heterogeneous system initiated by anhydrous FeCl_3 was compared (table IV).

With water as cocatalyst, its minimal concentration is about 0.016 M to give quantitative yield in 30 minutes.

The cocatalytic effect of methanol is practically the same as that of water.

Table IV. Effect of various cocatalysts on the heterogeneous polymerization of 2-methylpropene (4.5M) initiated by FeCl_3 in hexane at -10°C

Run n°	FeCl_3 , 10^2 .mol.l ⁻¹	Cocatalysts 10^2 .mol.l ⁻¹	Time min.	yield %
1	6.2	Water: 0.8	30	21
2	6.2	Water: 1.6	30	100
3	6.2	Methanol: 1.6	30	100
4	6.2	Triflic acid: 0.6	30	100

With trifluoromethanesulfonic (triflic) acid, 100% yield was obtained in 30 minutes with a low concentration (0.006M). Triflic acid is the most efficient cocatalyst used in this study, more than water or methanol.

The effect of water as a cocatalyst was more quantitatively studied. In a series of experiments the added water concentration was increased for polymerization initiated in the presence of anhydrous ferric chloride at a nominal concentration of 6.10^{-2}M at -10°C , and the effect on the polymerization yield is shown on figure 1. On the ordinates, the concentration of produced macromolecules is quoted as a function of the added water content. This concentration was calculated from the weight of collected polymer and the corresponding number average molecular weight. It can be seen that the quantity of macromolecules is proportional to the quantity of water up to around 1.5 M. This finding is in agreement with the cocatalytic initiation which was deduced above from the preliminary study. It can be concluded that the concentration of active species is proportional to the concentration of added water, in agreement with the theory of cocatalysis. The slope of the line shown on figure 1 shows that each water molecule approximately produced 7 macromolecules showing that transfer is the predominant macromolecular chain breaking process.

Influence of FeCl_3 Concentration. In the same way, the polymerization behavior as a function of catalyst concentration was followed. The experiments were first carried out with anhydrous ferric chloride (fig.2). On this figure it can be seen that in the concentration range used, the polymerization yield in a given time (30 min.) increases linearly up to only 10 %. The reason for which the straight line does not go exactly through the origin is probably due to experimental difficulties, more particularly in an accurate determination of the yield for such experiments giving low amount of polymer. Using a hydrated Lewis acid, the same type of experiments showed the same behavior, but on a much larger scale. the results are shown on figure 3. Within the same nominal concentration range, the hydrated form revealed to be very active giving up to 100 % yield, as already reported on table I. The most interesting feature of these experiments is the linear variation exhibited in figure 3. This linearity is easily accounted for assuming that the number of active species is

proportional to the ferric chloride surface, that they are permanently active, and that the propagation step is independent of monomer concentration. This point will be verified later in the kinetic study.

However, in order to check the insensitivity of the polymerization yield to monomer concentration, it was decided to carry out experiments at different monomer concentrations all other parameters being kept constant such as temperature (-10°C), and anhydrous ferric chloride nominal concentration ($6.2 \cdot 10^{-2} \text{ M}$). However, in order to favour experimental accuracy, the polymerization time was increased to 60 min. The results are shown in Figure 4. From this figure it can be reasonably concluded

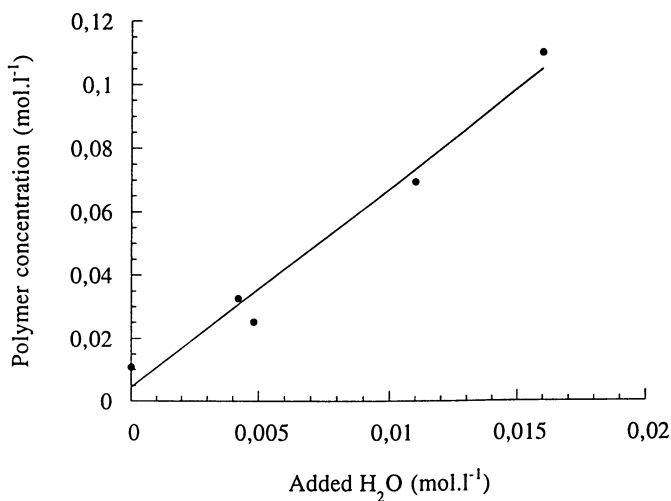


Figure 1. Concentration of produced polymer versus added water concentration plot, in the polymerization of 2-methylpropene (4.5 M) with anhydrous FeCl_3 ($6 \cdot 10^{-2} \text{ M}$).

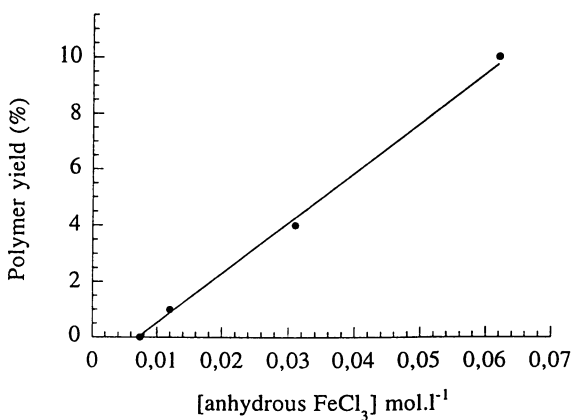


Figure 2. Polymer yield versus anhydrous FeCl_3 concentration plot, in the polymerization of 2-methylpropene (4.5 M) in hexane, 30 min. at -10°C .

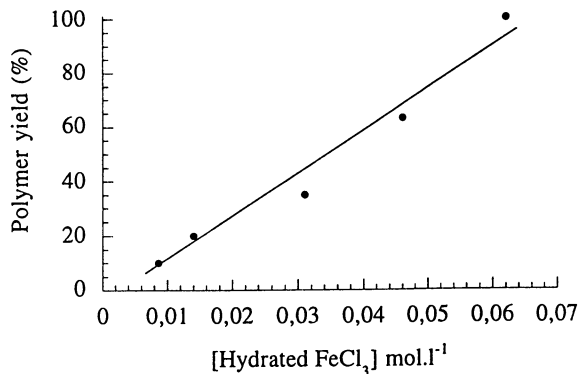


Figure 3. Polymer yield versus hydrated FeCl₃ concentration plot, in the polymerization of 2-methylpropene(4.5 M) in hexane, at -10°C during 30 min.

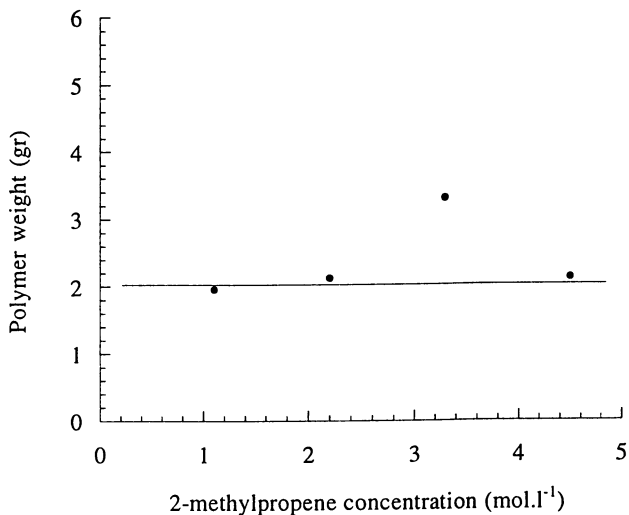


Figure 4. Polymer weight versus 2-methylpropene concentration plot with anhydrous FeCl₃ ($6.2 \cdot 10^{-2}$ M) in hexane, 60 min. at -10°C

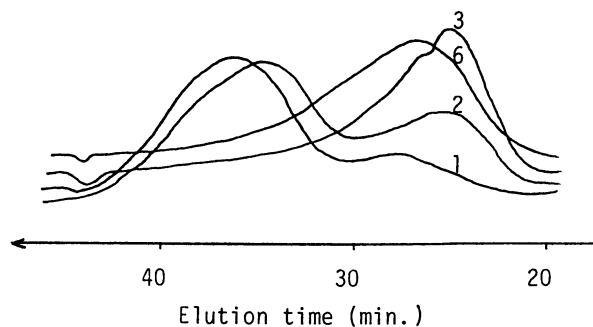


Figure 5. SEC Chromatograms of poly-2-methylpropene with various added water concentrations. Experimental conditions as in table V. 1: $[H_2O] = 0$ M; 2 = $4.2 \cdot 10^{-3}$ M; 3 = $4.8 \cdot 10^{-3}$ M; 6 = $21 \cdot 10^{-3}$ M.

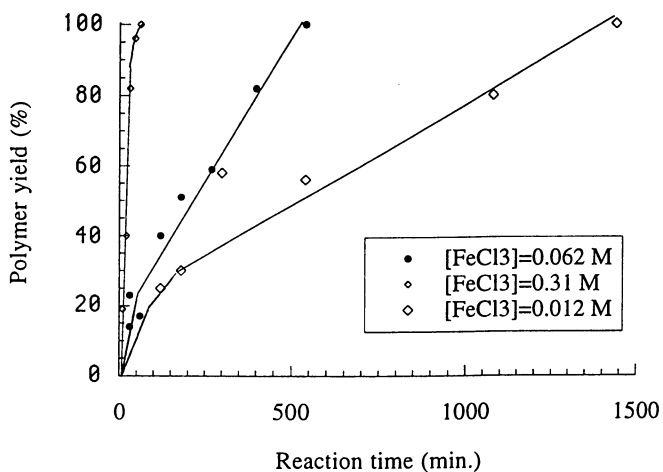


Figure 6. Evolution of the polymer yield with various anhydrous $FeCl_3$ concentrations in the Polymerization of 2-methylpropene (4.5 M) in hexane at $-10^\circ C$.

that the yield is approximately independent of monomer concentration. This finding supports the above conclusion on a stationary state of active species concentration combined with a propagation step independent of monomer concentration.

Some eluograms corresponding to the molecular weight determination of the above polymers are shown figure 5. The shape of these eluograms is strongly varying with added water concentration. At low water concentration the molecular weight distribution is clearly bimodal, and the low molecular weight peak is important. When the water concentration increases, the importance of the low molecular weight peak decreases, and finally disappears for higher concentration. The observed bimodality explains the high polydispersity indices which have been previously measured. It must be noticed that even in the case of the two highest water concentrations (Curves 3 and 6, figure 5) the molecular weight distribution is still bimodal, but the low molecular weight peak comes closer to the high one. It is assumed that these different molecular weight distributions correspond to different active species on the catalyst surface.

Kinetic Study

We have carried out a kinetic study in order to obtain a better understanding of the parameters which govern this type of polymerization. However, since the initiator remained heterogeneous in the reaction medium, most of the experiments were effected individually, and not by sampling from a reactor which always induces a risk of leak for a system which was always under vacuum, and a risk of introduction of water. This technique was preferred despite a possible source of irreproducibility if the control of adventitious water is not good.

With high FeCl_3 concentration ($3.1 \cdot 10^{-1} \text{ M}$) the yield of polymer is a linear function of time, as shown in figure 6: the stationary state is very rapidly reached. From the two others plots, it appears that stationary or quasi-stationary state in active species is reached the more rapidly as catalyst concentration increases. However, it is remarkable that with undried FeCl_3 , the yield of polymer is a linear function of time even at low catalyst content ($6.2 \cdot 10^{-3} \text{ M}$) (see fig.7). Like above, the 100% yield is always achieved in all cases. So, it seems that there is little or no termination reaction in those systems.

Rate Order in Monomer. As shown in figure 4, the rate of polymerization is independent of the monomer concentration at constant Lewis acid concentration, polymerization time and temperature (zero order in monomer concentration). In fact, the quantity of polymer obtained is nearly constant in the interval of monomer concentration studied (from 1 to 4.5 M).

Rate Order in Cocatalyst. To determine the order in cocatalyst (water in the present case) of the polymerization rate, we realized a series of polymerizations where only the concentration of cocatalyst changed (see table V and fig.8). With a water concentration lower than $1.6 \cdot 10^{-2} \text{ M}$, the polymer concentration is proportional to the quantity of added water in the presence of anhydrous FeCl_3 . This suggests that the order in cocatalyst concentration is 1. The SEC analysis (in fig.5) shows that we have noticeable bimodal MMD for lower concentration of added water and consequently for low polymer yields. This result can be explained by the existence of two different active species. With higher cocatalyst concentration, as the yield of polymer increases, the lower molecular weight distribution disappears and the bimodal distribution gets narrower on the higher mass side. However, it is worth noticing that the distribution still remains bimodal, as if the active species corresponding to the low molecular weight would have been replaced by a new active species giving higher

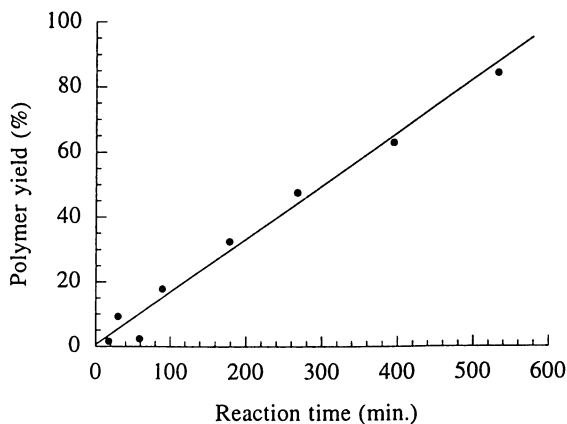


Figure 7. Polymer yield versus reaction time plot in the polymerization of 2-methylpropene (4.5 M) with undried FeCl_3 ($6.2 \cdot 10^{-3} \text{M}$) in hexane at -10°C .

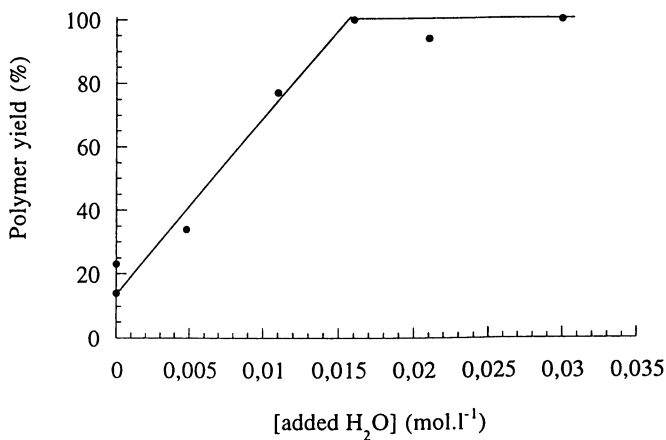


Figure 8. Yield of polymer versus added water concentration plot, with respectively 4.5 M and $6.2 \cdot 10^{-1} \text{M}$ monomer and anhydrous FeCl_3 concentrations in hexane at -10°C , during 10 min.

molecular weight. Furthermore, the high molecular mass peak rises more rapidly than that of low mass (plot 6 in fig. 5).

Table V. Effect of added water on the polymerization of 2-methylpropene (4.5M) initiated by anhydrous FeCl_3 , 30 mn in hexane at -10°C

Run n°	FeCl_3 $10^2 \cdot \text{mol} \cdot \text{l}^{-1}$	Added water $10^2 \cdot \text{mol} \cdot \text{l}^{-1}$	Yield %	Mn	Polydisp Index
1	6.2	0	14	600	12
2	6.2	0.42	12	850	22
3	6.2	0.48	34	3400	12
4	6.4	1.1	77	2800	9
5	6.3	1.6	100	2300	9
6	6.2	2.1	94	3300	8

Rate of Polymerization. We have plotted the yield of polymer versus the reaction time with two different monomer concentrations (fig.9) 2.2 and 4.5 M. In the two cases, 100% yield was obtained and the progression becomes rapidly linear after 30 minutes of polymerization.

We have calculated the global rate of polymerisation in the linear part of the two plots, by the slope of the straight line (table VI).

Table VI. Rate of polymerization expressed as the quantity of monomer consumed per mole of catalyst and per minute

Initial monomer concentration ($\text{mol} \cdot \text{l}^{-1}$)	$r(\text{mol}_{\text{mono}} \cdot \text{mol}_{\text{cat}}^{-1} \cdot \text{min}^{-1})$
2.2	0.11
4.2	0.12

The values of the polymerization rate calculated from the slopes on fig. 9 are low (in apolar medium and at -10°C) and close to each other. This confirms that the kinetic of the reaction is independent of the monomer concentration. Furthermore, the rate of polymerization reaction does not vary with time, in spite of the progressive diminution of the monomer concentration, as suggested by the results quoted on Fig.9.

From the two curves (Fig. 9) it can be deduced that a stationary or a quasi stationary state of active species concentration is observed after 40% of polymerization yield. The concentration in active species is constant or quasi-constant beyond 40% yield. Since the order of propagation reaction in monomer concentration is zero, and since it is one in ferric chloride concentration, it can be decided which one of the kinetic state, stationary or quasi-stationary state in active species, is reached from this value of 40% yield. Actually, it will be seen below that the active sites are long-lived species, which rule out the quasi-stationary state since the termination reaction is negligible.

Influence of the Polymerization Temperature. We studied also the evolution of the polymer yield with temperature. Figure 10 shows that the yield decreases when temperature decreases in the range $+20^\circ\text{C}$ and -20°C . For these polymerizations, an anhydrous salt was used. On the same plot a polymerization yield for a reaction initiated by a hydrated ferric chloride at -40°C is also shown. It is clear that the hydrated Lewis acid keeps an activity at -40°C which is not observed for the anhydrous form. This point would certainly deserve more attention in the future.

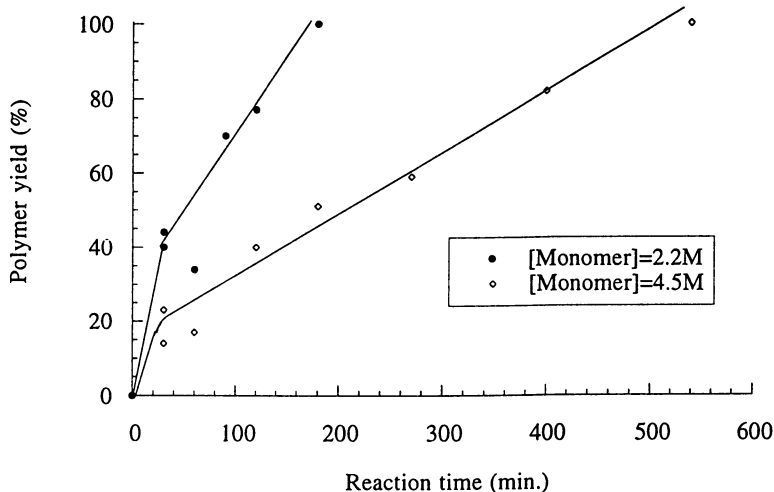


Figure 9. Evolution of the polymer Yield with two different 2-methylpropene concentrations in hexane at -10°C , with anhydrous FeCl_3 (7.10^{-2}M).

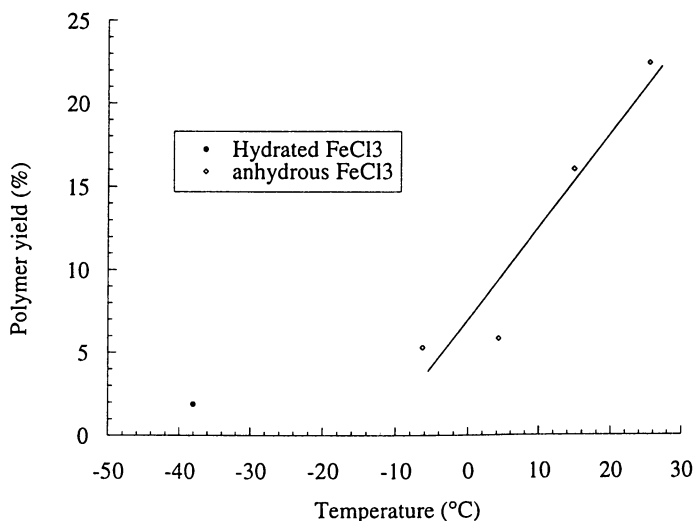


Figure 10. Yield of polymer versus reaction temperature plot in the polymerization of 2-methylpropene (4.5 M) with FeCl_3 ($6.2.10^{-2}\text{M}$), 30 min. in hexane.

We can estimate the activation energy E of the polymerization from the rate expression we have demonstrated :

$$v_p = k [\text{FeCl}_3]^1 [\text{Monom.}]^0 [\text{Cocat.}]^1 = k.C \quad (C=\text{constant})$$

for constant $[\text{H}_2\text{O}]$ and $[\text{FeCl}_3]$; thus $v_p = A e^{-E/RT}$. The slope of the straight line - $\ln v_p$ versus $1/T$ gives $E = 13.3 \text{ KJ.mol}^{-1}$.

Partially or Totally Heterogeneous System. We have conducted specially designed experiments in order to determine at least qualitatively the partially or totally heterogeneous aspect of the { FeCl_3 - 2-methylpropene - hexane } system.

In a first experiment, hydrated FeCl_3 was introduced in hexane and the solution was filtered under vacuum before being introduced in the reactor. After 30 minutes, 2-methylpropene was added on the yellow filtrate and the typical polymerization conditions were realized, but no polymerization occurred.

In an another experiment, we used two reactors joined by a cintered glass filter $n^\circ 3$. FeCl_3 , hexane and monomer in typical concentrations were respectively introduced and stirred. A part of the mixture was then transferred in the second reactor via the cintered glass filter,. After 30 minutes of reaction at -10°C and after quenching by methanol, the yield of polymer was found very low.

Taking into account the results of these two experiments, it is allowed to conclude that the system { FeCl_3 - 2-methylpropene - hexane } proceeds essentially via heterogeneous initiation.

Permanent Catalyst. We have above observed that 100% yield of polymer was always obtained when the polymerization was allowed to run for a sufficient time. We have verified adding a new charge of monomer that the catalyst continue to be active, by sequential heterogeneous polymerization.

In the first step, polymerization of 2-methylpropene was carried out during 16 hours to ensure that 100% yield was achieved. The reaction mixture was then allowed to stand 7 hours at the temperature of the reaction (-10°C) (with no quenching). In a second step, a second charge of monomer was added and allowed to react during 16 hours. 100% of polymerization yield was again obtained. From this experiment, it can be concluded that FeCl_3 behaves as a solid state permanent catalyst.

Active Species. We have mentioned above that, according to the bimodal MMD in SEC chromatogramm, there are two different active species. We have followed the evolution of this distribution during the course of the polymerization reaction (fig.11). The shoulder at low molecular weight is more and more important. It seems that the two active species, which explain the bimodal molecular weight distribution, induce propagation with a slightly different rate.

This bimodal distribution can be explained assuming that when the initial water concentration is low there is competition between two types of active species. One is given by direct intiation, proceeds at high rate but includes termination, and is only detected at low water concentration (see fig. 6). The second is given by water cocatalysis, proceeds at lower rate, but does not involve termination reation so that when the polymerization yield is about 40 %, propagation takes place only on the active species induced by water cocatalysis. This analysis is supported by the plots corresponding to the hydrated catalyst. (fig. 7). On this plot, it is clear that the initial fast polymerization is not detected, showing that the assumed direct initiation mechanism proceeds only at a negligible rate. It is clear that the sites corresponding

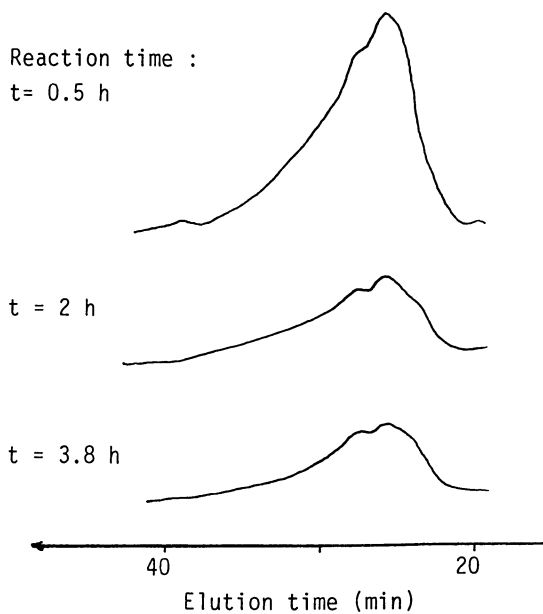
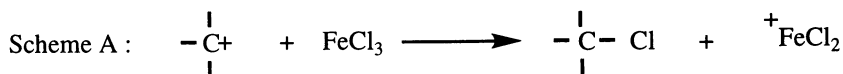


Figure 11. Evolution of the SEC chromatograms in the course of the polymerization of 2-methylpropene (4.5 M), with hydrated FeCl_3 ($1.3 \cdot 10^{-2}$ M) at -10°C .

to direct initiation must be very acidic. When water is present, it must react first with these highly acidic sites. There is no clear indication on the nature of the termination reactions which are involved in the assumed direct initiation mechanism.

As for the mechanism of transfer reaction, two types of transfer at the catalytic surface can be invoked (scheme A and B)



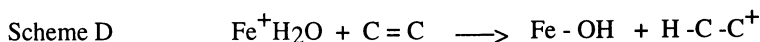
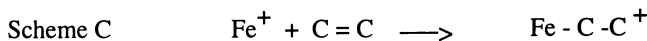
Scheme B :



Spectroscopic analysis of the polymers showed the presence of Cl, on the one hand, and terminal unsaturations, on the other hand. However, since some chlorine atom can be fixed on the polymers during quenching, it cannot be quantitatively decided at present the extent of these steps.

Conclusion

FeCl₃ in hexane promote the cationic polymerization of 2-methylpropene in an heterogeneous system. We suggest that both cocatalysis and direct initiation mechanism take place. They occur on the surface of the catalyst illustrated in simplified scheme C and D.



The scheme C is equivalent to the direct initiation mechanism postulated for self ionizing Lewis acids (12). Direct initiation can explain the initial fast polymerization giving low yield observed in the yield versus time plot. It explains also the polymerization initiated by the mixture FeCl₃-BCl₃ the ionization of which forms the positively charged FeCl₂⁺ (3)

The cocatalytic initiation mode in scheme D was already proposed by Addecott et al (7). Cocatalysis by water explains the effect of the FeCl₃ concentration at constant hydration degree and the effect of added water at constant FeCl₃ concentration.

The quantity of active species is proportional to the FeCl₃ surface, and to the initial water concentration which is able to activate the surface.

The overall polymerization rate is independent not only of initial monomer concentration, but also of the instantaneous monomer concentration. This is explained assuming that the rate determining step is the isomerization of the monomer molecule in the active species, and not the diffusion of the monomer molecule towards the active species, and assuming that the rate of termination is negligible during the polymerization time.

FeCl₃ behaves as a solid state permanent catalyst for the polymerisation of 2-methylpropene in hexane.

Acknowledgements. Paramins of Exxon Chemicals is gratefully acknowledged for a support for this research.

Literature Cited

1. COLLOMB, J. *Thèse de Doctorat d'Etat*, INP Grenoble **1981**.
2. COLLOMB, J.; ARLAUD, P.; GANDINI, A.; CHERADAME, H. *Cationic Polymerization and Related Processes*, IUPAC, **1984**, pp.49-67.
3. MAREK, M.; PECKA, J.; HALASKA, V. *Makromol. Chem., Makromol. Symp.* **1988**, Vol. 13/14, pp.443 -455.
4. SCOTT, H.; FROST, R.E.; BELT, R.F.; O'REILLY D.E. *J. Polym. Sci.* **1964**, Vol. A2, pp.3233-3257.
5. ANDERSON, W.S.; *J. Polym. Sci.* **1967**, Vol. A15, pp. 429.
6. COLLOMB, J.; GANDINI, A.; CHERADAME, H. *Makromol. Chem. Rapid Commun.* **1980**, Vol. 1, pp. 489.
7. ADDECOTT K.S.B.; MAYOR L.; C.N. TURTON C.N. *Eur. Polym. J.* **1967**, Vol. 3, pp. 601.
8. CHERADAME, H.; RISSOAN, G.; FAVIER F.; PASCAL J. L.; CHEN F. J. *C. R. Acad. Sci.Paris*, t. 318, Série II, **1994**, pp.329-334.
9. MOULIS, J. M.; COLLOMB, J.; GANDINI, A.; CHERADAME, H. *Polym. Bull.* **1980**, Vol. 3, pp.197.
10. KHALAFOV, F. R. and coll., *Makromol. Chem., Rapid Commun.* **1985**, Vol.6, pp.29.
11. KWON, O.S.; GHO, C. G.; CHOI, B. S.; CHOI, S.K. *Makromol. Chem. Phys.* **1994**, Vol. 195, pp.2187.
12. BOENE, R.; REICHERT, K. H. W.; *Makromol. Chem.* **1976**, Vol.177, pp.3545 .

Chapter 13

Amphiphilic Block Copolymers via Cationic Polymerization

Oskar Nuyken, Saehoon Oh, and Stefan Ingrisch

Lehrstuhl für Makromolekulare Stoffe, Technische Universität München,
Lichtenbergstrasse 4, D-85747 Garching, Germany

1. Introduction

Cationic polymerization of vinyl ethers initiated by HI/I_2 , HI/ZnI_2 , $\text{CH}_3\text{CHI(OR)/NR}_4\text{ClO}_4$, $\text{CH}_3\text{CHI(OR)/KClO}_4$ (crown ether) and $\text{CH}_3\text{CHI(OR)/LiClO}_4$ (crown ether) show the characteristics of a living polymerization [1-10]. The potential of this polymerization for the synthesis of telechelics, macromonomers, star- and block copolymers was discovered mainly by Higashimura and his group [1-7]. These authors and others [8-10] have demonstrated in a great variety of systematic studies that

- initiation is spontaneous
- molar mass is controlled by [monomer] : [initiator]
- molar mass increases with conversion
- molar mass increases by sequential addition of monomer
- molar mass distribution is narrow
- well defined initiation and termination allows the synthesis of taylor made polymers (macromonomers, telechelics ...)

It was of great interest to us to apply this method to the synthesis of amphiphilic block copolymers containing poly(methyl vinyl ether) (PMVE) as hydrophilic segment.

2. Homopolymerization of methyl vinyl ether (MVE)

From earlier work we know that $\text{CH}_3\text{CHI(OR)/NR}_4\text{ClO}_4$ is a very efficient initiator. In this study we have applied successfully **1** and **2** as initiators for the polymerization of MVE as shown in the following scheme. The advantage of pathway b) over a) is the possibility of molar mass determination via end group analysis ($^1\text{H-NMR}$). Both initiators (**1**, **2**) show identical polymerization behavior (Fig.1).

It was also shown that experimental and theoretical molar masses are very similar (Table I). These molar masses are controlled by the ratio $[\text{M}] : [\text{I}]$.

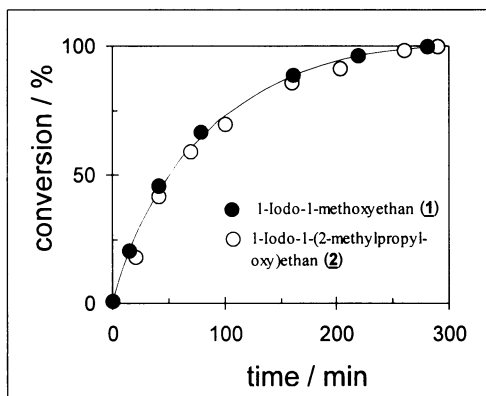
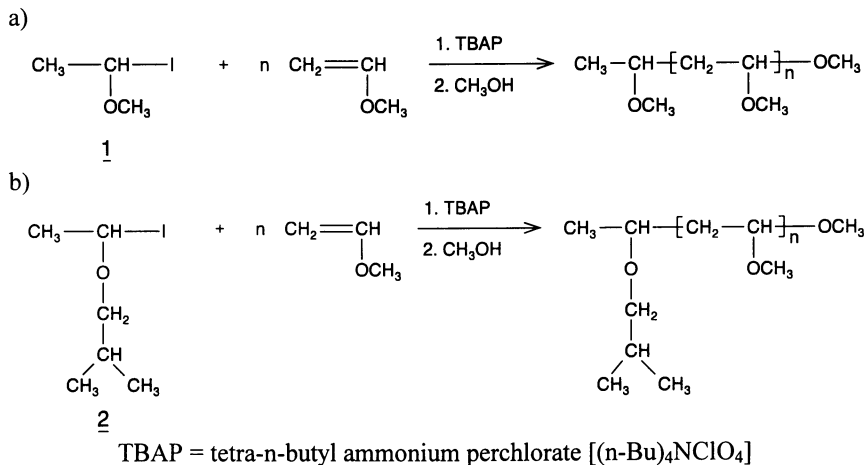


Fig. 1: Polymerization of MVE with 1 / TBAP (●) and 2 / TBAP (○) in CH_2Cl_2 at -25°C ; $[\text{MVE}] = 0,36 \text{ mol l}^{-1}$; $[\text{1}], [\text{2}] = 5 \text{ mmol l}^{-1}$; $[\text{TBAP}] = 5 \text{ mmol l}^{-1}$

Table I: Polymerization of MVE in CH_2Cl_2 initiated by 1/TBAP

$[\text{MVE}]$ <i>mol/l</i>	<u>1</u> <i>mmol/l</i>	[TBAP] <i>mmol/l</i>	temp. $^\circ\text{C}$	time <i>min</i>	\bar{M}_n ^{a)} <i>g·mol⁻¹</i>	$\bar{M}_{n,\text{calc}}$ ^{b)} <i>g·mol⁻¹</i>	\bar{M}_w / \bar{M}_n ^{a)}
0.42	13	13	-30	120	1740	1960	1.13
0.51	15	15	-30	130	1980	2060	1.12
0.72	9	9	-25	160	4760	4730	1.17
0.36	5	5	-25	280	4360	4270	1.18
0.36	9	9	-25	140	2380	2410	1.21
1.00	14	14	-15	65	4250	4230	1.20
0.36	5	5	-15	190	4240	4270	1.19

a) from GPC (polystyrene standards)

b) $\bar{M}_{n,\text{calc}} = \{M_{\text{MVE}} \times ([\text{MVE}]/[\text{1}])\} C + M_{\text{MeOH}} + M_{\text{MVE}}$; (C = conversion)

The polymerization rate depends on the concentration of monomer and initiator but also on the temperature. Linear increase of the molar masses were observed in case of sequential monomer addition (Figure 2, Table II).

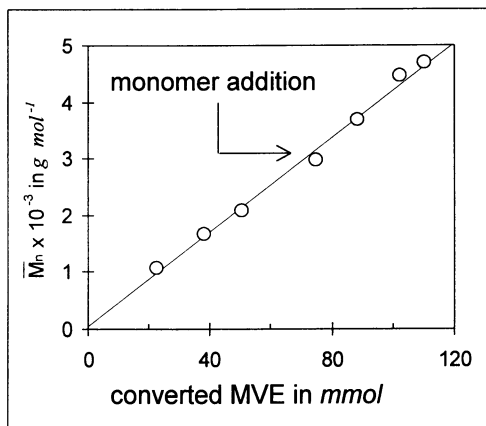


Fig.2: Polymerization of MVE with **1** / TBAP in CH_2Cl_2 at $-25^\circ C$; monomer addition experiment; $[MVE]_0 = 0,37 \text{ mol l}^{-1}$; **1**, [TBAP] = 7 mmol l^{-1}

Table II: Polymerization of MVE with **1**/TBAP in CH_2Cl_2 at $-20^\circ C$; monomer addition experiment; ($[MVE]_0 = 0,37 \text{ mol l}^{-1}$; **1**, [TBAP] = 7 mmol l^{-1})

time <i>min</i>	converted MVE <i>mmol</i>	conversion ^{a)} c, %	\bar{M}_n ^{b)} , $g \cdot mol^{-1}$	$\bar{M}_{n, calc}$ ^{c)} , $g \cdot mol^{-1}$	\bar{M}_w / \bar{M}_n ^{b)}
15	22	30	1120	1010	1.19
30	38	51	1730	1650	1.18
50	50	68	2090	2180	1.19
150	74	100	3070	3160	1.17
----- addition of 37 mmol MVE -----					
160	88	38	3790	3740	1.21
190	102	76	4480	4320	1.21
235	110	97	4710	4640	1.22

a) numbers are related to second portion of monomer

b) from GPC (polystyrene standards)

c) $\bar{M}_{n, calc} = \{M_{MVE} \times ([MVE]/[1])\} C + M_{MeOH} + M_{MVE}$

A typical GPC-diagram is shown in the Figure 3 and the change of the polymerization rate of MVE with the temperature is demonstrated in Figure 4.

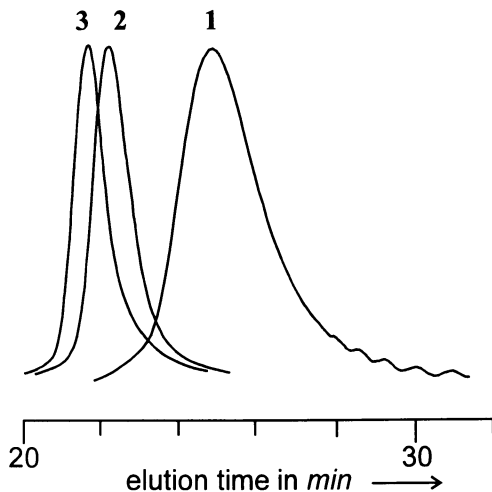


Fig.3: Polymerization of MVE with 1 / TBAP in CH_2Cl_2 at -25°C

1: $\bar{M}_n = 1120 \text{ g/mol}$	$\bar{M}_w/\bar{M}_n = 1.19$
2: $\bar{M}_n = 3070 \text{ g/mol}$	$\bar{M}_w/\bar{M}_n = 1.17$
3: $\bar{M}_n = 4710 \text{ g/mol}$	$\bar{M}_w/\bar{M}_n = 1.22$

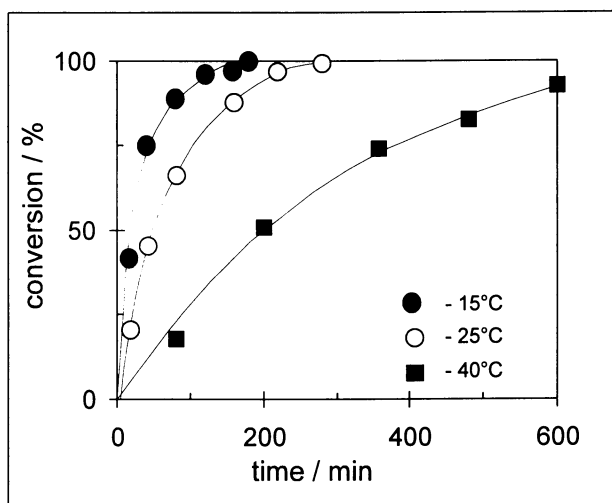


Fig.4: Polymerization of MVE with 1 / TBAP in CH_2Cl_2 at different temperatures
 $[\text{MVE}] = 0,36 \text{ mol l}^{-1}$; $[\text{1}], [\text{TBAP}] = 5 \text{ mmol l}^{-1}$

The consumption of MVE follows a first order kinetics (Fig.5). The activation energy of this process was determined to be 38 kJ/mol [compare isobutyl vinyl ether (IBVE): 60 kJ/mol].

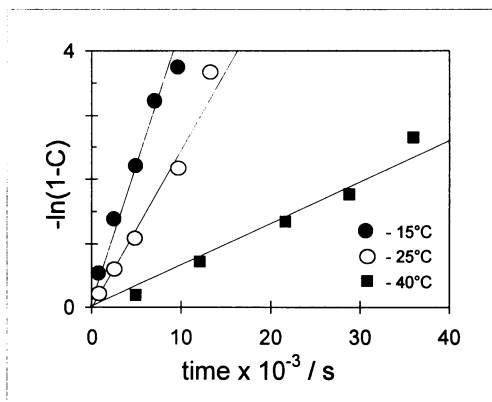


Fig. 5: Polymerization of MVE with **1** / TBAP in CH₂Cl₂ at different temperatures; 1st order plot; [MVE] = 0,36 mol l⁻¹; [**1**], [TBAP] = 5 mmol l⁻¹ C = conversion

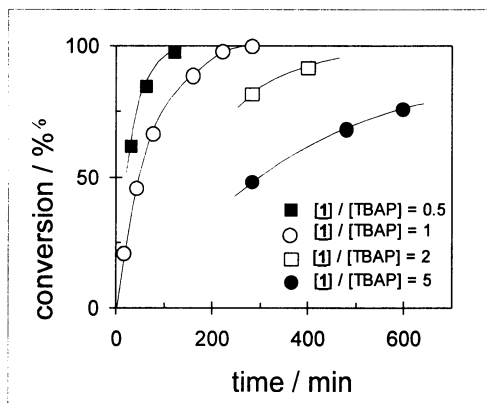


Fig. 6: Polymerization of MVE with **1** / TBAP in CH₂Cl₂ at -25°C; effect of [**1**] : [TBAP]

Table III: Polymerization of MVE with **1**/TBAP in CH₂Cl₂ at -25°C; effect of [**1**] : [TBAP]

[MVE] mol/l	[1] mmol/l	[TBAP] mmol/l	[1]/ [TBAP]	time min	conversion %	\bar{M}_w / \bar{M}_n ^{a)}	\bar{M}_n ^{a)} g/mol	$\bar{M}_{n,calc}$ g/mol
0.36	5	10	0.5	30	62	1.19	2650	2645
0.36	5	10	0.5	60	85	1.18	3780	3626
0.36	5	10	0.5	120	98	1.18	4180	4180
0.36	5	5	1	280	100	1.18	4430	4260
0.36	5	2.5	2	280	82	1.19	3510	3498
0.36	5	2.5	2	400	92	1.20	4120	3925
0.36	5	1	5	280	48	1.17	2060	2048
0.36	5	1	5	480	69	1.17	2930	2943
0.36	5	1	5	600	76	1.18	3290	3242

^{a)} from GPC (polystyrene standards)

From earlier studies we know that the ratio of [initiator (**1** or **2**)]: [TBAP] has a strong effect on the polymerization rate of vinyl ethers. A similar effect was found for the polymerization of MVE (Figure 6, Table III).

It was also of interest to compare the rate of polymerization of MVE with that of IBVE. The result is shown in Figure 7.

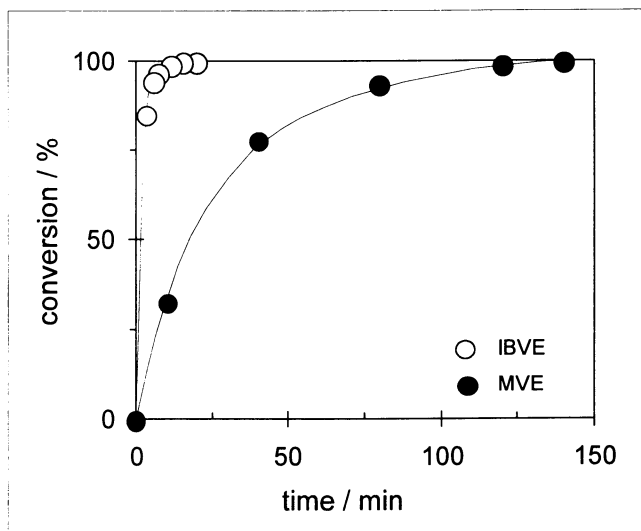


Fig.7: Polymerization of MVE (●) and IBVE (O) in CH_2Cl_2 at -25°C ; initiated by **1**/TBAP; $[\text{MVE}]$, $[\text{IBVE}] = 0,36 \text{ mol l}^{-1}$; **1**, [TBAP] = 9 mmol l^{-1}

As one can see from Figure 7 IBVE polymerizes faster than MVE. It is trivial that this comparison holds in a certain temperature region only, since both monomers polymerize with different activation energies.

The rate of the MVE polymerization can be influenced over a wide range by different factors:

- solvent
- concentration of monomer
- concentration of initiator
- concentration of TBAP
- temperature
- type of initiator

It could be demonstrated also that it is possible to polymerize MVE with **1**/ ZnI_2 as shown in the following scheme. Experimental results are summarized in Table IV. Molar masses increase with conversion (Fig.8).

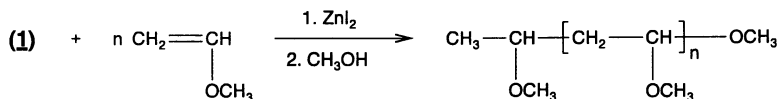


Table IV: Polymerization of MVE initiated by **1**/ZnI₂ in CH₂Cl₂ at -25 °C;
 ([MVE] = 0.36 mol·l⁻¹, [**1**] = 9 mmol·l⁻¹, [ZnI₂] = 0.9 mmol·l⁻¹)

time min	conversion C, %	$\bar{M}_{n,calc}$ ^{a)} g·mol ⁻¹	\bar{M}_n ^{b)} g·mol ⁻¹	\bar{M}_w / \bar{M}_n ^{b)}
20	38	971	980	1.17
40	55	1018	1210	1.15
120	79	1923	2030	1.16
210	94	2270	2320	1.19
250	99.5	2398	2450	1.15

a) $\bar{M}_{n,calc} = \{ M_{MVE} \times ([MVE]/[**1**]) \} C + M_{MVE} + M_{MeOH}$

b) from GPC (polystyrene standards)

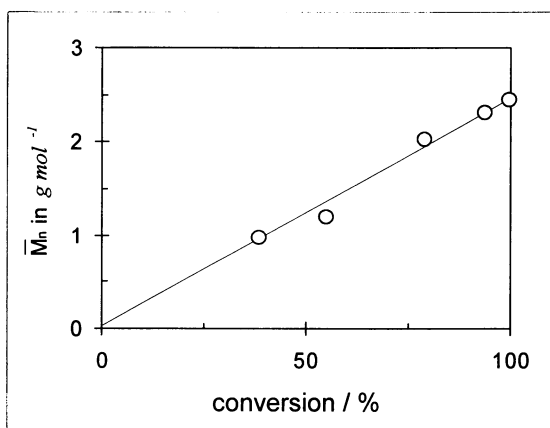


Fig.8: Polymerization of MVE with **1** / ZnI₂ in CH₂Cl₂ at -25°C;
 [MVE] = 0,36 mol l⁻¹; [**1**] = 9 mmol l⁻¹; [ZnI₂] = 0,9 mmol l⁻¹

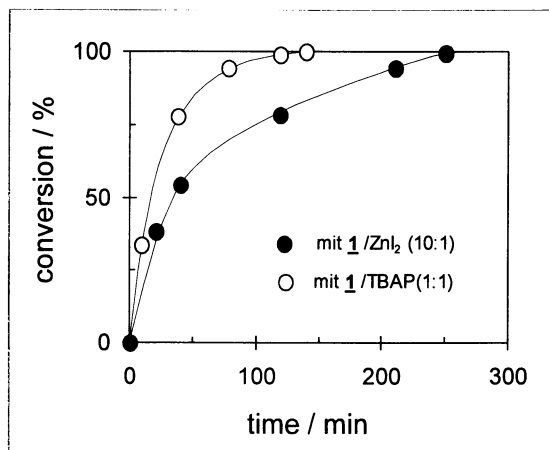


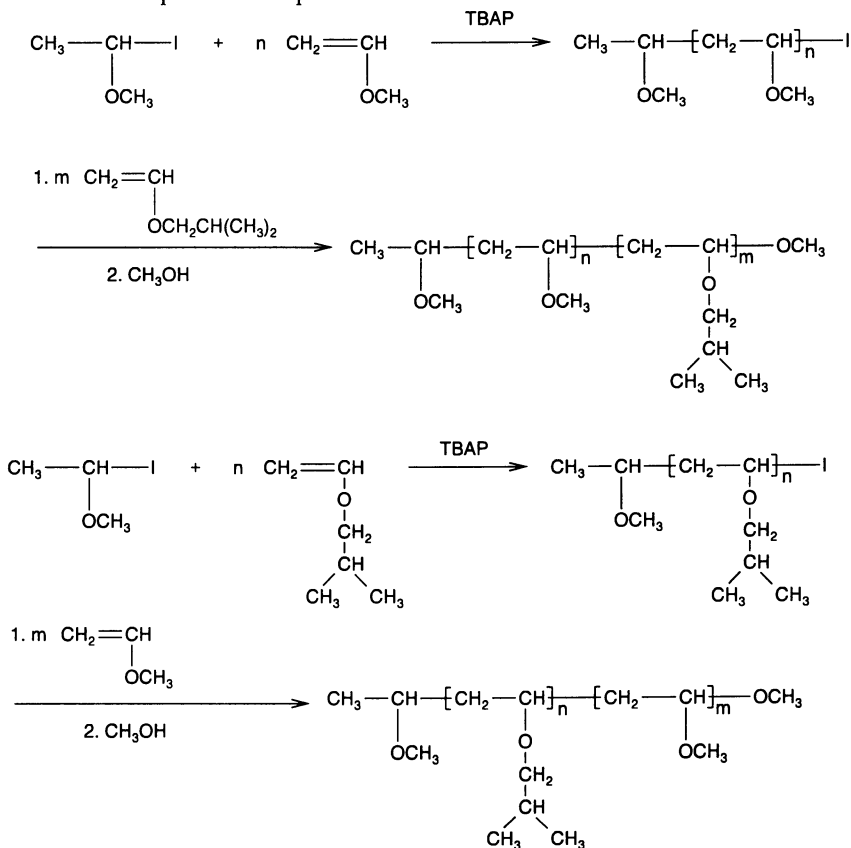
Fig.9: Polymerization of MVE with **1** / ZnI₂ (•) and **1**/TBAP (o) in CH₂Cl₂ at -25°C;
 [MVE] = 0,36 mol l⁻¹; [**1**], [TBAP] = 9 mmol l⁻¹; [ZnI₂] = 0,9 mmol l⁻¹

The rate of polymerization depends on the amount of coinitiator, meaning similar rates can be adjusted for $\underline{1}/\text{TBAP}$ and $\underline{1}/\text{ZnI}_2$ by varying the amount of TBAP and ZnI_2 (Fig.9). For $\text{MVE}/\underline{1}/\text{ZnI}_2$ the consumption of MVE follows first order kinetics and the monomer addition experiment shows similar characteristics as the system $\text{MVE}/\underline{1}/\text{TBAP}$.

Narrow molar masses were observed in all cases of poly(MVE) polymers initiated by $\underline{1}/\text{TBAP}$, $\underline{2}/\text{TBAP}$ and $\underline{1}/\text{ZnI}_2$ controlled by $[\text{M}] : [\underline{1}]$ or $[\underline{2}]$. It was not the intention of our work to reach for high molar masses. However, it was important to find conditions which allow block copolymer formation by sequential addition of different monomers. Before one can do that, it was essential to demonstrate that MVE segments of controlled size could be synthesized.

3. Block copolymers from MVE and IBVE, initiated by $\underline{1}/\text{TBAP}$

The following scheme describes the two strategies of the synthesis of AB-type block copolymers from MVE and IBVE; both, MVE and IBVE, have been polymerized first. After complete consumption of the first monomer the second one was added.



A solution of MVE (or IBVE) and TBAP in CH_2Cl_2 was kept at -25°C .

The polymerization of the first segment was started by addition of **1**, dissolved in hexane. After the complete conversion of the first monomer (monomer consumption followed via gas chromatography) the second monomer was added. In this case the sequence of monomer addition has no effect on the structure of the resulting block copolymer. The same narrow distributed products were received when the polymerization was started or finished by MVE addition (Table V).

Table V: Block copolymerization of MVE and IBVE with **1**/TBAP in CH₂Cl₂ at -25 °C; ([**1**] = [TBAP] = 9 mmol·l⁻¹)

[MVE] A mol/l	[IBVE] B mol/l	[A]/[B]	\bar{M}_n , calc ^{a)} g/mol	\bar{M}_n ^{b)} g/mol	\bar{M}_w/\bar{M}_n ^{b)}	type
0.72	0.18	4	6730	6920	1.25	AB
0.72	0.36	2	8730	8910	1.20	AB
0.36	0.36	1	6410	6330	1.25	AB
0.18	0.36	0.5	5250	5600	1.23	AB
0.72	0.36	2	8730	8340	1.18	BA
0.36	0.36	1	6410	6580	1.23	BA

a) \bar{M}_n , calc = $M_{\text{MVE}} \times ([\text{MVE}]/[\mathbf{1}]) + M_{\text{IBVE}} \times ([\text{IBVE}]/[\mathbf{1}]) + M_{\text{MeOH}} + M_{\text{MVE}}$

b) from GPC (polystyrene standards)

The molar mass is controlled by the ratio of [A] : [**1**] and [B] : [**1**]. This indicates that all chain ends remain active and AB respectively BA type polymers are formed exclusively. Narrow monomodal peaks of the AB-(BA)-type copolymers in the GPC-diagram support this view (Figure 10).

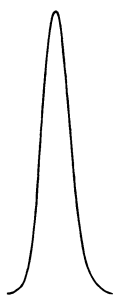


Fig.10: Block copolymerization of MVE and IBVE in CH₂Cl₂ initiated by **1**/TBAP;
 $\bar{M}_n = 8340$ g/mol; $\bar{M}_w/\bar{M}_n = 1.18$
(MVE : IBVE = 2 : 1)

The composition of the block copolymers was analysed by ¹H-NMR. The results are summarized in Table VI.

Table VI: Block copolymers of MVE and IBVE (AB and BA type) synthesized by sequential monomer addition in CH_2Cl_2 at -25°C , initiated by $\underline{1}$ /TBAP; ($[\underline{1}] = [\text{TBAP}] = 7 \text{ mmol}\cdot\text{l}^{-1}$)

monomer			block copolymer	
[MVE(A)], <i>mol/l</i>	[IBVE(B)], <i>mol/l</i>	[A]/[B]	composition n / m ^{a)}	type
0.72	0.18	4	4.17	AB
0.72	0.36	2	1.90	AB
0.36	0.36	1	1.06	AB
0.18	0.36	0.5	0.49	AB
0.36	0.36	1	1.05	BA
0.72	0.36	2	2.07	BA

^{a)} by $^1\text{H-NMR}$ (n/m corresponds to $[\text{A}]/[\text{B}]$)

4. Block copolymers from 2-chloroethyl vinyl ether (CEVE) and MVE

The block copolymerization of CEVE and IBVE has already been described in some detail [11-13]. However, little is known about the combination of MVE/CEVE in block copolymers. It was essential to study the homopolymerization of CEVE before this monomer could be applied for the synthesis of block copolymers.

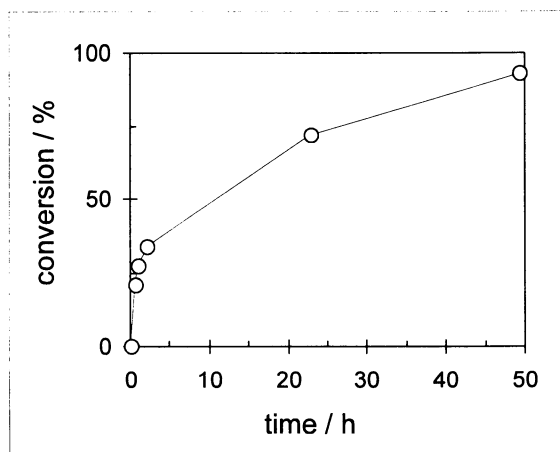
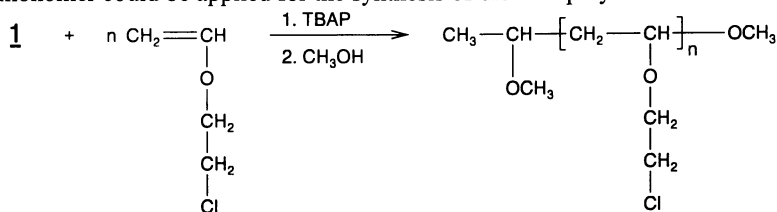


Fig. 11: Polymerization of CEVE with $\underline{1}$ / TBAP in CH_2Cl_2 at -25°C ; $[\text{CEVE}] = 0,36 \text{ mol l}^{-1}$; $[\underline{1}]$, $[\text{TBAP}] = 9 \text{ mmol l}^{-1}$

The system CEVE/**1**/TBAP was rather slow (Figure 11). Although molar masses are controlled by the ratio [monomer] : [initiator] products were rather broadly distributed ($\overline{M}_w/\overline{M}_n = 1.4$). Faster polymerization was observed when **1**/ ZnI_2 was used as initiator (polymerization was completed in less than 2 hours instead of more than 50 hours for **1**/TBAP, compare Figure 12). The reaction is shown in the scheme below.

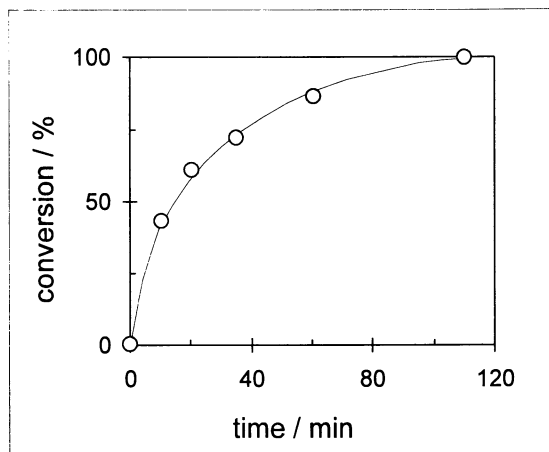
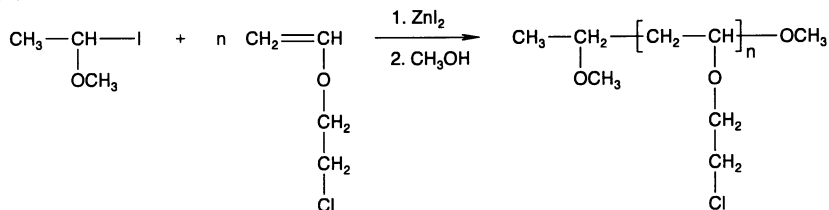


Fig.12: Polymerization of CEVE with **1** / ZnI_2 in CH_2Cl_2 at -25°C ;
 $[\text{CEVE}] = 0,36 \text{ mol l}^{-1}$;
 $[\mathbf{1}] = 9 \text{ mmol l}^{-1}$; $[\text{ZnI}_2] = 0,9 \text{ mmol l}^{-1}$

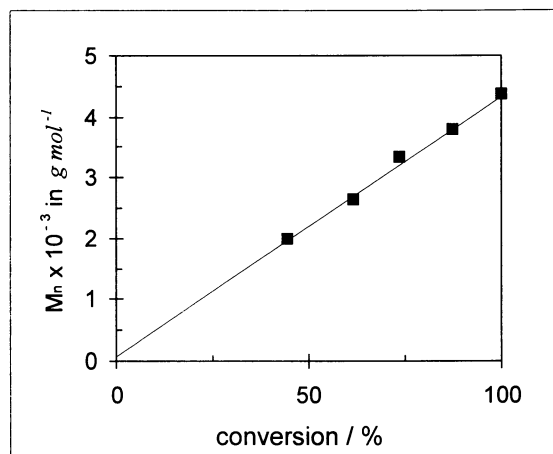


Fig.13: Polymerization of CEVE with **1** / ZnI_2 in CH_2Cl_2 at -25°C ;
 $[\text{CEVE}] = 0,36 \text{ mol l}^{-1}$;
 $[\mathbf{1}] = 9 \text{ mmol l}^{-1}$; $[\text{ZnI}_2] = 0,9 \text{ mmol l}^{-1}$

From the results summarized in Table VII one can see the good agreement between experimental and theoretical molar masses. Furthermore, the polymerization is reasonable fast and the polydispersity ($\overline{M}_w/\overline{M}_n = 1.18$) is narrow. Molar mass increases linearly with conversion (Figure 13). The monomer addition experiment showed the characteristic increase of the molar mass and the complete shift of the GPC peaks to higher molar masses (Figure 14).

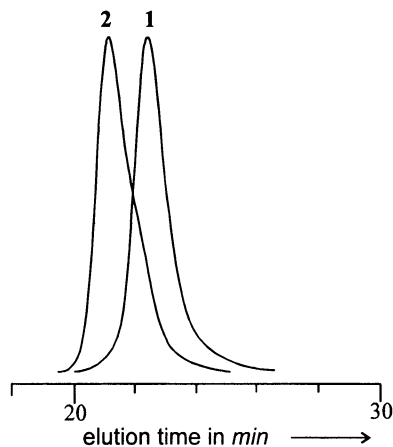


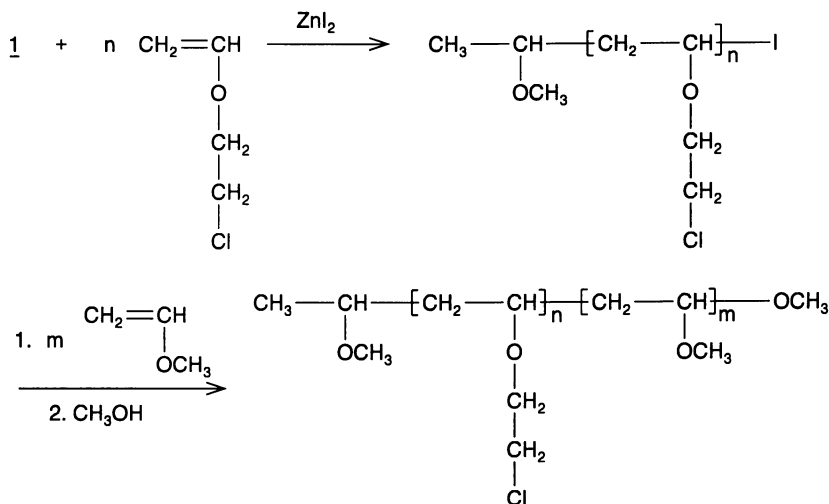
Fig.14: CEVE - polymerization; monomer-addition experiment:

Initiator = **1** / ZnI_2 (9 : 0,9 mmol)

1: $\overline{M}_n = 4190$ g/mol (before monomer addition)

2: $\overline{M}_n = 8340$ g/mol (after monomer addition)

Since we have shown that **1**/ ZnI_2 is an efficient initiator not only for CEVE but also for MVE, it should be possible to obtain block copolymers via sequential monomer addition and initiated with **1**/ ZnI_2 according to the following scheme:



In addition, it was also possible to polymerize first MVE and to add CEVE as second monomer. Some of the results are summarized in Table VII:

Table VII: Block copolymerization of CEVE and MVE with **1**/ZnI₂ in CH₂Cl₂ at -25 °C; ([**1**] = 9 mmol·l⁻¹, [ZnI₂] = 0.09 mmol·l⁻¹)

[CEVE] A mol/l	[MVE] B mol/l	[A]/[B]	$\bar{M}_{n,calc}$ ^{a)} g/mol	\bar{M}_n ^{b)} g/mol	\bar{M}_w/\bar{M}_n ^{b)}	type
0.36	0.36	1	6670	6550	1.25	AB
0.36	0.18	2	5510	5490	1.22	AB
0.36	0.72	0.5	8990	8530	1.35	AB
0.36	0.18	2	5510	5710	1.28	BA
0.36	0.36	1	6670	6480	1.26	BA
0.18	0.36	0.5	4540	4280	1.28	BA

a) $\bar{M}_{n,calc} = M_{MVE} \times ([MVE]/[**1**]) + M_{CEVE} \times ([CEVE]/[**1**]) + M_{MeOH} + M_{MVE}$

b) from GPC (polystyrene standards)

Monomodal GPC curves, narrow molar mass distribution, and last but not least perfect control of the molar masses ($\bar{M}_{n,calc}$ and $\bar{M}_{n,exp}$ are very similar) indicate that exclusively poly(MVE-b-CEVE) and poly(CEVE-b-MVE) are formed by sequential monomer addition. The composition of the block copolymers is simply controlled by the amount of each monomer when both monomers are converted completely (Table VIII).

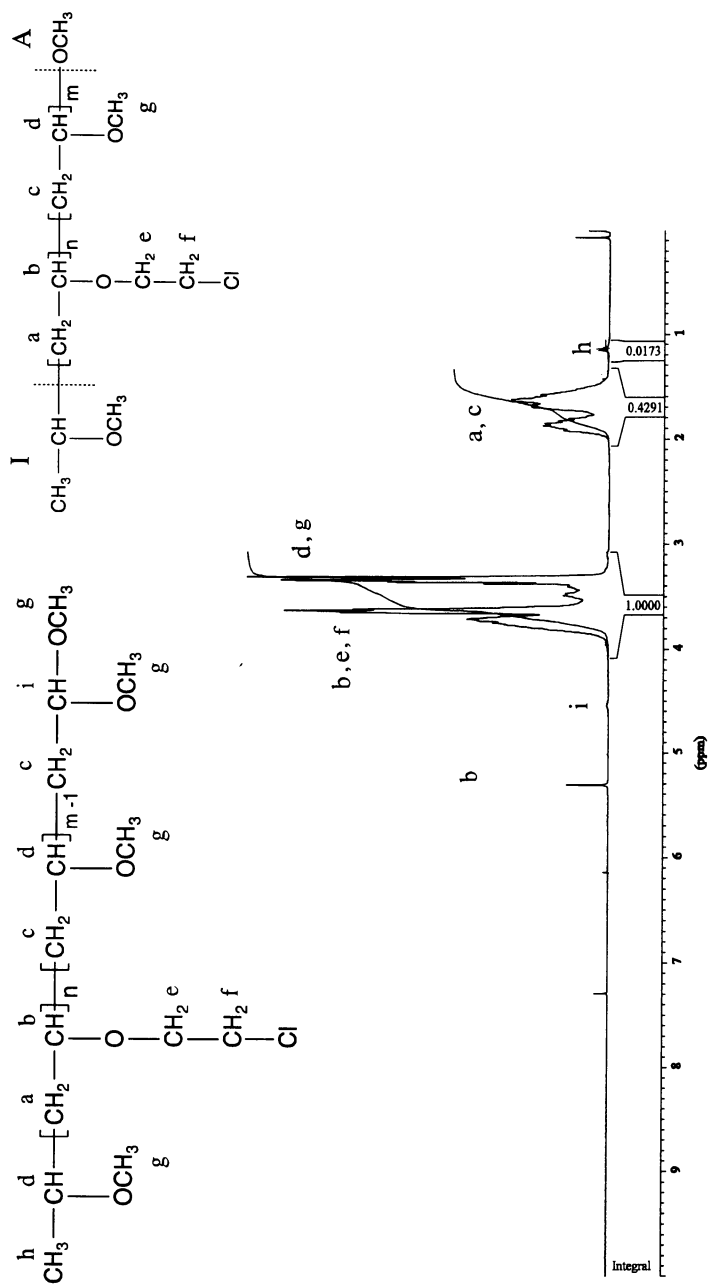
Table VIII: Block copolymerization of CEVE and MVE with **1**/ZnI₂ in CH₂Cl₂; ([**1**] = 9 mmol·l⁻¹, [ZnI₂] = 0.9 mmol·l⁻¹)

monomer			block copolymer	
[CEVE(A)] mol/l	[MVE(B)] mol/l	[A]/[B] ^{a)}	composition n / m ^{b)}	type
0.36	0.36	1	0.94	AB
0.36	0.18	2	1.94	AB
0.36	0.72	0.5	0.46	AB
0.36	0.18	2	1.91	AB
0.36	0.36	1	1.05	BA
0.18	0.36	0.5	0.47	BA

a) theoretical value

b) from ¹H-NMR (n/m corresponds to [A]/[B])

The analysis of the composition of poly(CEVE-b-MVE) and poly(MVE-b-CEVE) is based on ¹H-NMR (Figure 15).

Fig.15: $^1\text{H-NMR}$ spectrum of poly(CEVE-b-MVE) in CDCl_3

In the following calculation protons of the head (I) and end (A) group were neglected. The $^1\text{H-NMR}$ of poly(CEVE-b-MVE) (Figure 15) shows two areas of peaks:

$$I_1 (4.1 - 3.1 \text{ ppm}) = n\text{H} (h_b + h_c + h_f) + m\text{H} (h_d + h_g)$$

$$I_2 (2.1 - 1.3 \text{ ppm}) = n\text{H} h_a + m\text{H} h_c$$

H: equivalent of one proton

h: number of protons of type (a to g)

n, m: number of the repeating units of CEVE and MVE

Therefore one can immediately write:

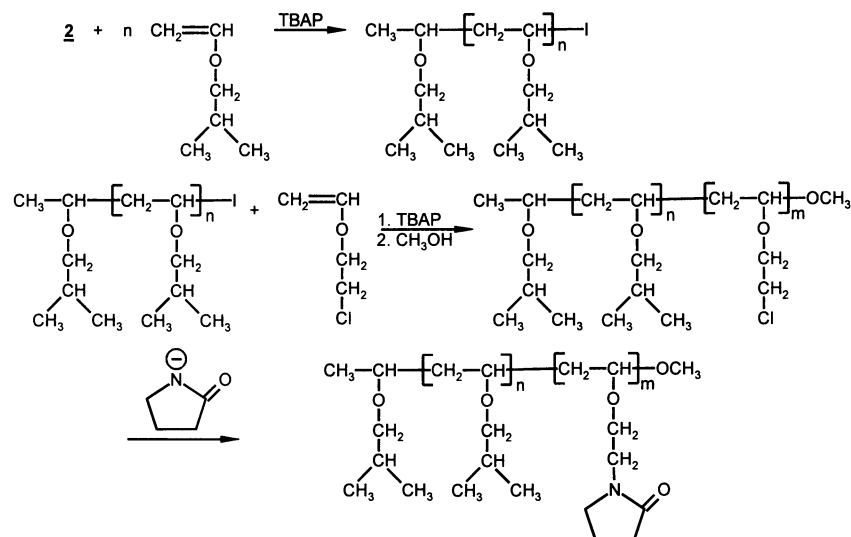
$$I_1 = 5n\text{H} + 4m\text{H}$$

$$I_2 = 2n\text{H} + 2m\text{H}$$

$$\text{resulting in } \frac{n}{m} = \frac{2I_1 - 4I_2}{5I_2 - 2I_1}$$

5. Block copolymers from IBVE and PEVE via polymer analog reaction

Poly(IBVE-b-PEVE) was synthesized via poly(IBVE-b-CEVE) as intermediate according to the following scheme:



PEVE: 2-(1-pyrrolidonyl)ethyl vinyl ether

The composition of the block copolymers can be determined by the $^1\text{H-NMR}$ spectroscopy. The agreement between calculated and experimental values is excellent for poly(IBVE-b-CEVE). The block formation is supported by a monomodal GPC diagram and the increase of the molar mass after addition of the

second monomer and the good agreement between molar masses from GPC and calculated values.

Since the initiating system which was used for the polymerization of IBVE and CEVE does not polymerize 2-(1-pyrrolidonyl)ethyl vinyl ether (PEVE), it was necessary to take a detour. Therefore, poly(IBVE-b-PEVE) was synthesized by reacting of poly(IBVE-b-CEVE) with the anion of pyrrolidone as shown in the scheme above.

Elemental analysis and $^1\text{H-NMR}$ indicate 100 % substitution of chlorine and good agreement between calculated and experimental \overline{M}_n . However, \overline{M}_n from GPC are much smaller than expected. The reason for this finding is the higher polarity of the product compared with the precursor. Therefore the elution time of GPC is extended.

6. Block copolymers from MVE and N-vinylcarbazole (NVC)

Polymerization of NVC initiated by $\underline{1}$ /TBAP is relatively uncontrolled concerning molar masses and their distribution ($\overline{M}_w/\overline{M}_n = 2.3 - 2.6$). Moreover, the polymerization is complete in a few seconds. Better results were received with solely $\underline{1}$ as initiator. Molar mass distribution narrows ($\overline{M}_w/\overline{M}_n = 1.4 - 1.7$) and the discrepancy between calculated and experimental molar masses became smaller. The polymerization time was extended to 50 min [14-16]. Further improvement was observed when the system $\underline{1}$ /TBAP/TBAI was applied as it is indicated in Table IX.

Table IX: Polymerization of NVC in CH_2Cl_2 initiated with $\underline{1}$ /TBAP/TBAI at -25°C ; $[\text{NVC}] = 0.3 \text{ mol/l}$, $[\underline{1}] = 10 \text{ mmol/l}$, $[\text{TBAP}] = [\text{TBAI}] = 9 \text{ mmol}$

time <i>min</i>	conversion %	$\overline{M}_{n, \text{calc}}$ ^{a)} <i>g·mol⁻¹</i>	\overline{M}_n ^{b)} <i>g·mol⁻¹</i>	$\overline{M}_w/\overline{M}_n$ ^{b)}
10	36	2180	1810	1.15
15	54	3220	3260	1.15
35	74	4380	4560	1.13
90	98	5770	5640	1.15
120	100	5890	5810	1.15

a) $\overline{M}_{n, \text{calc}} = \{M_{\text{NVC}} \times ([\text{NVC}]/[\underline{1}])\} C + M_{\text{MVE}} + M_{\text{MeOH}}$

b) from GPC (polystyrene standards)

In contrast to the successful block copolymerization of NVC/IBVE [15], we did not succeed in the synthesis of poly(NVC-b-MVE). Bimodal GPC curves were a clear indication that block copolymers were always accompanied by corresponding homopolymers.

7. References

1. M.Miyamoto, M.Sawamoto, T.Higashimura, *Macromolecules* **17**, 265 (1984)

2. M.Miyamoto, M.Sawamoto, T.Higashimura, *Macromolecules* **17**, 2228 (1984)
3. T.Higashimura, M.Miyamoto, M.Sawamoto, *Macromolecules* **18**, 611 (1985)
4. T.Higashimura, M.Sawamoto, *Makromol. Chem. Suppl.* **12**, 153 (1985)
5. T. Higashimura, S.Aoshima, M.Sawamoto, *Makromol. Chem., Macromol. Symp.* **3**, 99 (1986)
6. T. Higashimura, S.Aoshima, M.Sawamoto, *Makromol. Chem., Macromol. Symp.* **13/14**, 457 (1988)
7. M.Sawamoto, C.Okamoto, T. Higashimura, *Macromolecules* **20**, 2693 (1987)
8. O.Nuyken, H.Kröner, *Makromol. Chem.* **191**, 1 (1990)
9. O.Nuyken, H.Kröner, S.Aechtner, *Makromol. Chem., Macromol. Symp.* **32**, 181 (1990)
10. O.Nuyken, H.Kröner, G.Rieß, S.Oh, S.Ingrisch, *Macromol. Symp.* **101**, 29 (1996)
11. F.P.Boettcher, *Makromol. Chem., Macromol. Symp.* **13/14**, 193 (1988)
12. M.Sawamoto, T.Higashimura, *Makromol. Chem., Macromol. Symp.* **47**, 67 (1991)
13. N.H.Houcourt, E.J.Goethals, M.Schappacher, A.Deffieux, *Makromol. Chem., Rapid Commun.* **13**, 329 (1992)
14. O.Nuyken, G.Rieß, J.A.Loontjens, *Macromol. Reports* **A32**, 25 (1995)
15. O.Nuyken, G.Rieß, J.A.Loontjens, R.van der Linde, *Macromol. Reports* **A32**, 227 (1995)
16. S.Oh, Ph.D Thesis, TU München 1995

Chapter 14

Capping of Polyisobutylene with 1,1-Diphenylethylene and Its Derivatives

Kinetic and Mechanistic Studies

Young Cheol Bae, Zsolt Fodor¹, and Rudolf Faust²

Polymer Science Program, Department of Chemistry, University of Massachusetts Lowell, One University Avenue, Lowell, MA 01854

Fundamental investigations have been carried out on the capping reaction of living polyisobutylene with 1,1-diphenylethylene (DPE) and its derivatives. Capping is a reversible reaction and the corresponding equilibrium constants have been determined. In accord with theoretical considerations, higher K_e was obtained at lower temperature, at higher solvent polarity, and for better stabilized diphenyl carbenium ions. With DPE ΔH was found to be -85.2 kJ/mole in hexane:methyl chloride 40:60 (v:v) solvent mixture and -83.1 kJ/mole in hexane:methyl chloride 60:40 (v:v) solvent mixture. Capping involves about -300 J/mole/°K of entropy change due to the decrease in the number of molecules involved. A simplified kinetic equation was developed to describe the time dependence of uncapped living chain end concentration. By fitting the experimental data the corresponding kinetic parameters have been calculated, and found to be in satisfactory agreement with that obtained from capped/uncapped living chain end concentration at equilibrium.

Living polymerizations have provided the synthetic chemist with two particularly powerful tools for the design of polymer architectures: block copolymerization by sequential monomer addition and end-functionalization with suitable electrophiles (in anionic polymerization) or nucleophiles (in cationic polymerization) (1) for the synthesis of end-functionalized polymers. With the advent of living cationic polymerization of isobutylene (IB) (2), extensive studies have been directed on these two themes, due to potential commercial importance (3). The applicability of block

¹Permanent address: Central Research Institute for Chemistry of the Hungarian Academy of Sciences, Pusztaszeri u. 59-67, P.O. Box 17, H-1525 Budapest, Hungary

²Corresponding author

copolymerization by sequential monomer addition from the polyisobutylene (PIB) living end however has been limited to monomers with similar reactivity. Up until recently, success also remained limited in the synthesis of end-functionalized PIB by in-situ functionalization of the living chain end, ascribed to the very low concentration of active species, i.e., the cations, in a fast equilibrium with the dormant PIB-Cl.

Recent success in the synthesis of functionalized PIBs with quantitative functionality and of block copolymers with high structural integrity is based on the applications of non-(homo)polymerizable monomers such as 1,1-diphenylethylene (DPE) and 1,1-di-*p*-tolylethylene (DTE) in carbocationic macromolecular engineering (4-13). These processes involve the intermediate capping reaction of living PIB with DPE or its derivatives. The resulting stable and fully ionized carbenium ions have been successfully employed for the quantitative end-functionalization of living PIB (4,5) with soft nucleophiles such as silyl ketene acetals and the controlled initiation of the second monomers such as *p*-methyl styrene (7), α -methyl styrene (8), isobutyl vinyl ether (9) and methyl vinyl ether (10).

Although the versatility of using DPE and its derivatives was successfully demonstrated, our knowledge of the kinetics and mechanism remains limited. Earlier experiments conducted to determine the efficacy of DPE in living IB polymerization were limited to -80°C / $\text{CH}_3\text{Cl}:\text{hexanes}$ (or $\text{CH}_3\text{Cl}:\text{methylcyclohexane}$) 40:60 (v:v) / TiCl_4 systems (4,5). Expanding the applicability of end-capping technique in living IB polymerization, it was found that the reaction of living PIB with DPE is a reversible reaction, sensitive to temperature (13). For this reason, it was of crucial importance to generate mechanistic understanding and reliable kinetic information essential to achieve the total control over the variables such as solvent polarity, temperature, Lewis acidity and aromatic substituents of DPE. Herein are reported the effects of these variables on the capping-decapping equilibrium.

Experimental

Materials. 1,1-Di-(*p*-chlorophenyl)ethylene (DiClDPE) was synthesized according to the literature (14). 1-*p*-chlorophenyl-1-phenylethylene (MCIDPE) was prepared by the Grignard reaction of 4-chlorobenzophenone (Fluka) with methylmagnesium bromide (Aldrich), followed by dehydration of the resulting carbinol with a catalytic amount of acid. 1,1-di-*p*-tolylethylene (DTE) was prepared using procedures analogous to those reported by Anschutz and Hilbert (15). All other solvents and chemicals were purified as described previously (4,5) or used as received.

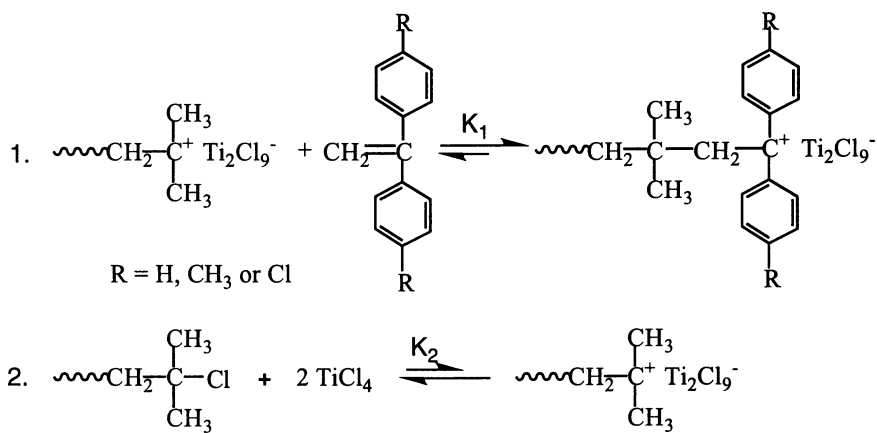
Polymerization, Capping, and Decapping Reaction. For the sake of analytical convenience by ^1H NMR, PIB with low molecular weight ($M_n \sim 1000$) were prepared by the 2,4,4-trimethyl-2-chloro-pentane (TMPCl)/ TiCl_4 /hexane:methyl chloride (Hex:MeCl) 60:40 (v:v)/ -80°C system in the presence of 2,6-di-*tert*-butylpyridine (DTBP) as a proton trap. Details for the polymerization of IB and the capping reaction have been described (5). PIB with diphenyl-methoxy functionality (PIB-DPE-OMe) was prepared by the procedure previously reported (5). PIB with ditolyl-methoxy functionality (PIB-DTE-OMe) was also prepared by the same procedure. For the study of decapping reaction, the stock solution of PIB-DPE-OMe (or PIB-DTE-OMe), prepared in Hex, was imparted to 75 mL test tubes and to these was added

DTBP stock solution, prepared in Hex, followed by MeCl to reach the desired Hex:MeCl ratio. At -80°C , TiCl_4 stock solution, prepared in Hex:MeCl solvent mixture, was added. The reaction was quenched with prechilled methanol (MeOH) after predetermined time intervals. The degree of capping was determined by ^1H NMR analysis.

Measurements. Conductivity measurements were carried out using a YSI Model 35 conductance meter equipped with a cell of 0.1 cm^{-1} cell constant and a BBC Goertz Metrawatt SE 120 plotter. ^1H NMR analysis was carried out by a Bruker 250 MHz spectrometer.

Results and Discussion

Capping Reaction of Living PIB with 1,1-Diarylethylenes. Capping reactions of living PIB with a series of diarylethylenes were first investigated at a constant temperature of -80°C . The results in the capping reaction of living PIB with two equivalents of 1,1-diarylethylenes are given in Table I. General schemes for the capping reaction and ionization of living PIB are given in Scheme 1.



Scheme 1

The equilibrium constant of the capping reaction of living PIB with DPE is given by

$$K_1 = \frac{k_c}{k_d} = \frac{[\text{PIBDPE}^+\text{Ti}_2\text{Cl}_9^-]}{[\text{PIB}^+\text{Ti}_2\text{Cl}_9^-] [\text{DPE}]} \quad (1)$$

The equilibrium constant of ionization of PIBCl is given by

$$K_2 = \frac{[\text{PIB}^+\text{Ti}_2\text{Cl}_9^-]}{[\text{PIBCl}] [\text{TiCl}_4]^2} \quad (2)$$

From the product of the two equilibrium constants, $K_1K_2=K_e$ (equation 3), the

Table I. Capping reaction of Living PIB with DPE and its derivatives at -80 °C^a

capping agent	reaction time, hr	solvent Hex:MeCl	capping efficiency ^b ,%	K _e , M ⁻³
DiClDPE	6	60:40	32	1.2 x 10 ⁵
MCIDPE	6	60:40	88	3.3 x 10 ⁶
MCIDPE	2	40:60	~100	-
DPE	1.25	60:40	~100	-
DPE ^c	3	60:40	91	8.6 x 10 ⁶
DTE	0.5	60:40	~100	-

^a Reaction conditions: [PIBCl]₀ ~ 0.002 M, [DTBP]₀ = 0.004 M, [TiCl₄] = 0.036 M and [capping agent] = 0.004M. ^b Determined after reaching limiting conductivity. ^c Reaction conditions: [PIBCl]₀ ~ 0.004 M, [DTBP]₀ = 0.004 M, [TiCl₄] = 0.026 M and [DPE] = 0.008M.

capped/uncapped ratio can be determined by K₁, K₂ and the equilibrium concentrations of the Lewis acid and DPE since [PIB⁺Ti₂Cl₉⁻] or [PIB⁺BCl₄⁻] << [PIBCl].

$$K_e = K_1 K_2 = \frac{[\text{PIBDPE}^+ \text{Ti}_2 \text{Cl}_9^-]}{[\text{PIBCl}]} \frac{1}{[\text{TiCl}_4]^2 [\text{DPE}]} \quad (3)$$

Equilibrium constants, K_e, in Table I were calculated from the capping efficiency measured by ¹H NMR analysis and from the equilibrium concentrations of Lewis acid and DPE. Capping reaction was paralleled with conductivity measurement. Figure 1 shows the corrected conductivity (κ-κ₀) vs. time plots during the capping reactions. As anticipated, under identical reaction conditions, substituted DPEs exhibited extremely large differences in reactivity depending on the substituents. With DiClDPE which has two *p*-chloro (i.e., electron withdrawing) substituents, limiting conductivity was reached after 6 hr of capping reaction. From ¹H NMR analysis of the product quenched after 6 hr, 32 % of maximum capping efficiency was obtained. The results with MCIDPE, which has one *p*-chloro substituent, are indicative of the significant effects of substituents and solvent polarity on the capping reaction. By substituting one chloro group in DiClDPE with hydrogen, the maximum capping efficiency was increased up to 88 % under the same reaction conditions and ~100 % of capping efficiency was obtained in 2 hr of reaction time by increasing solvent polarity from Hex:MeCl 60:40 (v:v) to Hex:MeCl 40:60 (v:v). While, in Hex:MeCl 60:40 (v:v) using the normal concentrations listed in Table I, virtually quantitative capping was observed with DPE, with different concentrations of reactants capping was not complete due to lower concentration of TiCl₄ and K_e could be obtained from the equilibrium capped/uncapped ratio. On the addition of DTE to living PIB solution, the reaction mixture exhibited a dark-red color and the conductivity increased instantaneously, reaching its limiting value in 10 minutes. From the ¹H NMR spectrum of the product obtained after 10 min, the characteristic resonance peaks of

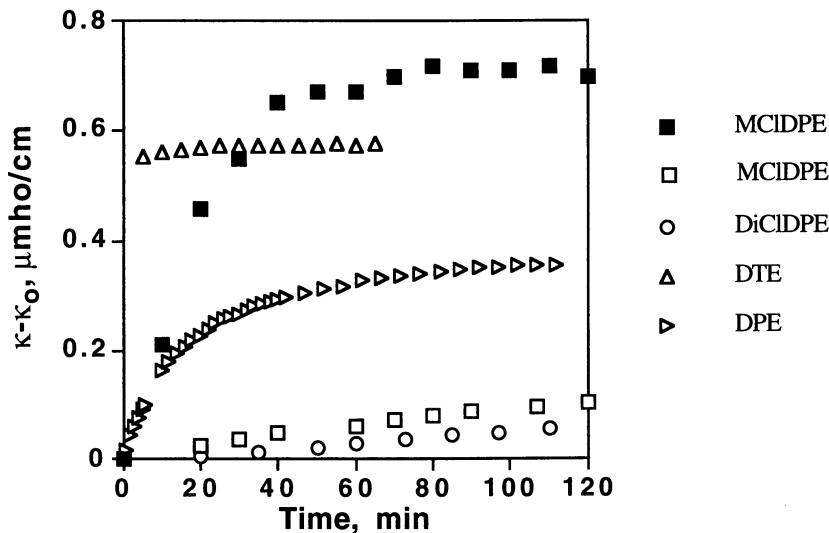


Figure 1. The corrected conductivity ($\kappa - \kappa_0$) vs time plot of the reaction mixtures in the capping reaction at -80°C . $[\text{P}(\text{B}(\text{C})\text{I})]_0 \sim 0.002\text{M}$ (or $[\text{TMPCl}]_0 = 0.0020\text{M}$ in the case of DiCIDPE), $[\text{TiCl}_4]_0 = 0.036\text{M}$, $[\text{DTBP}] = 0.0030\text{M}$ (open symbols Hex:MeCl 60:40 (v:v), solid symbols Hex:MeCl 40:60 (v:v)).

the *tert*-Cl end groups ($\text{PIB}-\text{CH}_2-\text{C}(\text{CH}_3)-\text{Cl}$) were absent indicating $\sim 100\%$ capping efficiency.

Decapping Reactions of PIB-DPE-OMe and PIB-DTE-OMe. If capping is an equilibrium reaction, the same equilibrium capped/uncapped ratio should be obtained from both directions. That is, upon mixing an isolated 100% capped PIB-DPE-Cl with TiCl_4 decapping should take place until the equilibrium $\text{PIBDPE}^+/\text{P}(\text{B}(\text{C})\text{I})$ is reached. Since PIB-DPE-Cl is unstable at room temperature the corresponding methoxy derivatives were used. We postulated that upon mixing with TiCl_4 the following reaction takes place:



A similar reaction was assumed to take place with PIB-DTE-OMe. The equilibrium concentrations of the PIB that remained capped was measured by ^1H NMR spectroscopy and used to calculate the equilibrium constant (K_e of equation 3) at several temperatures. The results of selected experiments are shown in Table II.

Reassuringly, using DPE at -80°C similar K_e was obtained from capping ($K_e = 8.6 \times 10^6$, in Table I) and from decapping of PIB-DPE-OMe ($K_e = 7 \times 10^6$, in Table II). K_e decreased about four orders of magnitude by increasing the temperature to -40°C . The equilibrium constants obtained in the more polar medium of Hex:MeCl 40:60 (v:v) are about two fold higher compared to that obtained in Hex:MeCl 60:40 (v:v), independently of temperature. Capping reaction of living PIB with DPE was extremely sluggish and low capping efficiency was obtained when BCl_3 was used in

Table II. The equilibrium capping efficiency (%), K_e (in terms of M^{-3} for $TiCl_4$ and M^{-2} for BCl_3)^a, and ΔS (J/mol⁰K)

capped PIB	Lewis acid	solvent Hex:MeCl	temp., °C	capping efficiency, %	K_e	ΔS
PIB-DPE-OMe	$TiCl_4$	60:40	-40	4.8 ^b	8.0×10^2	-301
			-60	10.4	6.0×10^4	-298
			-80	75.7	7.0×10^6	-299
		40:60	-40	8.8 ^b	1.6×10^3	-304
			-60	15.1	9.7×10^4	-304
			-80	81.5	1.3×10^7	-305
PIB-DTE-OMe	BCl_3	60:40	-80	7.8	8.6×10^3	
	$TiCl_4$	60:40	-40	30.2	2.9×10^5	
			-80	~100	-	
		40:60	-80	~100	-	

^a Reaction conditions: $[DTBP] = 0.003$ M and $[PIB-DPE-OMe]_0 = [PIB-DTE-OMe]_0 = 0.002$ M. ^b Calculated by extrapolation.

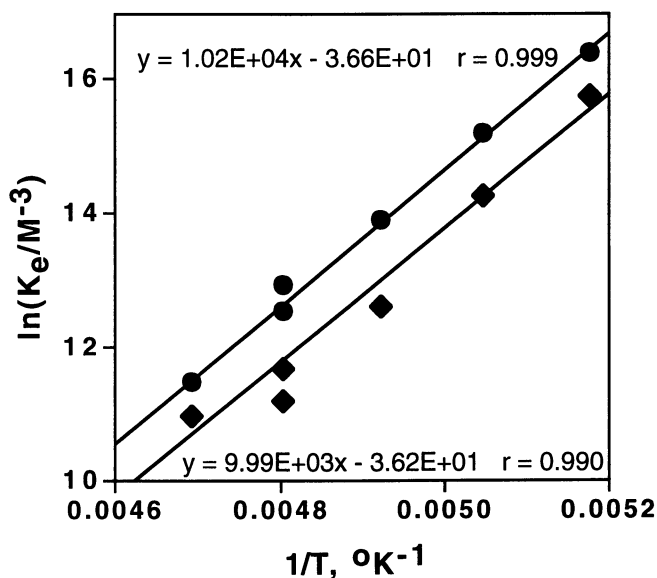


Figure 2. The Arrhenius plots of the equilibrium constants (K_e) of equation 3; $[PIB-DPE-OMe]_0 = 0.0020$ M, $[TiCl_4]_0 = 0.036$ M and $[DTBP] = 0.0030$ M (● Hex:MeCl 40:60 v:v, $\Delta H = -85.2$ kJ/mol (-20.4 kcal/mol); ◆ Hex:MeCl 60:40 v:v, $\Delta H = -83.1$ kJ/mol (-19.8 kcal/mol).

place of TiCl_4 . K_e can be obtained similarly for BCl_3 (however BCl_3 forms monomeric BCl_4^- gegen ions). The low K_e obtained for BCl_3 from the decapping experiments indicate that K_2 is extremely low. Thus the nature of Lewis acid also affects the equilibrium.

The Arrhenius plots for TiCl_4 are shown in Figure 2. In accord with the results of capping reactions, higher K_e was obtained at lower temperature, at higher solvent polarity, and for better stabilized diphenylcarbenium ions. For DPE, ΔH was calculated to be -85.2 (-20.4kcal/mol) (Hex:MeCl, 40:60, v:v), and 83.1 kJ/mol (-19.8kcal/mol) (Hex:MeCl, 60:40, v:v). It is interesting to note that it is about 10 kcal/mol higher than the π - σ transition and this is attributed to the energy gain due to ionization of the chain end (versus covalent PIB-Cl). This also explains the effect of solvent polarity. When DPE is substituted ΔH (and K_e) should be higher when the substituents (e.g. -Me) stabilize the cation and lower when the substituent (e.g. -Cl) produces a less stable cation.

The entropy change is about $-300\text{kJ/mol}^\circ\text{K}$ in all cases. This value is the combined ΔS of at least two reactions. The number of moles decreases in both the capping reaction and in the reaction of PIBCl with the TiCl_4 which explains the decrease in the entropy. A further decrease occurs as a strained chemical bond forms in the capping reaction. Nonetheless, the change in the enthalpy is high enough to compensate for that entropy decrease and the free enthalpy of the system decreases.

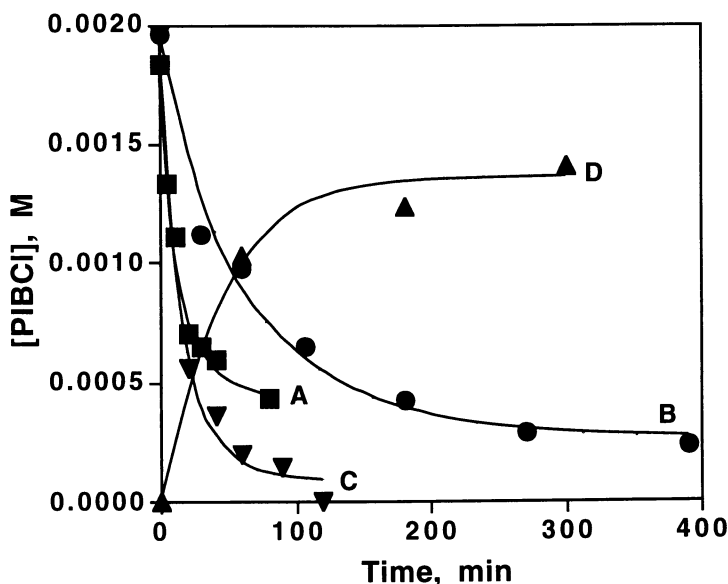
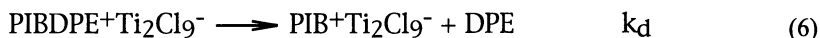
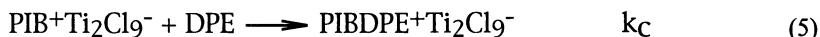


Figure 3. The experimental (symbols) and the calculated (solid line) values of $[\text{PIBCl}]$ plotted against the reaction time. For experimental details see Table III.

For the kinetical treatment of the capping-decapping reactions a simplified scheme was constructed. It was assumed that $[\text{TiCl}_4]$ is constant and considered the following two reactions:



After solving the corresponding differential equation $[\text{PIBCl}]$ is obtained as a function of time (equation 11), from which $k_c K_2$ and k_d can be calculated. The details are shown in the Appendix. $k_c K_2$ and k_d were calculated from four groups of data. The experimental and the calculated values of $[\text{PIBCl}]$ are plotted against time in Figure 3. As Figure 3 shows the equation satisfactorily describes $[\text{PIBCl}] = f(\text{time})$. The reaction conditions and the constants are listed in Table III.

Using Equation 11 one can calculate the equilibrium constant if the values of equilibrium concentrations are not available. The equilibrium constants calculated with the two different methods i.e., calculated by equation 11 or from the equilibrium concentrations using Equation 3 are in good agreement in the experiments B and D. In the case of experiment A however, higher K_e was obtained from the equilibrium concentrations. This is most probably the result of higher experimental errors due to very low decapping rate.

Table III. Rate constants and equilibrium constants in the capping and decapping reactions^a

exp.	temp., °C	solvent Hex:MeCl	capping agent (conc.)	$k_c K_2$, $\text{M}^{-3}\text{s}^{-1}$	k_d , s^{-1}	K_e^b, K_e^c , M^{-3}	M^{-3}
A	-80	60:40	DPE (0.002M)	430	1.2×10^{-6}	3.5×10^6	7.0×10^6
B			MCIDPE (0.0039M)	60.5	2.4×10^{-5}	2.5×10^6	3.3×10^6
C		40:60	MCIDPE (0.0039M)	278	3.0×10^{-5}	9.3×10^6	-
D ^d	-65	40:60	DPE	62.5	2.0×10^{-4}	3.1×10^5	2.9×10^5

^a Reaction conditions: $[\text{TiCl}_4] = 0.0364 \text{ M}$, $[\text{PIBCl}]_0 = 0.002 \text{ M}$ and $[\text{DTBP}] = 0.003 \text{ M}$.

^b Calculated by equation 11 ($K_e = k_c K_2 / k_d$). ^c Calculated from the equilibrium concentrations using equation 3. ^d Decapping

Acknowledgment. The authors gratefully acknowledge the National Science Foundation for financial support (DMR-9502777).

Appendix. Using equations 5 and 6, a differential equation for the time dependence of $[\text{PIBCl}]$ can be written as:

$$\frac{d([\text{PIBCl}] + [\text{PIB}^+\text{Ti}_2\text{Cl}_9^-])}{dt} = -k_c[\text{PIB}^+\text{Ti}_2\text{Cl}_9^-][\text{DPE}] + k_d[\text{PIBDPE}^+\text{Ti}_2\text{Cl}_9^-] \quad (7)$$

The stoichiometric relationships in capping and decapping reactions are

$$[\text{PIBCl}]_o - [\text{PIBCl}] = [\text{DPE}]_o - [\text{DPE}] \quad (8)$$

$$[\text{PIBCl}]_o - [\text{PIBCl}] = [\text{PIBDPE}^+\text{Ti}_2\text{Cl}_9^-] - [\text{PIBDPE}^+\text{Ti}_2\text{Cl}_9^-]_o \quad (9)$$

Using equations 2, 8 and 9, equation 7 can be rewritten as:

$$(1 + K_2[\text{TiCl}_4]^2) \frac{d[\text{PIBCl}]}{dt} = -k_c K_2 [\text{TiCl}_4]^2 [\text{PIBCl}] ([\text{DPE}]_o - [\text{PIBCl}]_o + [\text{PIBCl}]) + k_d ([\text{PIBCl}]_o + [\text{PIBDPE}^+\text{Ti}_2\text{Cl}_9^-]_o - [\text{PIBCl}]) \quad (10)$$

Since $[\text{PIBCl}^+\text{Ti}_2\text{Cl}_9^-] \ll [\text{PIBCl}]$ and therefore $K_2[\text{TiCl}_4]^2 \ll 1$ (see equation 2), the term $K_2[\text{TiCl}_4]^2$ on the left hand side of equation 10 can be neglected and equation 10 will have the form

$$\frac{d[\text{PIBCl}]}{dt} = -k_c K_2 [\text{TiCl}_4]^2 [\text{PIBCl}] ([\text{DPE}]_o - [\text{PIBCl}]_o + [\text{PIBCl}]) + k_d ([\text{PIBCl}]_o + [\text{PIBDPE}^+\text{Ti}_2\text{Cl}_9^-]_o - [\text{PIBCl}]) \quad (11)$$

Equation 11 can be solved since there is only one variable $[\text{PIBCl}]$. The solution is given in equation 12:

$$[\text{PIBCl}] = D \frac{[\text{DPE}]_o + [\text{PIBCl}]_o + A + 2D \tanh(k_c K_2 [\text{TiCl}_4]^2 Dt)}{2D + ([\text{DPE}]_o + [\text{PIBCl}]_o + A) \tanh(k_c K_2 [\text{TiCl}_4]^2 Dt)} - \frac{[\text{DPE}]_o - [\text{PIBCl}]_o + A}{2} \quad (12)$$

where

$$A = k_d / (k_c K_2 [\text{TiCl}_4]^2)$$

$$D = \left\{ \left(\frac{[\text{DPE}]_o - [\text{PIBCl}]_o + A}{2} \right)^2 + A ([\text{PIBDPE}^+\text{Ti}_2\text{Cl}_9^-]_o + [\text{PIBCl}]_o) \right\}^{1/2}$$

The parameters $k_c K_2$ and k_d can be obtained from Equation 12 when $[\text{PIBCl}]$ is known as a function of time. Using the stoichiometric relations, $[\text{DPE}]$ and $[\text{PIBDPE}^+\text{Ti}_2\text{Cl}_9^-]$ can be calculated as well.

Literature Cited

- (1) Webster, O. W. *Science* **1991**, *251*, 887.
- (2) Faust, R.; Kennedy, J. P. *Polym. Bull.* **1986**, *15*, 317.
- (3) Kennedy, J. P.; Ivan, B. *Designed Polymers by Carbocationic Macromolecular Engineering*; Hanser: Munich, 1991.

- (4) Fodor, Zs.; Hadjikyriacou, S.; Li, D.; Faust, R. *Polym. Prepr. (Am. Chem. Soc., Div. Polym. Chem.)* **1994**, 35(2), 492.
- (5) Hadjikyriacou, S.; Fodor, Zs.; Faust, R. *J. Macromol. Sci., Pure Appl. Chem.* **1995**, A32(6), 1137.
- (6) Takacs, A.; Faust, R. *Macromolecules* **1995**, 28, 7266.
- (7) Fodor, Zs.; Faust, R. *J. Macromol. Sci., Pure Appl. Chem.* **1994**, A31(12), 1985.
- (8) Li, D.; Faust, R. *Macromolecules* **1995**, 28, 1383.
- (9) Hadjikyriacou, S.; Faust, R. *Macromolecules* **1995**, 28, 7893.
- (10) Hadjikyriacou, S.; Faust, R. *Macromolecules* **1996**, 29, 5261.
- (11) Fodor, Zs.; Faust, R. *J. Macromol. Sci., Pure Appl. Chem.* **1995**, A32(3), 575.
- (12) Li, D.; Faust, R. *Macromolecules* **1995**, 28, 4893.
- (13) Li, D.; Hadjikyriacou, S.; Faust, R. *Macromolecules* in press.
- (14) Grummitt, O.; Buck, O.; Baker, A. C. *J. Am. Chem. Soc.* **1945**, 67, 2265.
- (15) Anschutz, R.; Hilbert, A. *Chem. Ber.* **1924**, 57, 1697.
- (16) Myer, H.; Schneider, R.; Schade, C. *Makromol. Chem., Macromol. Symp.* **1988** 13/14, 43.

Chapter 15

Multiarm Star Polyisobutylenes

Polyisobutylene Arms Connected to a Cyclosiloxane Core

Naoki Omura^{1,3}, Alexander V. Lubnin², and Joseph P. Kennedy^{1,4}

¹Maurice Morton Institute of Polymer Science, University of Akron,
Akron, OH 44325-3909

²BFGoodrich Company, 9921 Brecksville Road, Brecksville, OH 44141-3289

The synthesis and characterization of novel multi-arm stars comprising polyisobutylene (PIB) arms connected to various cyclo-siloxane cores are described. The syntheses have been achieved by hydrosilating allyl- or isopropenyl-capped PIB with cyclosiloxanes carrying 6 or 8 Si-H groups. The products were characterized by ¹H and ¹³C-NMR spectroscopy and GPC equipped with refractive index and laser light scattering detectors. The stars with close to the expected structures can be obtained under carefully controlled polymerization conditions. Traces of water in the charge may give higher-order stars by star-star coupling, however, this byproduct can be eliminated by the use of allyl-capped PIB and/or high [C=C]/[Si-H] ratios.

Key words: Star polymers, star-shaped polymers, secondary stars, octopus molecules, polyisobutylene, allyl endgroups, isopropenyl endgroups, hydrogensiloxanes, hydrogencyclosiloxanes, silicones, hydrosilation, hexachloroplatinic acid, NMR spectroscopy, GPC, light scattering.

³Permanent address: Shin-Etsu Chemical Company, Limited, Silicone-Electronics Materials Research Center, 1-10 Hitomi Matsuida Usui Gunma 379-02, Japan

⁴Corresponding author

NOTE: This article is part four of a series. For part three of this series of publications, see T. Marsalko, I. Majoros, and J. P. Kennedy, in *Macromol. Symp.*, **107**, 319 (1996).

In the course of our fundamental studies concerning novel multi-arm stars [1, 2], we became interested in the possibility of assembling architectures consisting of multiple PIB arms connected to a well-defined cyclosiloxane core. Recently, we have gained considerable experience in working with PIB stars having a crosslinked and therefore difficult-to-characterize aromatic (i.e., polydivinylbenzene) core [1], however, have not yet explored the potentialities offered by readily characterizable siloxane cores.

The PIB-based stars with polydivinylbenzene cores [1,2] are still being evaluated and tested, particularly in regard to their potential application as motor oil additives. In the latter field shear stability is of critical importance. In view of the demonstrated superior shear stability of silicone oils over hydrocarbon oils [3], siloxane cores appeared to be of particular interest; for example, in an aircraft gear pump, the viscosity of a silicone oil decreased less than 2 % after 105000 cycles, whereas, that of a petroleum oil dropped more than 50% after only 18000 cycles [3].

We theorized that the synthesis of the target PIB-arm cyclosiloxane-core stars could be accomplished in two steps: 1) Preparation of olefin (allyl or isopropenyl)-terminated PIB-prearms of desired molecular weights, followed by 2) Linking these PIB prearms by hydrosilation to well-defined cyclic siloxanes containing a desirable number of Si-H functions. According to recent literature, both steps are efficient: Allyl- or isopropenyl-ended PIBs have been prepared by living polymerization of isobutylene to practically any lengths [4] followed by quantitative end-functionalization to the $-\text{CH}_2\text{CH}=\text{CH}_2$ [5] or $-\text{CH}_2\text{C}(\text{CH}_3)=\text{CH}_2$ [6] terminus; hydrosilation was also demonstrated to be a quantitative reaction [7, 8]. Fig. 1 shows the structure of the siloxane fragments and molecules employed in these studies together with their abbreviations, and Scheme 1 helps to visualize the synthetic strategy to the target stars.

One of the great advantages of the D_6H and T_8H cores over those of polydivinylbenzene cores is that the formers are individual well-defined cyclic compounds and thus should yield relatively simple core architectures. In contrast, polydivinylbenzene cores are complex networks whose detailed structural characterization is well-nigh impossible.

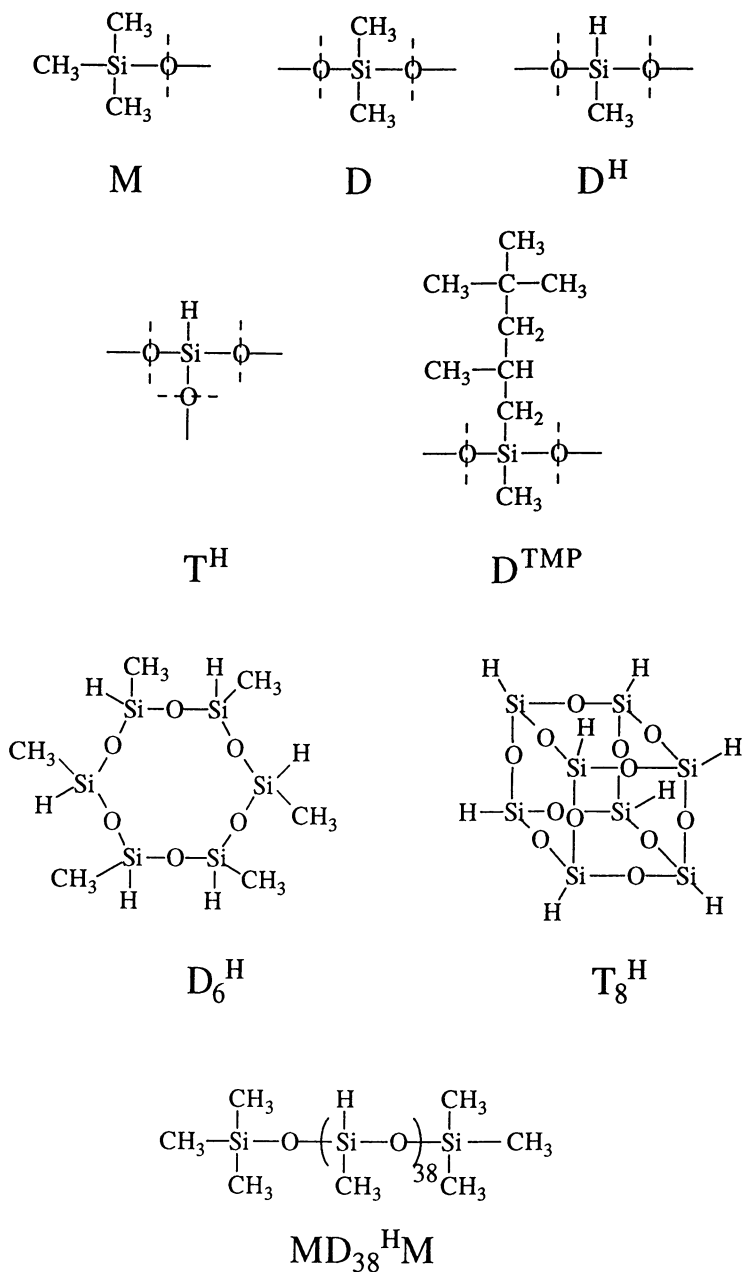
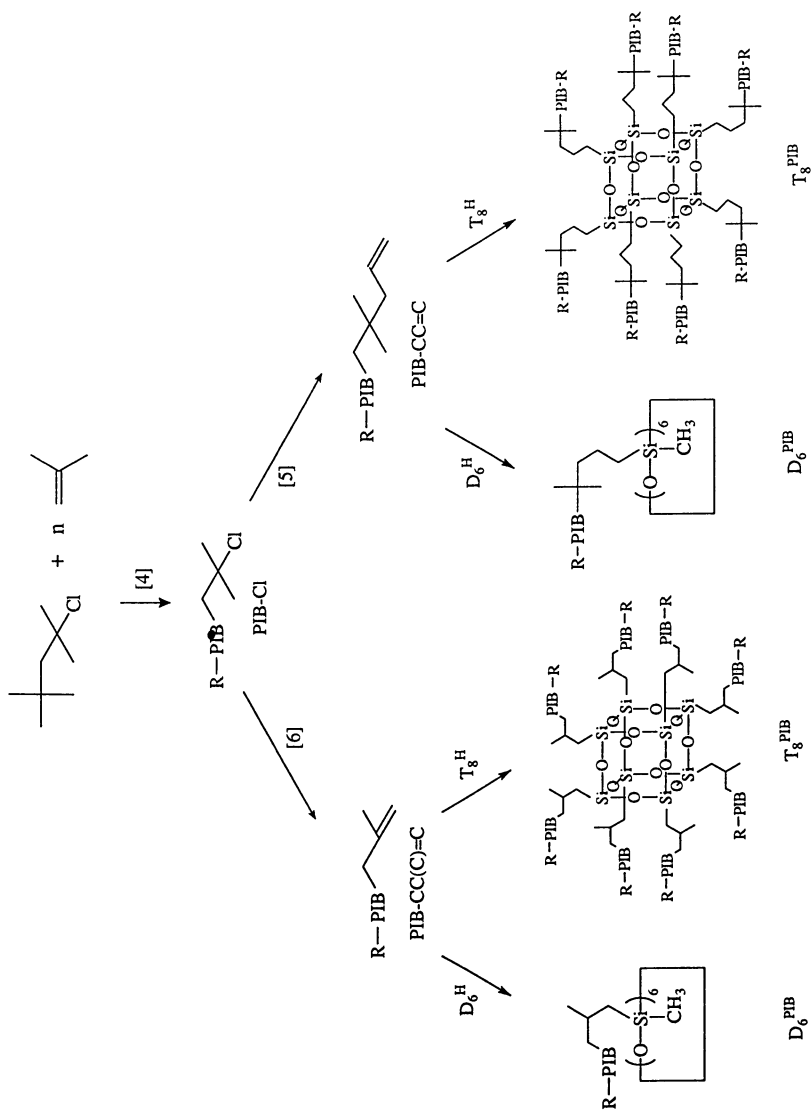
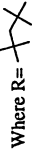


FIG 1. Structures and abbreviations of siloxane fragments and compounds used.



Where R =  residue, i.e., the 2,4,4-trimethylpentyl group

SCHEME 1. Outline of Synthesis Strategies.

Experimental

Materials. 2,4,4-Trimethyl-1-pentene (TMP) (Aldrich) was distilled from CaH_2 (Aldrich) before use. Benzene, toluene, SiHCl_3 , MeSiHCl_2 , FeCl_3 (anhydrous), and activated carbon were from Aldrich; *tert*-butanol, methanol, hexanes, Na_2CO_3 , MgSO_4 were from Fisher and used as received. Poly(methylhydrogensiloxane) MD₃₈HM (where 38 is the number average degree of polymerization) and H_2PtCl_6 catalyst solutions in toluene (0.5 wt.% Pt) are received from Shin-Etsu Chemical Co., Ltd and used as received.

Syntheses of starting materials. *Hexamethylcyclododecylsiloxane* (D_6H), *Dodecamethylcyclododecylsiloxane* (D_{12}H) was distilled from the mixture polymethylcyclododecylsiloxane (D_nH , $n=5,6,7,8,9,\dots$, Product name: X-92-154) received from Shin-Etsu Chemical Co., Ltd. Mixture of siloxanes was distilled under reduced pressure on a spinning band column (Nester/Faust, 75 theoretical plates). a fraction of bp 168°C , $37^\circ\text{C}/30,50$ mm Hg (compare with bp $92.6\text{--}93^\circ\text{C}/21$ mm Hg [10]) was collected. Yield = 11.1 g (12.4%). GC analysis showed this fraction to be essentially pure D_6H (>98 %). another fraction The product was stored over CaH_2 in a capped polypropylene test tube. $^1\text{H-NMR}$ (CDCl_3): $\delta = 0.19$ (s, 3H in Si-CH_3); 4.80 (s, 1H in Si-H).

Hydrogenoctasilsesquioxane (T_8H) was prepared by the hydrolysis of 26.6 g trichlorosilane [11]. The pure product (1.24 g, 12.0% yield) was obtained as colorless needles by recrystallization from hexanes solution. $^1\text{H-NMR}$ (CDCl_3): $\delta = 4.23$, $^1J_{\text{H,Si}} = 170$ Hz.

Model Compounds. D_6TMP . A mixture of 1.08 g (9.6 mmol) TMP, 0.29 g (0.80 mmol) D_6H , and $3.3 \mu\text{L}$ H_2PtCl_6 solution of a 2 wt.% Pt in 2-ethylhexanol was stirred at 70°C for 16 h. The $^1\text{H-NMR}$ spectrum indicated complete consumption of Si-H (absence of signal at 4.8 ppm). The solution was treated with 1 mg activated carbon to remove the catalyst and filtered. Excess TMP was removed in vacuo to yield a viscous liquid. $^1\text{H-}$

NMR (CDCl₃): δ = 0.10 (s, 3H, Si-CH₃); 0.37-0.75 (m, 2H, Si-CH₂); 0.87 (s, 9H, 3CH₃ in *t*Bu group); 0.95 (d, 3J = 6.8 Hz, 3H, CH₃ in CH₃-CH<); 1.09-1.38 (m, 2H, CH₂ in *t*Bu-CH₂); 1.70-1.88 (m, 1H, CH in CH₃-CH<). ¹³C-NMR (CDCl₃): δ = 1.3 (Si-CH₃); 25.5 (CH in CH₃-CH<); 25.6 (CH₃ in CH₃-CH<); 29.6 (CH₂ in CH₂-Si); 30.4 (3CH₃ in *t*Bu); 31.3 (C in *t*Bu); 55.2 (CH₂ in *t*Bu-CH₂-).

MD₃₈^{TMP}M was synthesized by the same procedure as D₆^{TMP}. ¹H-NMR (CDCl₃): δ = 0.09 (s, 3H, Si-CH₃); 0.38-0.78 (m, 2H, Si-CH₂-); 0.88 (s, 9H, 3CH₃ in *t*Bu); 0.97 (d, 3J = 6.0 Hz, 3H, CH₃ in CH₃-CH<); 1.04-1.32 (m, 2H, CH₂ in *t*Bu-CH₂-); 1.74 (m, 1H, CH in CH₃-CH<). ¹³C-NMR (CDCl₃): δ = 1.3 (Si-CH₃); 25.5 (CH in CH₃-CH<); 25.6 (CH₃ in CH₃-CH<); 29.6 (CH₂ in -CH₂-Si); 30.4 (3CH₃ in *t*Bu); 31.3 (C in *t*Bu); 55.2 (CH₂ in *t*Bu-CH₂-).

T₈^{TMP}. The above procedure was also used to obtain T₈^{TMP}. TMP was used in 2.5 molar excess and the reaction was carried out for 40 h. Product was a viscous liquid. ¹H-NMR (CDCl₃): δ = 0.46-0.75 (m, 2H, Si-CH₂-); 0.87 (s, 9H, 3CH₃ in *t*Bu); 0.97 (d, 3J = 6.6 Hz, 3H, CH₃ in CH₃-CH<); 1.09-1.38 (m, 2H, CH₂ in *t*Bu-CH₂-); 1.70-1.88 (m, 1H, CH in CH₃-CH<). ¹³C-NMR (CDCl₃): δ = 23.5 (CH₂ in -CH₂-Si); 24.9 (CH in CH₃-CH<); 25.7 (CH₃ in CH₃-CH<); 30.6 (3CH₃ in *t*Bu); 31.2 (C in *t*Bu); 53.9 (CH₂ in *t*Bu-CH₂-).

Polymerizations. The synthesis of the olefin-ended PIB starting materials are outlined in Scheme 1. α -*tert*-Butyl- ω -allyl-polyisobutylenes (PIB-CC=C) were prepared by a one-pot two-step method. First, chlorine-terminated PIBs (PIB-Cl) were obtained by using the 2-chloro-2,4,4-trimethylpentane/TiCl₄/N,N-dimethylacetamide system [4]. After completion of polymerizations, the living polymers were quenched *in situ* by a 10-fold excess of allyltrimethylsilane (AllSiMe₃) [5]. α -*tert*-Butyl- ω -isopropenyl-polyisobutylenes (PIB-CC(C)=C) were obtained by dehydrochlorination of PIB-Cl [6]. The products were characterized by ¹H-NMR spectroscopy and GPC.

Syntheses of Star Polymers. Typical procedures used for the preparation of star polymers follow.

D₆^{PIB}. PIB-CC=C (0.62 g, \overline{M}_n = 12300 g/mol), D₆^H (3.0 mg, 0.0083 mmol), and 15 μ L H₂PtCl₆ solution (0.5 wt.% Pt) in toluene were mixed in a vial, transferred into a dry ampule,

and sealed under vacuum. The ampule was placed in an oven at 180°C for 3 days.

T₈PIB. T₈H (2.7 mg, 0.0063 mmol) was ground in an agate mortar by a pestle in the presence of PIB-CC=C (0.62 g, $\overline{M}_n = 12300$ g/mol), Then 15 μ L H₂PtCl₆ solution (0.5 wt.% Pt) in toluene was added, and the mixture was transferred into a dry ampule. The ampule was sealed under vacuum and placed in the oven at 180°C for 3 days.

The viscous PIB prearms ($\overline{M}_n = 19,200$ g/mol) used for the preparation of relatively high molecular weight stars were diluted with a small amount of cyclopentane to facilitate stirring. Before sealing the ampules, most of the solvent was removed in vacuo.

Procedures. *Prearms.* The number and weight average molecular weights (\overline{M}_n and \overline{M}_w) and molecular weight dispersities ($\overline{M}_w/\overline{M}_n$) of the PIB prearms were determined by a GPC instrument (Waters) equipped with a series of five μ -Styragel columns (100, 500, 10³, 10⁴, 10⁵ Å, Waters), and a refractive index (RI) detector (Waters 410 Differential Refractometer, operating with Nelson Analytical Interfaces). Calibration and other details of the procedure have been described [1].

Stars. The number and weight average molecular weight (\overline{M}_n and \overline{M}_w) and dispersities ($\overline{M}_w/\overline{M}_n$, star) of stars were obtained by a laser light scattering (LLS) detector (Minidawn, Dawn F. Wyatt Technology Co.) in conjunction with an Optilab (Wyatt Technology Co.) instrument which provided dn/dc values, both attached to the GPC instrument. Astra software (version 4.00, Wyatt Technology Corp.) was used for data evaluation. The procedure has been described [1].

Very narrow molecular weight distributions of stars (less than ~1.2, see Table 2) allowed us to use calculated number average molecular weights from the primary weight average data. The number of arms were calculated as follows:

$$\overline{N}_n = \frac{\overline{M}_{n, \text{star}} - MW_{\text{core}}}{\overline{M}_{n, \text{arm}}}$$

where \overline{N}_n is the number average number of arms, $\overline{M}_{n, \text{star}}$ is the number average molecular weight of the star (calculated from \overline{M}_w), $\overline{M}_{n, \text{arm}}$ is the number average molecular weight of PIB prearms, and MW_{core} is the molecular weight of the well-defined silicone core. The number average numbers of arms can be directly correlated with the reaction stoichiometry.

NMR spectra were recorded by the use of a Varian Gemini-200 spectrometer using standard 5 mm tubes at ambient temperature. Sample concentrations for proton spectroscopy were ~50 mg/mL in CDCl_3 . Usually 64 FIDs were collected with 4 s repetition time for 15° pulses (6.7 μs); further spectroscopic details are given in Ref. [12].

Results and Discussion

Model Studies with TMP. The allyl endgroups in PIB-CC=C are relatively unencumbered, thus hydrosilation was expected to proceed rapidly and without significant steric hindrance [13]. In contrast, the isopropenyl termini in PIB-CC(C)=C are somewhat hindered and were therefore expected to have somewhat lower reactivity. Satisfactory hydrosilation conditions were established with this intermediate by carrying out hydrosilation model experiments with TMP which mimics the isopropenyl termini in PIB-CC(C)=C.

Table 1 summarizes the findings and shows the rate of disappearance of the Si-H groups (as determined by $^1\text{H-NMR}$ spectroscopy) for the three siloxanes studied. Fig. 2 shows a representative spectrum of a charge and gives experimental details. The conversions of Si-H groups were determined after removing excess TMP and comparing the integrated intensity of the Si-H signals at ~4.8 ppm (4.1 ppm in case of T_8H) with that of the *t*-butyl group signal at ~0.9 ppm. Conversions were calculated by:

$$\text{Conversion} = \frac{I_{0.9/9}}{I_{0.9/9} + I_{4.8}} 100\%$$

where $I_{0.9}$ and $I_{4.8}$ are the integrated intensities of the Si-H and $(\text{CH}_3)_3\text{C}$ signals, respectively.

Close to quantitative conversions were obtained with all

Table 1. Hydrosilation of TMP by D₆H, MD₃₈H^M, and T₈H.¹⁾

Time h	Conversion of Si-H, %		
	D ₆ H	MD ₃₈ H ^M	T ₈ H
1	90	88	69
2	91	91	70
4	92	92	76
8	94	90	83
16	95	92	90

¹⁾ 70°C, [Pt] = 16 ppm, 980 mg TMP, 20 mg siloxane. The low siloxane concentration was due to the limited solubility of T₈H in TMP. All mixtures were homogeneous.

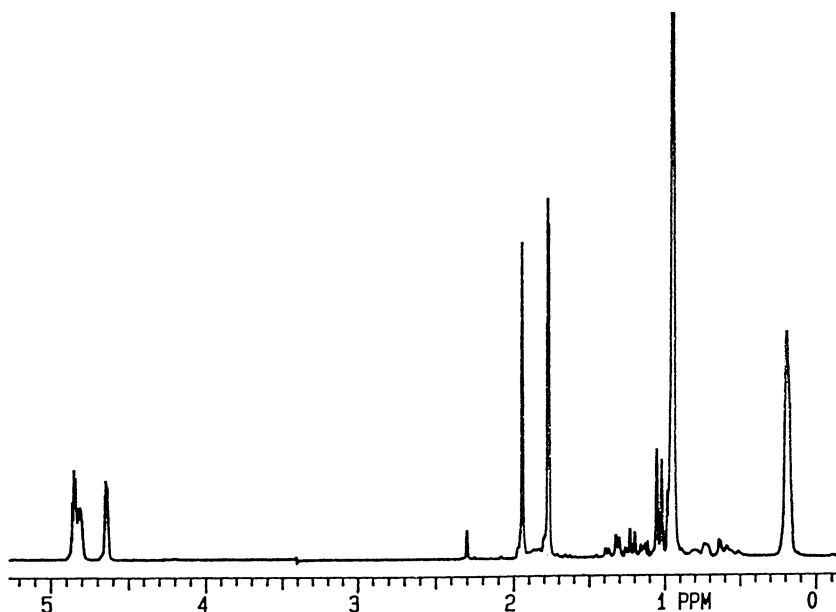


FIG. 2. ¹H-NMR (200 MHz) spectrum of the reaction mixture of D₆H plus TMP ([Si-H]/[C=C] = 1, [Pt] = 16 ppm) after 2 hours at room temperature. For assignments, see Experimental. Methyl protons of toluene (solvent for catalyst) at 2.3 ppm were used to reference the spectrum.

three hydrosiloxanes even under the mild conditions employed. The rates of hydrosilation with D_6H and $MD_{38}HM$ were essentially identical, while T_8H was found to be somewhat less reactive which may be due to the steric hindrance and rigidity of the T_8H skeleton.

According to these data, hydrosilation of TMP occurs readily and yields essentially quantitative conversions. In view of these encouraging results, we proceeded to study the syntheses of the target star polymers.

Stars with Multiple PIB Arms Emanating from Cyclic Siloxane Cores. Table 2 summarizes critical information needed to obtain N_n , the average number of arms of our stars. The first three columns show the number of the experiment (Run No.) and molecular characteristics of the olefin-ended PIB prearms (\overline{M}_n , $\overline{M}_w/\overline{M}_n$). The fourth column shows the molar ratio of the olefin endgroup (allyl or isopropenyl) relative to the Si-H groups in the synthesis charge. Column five gives the conversion of Si-H which was calculated from the ratio of product and remaining PIBs. Column six gives the number average molecular weight of the stars. Refractive index increments(dn/dc), which are necessary to calculate M_n , were measured for several linear and star PIBs and were found to be in the range of 0.112 - 0.119mL/g. The data in the sixth column shown in parentheses are "apparent" star molecular weights calculated from RI data using linear PIBs for calibration. The purpose of including these data in Table 2 is to show that, as expected, these "apparent" molecular weights are consistently lower than those obtained by LLS because of the highly branched structure of the stars. Column eight shows the dispersity of our stars obtained by LLS and the final column gives N_n calculated by the procedure described in Experimental.

The data are subdivided into four groups, i.e. the results obtained in the reaction with PIB-CC=C or PIB-CC(C)=C plus the six-functional cyclosiloxane D_6H (Runs 1-4 and 5-6, respectively), and the same prearms plus the eight-functional T_8H (Runs 7-11 and 12-14, respectively).

As shown by the data in Run 1 together with the corresponding GPC trace (Fig. 3a), the PIB-CC=C + D_6H system yielded exclusively the expected star. The presence of the

Table 2. Synthesis and Characterization of Star Polymers with PIB Arms and Silicone Cores.¹⁾

Run No.	PIB prearms ²⁾		[C=C]/[Si-H] of Si-H (%)	Conversion (%)	PIB stars			
	\bar{M}_n g/mol	\bar{M}_w/\bar{M}_n			\bar{M}_n ³⁾ g/mol	(R ¹²⁾	\bar{M}_w/\bar{M}_n ³⁾	\bar{N}_n
D₆H + PIB-CC=C								
1	5200	1.23	1	78	26000	(24000)	1.05	4.9
2 ⁴⁾	12600	1.10	1	84	58000	(57000)	1.02	4.6
3	12600	1.10	2	~100	180000		1.16	17
4	19200	1.11	2	76	63000	(57000)	1.05	5.0
					91000	(84000)	1.19	4.7
D₆H + PIB-CC(C)=C								
5	670	1.19	1	63		(3400)	1.21 ⁵⁾	5.8 ⁶⁾
6 ⁷⁾	3800	1.06	1	45	15000	(14200)	1.02	3.9 (50%)
					56000	(35000)	1.19	15 (50%)
T₈H + PIB-CC=C								
7	5200	1.23	1	64	33000	(32000)	1.15	6.3
8 ⁴⁾	12600	1.10	1	84	59000	(60000)	1.08	4.7
					260000		1.10	21

94)	12600	1.10	2	~100	66000	(62000)	1.03	5.2
					230000		1.13	18
104)	19200	1.11	2	80	100000	(94000)	1.03	5.2
					250000		1.13	13
114,8)	19200	1.11	2	~100	91000	(102000)	1.05	4.7
					330000		1.20	17
T_gH + PIB-CC(C)=C								
12	670	1.19	1	61	4900	(4400)	1.20	6.7
134)	3800	1.06	1	25	18000	(23000)	1.01	4.6
					60000		1.45	16
144)	3800	1.06	2	51	23000	(22000)	1.01	6.0
					87000		1.22	23

- 1) Synthesis in bulk at 180°C, [Pt] = 100 ppm: 3 days for PIB-CC=C, 7 days for PIB-CC(C)=C.
- 2) Determined by refractive index detector, linear PIB standards for calibration.
- 3) Determined by laser light scattering (see Experimental).
- 4) GPC traces show a shoulder at high molecular weight (see for example, Figs. 4a and 5a). These shoulders are unresolved from the main peak by RI but separate by LLS.
- 5) By RI data.
- 6) Calculated from the ¹H-NMR spectrum by comparing integrated intensities of *tert*-butyl group and unreacted Si-H.
- 7) RI trace shows two separate peaks.
- 8) 2.5 mol water per 1 equivalent of Si-H was added.

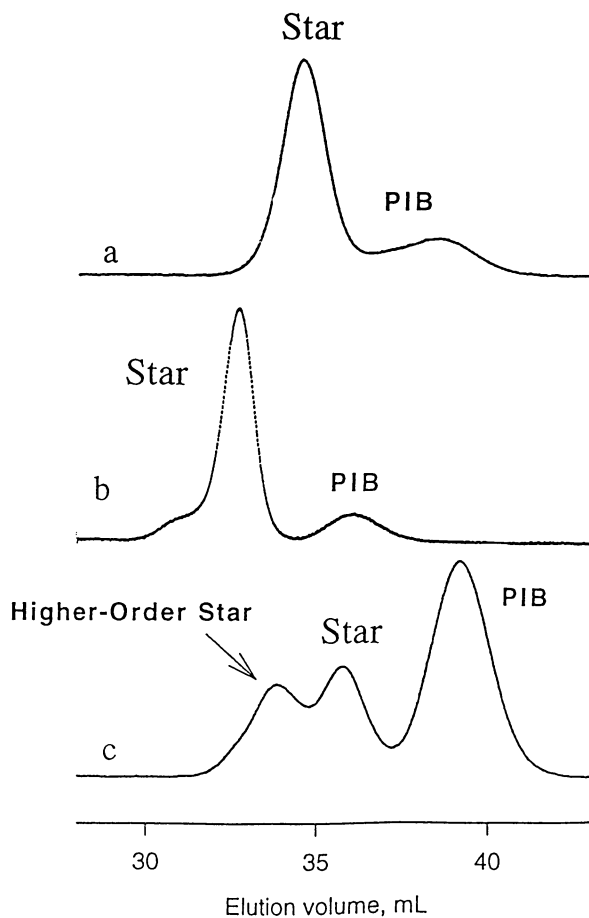
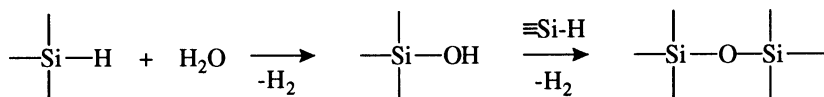


FIG. 3. GPC traces of the products obtained in: (a) - Run 1, (b) - Run 2, and (c) - Run 6 of Table 2.

small amount of unreacted PIB-CC=C (elution volume ~38 mL) indicated by the GPC trace of this product (Fig. 3a) suggests that the reaction must have slowed down at high conversions (i.e., when the concentration of the reacting species has strongly diminished).

When a relatively higher molecular weight prearm ($\overline{M}_n = 12600$ g/mol, Run 2) was used, the product contained the expected star ($\overline{M}_n = 59000$ g/mol) and a much higher molecular weight component ($\overline{M}_n \sim 260000$ g/mol) as evidenced by a distinct shoulder at lower elution counts in the RI trace (Run 2, Fig. 3b). The higher molecular weight component most likely arose by star-star coupling in the presence of adventitious water by the following reaction:



The Pt catalyst used for hydrosilation also accelerates this coupling reaction [8].

In the presence of PIB-CC(C)=C, the amount of unreacted starting olefin in the final product was much higher (~50%) than with the PIB-CC=C even though the molecular weight of the former was relatively low (Run 5). Evidently the methyl group adjacent to the unsaturation reduces the rate of hydrosilation. According to GPC evidence, star-star coupling also proceeds in this system (Run 6, Fig. 3c).

Experiments 7-14 (Table 2) were carried out with T_8^{H} . In contrast to hydrosilation with D_6^{H} (Runs 1-6) in which both PIB-CC=C and PIB-CC(C)=C readily gave the close to theoretical stars (Runs 1-5), the experiments with T_8^{H} yielded the star with significantly less than the expected 8 arms even with relatively low molecular weight prearms (Runs 7 and 12). With higher molecular weight PIB prearms (Runs 8-10) the number of arms of the primary stars was only 4.7-5.2 at 60-65% conversion of Si-H groups. These cyclic siloxanes mostly yielded higher than expected molecular weight stars probably by star-star coupling.

The proposition of star-star coupling was substantiated by two independent experiments:

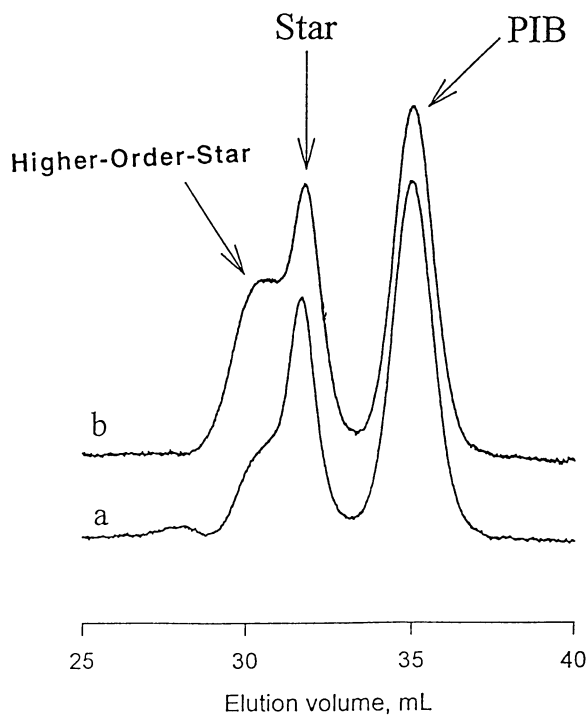


FIG. 4. GPC traces of the products obtained in: (a) - Run 10 and (b) - Run 11 (2.5-fold molar excess of water over Si-H) of Table 2.

1) An experiment in which H₂O was purposely added (specifically, 2.5 mole H₂O / Si-H) to the charge (Run 11). Under these conditions, the GPC trace of the product (shown in Fig. 4) clearly indicated the formation of significant amount of high molecular weight product.

2) An experiment in which the [C=C]/[Si-H] ratio was increased, in this case to 2.0 (i.e., to "outcompete" the parasitic reaction with H₂O); the formation of the high molecular weight product was completely eliminated even in the presence of relatively high molecular weight prearms (compare Runs 2 with Run 3, and Run 8 with Run 9 in Table 2; and Fig. 5).

Results obtained with the PIB + T₈^H systems correlate well with those of model experiments (see above): Thus the reaction between T₈^H plus TMP reached ~70% conversion within 1-2 hours, however, the rate significantly diminished after that (cf. Table 1).

It has been reported that in highly substituted aromatic compounds ("octopus molecules") steric interaction exists between the substituents (i.e, arms) due to their close proximity [14]. We hypothesize that the reason for the reduced reactivity of T₈^H we have observed could be due to such a steric hindrance at the rigid and compact T₈ core.

¹³C Relaxation Times. Carbon-13 spin-lattice relaxation time (¹³C T₁) is a sensitive tool for studying the segmental and overall dynamics of molecules ([12] and references therein). Thus we have measured ¹³C T₁'s for several purposefully synthesized model compounds.

A representative ¹³C-NMR spectrum of a multi-arm PIB is shown on Fig. 6. The signal assignments and the relaxation times are summarized in Schemes 2 and 3.

The T₁ of α-methylene carbon of T₈^{TMP} is significantly shorter than that in the open-chain MD₃₈^{TMPM} (0.20 and 0.31 s, respectively) indicating slower tumbling of this group in T₈^{TMP}. However, a two arm star, i.e., a product obtained by the reaction of two moles of PIB-CC(C)=C with one mole of T₈^H in which the T₈ core bears only two PIB arms (abbreviated by T₈^{HT₂PIB}) and has approximately the same molecular weight as

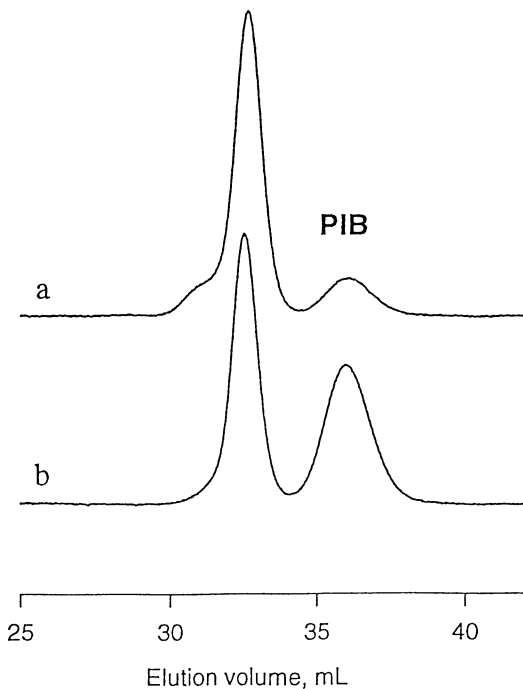


FIG. 5. GPC traces of star polymers obtained with PIB- $\text{CC}=\text{C}$ and T_8H : (a) - $[\text{C}=\text{C}]/[\text{Si}-\text{H}] = 1$ (Run 8, Table 2) and (b) - $[\text{C}=\text{C}]/[\text{Si}-\text{H}] = 2$ (Run 9, Table 2).

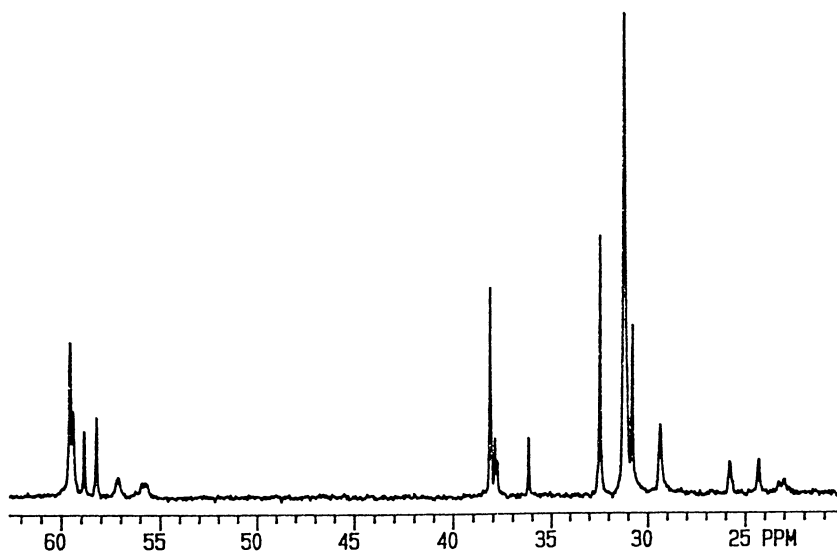
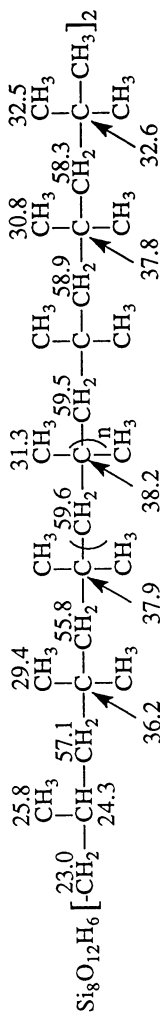
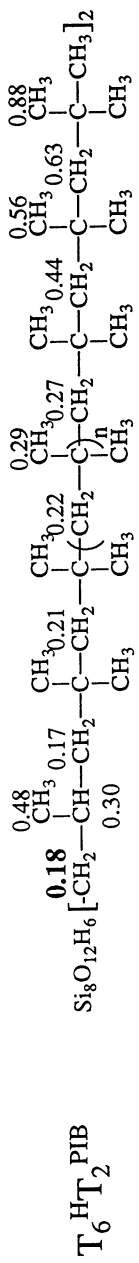
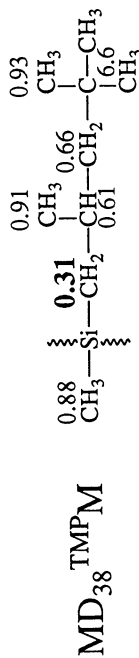


FIG. 6. ^{13}C -NMR (50.3 MHz) spectrum of $\text{T}_6\text{HT}_2\text{PIB}$. For assignment, see Scheme 2.



SCHEME 2. ^{13}C chemical shifts and assignments for $\text{T}_6\text{T}_2\text{PIB}$.



SCHEME 3 ^{13}C spin-lattice relaxation times for model compounds (50.3 MHz, 0.5 g in 0.5 mL CDCl_3).

T_8^{TMP} (ca. 1800 and 1323 g/mol, respectively), has practically the same ^{13}C T_1 of the α -methylene carbon (0.18 s) as that in T_8^{TMP} (0.20 s). This indicates that short ^{13}C T_1 's in T_8^{TMP} are due to the rigid silicone core rather than to steric compression between hydrocarbon branches. The same effect of the rigid fragment on ^{13}C T_1 's was also observed for isobutylene units next to an aromatic ring of initiator fragment incorporated in the chain of telechelic PIBs [12].

These studies indicate that, though the silicone core restricts the mobility of hydrocarbon arms, there is no evidence of steric interaction between the arms. Apparently there is enough room around T_8 to place eight TMP fragments, but after reaching ~70 % conversion of Si-H groups (5-6 arms), the access of the bulky catalytic complex to the unreacted Si-H functions groups becomes limited.

Conclusions

This investigation has demonstrated that star-shaped polyisobutylenes with well-defined siloxane cores can be synthesized by linking the olefin-capped (allyl or isopropenyl) PIB arms with multifunctional hydrogencyclosiloxanes via hydrosilation. The existence of star architecture was demonstrated by model experiments, LLS studies, and NMR spectroscopy.

Allyl-terminated PIBs prearms give well defined star polymers whereas isopropenyl terminated PIBs produce higher order coupled stars as well. In the presence of adventitious traces of water higher order star polymers may arise.

^{13}C relaxation time studies indicate that though the rigid T_8 silicone core restricts the mobility of hydrocarbon arms, there is no evidence of steric interaction between the arms.

Acknowledgement

This material is based upon work partly supported by the National Science Foundation under Grant DMR-94-23202 and by Shin-Etsu Chemical Co., Ltd., Japan, Shin-Etsu Silicones of America, Inc., and Shincor Silicones, Inc.

Literature Cited

- [1] T. M. Marsalkó, I. Majoros, and J. P. Kennedy, *Polym. Bull.*, **31**, 665 (1993).
- [2] J. P. Kennedy, T. M. Marsalkó, and I. Majoros, U.S. Patent No. 5,395,885 (1995).
- [3] V. G. Fitzsimmons, D. L. Pickett, R. O. Militz, and W. A. Zisman, *Trans. ASME*, **68**, 361 (1946).
- [4] G. Kaszas, J. E. Puskas, J. P. Kennedy, and C. C. Chen, *J. Macromol. Sci.-Chem.*, **A26**, 1099 (1989).
- [5] L. Wilczek and J. P. Kennedy, *J. Polym. Sci.: Polym. Chem.*, **25**, 3255 (1987).
- [6] J. P. Kennedy, V. S. C. Chang, R. A. Smith, and B. Iván, *Polym. Bull.*, **1**, 575 (1979).
- [7] F. C. Whitmore, F. W. Pietrusza, and L. H. Sommer, *J. Am. Chem. Soc.*, **69**, 2108 (1947).
- [8] K. Itoh, "Silicone Handbook" (*In Japanese*), Nikkan Kogyo Shinbunshya: Tokyo, 1990, p. 23.
- [9] J. W. Curry, U.S. Patent No. 3484468 (1969).
- [10] V. Bazant, V. Chvalovsky, J. Rathousky, "Organosilicone Compounds", Academic Press: New York and London, 1965, Vol. 2(2), p. 512.
- [11] P. A. Agaskar, *Inorg. Chem.*, **30**, 2707 (1991).
- [12] A. V. Lubnin and J. P. Kennedy, *J. Macromol. Sci.-Pure Appl. Chem.*, **A32**, 191 (1995).
- [13] B. Marcinec, "Comprehensive Handbook on Hydrosilylation", Oxford, New York: Pergamon Press, 1992.
- [14] F. Vögtle and E. Weber, *Angew. Chem., Int. Ed.*, **13**, 814 (1974).

Chapter 16

Coupling Reaction of Living Polyisobutylene Using Bis(diphenylethenyl) Compounds as Coupling Agents

Young Cheol Bae, S. Coca¹, P. L. Canale, and Rudolf Faust²

Polymer Science Program, Department of Chemistry, University of Massachusetts Lowell, One University Avenue, Lowell, MA 01854

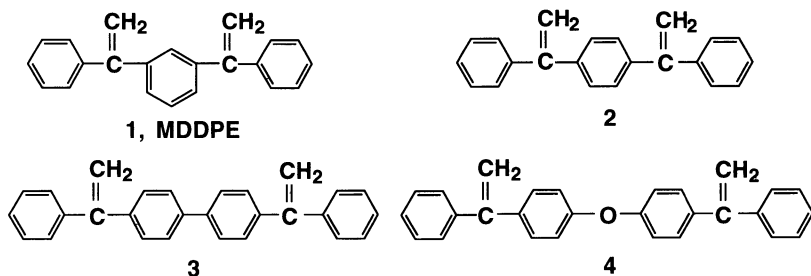
In-situ coupling reaction of living polyisobutylene (PIB), prepared by the 2,4,4-trimethyl-2-chloropentane/TiCl₄/hexane:methyl chloride (6:4, v:v)/-80 °C system, has been studied using 1,3-bis(1-phenylethenyl)benzene (MDDPE), 2,2-bis[4-(1-phenylethenyl)phenyl]propane (BDPEP), and 2,2-bis[4-(1-tolylolethenyl)phenyl]propane (BDTEP) as coupling agents. The reaction of living PIB with MDDPE yielded the monoadduct, possibly due to delocalization of positive charge over the *meta*-substituted benzene ring upon monoaddition and thereby decreased reactivity of the second double bond. Using BDPEP and BDTEP, rapid and quantitative coupling was achieved and the coupled product exhibited doubled molecular weight and narrowed molecular weight distribution. Direct evidence of the quantitative coupling reaction was also obtained by comparison of the ¹H NMR spectra of the samples before and after the coupling reaction. Kinetic studies by ¹H NMR spectroscopy indicated the coupling reaction of living PIB by BDPEP and BDTEP is a consecutive reaction where the second addition is faster than the first one. As a result, high coupling efficiency was also observed when excess BDPEP was used.

We recently introduced the foundation and methodology of using non(homo)polymerizable monomers, such as 1,1-diphenylethylene (DPE) and 1,1-ditolylethylene (DTE), in carbocationic macromolecular engineering (1-9). These processes involved the intermediate capping reaction of living polyisobutylene (PIB) with DPE or DTE, in the courses of quantitative end-functionalization of PIB (1,2), coupling reaction of two homopolymers prepared by different mechanisms (cationic and anionic) (3), and the clean synthesis of diblock (4-7) or triblock copolymers (8,9).

¹Current address: Department of Chemistry, Carnegie Mellon University, 4400 Fifth Avenue, Pittsburgh, PA 15213

²Corresponding author

As an extension of our recent efforts on the applications of non(homo)polymerizable monomers in carbocationic polymerization, it was conceived that bis-DPE compounds, which have two DPE moieties, could be useful as coupling agents for living PIB. In fact, this concept of coupling living polymers by bis- or double-DPE compounds has been reported in anionic polymerization (10-15). Tung et al. investigated the coupling reaction of *sec*-butyllithium or oligomeric poly(styryl)lithium with bis(1-phenylethenyl) compounds of *m*-phenylene (1), *p*-phenylene (2), *p,p'*-biphenyl (3), or *p,p'*-diphenyl ether (4) (10-12).



More recently, the full potential of coupling reaction of living poly(styryl)lithium by 1,3-bis(1-phenylethenyl)benzene (1 or *meta*-double DPE, MDDPE) was exploited by Quirk et al. in the preparation of star-block copolymers (13-15). In addition to this type of coupling reaction of living anionic polymers, the ability of stable polymeric carbanions to react with certain electrophilic species such as phosgene or dichlorodimethylsilane has rendered the coupling of living anionic diblocks a useful method for the preparation of ABA triblock copolymers where the quantitative crossover from monomer B to monomer A is unavailable (16,17). And also, multifunctional silicon halides have been utilized to prepare symmetrical or asymmetrical star block copolymers (18).

Although several coupling agents for living poly(vinyl ethers) and poly(α -methylstyrene) have been reported in cationic polymerization (19-21), quantitative coupling was limited to the living polymers with low molecular weight ($DP_n \sim 10$). No report has appeared in the literature on the quantitative coupling reaction of living PIB. Based on the recent successful applications of non(homo)polymerizable monomers, herein are reported the results in the coupling reaction of living PIB using bis-DPE compounds such as 2,2-bis[4-(1-phenylethenyl)phenyl]propane (or bis(diphenylethenyl)propane, BDPEP) and 2,2-bis[4-(1-tolylolethenyl)phenyl]propane (or bis(ditolylolethenyl)propane, BDTEP) as coupling agents.

Experimental

Materials. Dichloromethane was treated with portions of concentrated sulfuric acid, washed with water, 5% aqueous sodium bicarbonate then water again. It was pre-dried over calcium chloride, and distilled from calcium hydride before use. 2,2-diphenylpropane was purified by vacuum distillation. All other solvents and chemicals were purified as described previously (4-6) or used as received. MDDPE was synthesized using procedures reported by Schulz and Hocker (22).

2,2-Bis(4-acetylphenyl)propane (5). Acetyl chloride (25.43 g, 0.32 mol) was added dropwise into a suspension of AlCl_3 (45.20 g, 0.34 mol) in 100 mL of anhydrous dichloromethane under nitrogen atmosphere. To this stirred solution was added dropwise 21.22 g (0.11 mol) of 2,2-diphenylpropane in 50 mL of dichloromethane at 0°C. After the addition was complete, the mixture was allowed to warm to room temperature and stirred for 24 h. Dichloromethane was replenished and the temperature was increased until gentle reflux started. After 2 h of reflux, the reaction mixture was quenched by pouring the mixture over 300 g of crushed ice containing 50 mL of concentrated hydrochloric acid. The aqueous phase was extracted with portions of dichloromethane. The organic phase was washed with water, 10% aqueous sodium bicarbonate solution and then water again until neutral. It was dried over magnesium sulfate and the solvent was evaporated to yield a dark-red viscous oil. **5** was separated from the resulting dark red viscous oil by "hot extraction" with portions of hexane in a water bath at 60 °C. Hexane layers were collected, reduced and allowed to crystallize. Recrystallization from hexane/ethanol (95/5, v/v) yielded colorless scintillating platelets. Mp: 63.6-65.2 °C; Yield: 47%; ^1H NMR (CDCl_3 , TMS): δ 1.75 (s, 6H, $-\text{C}(\text{CH}_3)_2-$), 2.60 (s, 6H, $-\text{C}(=\text{O})\text{CH}_3$), 7.32 (m, 4H, Ar-H), 7.89 (m, 4H, Ar-H).

2,2-Bis[4-(1-phenylethenyl)phenyl]propane(BDPEP). Phenylmagnesium bromide (3 M in diethyl ether, Aldrich; 26.67 mL, 0.08 mol) was added dropwise to the stirred solution of **5** (5.42 g, 0.02 mol) in 200 mL of diethyl ether under nitrogen atmosphere at -4 °C. After the addition was complete, the mixture was allowed to warm to room temperature and stirred overnight. The reaction mixture was then hydrolyzed by pouring over a mixture of 10 g of ammonium chloride and 100 g of crushed ice. The aqueous phase was extracted three times with 100 mL of diethyl ether. The combined organic phase was washed with water, 5% aqueous sodium bicarbonate solution and then water again until neutral and dried over magnesium sulfate. The resulting yellowish-viscous dicarbinol, without further purification, was used for dehydration according to the literature (23). The crude BDPEP was obtained as yellowish-viscous oil and purified by flash chromatography using a 5 cm x 20 cm of 130-270 Å silica gel (Aldrich) column using hexane as an eluent. The colorless effluent was collected, reduced and allowed to crystallize to yield a white solid. Recrystallization from ethanol yielded colorless scintillating platelets. Mp: 79.1-80.6 °C; Yield: 80%; ^1H NMR (CDCl_3 , TMS): δ 1.75 (s, 6H, $-\text{C}(\text{CH}_3)_2-$), 5.44 and 5.50 (d, 4H, $=\text{CH}_2$), 7.23 (m, 14H, Ar-H).

2,2-Bis[4-(1-tolylenyl)phenyl]propane (BDTEP). BDTEP was synthesized by the Grignard reaction of **5** with *p*-tolylmagnesium bromide and subsequently by dehydration of the resulting dicarbinol with a catalytic amount of phosphoric acid in *p*-xylene. The overall procedure and reaction conditions were similar to those employed for the synthesis of BDPEP. Recrystallization from ethanol/acetone (95/5, v/v) yielded colorless scintillating platelets. Mp: 96.5-96.8 °C; Yield: 81.2%; ^1H NMR (CDCl_3 , TMS): δ 1.75 (s, 6H, $-\text{C}(\text{CH}_3)_2-$), 2.40 (s, 6H, Ar- CH_3), 5.41 and 5.44 (d, 4H, $=\text{CH}_2$), 7.16 (m, 14H, Ar-H).

Polymerization and Coupling Reaction. Polymerizations were carried out in a three-neck flask equipped with an overhead stirrer at -80 °C under a dry ($[\text{H}_2\text{O}] < 1.0$

ppm) nitrogen atmosphere in an MBraun 150-M glovebox (Innovative Technology Inc.). A hexane (Hex) stock solution containing 2-chloro-2,4,4-trimethylpentane (TMPCl), as an initiator, and 2,6-di-*tert*-butylpyridine (DTBP), as a proton trap, was prepared and charged to the flask followed by the addition of methyl chloride (MeCl) at -80 °C. Then TiCl₄ (dissolved in Hex with TiCl₄/Hex = 1/3 (v/v)) was added. Isobutylene (IB) was introduced to the flask 10 min after the addition of TiCl₄. The following polymerization conditions were employed except when specified: [TMPCl] = 0.002 M, [TiCl₄] = 0.036 M, [IB] = 0.04 M, and [DTBP] = 0.003 M; in Hex:MeCl (60:40, v:v) at -80 °C. After 1 h of polymerization (~100% conversion), a portion of the reaction mixture was withdrawn from the flask and quenched with prechilled methanol for molecular weight measurement of the original PIB. Coupling reactions were effected by adding a stoichiometric amount of coupling agent dissolved in Hex/MeCl=5/5 (v/v) at -80 °C. At predetermined time intervals, aliquots of the reaction mixture were withdrawn and quenched with prechilled methanol inside the glovebox and poured over excess 10% ammoniacal methanol outside of the glovebox to preserve diarylmethoxy functionality. The purification procedure of the product has already been reported (4-6).

Characterization. Molecular weights were measured using a Waters HPLC system equipped with Model 510 HPLC pump, Model 410 differential refractometer, Model 486 tunable UV/vis detector, Model 250 viscometer (Viscotek), on-line multiangle laser light scattering (MALLS) detector (Wyatt Technology Inc.), Model 712 sample processor, and five Ultrastaygel GPC columns connected in the following series: 500, 10³, 10⁴, 10⁵ and 100 Å. The flow rate of THF was 1.0 mL/min. ¹H NMR spectroscopy for structural analysis was carried out by a Bruker 250 MHz spectrometer.

Results and Discussion

Coupling Reaction of Living PIB by MDDPE. Our initial interest was focused on MDDPE, since the efficacy of this compound as a coupling agent in anionic polymerization has already been reported (11-15). The coupling reaction of living PIB by MDDPE was carried out by adding a stoichiometric amount ([MDDPE]/[living PIB] = 0.5) of MDDPE to the reactor at ~100% IB conversion. Just before the addition of MDDPE, a portion of reaction mixture was withdrawn from the reactor to characterize the molecular weight of the original PIB. After the addition of MDDPE solution, a dark-red color gradually developed in minutes, indicating relatively slow formation of diarylalkylcarbenium ions. During the reaction, aliquots of the reaction mixture were withdrawn at predetermined time intervals, quenched with prechilled methanol, and analyzed by GPC to monitor the progress of the coupling reaction. A summary of the reaction of living PIB with MDDPE is given in Table I. Even after a 2 h reaction time (no. 5 in Table I), there is no appreciable increase in the molecular weight of the product. GPC traces of all products showed monomodal distribution with identical molecular weight distribution reflecting the absence of coupling of living PIB by MDDPE. All products, however, became UV active, indicating monoaddition of living PIB to MDDPE. This monoaddition reaction was also confirmed by comparison of the ¹H NMR spectra of the original PIB-Cl, which exhibits characteristic

Table I. Reaction of Living PIB with MDDPE ^a

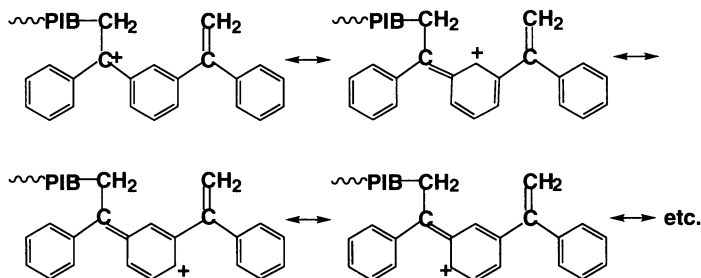
no.	reaction time, min	$10^{-3} M_n$	M_w/M_n	UV activity ^c
1 ^b	-	1.3	1.2	no
2	30	1.5	1.2	yes
3	60	1.5	1.2	yes
4	90	1.4	1.2	yes
5	120	1.4	1.2	yes

^aReaction condition: [MDDPE]/[living PIB] = 0.5. ^bOriginal PIB. ^cRecorded on a Waters 486 tunable absorbance detector at 254 nm.

proton resonances due to the methylene and methyl group with a *tert*-chlorine end (-CH₂-C(CH₃)₂-Cl) at δ = 1.66 and 1.92 ppm, respectively, and the resulting PIB. This exhibited characteristic resonance peaks for the terminal diphenylalkylmethoxy protons at δ = 3.0 ppm in addition to those characteristic peaks of the unreacted PIB.

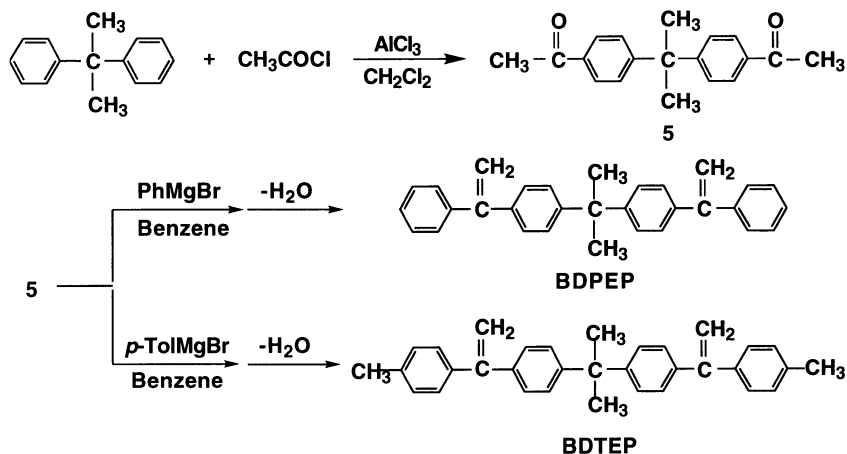
This monoaddition of living PIB to MDDPE could be explained in terms of the lower reactivity of the second double bond. Scheme 1 shows the resonance structures of the product upon monoaddition. The reactivity of the second double bond is reduced due to the electron deficient α -substituent, arising from the delocalization of positive charge over the two phenyl rings adjacent to the carbenium ion. In addition to this charge-delocalization effect, the relative steric hindrance of the second double bond might also contribute to its reduced reactivity.

Scheme1. Resonance Structures upon Monoaddition of Living PIB to MDDPE



Synthesis of Bis-DPE Compounds. In line with the result for MDDPE, we found that the reaction of living PIB with DPE is an equilibrium reaction and that this equilibrium is shifted toward the right or to completion by increasing the Lewis acidity, solvent polarity, electron-donating ability of *para*-substituents, or concentration of reactants such as DPE and Lewis acid or by decreasing the reaction temperature (24). Without affecting the living system, this can be accomplished by designing the structure of bis-DPE compounds which helps the possible equilibrium to shift to completion. It appears that, for the quantitative coupling of living PIB by bis-

Scheme 2. Synthesis of BDPEP and BDTEP

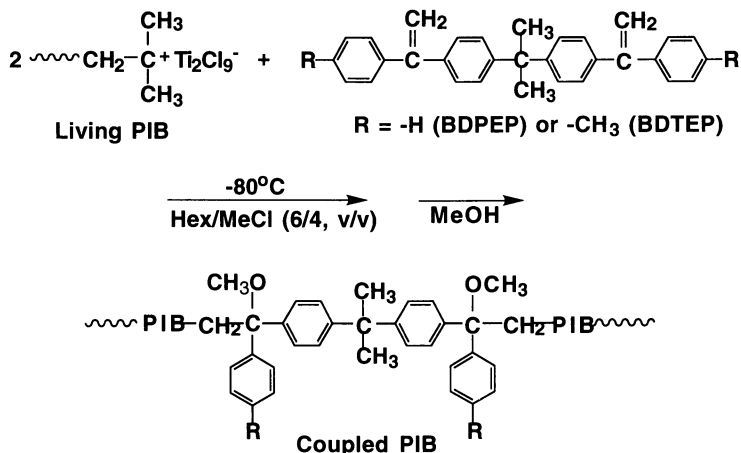


DPE compounds, the two DPE moieties should be separated by a spacer group which not only excludes the charge-delocalization effect but increases its electron-donating ability as *para*-substituent.

A potential candidate, 2,2-bis[4-(1-phenylethenyl) phenyl]propane (BDPEP), could be found in the work by Tung et al. (10,12). According to their reports, the synthesis of BDPEP was carried out by Friedel-Crafts benzylation of 2,2-diphenylpropane, followed by Wittig olefination of the resulting diketone. The final product, a brownish-viscous oil, was ~ 90% pure by GC, however. We undertook the synthesis and succeeded in the clean synthesis of this compound by modifying their procedure as shown in Scheme 2. First, **5** was prepared by Friedel-Crafts acylation of 2,2-diphenylpropane with acetyl chloride. The crude **5** has a tendency to separate as an oil, but after extraction with hexane in a water bath at 60 °C (impurities are less soluble in nonpolar solvent), it can be obtained as a solid in good yield (> 47%) with defined physical property (Mp: 63.6-65.2). This process seems more flexible, since the resulting diketone, **5**, can be converted to various bis-DPE derivatives by selecting appropriate Grignard reagents. Dicarbinols were prepared by the Grignard reaction of **5** with phenylmagnesium bromide or *p*-tolylmagnesium bromide. Finally, BDPEP and BDTEP were obtained by dehydration of the resulting dicarbinols according to the procedure reported by Rosser and Neville (23). Both BDPEP and BDTEP were obtained in excellent yield (> 80%) on the basis of **5**.

Coupling Reaction of Living PIB by Bis-DPE Compounds. The general scheme for the coupling reaction of living PIB by BDPEP or BDTEP is shown in Scheme 3. In the coupling reaction of living PIB by BDPEP, in which the two DPE moieties are separated by an electron-donating spacer group, the characteristic dark-red color of diarylalkylcarbenium ions developed instantaneously upon addition of BDPEP solution to the reactor at ~100% conversion of IB. The GPC RI traces of the original PIB (A) and the products (B and C) are shown in Figure 1. After 15 min of the coupling reaction, the GPC trace of the intermediate product (B) showed a significant

Scheme 3. Coupling Reaction of Living PIB by Bis-DPE Compounds



extent of coupling (> 50%) with a distinct bimodal distribution representing a mixture of the original PIB and the coupled product. After 3 h of the coupling reaction, the product (C) showed monomodal distribution with doubled molecular weight and narrowed molecular weight distribution. By comparison of the ^1H NMR spectra of the original PIB and the product, it was also confirmed that virtually quantitative coupling of living PIB was achieved by BDPEP.

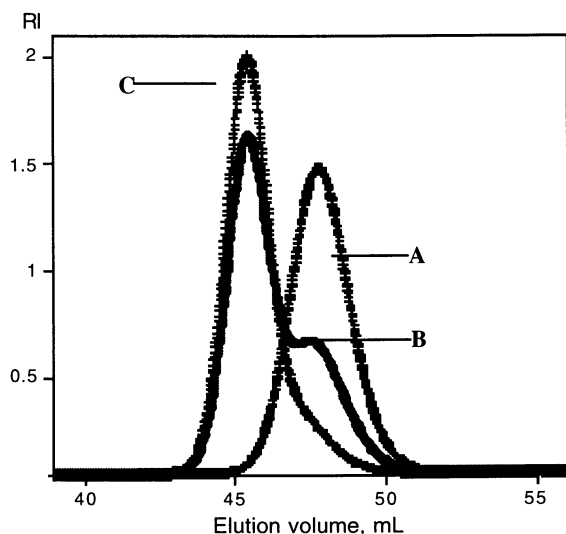


Figure 1. GPC RI traces of the original PIB (A) with $M_n = 1600$ and $M_w/M_n = 1.1$, the intermediate product (B) quenched after 15 min with $M_n = 2700$ and $M_w/M_n = 1.3$, and the coupled product (C) with $M_n = 3500$ and $M_w/M_n < 1.1$.

In the original PIB (or PIB-Cl, A in Figure 2), the terminal *tert*-chlorine exerts a strong electron-withdrawing effect on the vicinal methyl and methylene groups and shifts the resonances of these groups downfield. The proton resonances of the methyl and methylene groups in the main chain appear at 1.09 (peak b) and 1.40 ppm (peak d), respectively, while those of the terminal repeating unit directly attached to chlorine appear at $\delta = 1.66$ (peak f) and 1.92 ppm (peak g) and those of the penultimate unit appear at 1.16 (peak c) and 1.46 ppm (peak e). Those four characteristic peaks (c, e, f, and g) of the original PIB were completely absent from the product which was quenched after a 3 hr coupling reaction (B in Figure 2), whereas new peaks characteristic of PIB capped with DPE units (h, i, j, and k) appeared as assigned.

Using BDTEP as a coupling agent, the coupling reaction was more rapid than the corresponding reaction with BDPEP. As can be seen in Figure 3, GPC results indicate the coupling reaction was complete in 1.5 h. It has been known that the addition reaction of living PIB to DPE or its derivatives exhibits extremely large differences in reactivity depending on the aromatic substituents (24). Under the same solvent and concentration of reactants as the coupling reaction, the capping equilibrium constant (K_e) was found to be $8.0 \times 10^2 \text{ M}^{-3}$ in the reaction of living PIB with a stoichiometric amount of DPE at $-40 \text{ }^\circ\text{C}$. With DTE, this equilibrium constant was almost three orders of magnitude ($K_e = 2.9 \times 10^5 \text{ M}^{-3}$) higher, with a simultaneous increase in the rate of capping, under identical conditions. Thus a significant effect of stabilization of the resulting diarylalkylcarbenium ions by the electron-donating substituent is exhibited. Hence it is not surprising that BDTEP, which yields a more stable carbenium ion in the coupling reaction, is a more efficient coupling agent than BDPEP.

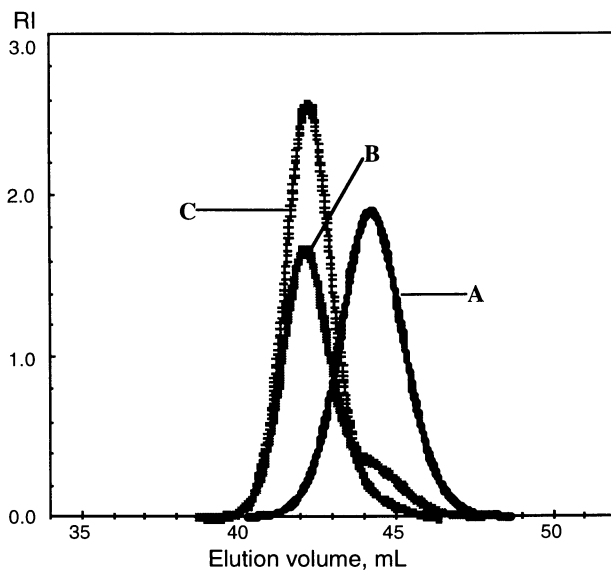


Figure 3. GPC RI traces of the original PIB (A) with $M_n = 2400$ and $M_w/M_n = 1.1$, the intermediate product (B) quenched after 15 min with $M_n = 4900$ and $M_w/M_n = 1.2$, and the coupled product (C) after 90 min with $M_n = 5200$ and $M_w/M_n < 1.1$.

Table II. Coupling Reaction of Living PIB with BDPEP

no.	reaction time, min	$10^{-3} M_n$		M_w/M_n	coupling efficiency, % ^a	unreacted PIB, % ^a	PIB-DPE ^b , % ^a
		¹ H NMR	GPC				
1 ^c	-	1.6	1.6	1.1	-	-	-
2	15	-	2.7	1.3	50.6	46.0	3.4
3	45	-	3.3	1.1	79.3	12.8	5.1
4	95	-	3.6	1.1	>95	~0	< 5
5	180	3.6	3.5	1.1	>98	~0	<2

^aBy ¹H NMR spectroscopy. ^bPIB-DPE: the monoadduct of PIB to BDPEP. ^cOriginal PIB.

Table III. Coupling Reaction of Living PIB with BDTEP

no.	reaction time, min	$10^{-3} M_n$		M_w/M_n	coupling efficiency, % ^a	unreacted PIB, % ^a	PIB-DTE ^b , % ^a
		¹ H NMR	GPC				
1 ^c	-	2.4	2.4	1.1	-	-	-
2	15	-	4.9	1.2	89	11	-
3	45	-	5.2	1.1	97	3	-
4	90	-	5.2	<1.1	~100	-	-
5	180	5.2	5.3	<1.1	~100	-	-

^aBy ¹H NMR spectroscopy. ^bPIB-DTE: the monoadduct of PIB to BDTEP. ^cOriginal PIB.

Kinetic studies of the addition of living PIB to a stoichiometric amount of bis-DPE compounds were also paralleled by ¹H NMR spectroscopy. The results with BDPEP and BDTEP are listed in Tables II and III, respectively. In Table II, it should be noted that the concentration of the monoadduct remains extremely low throughout the coupling reaction compared to that of unreacted PIB. It is evident that the addition of living PIB to BDPEP is a consecutive reaction where the second addition is faster than the first one. With BDTEP (Table III) the reaction was too fast to compare the relative amount of the unreacted PIB and the monoadduct, however. In order to prove the faster rate of the second addition, excess BDPEP was employed in the coupling reaction. Supporting our previous experimental results, a high coupling efficiency was also observed when excess BDPEP ($[\text{BDPEP}]/[\text{living PIB}] = 1$) was used. Interestingly, the GPC trace of the product was followed by that of unreacted BDPEP at ~53 mL of elution volume (D in Figure 4). This was also proved by recent kinetic studies (25) where the ratio of the rate constants of the first and second addition (k_1/k_2) was found to be 0.39 ± 0.02 . This indicates that the second addition is about 5 times faster than the first one.

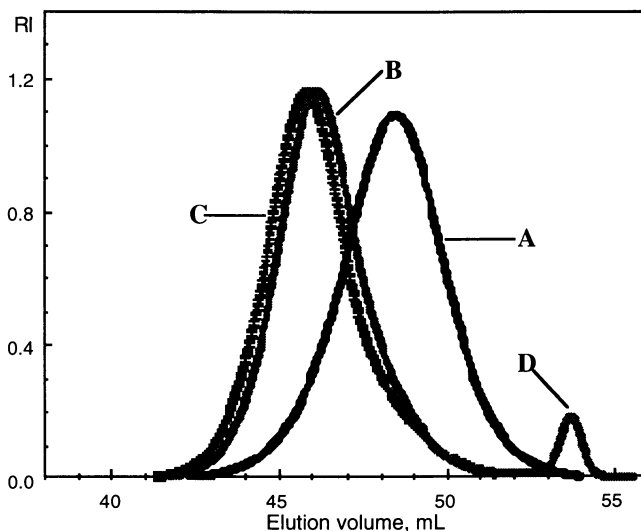
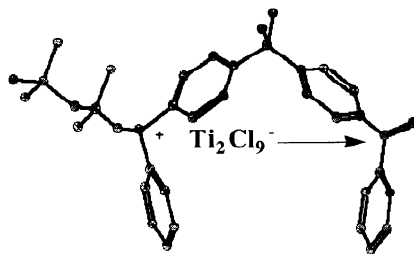


Figure 4. GPC RI traces of the original PIB (A) with $M_n = 1300$ and $M_w/M_n = 1.3$, the coupled product (B) with $M_n = 2800$ and $M_w/M_n = 1.2$ ($[\text{BDPEP}]/[\text{living PIB}] = 1$) and the coupled product (C) with $M_n = 3000$ and $M_w/M_n = 1.2$ ($[\text{BDPEP}]/[\text{living PIB}] = 0.5$). Polymerization conditions: $[\text{TMPCl}] = 0.005 \text{ M}$, $[\text{TiCl}_4] = 0.023 \text{ M}$, $[\text{DTBP}] = 0.003 \text{ M}$ and $[\text{IB}] = 0.09 \text{ M}$.

A similar observation was reported by McGrath et al. (26) in the coupling reaction of *sec*-butyllithium by MDDPE in cyclohexane. Their experimental results were consistent with the computer simulated plot for a consecutive reaction mechanism where the second rate constant was assumed to be an order of magnitude larger than the first rate, presumably due to chain association in nonpolar solvent. Since viscosity studies indicated that there is no chain end association in cationic polymerization of IB (27), this mechanism is not applicable to the anomalous addition behavior of living PIB to BDPEP. It would appear to be more germane to consider topological aspects of the bulky gegenion, Ti_2Cl_9^- , and the monoadduct of living PIB to BDPEP. The model to explain this hypothesis is shown below.



For simplicity the PIB segment has been replaced with the trimethylpentyl group (head group of PIB) and hydrogen atoms have been omitted. Stucky et al. reported the

adduct of $[\text{PCl}_4][\text{Ti}_2\text{Cl}_9]$ in the reaction of PCl_5 with TiCl_4 in SOCl_2 and the face-shared bioctahedral structure of Ti_2Cl_9^- by X-ray structural analysis (28). If a similar bulky structure could be applied to Ti_2Cl_9^- in the solution state, we can easily imagine the interaction between the bulky gegenion and the second double bond upon monoaddition. This interaction is expected to increase the electron density of the second double bond. Thereby, the second double bond will be activated, rendering the monoaddition rate-determining step. In order to prove this hypothesis, ab initio or semi-empirical molecular orbital calculations may be necessary.

Conclusions

The reaction of living PIB with MDDPE yielded the monoadduct, this can be attributed to the charge delocalization effect and steric hindrance of the second double bond. Clean synthesis of new types of bis-DPE compounds, such as BDPEP and BDTEP, has been achieved and successfully utilized in the coupling reaction of living PIB. Using BDPEP and BDTEP, rapid and quantitative coupling was accomplished for the first time. The rate of this coupling reaction is dependent on aromatic *para*-substituents of bis-DPE compounds; a faster rate was observed when the more stabilized carbenium ions were produced. The observed faster rate of second addition is proposed to involve the activation of the second double bond by the bulky inorganic gegenion, Ti_2Cl_9^- , upon monoaddition. Investigations of the versatility and limitations of bis-DPE derivatives in the living carbocationic polymerization are in progress.

Acknowledgment. The authors gratefully acknowledge the National Science Foundation for financial support (DMR-9502777). We are also grateful to Camille and Henry Dreyfus Foundation for funding the Model 250 viscometer (Viscotek).

Literature Cited

1. Fodor, Zs.; Hadjikyriacou, S.; Li, D.; Faust, R. *Polym. Prepr. (Am. Chem. Soc., Div. Polym. Chem.)* **1994**, 35 (2), 492.
2. Hadjikyriacou, S.; Fodor, Zs.; Faust, R. *J. Macromol. Sci., Pure Appl. Chem.* **1995**, A32 (6), 1137.
3. Takacs, A.; Faust, R. *Macromolecules* **1995**, 28, 7266.
4. Fodor, Zs.; Faust, R. *J. Macromol. Sci., Pure Appl. Chem.* **1994**, A31 (12), 1985.
5. Li, D.; Faust, R. *Macromolecules* **1995**, 28, 1383.
6. Hadjikyriacou, S.; Faust, R. *Macromolecules* **1995**, 28, 7893.
7. Hadjikyriacou, S.; Faust, R. *Macromolecules* **1996**, 29, 5261.
8. Fodor, Zs.; Faust, R. *J. Macromol. Sci., Pure Appl. Chem.* **1995**, A32 (3), 575.
9. Li, D.; Faust, R. *Macromolecules* **1995**, 28, 4893.
10. Tung, L. H.; Lo, G. Y.-S.; Beyer, D. E. *Macromolecules* **1978**, 11, 616; U.S. Patent 4,172,100, 1979.
11. Tung, L. H.; Lo, G. Y.-S. U.S. Patent 4,182,818, 1980; *Macromolecules* **1994**, 27, 1680.
12. Tung, L. H.; Lo, G. Y.-S.; Rakshys, J. W.; Beyer, D. E. U.S. Patent 4,205,016, 1980.
13. Quirk, R. P.; Hoover, F. I. In *Recent Advances in Anionic Polymerization*; Hogen-Esch, T. E., Smid, J., Eds.; Elsevier: New York, 1987; pp 393-401.

14. Quirk, R. P.; Yoo, T.; Lee, B. *J. Macromol. Sci., Pure Appl. Chem.* **1994**, *A31* (8), 911.
15. Quirk, R. P.; Yoo, T. *Polym. Prepr. (Am. Chem. Soc., Div. Polym. Chem.)* **1993**, *34* (2), 578.
16. Heller, J. G.; Schimsheimer, J. F.; Pasternak, R. A.; Kingsley, C. B.; Moacanin, J. *J. Polym. Sci., Polym. Chem. Ed.* **1969**, *7*, 73.
17. Morton, M.; Kammereck, R. F.; Fetters, L. *J. Macromolecules* **1971**, *4*, 11.
18. Iatrou, H.; Hadjichristidis, N. *Macromolecules* **1992**, *25*, 4649, and references therein.
19. Fukui, H.; Sawamoto, M.; Higashimura, T. *J. Polym. Sci., Part A: Polym. Chem.* **1993**, *31*, 1531.
20. Fukui, H.; Sawamoto, M.; Higashimura, T. *Macromolecules* **1993**, *26*, 7315.
21. Fukui, H.; Yoshihashi, S.; Sawamoto, M.; Higashimura, T. *Macromolecules* **1996**, *29*, 1862, and references therein.
22. Schulz, G. G. H.; Hocker, H. *Macromol. Chem.* **1977**, *178*, 2589.
23. Rosser, R. W.; Neville, R. G. *J. Appl. Polym. Sci.* **1969**, *13*, 215.
24. Bae, Y. C.; Fodor, Zs.; Faust, R. *Polym. Prepr. (Am. Chem. Soc., Div. Polym. Chem.)* **1996**, *37* (1), 801.
25. Bae, Y. C.; Fodor, Zs.; Faust, R. *Macromolecules* **1997**, in press.
26. Broske, A. D.; Huang, T. L.; Allen, R. D.; Hoover, J. M.; McGrath, J. E. In *Recent Advances in Anionic Polymerization*; Hogen-Esch, T. E., Smid, J., Eds.; Elsevier: New York, 1987; pp 363-380.
27. Gyor, M.; Faust, R. Unpublished results.
28. Kistenmacher, T. J.; Stucky, G. D. *Inorg. Chem.* **1971**, *10*, 122.

Author Index

- Bae, Young Cheol, 168,198
Basko, M., 41
Canale, P. L., 178
Cheradame, H., 135
Coca, S., 198
Crivello, J. V., 83
de Jong, Feike, 63
Faust, Rudolf, 168,198
Fodor, Zsolt, 168
Gandini, Alessandro, 113
Graafland, Teun, 63
Held, Daniela, 63
Ingrisch, Stefan, 151
Iván, Béla, 63
Kaluzynski, Krzysztof, 75
Kamigaito, Masami, 106
Katayama, Hiroshi, 106
Kennedy, Joseph P., 178
Kubisa, P., 41
Lai, Y.-L., 83
Lang, Gabriele, 25
Libiszowski, Jan, 75
Lubnin, Alexander V., 178
Malik, R., 83
Matyjaszewski, Krzysztof, 12
Mayr, Herbert, 25
Mohamed, F., 50
Moreau, M., 50
Müller, Axel H. E., 63
Nuyken, Oskar, 151
Oh, Saehoon, 151
Omura, Naoki, 178
Penczek, Stanislaw, 41,75
Pretula, Julia, 75
Randriamahefa, S., 135
Rissoan, G., 135
Roth, Michael, 25
Satoh, Kotaro, 106
Sawamoto, Mitsuo, 106
Shaffer, Timothy D., 1,96
Szymanski, Ryszard, 75
Vairon, J. P., 50
Yang, Yao-Hong, 113

Affiliation Index

- BFGoodrich Company, 178
Carnegie Mellon University, 12,198
Ecole Française de Papeterie et des
Industries Graphiques, 113
Exxon Chemical Company, 1,96
Kyoto University, 106
Ludwig-Maximilians-Universität, 25
Polish Academy of Sciences, 41,75
Rensselaer Polytechnic Institute, 83
Shell Research and Development
Centre, 63
Technische Universität München, 151
Université Pierre et Marie Curie, 50
University of Akron, 178
University of Evry, 135
University of Mainz, 63
University of Massachusetts Lowell,
168,198

Subject Index

A

Acetals

- cyclic ketene, *See* Cyclic ketene acetals
living cationic copolymerization with
methyl glyoxylate, 41–48

- Aliphatic aldehydes, polymerization for
formation of polyacetals, 50–51

- Alkene(s), heterogeneous cationic
polymerization by aluminum triflate,
113–134

- Alkene–vinyl polymerization, living, *See*
Living vinyl–alkene polymerization
Alkyldiphenylcarbenium ions, 32–33
Allylic positions, hydride abstractions,
37–38

Author Index

- Bae, Young Cheol, 168,198
Basko, M., 41
Canale, P. L., 178
Cheradame, H., 135
Coca, S., 198
Crivello, J. V., 83
de Jong, Feike, 63
Faust, Rudolf, 168,198
Fodor, Zsolt, 168
Gandini, Alessandro, 113
Graafland, Teun, 63
Held, Daniela, 63
Ingrisch, Stefan, 151
Iván, Béla, 63
Kaluzynski, Krzysztof, 75
Kamigaito, Masami, 106
Katayama, Hiroshi, 106
Kennedy, Joseph P., 178
Kubisa, P., 41
Lai, Y.-L., 83
Lang, Gabriele, 25
Libiszowski, Jan, 75
Lubnin, Alexander V., 178
Malik, R., 83
Matyjaszewski, Krzysztof, 12
Mayr, Herbert, 25
Mohamed, F., 50
Moreau, M., 50
Müller, Axel H. E., 63
Nuyken, Oskar, 151
Oh, Saehoon, 151
Omura, Naoki, 178
Penczek, Stanislaw, 41,75
Pretula, Julia, 75
Randriamahefa, S., 135
Rissoan, G., 135
Roth, Michael, 25
Satoh, Kotaro, 106
Sawamoto, Mitsuo, 106
Shaffer, Timothy D., 1,96
Szymanski, Ryszard, 75
Vairon, J. P., 50
Yang, Yao-Hong, 113

Affiliation Index

- BFGoodrich Company, 178
Carnegie Mellon University, 12,198
Ecole Française de Papeterie et des
Industries Graphiques, 113
Exxon Chemical Company, 1,96
Kyoto University, 106
Ludwig-Maximilians-Universität, 25
Polish Academy of Sciences, 41,75
Rensselaer Polytechnic Institute, 83
Shell Research and Development
Centre, 63
Technische Universität München, 151
Université Pierre et Marie Curie, 50
University of Akron, 178
University of Evry, 135
University of Mainz, 63
University of Massachusetts Lowell,
168,198

Subject Index

A

Acetals

- cyclic ketene, *See* Cyclic ketene acetals
living cationic copolymerization with
methyl glyoxylate, 41–48
Aliphatic aldehydes, polymerization for
formation of polyacetals, 50–51

- Alkene(s), heterogeneous cationic
polymerization by aluminum triflate,
113–134
Alkene–vinyl polymerization, living, *See*
Living vinyl–alkene polymerization
Alkyldiphenylcarbenium ions, 32–33
Allylic positions, hydride abstractions,
37–38

Aluminum triflate, heterogeneous cationic polymerization of aromatic alkenes, 113–134

Amphiphilic block copolymers via cationic polymerization
 block copolymers
 from 2-chloroethyl vinyl ether and methyl vinyl ether, 160–165
 from isobutyl vinyl ether and poly(ethyl vinyl ether) via polymer analogue reaction, 165–166
 from methyl vinyl ether and isobutyl vinyl ether, 158–160
 from methyl vinyl ether and *N*-vinyl-carbazole, 166
 homopolymerization of methyl vinyl ether, 151–158
 via living vinyl–alkene polymerization, 6

Anion(s), noncoordinating, use in carbocationic polymerization, 96–105
 Anionic polymerization, thermodynamics of *n*-butyraldehyde, 59–61
 Aromatic alkenes, heterogeneous cationic polymerization by aluminum triflate, 113–134

B

Batch homopolymerization
 indene, 126–131
 4-methylstyrene, 116–127
 Benzhydryl cations, constant selectivity relationships, 35
 Bis(diphenylethenyl) compounds, coupling reaction of living polyisobutylene, 198–209
 1,3-Bis(1-phenylethenyl)benzene, use in coupling reaction of living polyisobutylene, 198–209
 2,2-Bis[4-(1-phenylethenyl)phenyl]propane, use in coupling reaction of living polyisobutylene, 198–209
 2,2-Bis[4-(1-tolylethenyl)phenyl]propane, use in coupling reaction of living polyisobutylene, 198–209

Block copolymers
 7-oxabicyclo[2.2.1]heptane and tetrahydrofuran, 81–82
See also Amphiphilic block copolymers via cationic polymerization
n-Butyraldehyde, thermodynamics of ionic polymerization, 50–61

C

Capping, polyisobutylene with 1,1-diphenylethylene, 168–176
 Carbocationic polymerization
 control problems, 12–13
 initiation using metallocene initiators that contain noncoordinating anions, 96
 living, *See* Living carbocationic polymerization
 use of noncoordinating anions, 96–105
 Cation–nucleophile combination reactions, rate constant determination methods, 26–27
 Cationic copolymerization of methyl glyoxylate with cyclic acetals
 comparison of structural determination systems, 47–48
 1,3-dioxolane
 with acetaldehyde, 42–45
 with methyl glyoxylate, 45–47
 Cationic polymerization
 amphiphilic block copolymers, 151–166
 aromatic alkenes by aluminum triflate, *See* Heterogeneous cationic polymerization of aromatic alkenes by aluminum triflate
 cyclic ketene acetals, 89–91
 thermodynamics of *n*-butyraldehyde, 53–59
 vinyl ethers, 151
 vinyl monomers, role of Lewis acids, 106
 Cationic polymerization initiators, *See* 2-Methylpropene polymerization with FeCl₃ in nonpolar medium
 2-Chloroethyl vinyl ether, block polymerization, 151–166

- Copolymer(s), *See* Amphiphilic block copolymers via cationic polymerization
- Copolymerization
indene, 131–133
4-methylstyrene, 131–133
- Coupling reaction of living polyisobutylene using bis(diphenylethenyl) compounds as coupling agents
coupling reaction
bis(diphenylethenyl) compounds, 203–209
1,3-bis(1-phenylethenyl)benzene, 201–202
experimental description, 199–201
synthesis, 202–203
- Cyclic acetals, living cationic copolymerization with methyl glyoxylate, 41–48
- Cyclic ketene acetals
cationic polymerization, 89–91
depolymerization, 93–95
experimental procedure, 85–87
monomer synthesis, 86–89
polymer microstructure determination, 92–93
structure, 83
- Cyclosiloxane core, connection to polyisobutylene arms, 178–196
- D
- Depolymerization, cyclic ketene acetals, 93–95
- 2,6-Di-*tert*-butylpyridine, role in stability of propagating species in living cationic polymerization of isobutylene, 65–67
- 1,4-Dienes, reactions as σ - or π -nucleophiles, 37
- N,N*-Dimethylacetamide, role in stability of propagating species in living cationic polymerization of isobutylene, 65–67
- 2,4-Dimethylpyridine, role in stability of propagating species in living cationic polymerization of isobutylene, 65–67
- 1,3-Dioxolane copolymerization
with acetaldehyde, 42–45
with methyl glyoxylate, 45–47
- 1,1-Diphenylethylene, capping of polyisobutylene, 168–176
- E
- Electrophiles, reactivity scales, 27–28
- Exchange reactions
living carbocationic polymerization, 13–15
living radical polymerization, 13–15
- F
- Ferric chloride, role in 2-methylpropene polymerization in nonpolar medium, 135–149
- G
- Gel permeation chromatography, polyisobutylene arms connected to cyclosiloxane core, 178–196
- H
- Heterogeneous cationic polymerization initiators, *See* 2-Methylpropene polymerization with FeCl_3 in nonpolar medium
- Heterogeneous cationic polymerization of aromatic alkenes by aluminum triflate
batch homopolymerization
indene, 126–131
4-methylstyrene, 116–127
copolymerization, 131–133
experimental description, 113–116
flow experiments, 133–134
- Homopolymers of methyl glyoxylate, thermal stability, 42
- Hydride donors, reactivities toward carbenium ions, 35–36
- Hydride transfer reactions, living carbocationic polymerizations, 34–38

Hyperbranched polymers, preparation using living vinyl-alkene polymerization, 6-8

I

Indene

batch homopolymerization, 126-131

copolymerization, 131-133

flow experiments, 133-134

Initiator

heterogeneous cationic polymerization,

See 2-Methylpropene polymerization

with FeCl₃ in nonpolar medium

role in thermodynamics of ionic

polymerization of *n*-butyraldehyde, 55

Ionic polymerization of *n*-butyraldehyde, thermodynamics, 50-61

Isobutyl vinyl ether, cationic

polymerization, 158-160, 165-166

Isobutylene

propagation rate constant, 30-34

stability of propagating species in

living cationic polymerization,

63-73

Isobutylene polymerization, catalysis

using tris(pentafluorophenyl)boron,

96-105

K

Kinetics

living carbocationic polymerizations

hydride transfer reactions, 34-38

propagation rate constants, 28-34

polyisobutylene capping with

1,1-diphenylethylene, 168-176

reactions of carbocations with uncharged nucleophiles

linear free energy relationship, 27-28

rate constant determination methods,

26-27

reactions, 25-26

reactivity scales for nucleophiles and electrophiles, 27-28

L

Lewis acid(s)

roles in cationic polymerizations of

vinyl monomers, 106

selection, 107

Lewis acid catalyst, use in carbocationic

polymerization, 96-105

Liquid-crystalline polymers, preparation

using living vinyl-alkene

polymerization, 1-8

Living carbocationic polymerization

additive(s), 64

additive effects, 65-67

applications, 63-64

chain end stability under monomer-

starved conditions, 67-68

comparison to conventional systems,

20-22

developments, 63

2,6-di-*tert*-butylpyridine effect on

mechanism of chain coupling, 68-71

exchange reactions, 13-16

formal stoichiometry of exchange

reactions, 16-18

initiator effects, 65-67

mechanism, 64

new polymers, 5-8

proton expulsion and double bond

formation, 64-65

requirements for controlled

polymerization, 18-20

Living cationic polymerization

kinetics, 25-38

stability of propagating species of

isobutylene

chain end stability under monomer-

starved conditions, 67-68

effect of additives, 65-67

effect of 2,6-di-*tert*-butylpyridine

on mechanism of chain coupling,

68-71

experimental procedure, 73

with ytterbium trifluoromethanesulfonate

as water-resistant recoverable Lewis

acid, 107-112

- Living polyisobutylene, coupling reaction using bis(diphenylethenyl) compounds as coupling agents, 198–209
- Living polymerization, design of polymer architectures, 168–169
- Living radical polymerization
comparison to conventional systems, 20–22
exchange reactions, 13–16
requirements for controlled polymerization, 18–20
- Living vinyl–alkene polymerization
amphiphilic block copolymers, 6
hyperbranched polymers, 6–8
initiation rate, 4
polyisobutylene thermoplastic elastomers, 5–6
propagation equilibria, 2–4
- M
- Macrocyclic polymers, preparation using living vinyl–alkene polymerization, 1–8
- Macromonomeric polymers, preparation using living vinyl–alkene polymerization, 1–8
- Metallocene initiators that contain noncoordinating anions, initiation of carbocationic polymerizations, 96
- Methyl glyoxylate
living cationic copolymerization with cyclic acetals, 41–48
polyacetal formation, 41–42
polymerization, 41
- Methyl vinyl ether, cationic polymerization, 151–166
- 2-Methylpropene polymerization with FeCl_3 in nonpolar medium
cocatalysts, 139,140f
cocatalyst initiation mechanism, 149
direct initiation mechanism, 149
experimental procedure, 136
 FeCl_3 concentration effect, 139–143
initiation mechanism, ferric salts in nonpolar medium, 136–137
- 2-Methylpropene polymerization with FeCl_3 in nonpolar medium—*Continued*
kinetics
active species, 147–149
partially and totally heterogeneous system, 147
permanent catalyst, 147
polymer yield vs. time, 142f,143,144f
polymerization temperature, 145–147
rate of polymerization, 145,146f
rate order in cocatalyst, 143
rate order in monomer, 143–144
- 4-Methylstyrene
batch homopolymerization, 116–127
copolymerization, 131–133
flow experiments, 133–134
Microstructure, determination, 92–93
Monomer synthesis, cyclic ketene acetals, 86–89
- Multiarm star polyisobutylenes, *See* Polyisobutylene arms connected to cyclosiloxane core
- N
- Neopentylidiphenylcarbenium ion, propagation rate constant, 32–33
- Nitrogen nucleophile, role in living cationic polymerization, 106–112
- NMR spectroscopy
coupling reaction of living polyisobutylene using bis(diphenylethenyl) compounds as coupling agents, 198–209
polyisobutylene arms connected to cyclosiloxane core, 178–196
thermodynamics of ionic polymerization of *n*-butyraldehyde, 51–61
- Noncoordinating anions, use in carbocationic polymerization, 96–105
- Nonpolar medium, 2-methylpropene polymerization with FeCl_3 , 135–149
- Nonpolymerizable monomers, use in carbocationic macromolecular engineering, 198
- Nucleophiles, reactivity scales, 27–28

O

- 7-Oxabicyclo[2.2.1]heptane, cationic polymerization, 75
- 7-Oxabicyclo[2.2.1]heptane–tetrahydrofuran copolymerization block copolymers, 81–82
- pseudoperiodic copolymers, 80–81
- reactivities of active species, 76–78
- statistical copolymers, 78–80

P

- π -nucleophiles, reactivities toward carbenium ions, 35–36
- Phosphine ion trapping, structure of active species of cationic copolymerization of methyl glyoxylate with cyclic acetals, 41–48
- Photoinitiated cationic polymerization, cyclic ketene acetals, 83–95
- Polyacetals
- formation from methyl glyoxylate, 41
 - thermal stability, 42
- Polyisobutylene, coupling reaction using bis(diphenylethenyl) compounds as coupling agents, 198–209
- Polyisobutylene arms connected to cyclosiloxane core
- advantages, 179
 - ^{13}C relaxation times, 193–196
 - experimental procedure, 182–185
 - model studies with 2,4,4-trimethyl-1-pentene, 185–187
 - stars with multiple polyisobutylene arms emanating from cyclic siloxane cores, 187–194
 - structure of siloxane fragments and molecules, 179, 180f
- Polyisobutylene capping with 1,1-diphenyl-ethylene
- calculation of kinetic parameters, 175–176
 - capping reactions, 170–172
 - decapping reactions, 172–175
 - experimental procedure, 169–170
- Polyisobutylene thermoplastic elastomers, preparation using living vinyl–alkene polymerization, 5–6
- Polymer analogue reaction, isobutyl vinyl ether and poly(methyl vinyl ether) block copolymers, 165–166
- Polymerization
- amphiphilic block copolymers, 151–166
 - aromatic alkenes by aluminum triflate, *See* Heterogeneous cationic polymerization of aromatic alkenes by aluminum triflate
 - living carbocationic, *See* Living carbocationic polymerization
 - living vinyl–alkene, *See* Living vinyl–alkene polymerization
 - 2-methylpropene with FeCl_3 in nonpolar medium, 135–149
- Polymerization initiators, *See* 2-Methylpropene polymerization with FeCl_3 in nonpolar medium
- Poly(methyl glyoxylate), preparation, 41
- Propagation rate constants, living carbocationic polymerizations, 28–31
- Pseudoperiodic copolymers, 7-oxabicyclo[2.2.1]heptane and tetrahydrofuran, 80–81
- Pyridine, role in stability of propagating species in living cationic polymerization of isobutylene, 65–67

R

- Radical polymerizations
- control problems, 12–13
 - living, *See* Living radical polymerization

S

- Solvent, role in thermodynamics of ionic polymerization of *n*-butyraldehyde, 59
- Star polyisobutylenes, *See* Polyisobutylene arms connected to cyclosiloxane core
- Statistical copolymers, 7-oxabicyclo[2.2.1]heptane and tetrahydrofuran, 78–80

T

- Telechelic polymers, preparation using living vinyl-alkene polymerization, 1-8
- Temperature, role in thermodynamics of ionic polymerization of *n*-butyraldehyde, 55-61
- Tetrahydrofuran-7 oxabicyclo[2.2.1]heptane copolymerization, *See* 7-Oxabicyclo-[2.2.1]heptane-tetrahydrofuran copolymerization
- Thermodynamics of ionic polymerization of *n*-butyraldehyde
- anionic polymerization, 59-61
 - cationic polymerization, 53-59
 - experimental procedure, 51-53
- Titanium(IV) chloride, role in stability of propagating species in living cationic polymerization of isobutylene, 65-67
- 2,4,4-Trimethyl-2-pentyl cation, propagation rate constants, 2-34
- Tris(pentafluorophenyl)boron as Lewis acid catalyst in carbocationic polymerization
- copolymerization of isobutylene with isoprene, 101-103
 - with *p*-methylstyrene, 103-104
 - experimental procedure, 104-105
 - homopolymerization of isobutylene kinetics, 97,99-101
 - reaction conditions, 97-98

U

- UV spectrophotometry, thermodynamics of ionic polymerization of *n*-butyraldehyde, 51-61

V

- Vinyl-alkene polymerization, living, *See* Living vinyl-alkene polymerization
- Vinyl ethers, cationic polymerization, 151
- Vinyl monomers, role of Lewis acids in cationic polymerizations, 106
- N*-Vinylcarbazole, cationic polymerization, 166

W

- Winstein equilibrium, schematic representation, 2

Y

- Ytterbium trifluoromethanesulfonate properties, 107
- use as Lewis acid in living cationic polymerization, 106-112